A UNIFIED SYNTHETIC APPROACH TO THE TRANSTAGANOLIDE AND BASILIOLIDE NATURAL PRODUCTS

Thesis by

Hosea Martin Nelson

In Partial Fulfillment of the Requirements

for the Degree of

Doctor of Philosophy

CALIFORNIA INSTITUTE OF TECHNOLOGY

Pasadena, California

2013

(Defended September 20, 2012)

To my mother, Patricia

ACKNOWLEDGEMENTS

First and foremost I would like to thank my family; without you guys this work wouldn't have been possible. Your relentless support has been the key ingredient to my success.

Brian Stoltz has been a tremendous advisor and deserves acknowledgement above all others. In a lot of ways we are very different, but Brian always accepted me for who I am, and tried his best to help me to succeed. When I first met Brian during visiting weekend, he asked me what I wanted to do in grad school. I said, "I dunno …. I just like molecules." He said, "Me too." I think that conversation has been representative of our relationship over the years: we both love chemistry and that shared passion has prevailed over all other concerns. I hope that I will be lucky enough to interact with him in the future, both personally and professionally.

All of the members of my committee have been great. Peter has a tremendous presence, and as chair of my committee he has always advocated for me and had my best interests at heart. His ability to gently control a room full of smart, opinionated people is a skill that I aspire to obtain. Bob's humility and kindness are traits that we should all learn from. He is incredibly down to earth and is an example that fame and success doesn't always diminish interpersonal skills. He is a *pretty* good fisherman too! Sarah is a fantastic mentor, and of my committee members, she asks the hardest questions. I am grateful to have witnessed her rise in the field and I will always think of her as a role model for how to start a research group. She has a notable skill for selecting graduate students: the social and scientific cultures that she has created within her group are second to none.

Throughout the years I have had the opportunity to collaborate with a number of talented scientists on and off campus and I would like to acknowledge them here: Jonny Gordon, Kei Murakami, Dr. Scott Virgil. Dr. Jeff Vieregg, Prof. Niles Pierce, Dr. Qingyu Sun, Prof. Ryan Julian, Prof. Vince Lavallo, Dr. Michael Day, Larry Henling, Anguel Alexiev, Josh Owens, Linda Choi, Michael Stepanian, Dr. Mona Shahgoli, and Dr. David VanderVelde.

The non-scientific support staff, who do an often thankless job, were imperative to this work. Lynne Martinez, Tess Legaspi, Ann Penney, Agnes Tong, Laura Howe, Joe Drew, Silva Virgil, and Stephen Gould have all been of great assistance.

The members of the Stoltz, Grubbs, and Reisman groups have truly been a joy to work with over the years. Regardless of hour, they always seemed to be around and willing to talk chemistry or give experimental advice. Their enthusiasm for science is violently contagious, and unsurpassed by any group of people that I have encountered thus far.

To all of the wonderful personal friends that I have made during my 6 years here, many of which are acknowledged above, thanks for the memories and stay in touch!

hosea

ABSTRACT

Herein are described the first total syntheses of several members of the transtaganolide and basiliolide natural product family. A general strategy, hinging upon the use of a biomimetic Ireland–Claisen rearrangement/Diels–Alder cycloaddition cascade, was developed. It allowed for the rapid assembly of the most structurally complex, and biologically active members of the family.

A brief introduction that surveys the use of the pyrone Diels–Alder cycloaddition in total synthesis precedes details of our synthetic efforts. The diversity of structural motifs accessible through this reaction manifold is described through literature examples.

The account of our experimental work begins with details of extensive model studies. First, a simple system was prepared which probed the ability to construct basiliolide B via an intramolecular pyrone Diels–Alder reaction. It was demonstrated that the sterically congested core could be constructed in a highly diastereoselective fashion using this technology. Second, a simple prenylated pyrone was constructed, and shown to undergo a facile Ireland–Claisen rearrangement under a variety of conditions.

Subsequently, the utilization of these two methods within a cascade allowed for the rapid construction of racemic transtaganolide C, transtaganolide D, basiliolide B, and *epi*-8-basiliolide B. Furthermore, a novel Pd-catalyzed [5+2] annulation technology is utilized to construct the venerable, carboxy-ketene-acetal containing C-ring present in most of the metabolites.

Integration of asymmetry into our general strategy is also described. Utilization of a chiral silane directing group allowed for the successful and rare application of an enantioselective Ireland–Claisen rearrangement, culminating in the total syntheses of (+)-transtaganolide C, (–)-transtaganolide D, (+)-transtaganolide B, and (–)-transtaganolide A. Furthermore, the impact of this work on existing biosynthetic hypotheses is discussed.

TABLE OF CONTENTS

LIST OF FIGURES

CHAPTER 2

APPENDIX 1

APPENDIX 2

APPENDIX 5

APPENDIX 6

CHAPTER 4

APPENDIX 8

APPENDIX 9

LIST OF SCHEMES

CHAPTER 1

CHAPTER 2

APPENDIX 3

CHAPTER 3

APPENDIX 4

CHAPTER 4

APPENDIX 7

LIST OF TABLES

APPENDIX 2

APPENDIX 6

CHAPTER 4

APPENDIX 9

LIST OF ABBREVIATIONS

$[\alpha]_D$	angle of optical rotation of plane-polarized light
Å	angstrom(s)
p-ABSA	*para*-acetamidobenzenesulfonyl azide
Ac	acetyl
AIBN	azobisisobutyronitrile
APCI	atmospheric pressure chemical ionization
app	apparent
aq	aqueous
Ar	aryl group
atm	atmosphere(s)
ATP	adenosine triphosphate
B	base
Bn	benzyl
Boc	*tert*-butoxycarbonyl
bp	boiling point
BTSA	bis(trimethylsilyl)acetamide
BSA	bis(trimethylsilyl)acetamide
br	broad
Bu	butyl
i-Bu	*iso*-butyl
n-Bu	butyl or *norm*-butyl

t-Bu	*tert*-butyl
Bz	benzoyl
c	concentration of sample for measurement of optical rotation
^{13}C	carbon-13 isotope
^{14}C	carbon-14 isotope
/C	supported on activated carbon charcoal
°C	degrees Celcius
calc'd	calculated
CAN	ceric ammonium nitrate
Cbz	benzyloxycarbonyl
CCDC	Cambridge Crystallographic Data Centre
CDI	1,1'-carbonyldiimidazole
cf.	consult or compare to (Latin: *confer*)
cm^{-1}	wavenumber(s)
cod	1,5-cyclooctadiene
comp	complex
conc.	concentrated
Cy	cyclohexyl
CSA	camphor sulfonic acid
d	doublet
d	dextrorotatory
D	deuterium
DABCO	1,4-diazabicyclo[2.2.2]octane

dba	dibenzylideneacetone
DBDMH	*N*,*N*'-dibromo-5,5-dimethylhydantoin
DBU	1,8-diazabicyclo[5.4.0]undec-7-ene
DCC	dicyclohexyl carbodiimide
DCE	1,2-dichloroethane
DDQ	2,3-dichloro-5,6-dicyanobenzoquinone
de	diastereomeric excess
DIAD	diisopropyl azodicarboxylate
DIBAL	diisobutyl aluminum hydride
DMA	dimethylacetamide
DMAD	dimethyl acetylenedicarboxylate
DMAP	4-dimethylaminopyridine
DME	1,2-dimethoxyethane
DMF	*N*,*N*-dimethylformamide
DMSO	dimethylsulfoxide
DMTS	dimethylthexylsilyl
DNA	deoxyribonucleic acid
DPPA	diphenylphosphorylazide
dppp	1,3-bis(diphenylphosphino)propane
dr	diastereomeric ratio
DTT	dithiothreitol
ee	enantiomeric excess
E	methyl carboxylate (CO_2CH_3)

E^+	electrophile
E	trans (entgegen) olefin geometry
EC_{50}	median effective concentration (50%)
e.g.	for example (Latin: *exempli gratia*)
EI	electron impact
eq	equation
ESI	electrospray ionization
Et	ethyl
et al.	and others (Latin: *et alii*)
FAB	fast atom bombardment
Fmoc	fluorenylmethyloxycarbonyl
g	gram(s)
G	guanine
h	hour(s)
^1H	proton
^2H	deuterium
^3H	tritium
[H]	reduction
HATU	2-(7-aza-1*H*-benzotriazol-1-yl)-1,1,3,3-tetramethyluronium hexafluorophosphate
HMDS	hexamethyldisilamide or hexamethyldisilazide
HMPT	hexamethylphosphoramide
$h\nu$	light
HPLC	high performance liquid chromatography

HRMS	high resolution mass spectrometry
Hz	hertz
IBX	2-iodoxybenzoic acid
IC_{50}	half maximal inhibitory concentration (50%)
ICR	Ireland–Claisen rearrangement
i.e.	that is (Latin: *id est*)
IMPDA	intramolecular pyrone Diels–Alder
iNOS	human-inducible nitric oxide synthase
IR	infrared spectroscopy
J	coupling constant
k	rate constant
kcal	kilocalorie(s)
kg	kilogram(s)
KHMDS	potassium bis(trimethylsilyl)amide
L	liter or neutral ligand
l	levorotatory
LA	Lewis acid
LD_{50}	median lethal dose (50%)
LDA	lithium diisopropylamide
LHMDS	lithium bis(trimethylsilyl)amide
LICA	lithium isopropylcyclohexylamide
LTMP	lithium 2,2,6,6-tetramethylpiperidide
m	multiplet or meter(s)

M	molar or molecular ion
m	meta
μ	micro
m-CPBA	*meta*-chloroperbenzoic acid
Me	methyl
mg	milligram(s)
MHz	megahertz
MIC	minimum inhibitory concentration
min	minute(s)
mL	milliliter(s)
MM	mixed method
mol	mole(s)
MOM	methoxymethyl
mp	melting point
Ms	methanesulfonyl (mesyl)
MS	molecular seives
m/*z*	mass-to-charge ratio
N	normal or molar
NBS	*N*-bromosuccinimide
nm	nanometer(s)
NMR	nuclear magnetic resonance
NOE	nuclear Overhauser effect
NOESY	nuclear Overhauser enhancement spectroscopy

Nuc	nucleophile
o	ortho
[O]	oxidation
t-Oct	*tert*-octyl (1,1,3,3-tetramethylbutyl)
p	para
PCC	pyridinium chlorochromate
PDA	pyrone Diels–Alder
PDC	pyridinium dichromate
Ph	phenyl
pH	hydrogen ion concentration in aqueous solution
Piv	pivalate
pK_a	acid dissociation constant
PKS	polyketide synthase
PMB	*para*-methoxybenzyl
ppm	parts per million
PPTS	pyridinium *para*-toluenesulfonate
Pr	propyl
i-Pr	isopropyl
n-Pr	propyl or *norm*-propyl
psi	pounds per square inch
py	pyridine
q	quartet
R	alkyl group

R	rectus
RCM	ring-closing metathesis
REDAL	sodium bis(2-methoxyethoxy)aluminum hydride
ref	reference
R_f	retention factor
s	singlet or seconds
s	selectivity factor = $k_{rel(fast/slow)} = \ln[(1 - C)(1 - ee)]/\ln[(1 - C)(1 + ee)]$, where C = conversion
S	sinister
sat.	saturated
SERCA	sarcoendoplasmic reticulum calcium atpase
SEM	2-(trimethylsilyl)ethoxymethyl
SOD	superoxide dismutase
Su	succinimide
t	triplet
T	thymine
TBAF	tetra-*n*-butylammonium fluoride
TBAT	tetra-*n*-butylammonium difluorotriphenylsilicate
TBDPS	*tert*-butyldiphenylsilyl
TBHP	*tert*-butyl hydroperoxide
TBS	*tert*-butyldimethylsilyl
TCA	trichloroacetic acid
temp	temperature
TES	triethylsilyl

Tf	trifluoromethanesulfonyl
TFA	trifluoroacetic acid
TFAA	trifluoroacetic anhydride
TFE	2,2,2-trifluoroethanol
THF	tetrahydrofuran
THIQ	tetrahydroisoquinoline
TIPS	triisopropylsilyl
TLC	thin layer chromatography
TMEDA	*N*,*N*,*N'*,*N'*-tetramethylethylenediamine
TMP	2,2,6,6-tetramethylpiperidine
TMS	trimethylsilyl
TOF	time-of-flight
tol	tolyl
Tr	triphenylmethane (trityl)
Troc	2,2,2-trichloroethoxycarbonyl
Ts	*para*-toluenesulfonyl (tosyl)
UV	ultraviolet
w/v	weight per volume
v/v	volume per volume
X	anionic ligand or halide
Z	cis (zusammen) olefin

CHAPTER 1

Highlights of The Pyrone Diels–Alder Reaction in Total Synthesis

1.1 Introduction

Among the organic reactions known to generate stereochemical complexity, the Diels–Alder reaction is perhaps the most well studied and frequently applied. Since initial literature accounts,[1] the [4+2] cycloaddition between a diene and a dienophile has been applied to the syntheses of countless natural products,[2] polymers,[3] materials,[3a] and has been invoked as a fundamentally important enzymatic process in nature.[4] Many variants of the Diels–Alder reaction have been disclosed, including hetero Diels–Alder reactions[5] and intramolecular Diels–Alder reactions.[6] Furthermore, several methods to impart stereoselectivity have been disclosed.[7]

Shortly after their initial report of the Diels–Alder reaction,[1] Diels and Alder disclosed that methyl coumalic acid (**1**) undergoes [4+2] cycloaddition with maleic anhydride (**2**) to yield mixtures of oxabicyclo[2.2.2]octene **3** and bicyclo[2.2.2]octene **5** (Scheme 1.1).[8] Oxabicyclo[2.2.2]octene **3** derives from direct cycloaddition of coumarin

1 and anhydride **2**, while bicyclo[2.2.2]octene **5** arises from the retro [4+2] extrusion of CO_2 from intermediate **3**, followed by a second [4+2] cycloaddition of an additional equivalent of maleic anhydride (**2**) to the resulting diene (**4**). The demonstrated ability to prepare substituted and structurally complex cyclohexenes in this early example foreshadows the utility of the Pyrone Diels–Alder (PDA) reaction manifold.

Scheme 1.1. Diels' and Alder's 1931 PDA

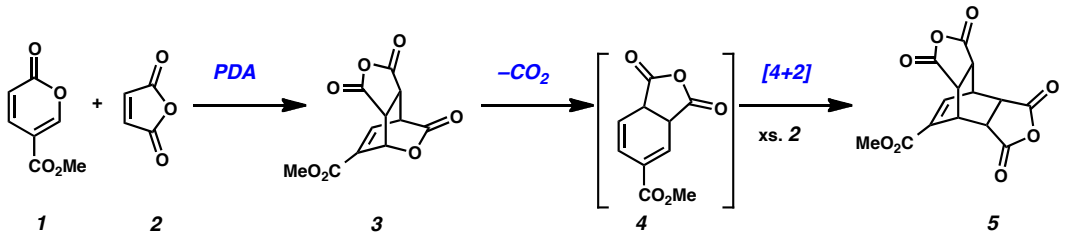

Indeed, in the 79 years since this seminal report, methods have been developed that allow for complete exploitation of the PDA reaction (Scheme 1.2).[9] Functionalized oxabicyclo[2.2.2]octenes (**7**), functionalized cyclohexenes (**8**), functionalized cyclohexadienes (**9**) and substituted aromatics (**10**), have all been prepared by PDA reactions.[9] Furthermore, methods for control of absolute and relative stereochemistry have been demonstrated.[10]

Scheme 1.2. The pyrone Diels–Alder (PDA) reaction manifold

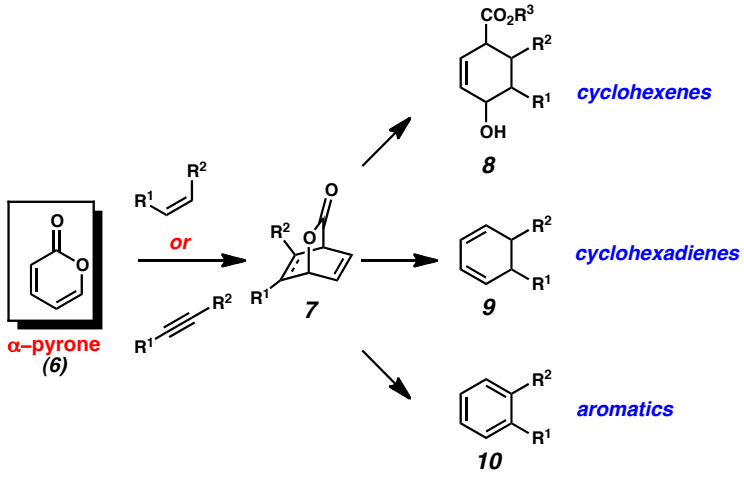

α-Pyrones (or *2*-pyrones) (**6**) undergo [4+2] cycloadditions less readily than other cyclic dienes due to their partial aromatic character (Scheme 1.3). This review highlights the many approaches necessary to overcome this inherent reactivity.[9b] Such techniques include: high temperature, high pressure, catalysis, template direction, and electronic perturbations through substrate design. The products obtained from the PDA reaction manifold are largely determined by the conditions employed. As shown in Scheme 1.2, the PDA reaction of α-pyrone **6** can yield oxabicyclo[2.2.2]octene **7**, highly oxygenated cyclohexene **8**, diene **9**, or aromatic ring **10** as dictated by the conditions employed.

*Scheme 1.3. Partial aromaticity of **6** due to resonance contribution from **6a***

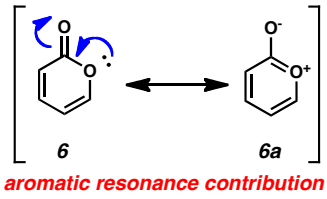

While multiple reviews have addressed the PDA from the perspective of methods development and mechanism,[9] it is the goal of this document to highlight its application

within the realm of total synthesis. In particular, we will survey the types of structural motifs accessible from this reaction manifold by a discussion of reactions and substrates utilized in complex molecule synthesis. This chapter is not meant to be comprehensive, but rather a brief survey that highlights an underutilized transformation in organic synthesis.

1.2 Synthesis of Aromatic Systems

Due to the aromatic character of α-pyrones (Scheme 1.3), the use of high temperatures to facilitate cycloaddition is often necessary. Under such conditions, extrusion of CO_2 *via* retro [4+2] is facile, which in turn leads to diene formation (Scheme 1.4). When the dienophile is either an alkyne or alkene, where X is a leaving group (**11**), aromatic products will be formed. In the case of alkynyl dienophiles, the intermediate bicyclo[2.2.2]octadiene **12** is highly strained, and *readily* decomposes by CO_2 extrusion to the corresponding aromatic ring.[11] When alkenyl dienophiles are substituted with a leaving group (**11**), HX elimination from the intermediate diene **13** is required to form aromatic systems. The necessary elimination can occur with or without the addition of exogenous base. Additionally, *in situ* oxidation of the intermediate diene **13** to the aromatic ring system has been demonstrated in polyaromatic systems.[9b]

Scheme 1.4. Formation of aromatic rings by PDA reactions

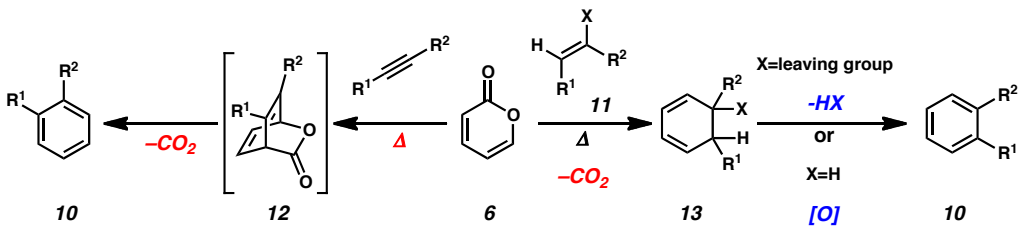

1.2.1 Boger's Synthesis of Azafluoranthene Alkaloids

In an early utilization of the PDA reaction, Boger and co-workers synthesized biologically active azafluoranthene alkaloids rufescine (**17**) and imeluteine (**18**) (Scheme 1.5).[12] Both 1,1-dimethoxyethylene and 1,1,2-trimethoxyethylene underwent smooth cycloaddition with electron-deficient coumarin **14** to yield the cores of rufescine (**15**) and imeluteine (**16**). It is notable that, while CO_2 extrusion was facile under the reaction conditions, treatment of the diene PDA product **16** with DBU was needed to facilitate the elimination of methanol to form the aromatic system of **18**. Conversely, aromatic product **15** was formed in situ, as the needed elimination of MeOH was accomplished without additional base. Intermediates **15** and **16** were advanced to the natural product targets after saponification and Cu-catalyzed decarboxylation.

*Scheme 1.5. Boger's total synthesis of and rufescine (**17**) and imeluteine (**18**)*

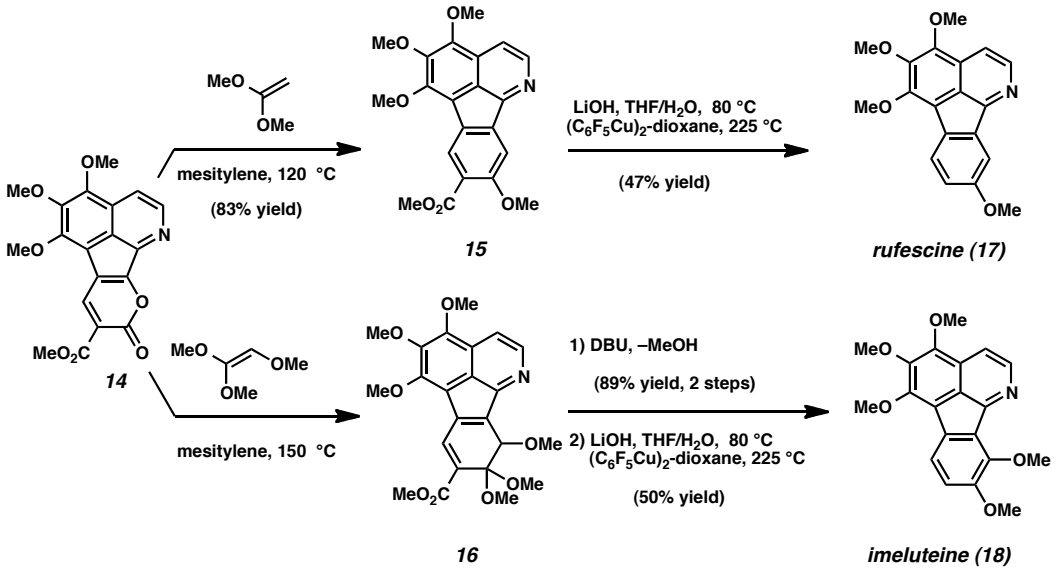

1.2.2 Utilization of Triple Bonds in the PDA Cycloaddition

α-Pyrones readily undergo [4+2] cycloaddition reactions with arynes. In Guitan's formal synthesis of nitidine (**23**),[13] cycloaddition of pyrone diene **19** with an aryne derived from catechol efficiently constructs the core of the target (Scheme 1.6). Notably, Dyke and co-workers had previously tried to utilize diene **20** in the synthesis of nitidine (**23**), but they only obtained trace yields of the desired product **21a**.[14] Subsequent to the key PDA reaction, saponification and decarboxylation yield tetracycle **22**, which had previously been advanced to the cationic natural product.[15] It is noteworthy that the α-pyrone ring reacts with the aryne dienophile, while the pyridone ring remains untouched; establishing the chemoselectivity between two analogous ring systems known to undergo [4+2] cycloaddition.[9b]

*Scheme 1.6. Guitan's synthesis of nitidine (**23**)*

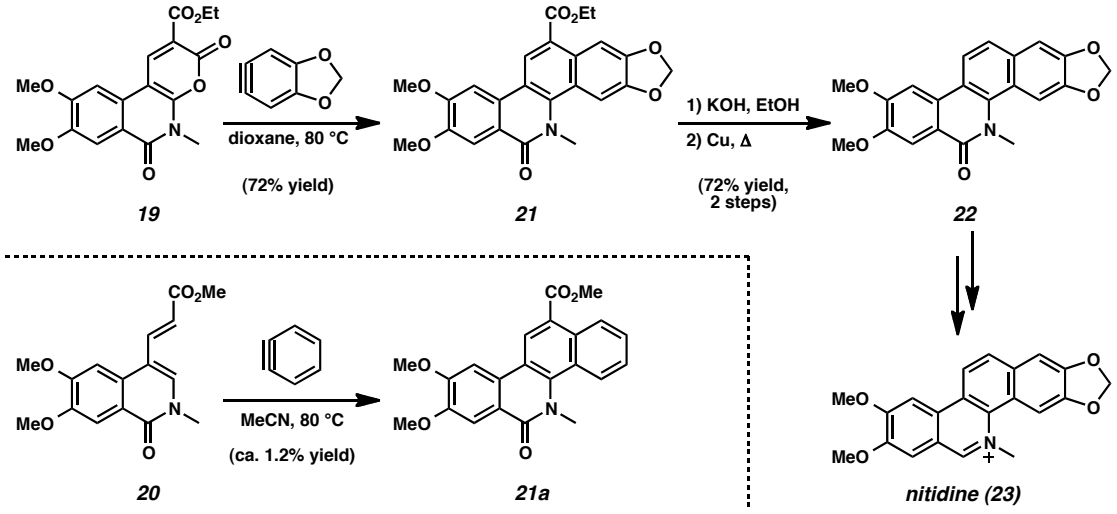

Perhaps the most daring utilization of an aromatic forming PDA cycloaddition comes from Baran and Burns. In particular, the unusual bent aromatic ring (highlighted

in red) was forged by microwave irradiation of alkyne-pyrone **24** to the yield the natural product (±)-haouamine A (**26**) (Scheme 1.7).[16] As noted by Baran, the formation of such a ring suggested to him "that a non-aromatic conformational mimic of the bent aromatic ring might serve as a viable precursor if it were able to undergo subsequent aromatization."[16] The PDA, with bicyclo[2.2.2]octene intermediate **25,** is particularly suited to this task. Further confounding his bold late-stage application of the PDA was the atropoisomerism of the bent aromatic ring and the daunting task of forming an 11-membered ring via intramolecular PDA. Remarkably, the reaction proceeded in greater than 10:1 atroposelectivity, and the natural product target was isolated in 21% yield.

*Scheme 1.7. Baran's total synthesis of (±)-haouamine A (**26**)*

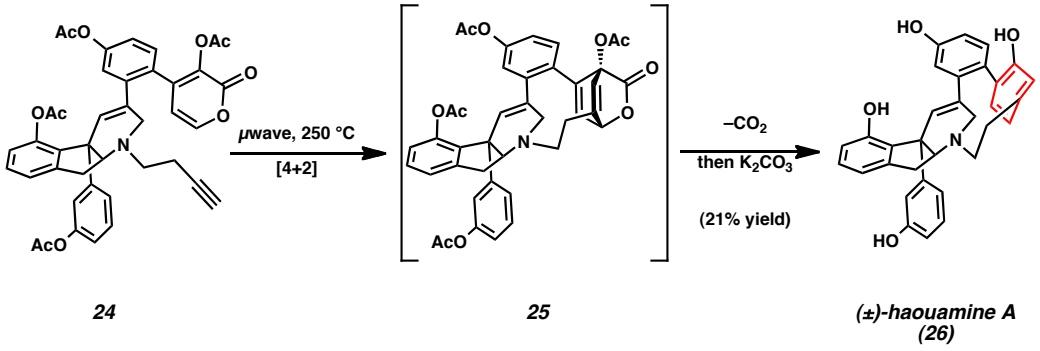

1.2.3 The Biosynthetic PDA

Attempts to characterize a putative Diels–Alderase, frequently evoked in biosynthetic pathways, have been extensive.[4] Perhaps the most well known of the candidates for this role is macrophomate synthase, an enzyme found in the phytopathogenic fungus *Macrophoma commelinae*.[17] It has been shown to catalyze the formation of benzoates such as macrophomate (**30**) from the corresponding oxaloacetate (**28**) and substituted α-pyrone **27** (Scheme 1.8). Macrophomate synthase has been

demonstrated to be imperative in decarboxylative enolate formation, C–C bond forming events, and CO_2 extrusion.[17] While the debate has raged in the literature as to whether this transformation is truly a concerted [4+2] cycloaddition[18] or a Michael–Aldol stepwise sequence, recent computational[19] and experimental evidence[20] that favor the latter mechanism has been reported. Nonetheless, this transformation represents the most debated PDA in the literature.[21]

Scheme 1.8. Macrophomate synthase catalyzed PDA from nature

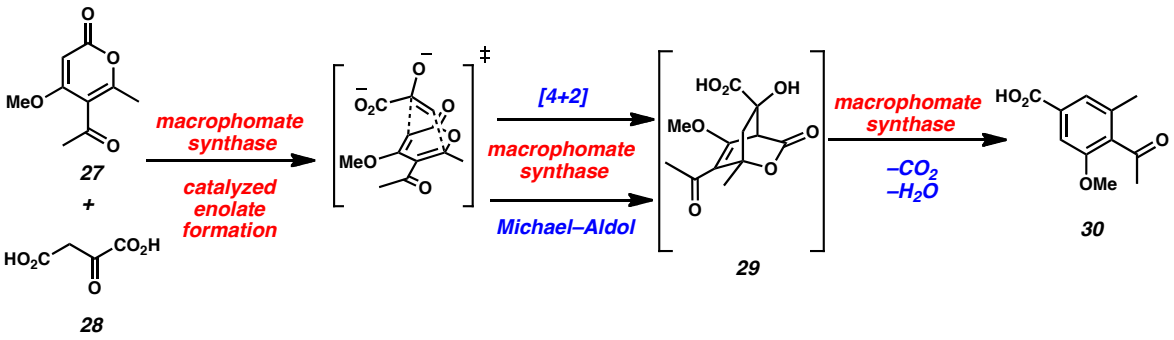

1.3. Synthesis of Dienes

In systems where an olefin dienophile is not substituted with a latent leaving group, or when no base or external oxidant is supplied, PDA reactions will often yield dienes by CO_2 extrusion from oxabicyclo[2.2.2]octene intermediate (Scheme 1.2). As early as 1972, E. J. Corey and co-workers recognized this, and exploited the PDA cycloaddition to prepare dienes in the key step of the syntheses of the copaenes and ylangenes (Scheme 1.9, **35**–**38**).[22] Heating of pyrone **31** with β,γ-unsaturated ketone **32** led to the formation of **34** with "remarkable selectivity".[22] Corey rationalized that the reaction proceeded through the enol tautomer (**32a**), which is consistent with the observed regioselectivity. Notably, dienophiles **39**, **40**, and **41** failed to react with pyrone

31 under similar conditions, a testament to the careful electronic matching required to carry out the PDA reaction (Scheme 1.10).

*Scheme 1.9. Corey's total syntheses of the copaenes (**35** and **37**) and ylangenes (**36** and **38**)*

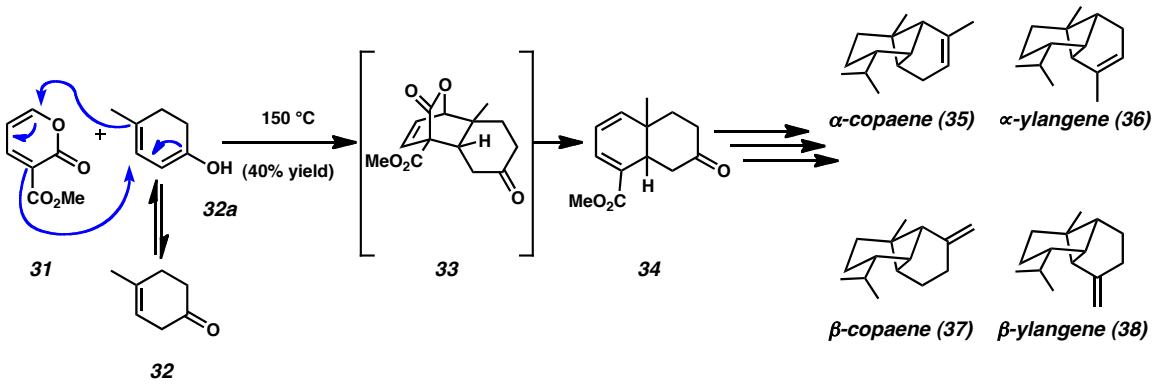

Scheme 1.10. Evidence for reactivity through enol tautomer

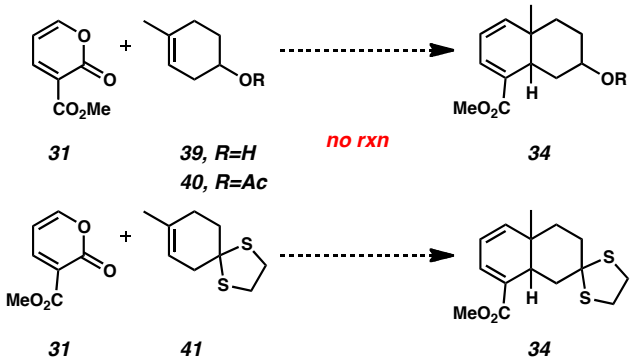

1.4 Synthesis of Substituted Cyclohexenes: PDA without CO_2 Extrusion

The application of the PDA to the synthesis of dienes and aromatics is a very powerful method, as discussed in sections 1.2 and 1.3. However, the examples in which CO_2 extrusion is not observed are perhaps the most powerful. In these cases up to four contiguous stereocenters are generated in the initial bicyclo[2.2.2]octene (**43**) and can be elaborated into a number of highly oxygenated cyclic systems (e.g., **44**, Scheme 1.11).

Scheme 1.11. PDA without CO_2 extrusion

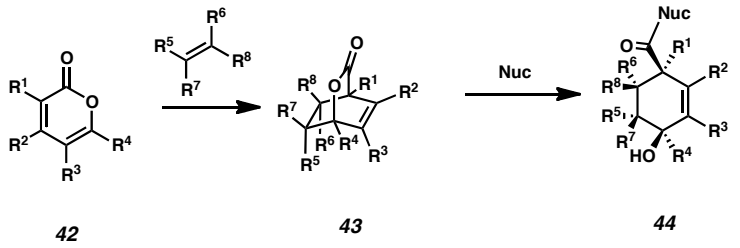

42 ***43*** ***44***

As discussed, the aromatic character of α-pyrones often necessitates harsh reaction conditions for efficient [4+2] cycloaddition. Unfortunately isolation of the stereochemically rich bicyclo[2.2.2]octene (**43**) or its derivatives is unlikely under such conditions, as intermediates such as **43** have been shown to extrude CO_2 at temperatures as low as 50 ºC.[9b] Therefore, careful choice of reactive partners and/or reaction conditions are required to allow for low temperature cycloadditions that do not favor CO_2 extrusion. Several approaches to address this challenge have been developed, including substituents that enhance electronic matching, catalysis, and use of intramolecular reactions.[9b] While it is more desirable to lower the HOMO-LUMO gap *via* catalysis, covalent substituents on the pyrone diene or olefinic dienophile have been used extensively.

1.4.1 Nicolaou's Total Synthesis of Taxol: Use of Templating in the PDA Reaction

The first total synthesis of Taxol (**50**),[23] which stands as one of the major chemical achievements of the 20th century, is an exemplary use of the PDA to rapidly install stereochemical complexity (Scheme 1.12 and 1.13). The cyclohexenyl C-ring, which contains four contiguous stereocenters, posed a significant challenge to standard Diels–Alder technology. As noted by the authors, "[the] ring C of Taxol (**50**), with its numerous stereocenters and high degree of oxygenation, presented a more serious

challenge [than the A-ring] to the Diels–Alder approach."[23b] Their initial efforts focused on the use of carboxymethyl pyrone **31** and dienophile **45** (Scheme 1.12). Much to the author's disappointment, heating of these reactants to 155 °C led to the formation of undesired intermediate **46**, instead of **47**, the former of which undergoes facile decarboxylation to yield unexpected diene **48**.

Scheme 1.12. First attempts at taxol C-Ring

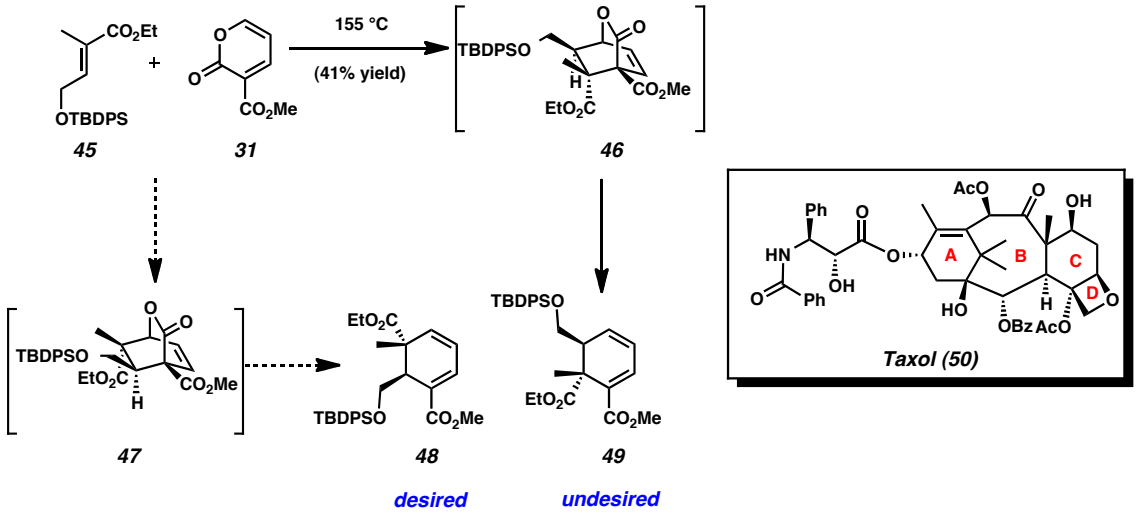

Despite this unfortunate result, Nicolaou and co-workers continued to work within the PDA reaction manifold, eventually finding the use of a temporary tether to force the desired stereochemical outcome (Scheme 1.13). Based on earlier work by Narasaka,[24] treatment of dienophile **51** and hydroxypyrone **52**, with phenylboronic acid under dehydrating conditions yielded bicycle **55** after cleavage of the temporary boronic ester linkage. It is worthy to note that, under reduced temperatures, the oxabicyclo[2.2.2]octene **54** did not undergo thermal decarboxylation and was isolable as

the initial product. Subsequent to decomplexation, intramolecular transacetalization yields the desired C-ring fragment (**55**) that was subsequently advanced to taxol (**50**).

Scheme 1.13. Synthesis of taxol C-Ring

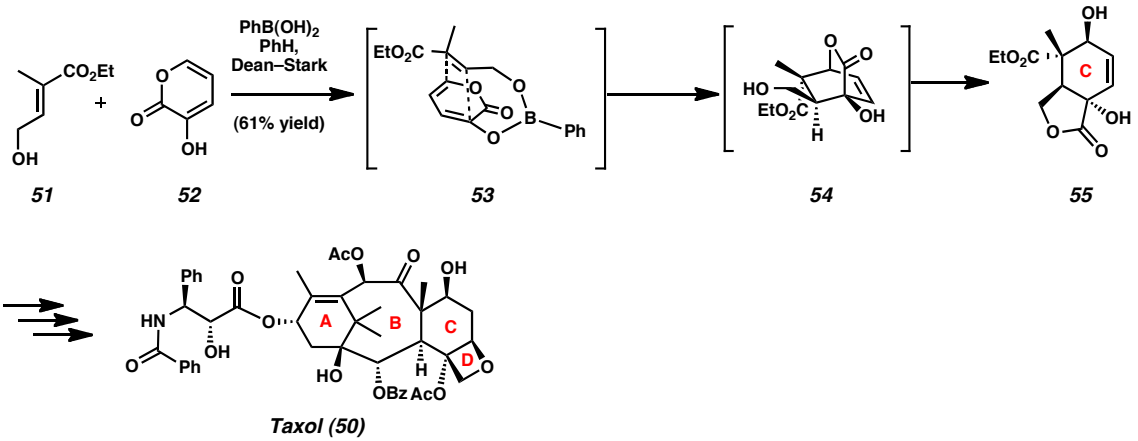

1.4.2. Posner's Covalent Modification Approach

Posner and co-workers have demonstrated that strongly electron withdrawing pyrone substituents, such as sulfinyls[25] and sulfonyls,[26] allow for low temperature inverse-demand cycloadditions. For example, *1,1*–dimethoxyethylene (**56**) undergoes cycloaddition with *3*-sulfinyl-*2*-pyrone **57** at a modest 25 ºC (Scheme 1.14). Bicyclo[2.2.2]octene **58** was resistant to CO_2 extrusion and easily isolated at this temperature.

Scheme 1.14. Substituent-assisted inverse-demand PDA

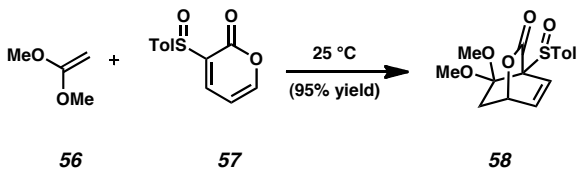

2-Pyridones (e.g., **60**, Scheme 1.15), which are normally more resistant to cycloaddition than their oxygen analogs, were also demonstrated to have enhanced reactivity due to sulfonyl substitution.[27] *1,3*-Disulfonyl-*2*-pyridone **60** underwent smooth cycloaddition with butyl vinyl ether **59** at low temperatures and near ambient pressures. Bicycle **61** was isolated, and the resulting olefin was reduced. Notably, further reduction with $NaBH_4$ allowed isolation of oxygenated aminocyclohexane **62**.

Scheme 1.15. Substituent-assisted normal-demand pyridone Diels–Alder

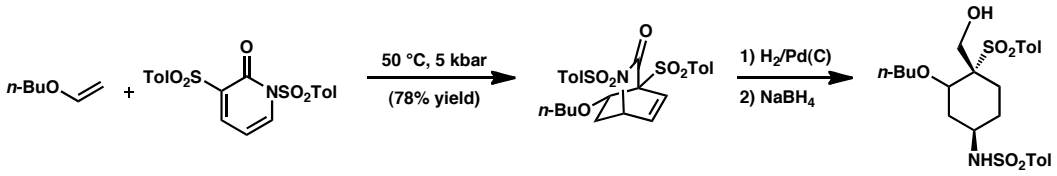

59 ***60*** ***61*** ***62***

A further example of the application of the PDA to complex molecule synthesis is Posner's synthesis of (–)-methyl triacetyl-*4*-epishikimate[28] (**68**, Scheme 1.16). This compound had been previously prepared by resolution of a racemate[29] or from the chiral pool.[30] Of note to Posner's synthesis is the use of the sulfone-modified pyrone **64**, which allows for a low temperature cycloaddition and isolation of bicycle **65**. Furthermore, in a rare example of a diastereoselective PDA, excellent facial selectivity was imparted from the non-racemic, chiral ether **63**, despite free rotation about the oxygen atom. The bridging ester (**65**) was hydrolyzed at low temperature by treatment with NaOMe. Importantly, cyclohexene **66** was desulfonylated by treatment with mercury-aluminum amalgam and oxidized to epoxide **67**, which was advanced to the target compound (**68**).

*Scheme 1.16. Synthesis of (–)-methyl triacetyl-4-epishikimate (**68**)*

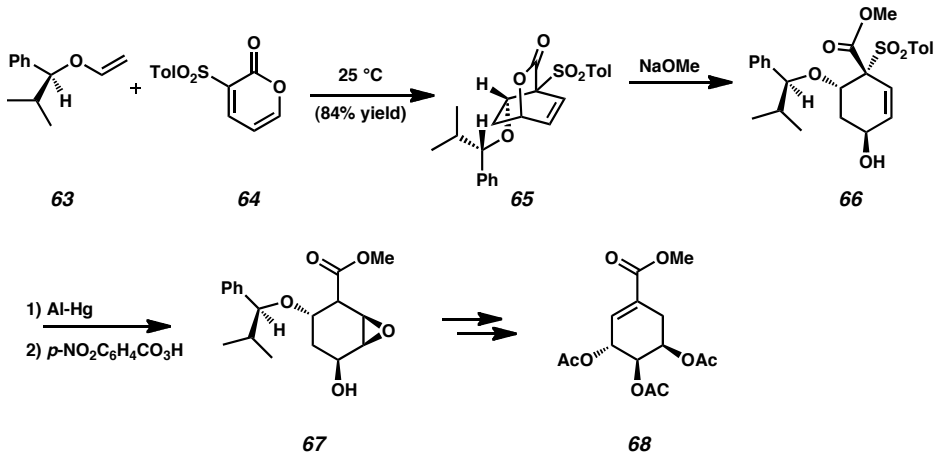

Modification of the α-pyrone skeleton with strong electron withdrawing groups is an effective method for lowering the activation barrier and allowing for isolation of the initial oxabicyclo[2.2.2]octene adduct, as exemplified by the previous examples. However, this modification is limited to inverse-demand PDAs with electron rich dienophiles. Furthermore, the conditions required to remove the activating group are harsh and suffer from low functional group compatibility.

Posner and co-workers have demonstrated that halogenation at the *3*- and/or *5*-positions of α-pyrones improves reactivity in both inverse- *and* normal-demand PDA cycloadditions.[31,9b] In early work toward calcitrol derivatives (**74a** and **74b**, Scheme 1.17), they demonstrated the propensity of brominated pyrones to undergo normal-demand PDAs.[32] Heating of 3-bromo-2-pyrone (**69**) with acrolien (**70**) yielded isolable oxabicyclo[2.2.2]octene **71** in good yield. Following functional group manipulations, the bridgehead bromine of bicycle **72** was reduced selectively and with high efficiency by treatment with tributyltin hydride and AIBN. This highly functionalized bicycle (**73**) was further manipulated to the C-ring of calcitrol derivatives **74a** and **74b**.

Scheme 1.17. Posner's use of bromopyrone for calcitrol synthesis

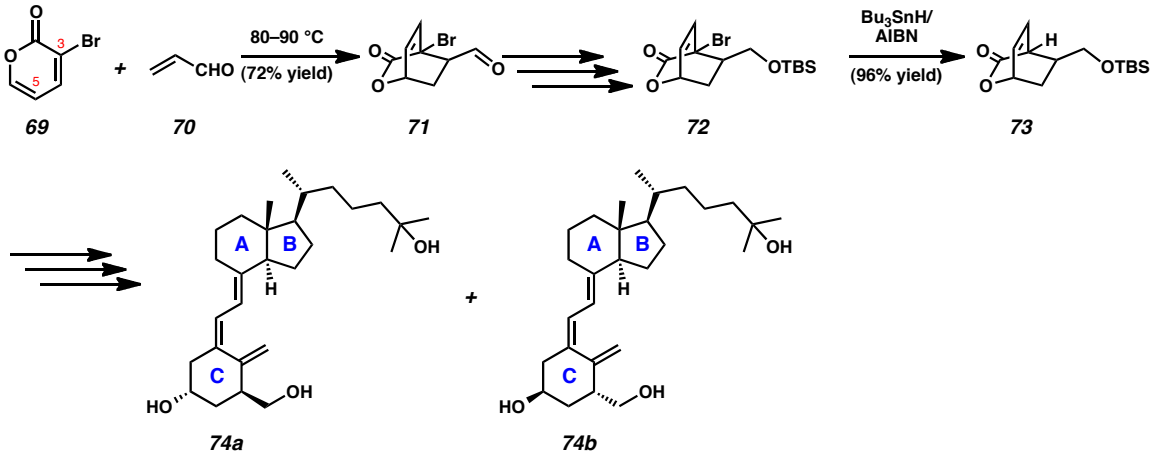

Perhaps there are no natural products better suited for synthesis *via* a PDA reaction than the transtaganolides (**75**) and basiliolides (**76**) (Scheme 1.18). These metabolites, recently isolated from plants belonging to the genus *thapsia*, possess a common oxabicyclo[2.2.2]octene core, which has been proposed to arise from a biosynthetic PDA cycloaddition.[33]

Scheme 1.18. The transtaganolides and basiliolides

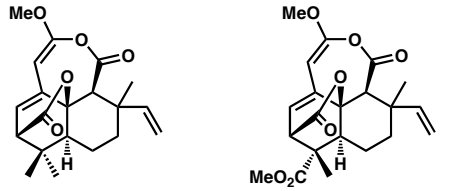

75a Transtaganolide C (C-8 β–Me, α–vinyl)

75b Transtaganolide D (C-8 α–Me, β–vinyl)

76a epi-Basiliolide B (C-8 α–Me, β–vinyl)

76b Basiliolide B (C-8 β–Me, α–vinyl)

Recognizing this structural motif, shortly after their isolation Nelson and Stoltz set out to prepare the transtaganolides (**75**) and basiliolides (**76**) utilizing the PDA reaction.[34] In their initial efforts, pyrone **77** was heated to 120 °C for three days, leading

to undesired CO_2 extrusion and formation of diene **79** (Scheme 1.19). Introduction of a bromine at the *3*-position (**80**), however, allowed for a lower-temperature cycloaddition, and oxabicyclo[2.2.2]octene **81** was isolated (Scheme 1.20). Following this report, several other groups reported transtaganolide model systems based on the PDA reaction.[35, 33c]

Scheme 1.19. Initial PDA reactions

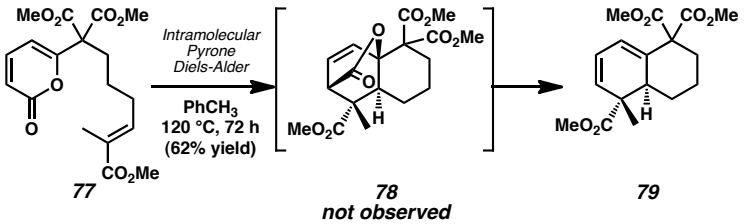

Scheme 1.20. Successful isolation of oxabicyclooctene intermediate

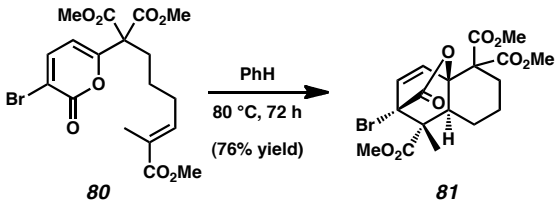

Nelson and Stoltz went on to prepare transtaganolides A–D (**75**, **85**) and basiliolide B (**76**) utilizing the PDA as part of a cascade reaction (Scheme 1.21).[36] Pyrone ester **82**, when exposed to *N,O*-bis(trimethylsilyl)acetamide (BSA), NEt_3, and heat, underwent an Ireland–Claisen rearrangement to produce intermediate **83**. Subsequent heating effected the desired PDA cycloaddition and formation of the oxabicyclo[2.2.2]octene-containing cores (**84**) of the natural product targets. It is notable that allylic strain dictated the reactive conformations of intermediate **83**, selectively

forming the desired stereoisomers. Intermediates **84** were rapidly advanced to the natural product targets (**75**, **76**, and **85**).

*Scheme 1.21. Utilization of the PDA in the total syntheses of the transtaganolides (**75** and **85**) and basiliolides (**76**)*

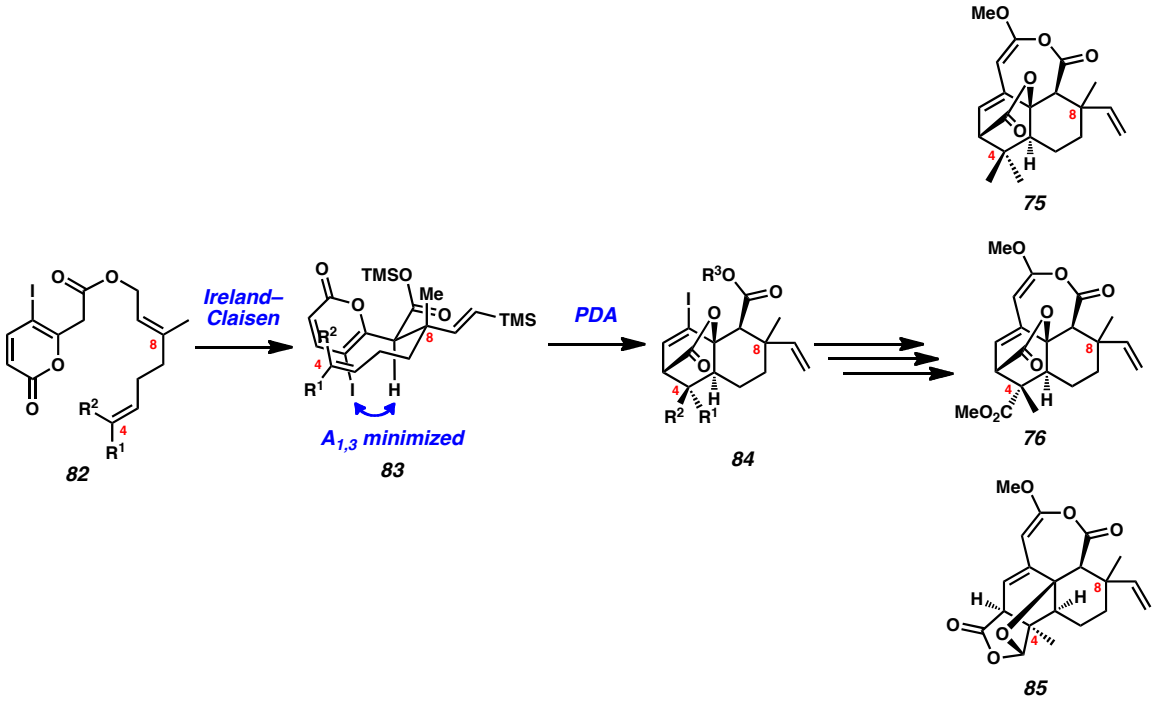

1.5 Conclusions and Outlook

Since its first report by Diels and Alder, the [4+2] cycloaddition, in which the diene component is an α-pyrone, has proven itself as an effective method for the construction of complex molecules. The ability to obtain aromatic, cyclohexadienyl, or cyclohexyl products based on reaction conditions and substitution patterns is a unique feature absent from all other common [4+2] cycloadditions. Furthermore, through the synthesis of natural products, α-pyrone has filled a niche as a dienophile capable of achieving stereoselectivity and reactivity not possible with an "average" acyclic or cyclic diene. Despite these facts, the pyrone Diels–Alder reaction remains underutilized.

It is the authors' opinion that this lack of use in medicinal chemistry and total synthesis is due to the dearth of catalytic asymmetric PDA methods available. While there are examples of diastereoselectivity utilizing chiral auxiliaries and diastereomeric reactions of chiral substrates, the number of catalytic asymmetric PDA reactions is exceedingly small.[10d] Development of chiral reagents that catalyze the [4+2] reaction of α-pyrones with both electron-rich and electron-poor dienophiles will surely increase the usage of the PDA reaction in complex molecule synthesis.

1.6. References and Notes

1) Diels, O.; Alder, K. *Liebigs Ann. Chem.* **1928**, *460*, 98–122.

2) Nicolaou, K. C.; Snyder, S. A.; Montagnon, T.; Vassilikogiannakis, G. *Angew. Chem. Int. Ed.* **2002**, *41*, 1668–1698.

3) a) Hall, D. J.; Van Den Berghe, H. M.; Dove, A. P. *Polym. Int.* **2011**, *60*, 1149–1157. b) Tasdelen, M. A. *Polym Chem-UK.* **2011**, *2*, 2133–2145.

4) a) Kelly, W. L. *Org. Biomol. Chem.* **2008**, *6*, 4483–4493. b) Kim, H. J.; Ruszczycky, M. W.; Liu, H.–w. *Curr. Opin. Chem. Biol.* **2012**, *16*, 124–131.

5) a) Jørgensen, K. A. *Angew. Chem., Int. Ed.* **2000**, *39*, 3558–3588. b) Tietze, L. F.; Kettschau, G. *Stereoselective Heterocyclic Synthesis I* **1997**, *189*, 1–120. c) Waldmann, H. *Synthesis-Stuttgart* **1994**, 535–551. d) Kametani, T.; Hibino, S. *Advances in Heterocyclic Chemistry* **1987**, *42*, 245–333. e) Schmidt, R. R. *Acc. Chem. Res.* **1986**, *19*, 250–259.

6) a) Tadano, K.-i. *Eur. J. Org. Chem.* **2009**, 4381–4394. b) Juhl, M.; Tanner, D. *Chem. Soc. Rev.* **2009**, *38*, 2983–2992. c) Takao, K.–i.; Munakata, R.; Tadano, K–i. *Chem. Rev.* **2005**, *105*, 4779–4807.

7) a) Kobuke, Y. *J. Syn. Org. Chem. Jpn.* **1972**, *30*, 992–1005. b) Corey, E. J. *Angew. Chem. Int. Ed.* **2002**, *41*, 1650–1667. b) Carmona, D.; Lamata, M. P.; Oro, L. A. *Coord. Chem. Rev.* **2000**, *200*, 717–772.

8) Diels, O.; Alder, K. *Liebigs Ann. Chem.* **1931**, *490*, 257–266.

9) a) Shusheri, N. P. *Usp. Khim.* **1974**, *43*, 1771–1793. b) Afarinkia, K.; Vinader, V.; Nelson, T. D.; Posner, G. H. *Tetrahedron* **1992**, *48*, 9111–9171.

10) a) Posner, G. H.; Carry, J. C.; Lee, J. K.; Bull, D. S.; Dai, H. *Tetrahedron Lett.* **1994**, *35*, 1321–1324. b) Okamura, H.; Urabe, F.; Hamada, T.; Iwagawa, T. *Bull. Chem. Soc. Jpn.* **2012**, *85*, 631–633. c) Wu, W.; Min, L.; Zhu, L.; Lee, C.-S. *Adv. Synth. Catal.* **2011**, *353*, 1135–1145. d) Wang, Y.; Li, H.; Wang, Y.-Q.; Liu, Y.; Foxman, B. M.; Deng, L. *J. Am. Chem. Soc.* **2007**, *129*, 6364–6365.

11) Goldstein, E. *J. Mol. Struct. THEOCHEM* **1987**, *151,* 297–305.

12) Boger, D. L.; Brotherton, C. E. *J. Org. Chem.* **1984**, *49*, 4050–4055.

13) Pérez, D.; Guitián, E.; Castedo, L. *J. Org. Chem.* **1992**, *57*, 5911–5917.

14) Dyke, S. F.; Sainsbury, M.; Brown, D. W.; Clipperton, R. D. J. *Tetrahedron* **1970**, *26*, 5969–5980.

15) Ninomiya, I.; Naito, T.; Ishii, H.; Ishida, T.; Ueda, M.; Harada, K. *J. Chem. Soc., Perkin Trans. 1* **1975**, 762–764.

16) Baran, P. S.; Burns, N. Z. *J. Am. Chem. Soc.* **2006**, *128*, 3908–3909.

17) Watanabe, K.; Oikawa, H.; Yagi, K.; Ohashi, S.; Mie, T.; Ichihara, A.; Hornma, M. *J. Biochem.* **2000**, *127*, 467–473.

18) Ose, T.; Watanabe, K.; Mie, T.; Honma, M.; Watanabe, H.; Yao, M.; Oikawa, H.; Tanaka, I. *Nature* **2003**, *422*, 185–189.

19) Guimaraes, C. R. W.; Udier-Blagovic, M.; Jorgensen, W. L. *J. Am. Chem. Soc.* **2005**, *127*, 3577–3588.

20) Serafimov, J. M.; Westfeld, T.; Meier, B. H.; Hilvert, D. *J. Am. Chem. Soc.* **2007,** *129*, 9580–9581.

21) a) Kelly, W. L. *Nature* **2011,** *473*, 35–36. b) Kim, H. J.; Ruszczycky, M. W.; Choi, S.–h.; Liu, Y.–n.; Liu, H. –w. *Nature* **2011,** *473*, 109–112.

22) Corey, E. J.; Watt, D. S. *J. Am. Chem. Soc.* **1973**, *95*, 2303–2311.

23) a) Nicolaou, K. C.; Yang, Z.; Liu, J. J.; Ueno, H.; Nantermet, P. G.; Guy, R. K.; Claiborne, C. F.; Renaud, J.; Couladouros, E. A.; Paulvannan, K.; Sorensen, E. J. *Nature* **1994**, *367*, 630–634. b) Nicolaou, K. C.; Liu, J. J.; Yang, Z.; Ueno, H.; Sorensen, E. J.; Claiborne, C. F.; Guy, R. K.; Hwang, C. K.; Nakada, M.; Nantermet, P. G. *J. Am. Chem. Soc.* **1995**, *117*, 634–644. C) Nicolaou, K. C.; Nantermet, P. G.; Ueno, H.; Guy, R. K.; Couladouros, E. A.; Sorensen, E. J. *J. Am. Chem. Soc.* **1995**, *117*, 624–633. d) Nicolaou, K. C.; Ueno, H.; Liu, J. J.; Nantermet, P. G.; Yang, Z.; Renaud, J.; Paulvannan, K.; Chadha, R. *J. Am. Chem. Soc.* **1995**, *117*, 653–659. e) Nicolaou, K. C.; Yang, Z.; Liu, J. J.; Nantermet, P. G.; Claiborne, C. F.; Renaud, J.; Guy, R. K.; Shibayama, K. *J. Am. Chem. Soc.* **1995**, *117*, 645–652.

24) Narasaka, K.; Shimada, S.; Osoda, K.; Iwasawa, N. *Synthesis* **1991**, 1171–1172.

25) Posner, G. H.; Harrison, W. *J. Chem. Soc., Chem. Commun.* **1985**, 1786–1787.

26) Posner, G. H.; Wettlaufer, D. G. *Tetrahedron Lett.* **1986**, *27*, 667–670.

27) Posner, G. H.; Switzer, C. *J. Org. Chem.* **1987**, *52*, 1642–1644.

28) Posner, G. H.; Wettlaufer, D. G. *J. Am. Chem. Soc.* **1986**, *108*, 7373–7377.

29) Grewe, R.; Kersten, S. *Chem. Ber.* **1967**, *100*, 2546–2553.

30) Snyder, C. D.; Rapoport, H. *J. Am. Chem. Soc.* **1973**, *95*, 7821–7828.

31) Afarinkia, K.; Posner, G. H. *Tetrahedron Lett.* **1992**, *33*, 7839–7842.

32) Posner, G. H.; Dai, H.; Afarinkia, K.; Murthy, N. N.; Guyton, K. Z.; Kensler, T. W. *J. Org. Chem.* **1993**, *58*, 7209–7215.

33) a) Appendino, G.; Prosperini, S.; Valdivia, C.; Ballero, M.; Colombano, G.; Billington, R. A.; Genazzani, A. A.; Sterner, O. *J. Nat. Prod.* **2005**, *68*, 1213–1217. b) Saouf, A.; Guerra, F. M.; Rubal, J. J.; Moreno-Dorado, F. J.; Akssira, M.; Mellouki, F.; Lopez, M.; Pujadas, A. J.; Jorge, Z. D.; Massanet, G. M. *Org. Lett.* **2005**, *7*, 881–884. c) Larsson, R.; Sterner, O.; Johansson, M. *Org. Lett.* **2009**, *11*, 657–660.

34) Nelson, H. M.; Stoltz, B. M. *Org. Lett.* **2007**, *10*, 25–28.

35) a) Kozytska, M. V.; Dudley, G. B. *Tetrahedron Lett*. **2008**, 49, 2899–2901. b) Zhou, X.; Wu, W.; Liu, X.; Lee, C.-S. *Org. Lett.* **2008**, *10*, 5525–5528.

36) a) Nelson, H. M.; Murakami, K.; Virgil, S. C.; Stoltz, B. M. *Angew. Chem. Int. Ed.* **2011**, *50*, 3688–3691. b) Nelson, H. M.; Gordon, J. R.; Virgil, S. C.; Stoltz, B. M., *manuscript in preparation.*

CHAPTER 2

Model Studies Aimed at The Total Syntheses of The Transtaganolide Natural Products

2.1 Introduction

2.1.1 Biological Activity

Thapsia garganica L., an herb native to Mediterranean countries, has a long history as a medicinal plant, with therapeutic attributes first reported by Hippocrates in 400 BC.[1] Its roots have traditionally been used for the treatment of pulmonary diseases, catarrh, and rheumatoid arthritis.[1] Thapsigargin (TG)(**86**, Scheme 2.1), the principal chemical component of *T. garganica* L., is a powerful histamine liberator and a non-TPA type tumor promoter.[2,3] However, TG (**86**) is best known as a selective and potent microsomal SERCA-ATPase inhibitor, and is widely used as a chemical tool for cell physiological studies.[4] Its utility as a biological tool is evident from its frequent appearance in the literature: since 1985, when TG (**86**) was first shown to selectively inhibit SERCA-ATPase, published reports involving TG (**86**) have averaged more than one a day.[5]

Because of its high cost[6] and variable concentration in *T. garganica* L., several

groups have attempted to isolate TG (**86**) analogues from *T. garganica* L., as well as from other members of the *Thapsia* genus. Recent efforts have led to the isolation of several new compounds, the transtaganolides and basiliolides (**75**, **76**, **85** and **87**–**91**, Scheme 2.2).[7]

Scheme 2.1. Thapsigargin and thapsigargin bound SERCA-ATPase

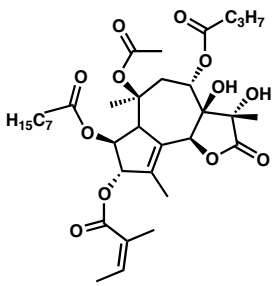

86

Thapsigargin (TG)

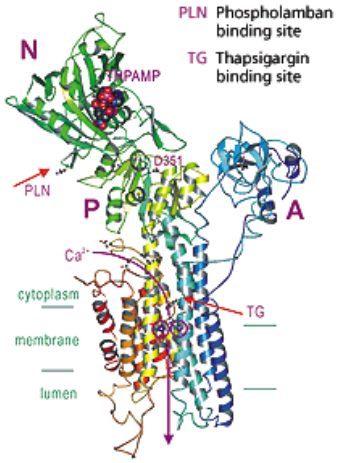

Scheme 2.2. The meroterpenoids of Thapsia transtagana

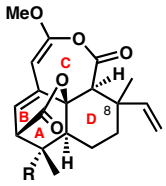

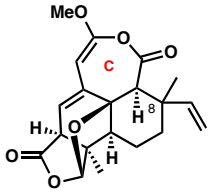

	R	
75a	Me	C-8 α–methyl, β–vinyl (Transtaganolide C)
75b	Me	C-8 β–methyl, α–vinyl (Transtaganolide D)
76a	CO_2Me	C-8 α–methyl, β–vinyl (Basiliolide B)
87	CH_2OAc	C-8 α–methyl, β–vinyl (Basiliolide C)

85a C-8 β–methyl, α–vinyl (Transtaganolide A)
85b C-8 α–methyl, β–vinyl (Transtaganolide B)

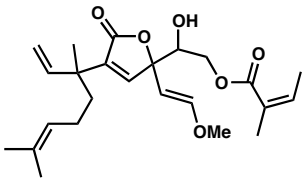

88

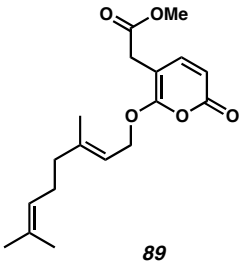

89

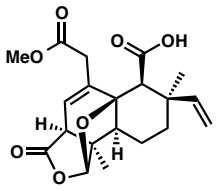

90

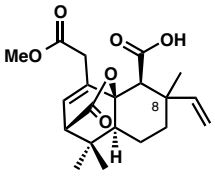

91a C-8 α–methyl, β–vinyl
91b C-8 β–methyl, α–vinyl

Interestingly, despite obvious structural differences between TG and the transtaganolides (**86** *vs.* **75** and **76**), compounds **75** and **76** have *also* been shown to induce an increase in cytosolic [Ca^{2+}]. This biological activity is the primary action of SERCA-ATPase inhibitors such as TG (**86**).[8] While it was initially suggested that compounds **75** and **76** were also SERCA-ATPase inhibitors, there is evidence that these compounds may act through a different mechanism.[7b,8] In particular, TG (**86**) is known to irreversibly inhibit SERCA-ATPase, causing an increase in cytosolic [Ca^{2+}] which leads to endoplasmic reticulum (ER) stress and eventual apoptosis.[9] However, it has been demonstrated that unlike TG, the cytosolic [Ca^{2+}] increase induced by compounds **75** and **76** is reversible.[8] Furthermore, *in vivo* studies show that the cytosolic [Ca^{2+}] concentration increase is limited and does not cause cell lysis.[8]

In addition to its potential application as a [Ca^{2+}] homeostasis probe, several structural comparisons have been made between the transtaganolides and the privileged anti-parasitic agent artemisinin.[10] While speculative at best, small molecule libraries inspired by the core ring system of the transtaganolides have been shown to be effective against African Sleeping Sickness, with potencies rivaling that of artemisinin.[11]

Beyond their biological activity, we were also drawn to the densely functionalized, structurally novel frameworks present in these natural products. In particular, the metabolites isolated from *T. garganica* L. and *T. transtagana* (**75** and **76**) contain an interesting tetracyclic core featuring a bicyclic lactone (Scheme 2.2, **75** and **76**, AB rings). Furthermore, the 7-methoxy-4,5-dihydro-3*H*-oxepin-2-one ring (C-ring) common to all of the transtaganolides is an unprecedented structural motif.

2.1.2 Biosynthetic Proposals

Since isolation, the transtaganolides (Scheme 2.2) have been the subject of multiple biosynthetic proposals. In 2005, Appendino and co-workers proposed a biosynthesis based on a polyolefin rearrangement of farnesyl pyrophosphate (**92**) with several subsequent CO_2 abstractions (Scheme 2.3).[7b] While polyolefin/cation cascades are well precedented in terpenoid biosynthesis,[12] carbon dioxide abstraction is not. Furthermore, with no robust method for olefin carboxylation, and no clear path of inducing stereochemical selectivity, we chose not to explore this biosynthetic hypothesis in a laboratory setting.

Scheme 2.3. Appendino's biosynthetic hypothesis

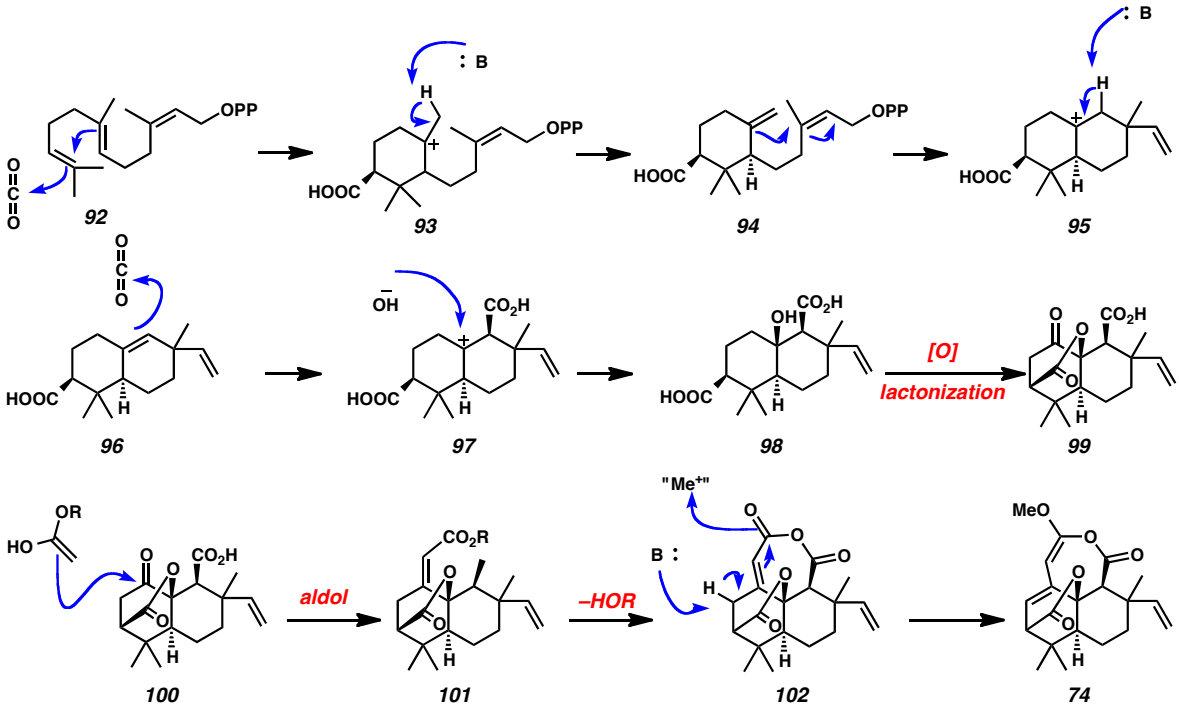

In 2007 Rubal and co-workers proposed a biosynthesis in which co-isolated coumarin **103** serves as the biosynthetic precursor of the transtaganolides.[13] Under this scenario, myriad biosynthetic pathways are possible. As shown in Scheme 2.4, a sequence of intramolecular pyrone diels–alder (IMPDA)/ claisen rearrangement (CR) /electrocyclic ring opening (ERO) reactions are responsible for the formation of the natural products (Scheme 2.4). At the time of this proposal, no particular order of transformations was proposed.

Scheme 2.4. Rubal's biosynthetic proposal

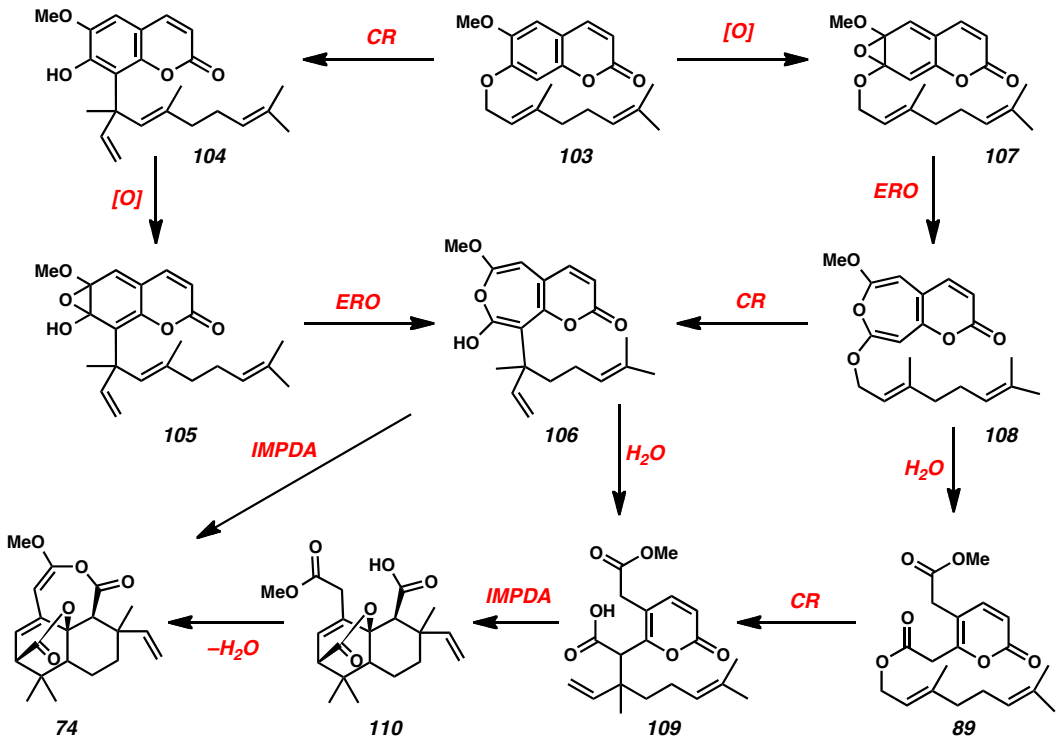

In 2008, Larsson and co-workers proposed a more specific version of Rubal's hypothesis (Scheme 2.5).[14] They posited that co-isolated, prenylated pyrone **89** is the direct biosynthetic precursor of transtaganolides C (**74a**) and D (**74b**). Under this scenario, they state that an unprecedented enzymatic enolate-Claisen rearrangement leads to the formation of intermediate **109**, which subsequently undergoes a spontaneous pyrone Diels–Alder (PDA) cycloaddition to yield the cores of the natural products (**91**, Scheme 2.5). It is noteworthy that the C8 diastereomers obtained by this biosynthetic pathway would likely share the same absolute stereochemistry at C8 and be of opposite enantiomeric series at all other stereocenters (**91a** and **91b**, Scheme 2.5).

Scheme 2.5. Larsson's biosynthetic proposal

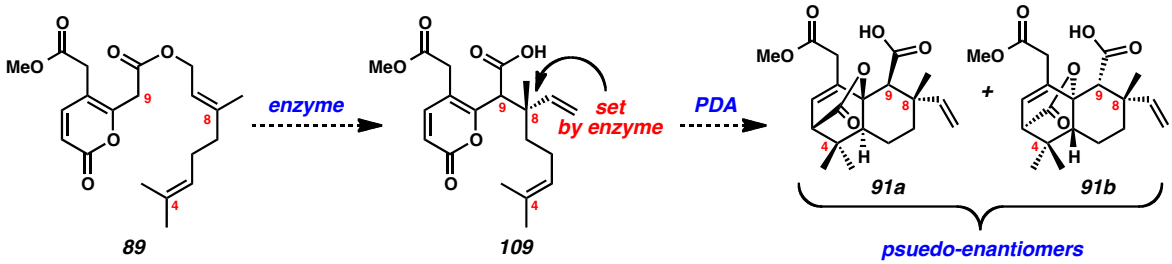

2.2 Synthetic Strategy

Inspired by these biosynthetic proposals, we envisioned that the cores of the transtaganolide natural products (**111**) could be prepared in the laboratory *via* an Ireland–Claisen rearrangement (ICR)/intramolecular pyrone Diels–Alder (IMPDA) sequence (Scheme 2.6). We proposed that the oxepinone ring (ring C) would need to be formed subsequent to the IMPDA, as formation of the oxepinone prior to the cycloaddition could potentially lead to the incorrect relative stereochemistry (**116** to **117**, Scheme 2.7). Furthermore, we envisioned that the reactivity of the C-ring could interfere with core-forming chemical transformations. Intermediate **111** would arise from pyrone **112** via an IMPDA. The IMPDA substrate **112** would be prepared from the ICR of pyrone ester **113**. The ICR substrate (**113**) could be synthesized by coupling of geraniol derivatives (**114**) to pyrone acid **115**.

Scheme 2.6. Retrosynthetic analysis

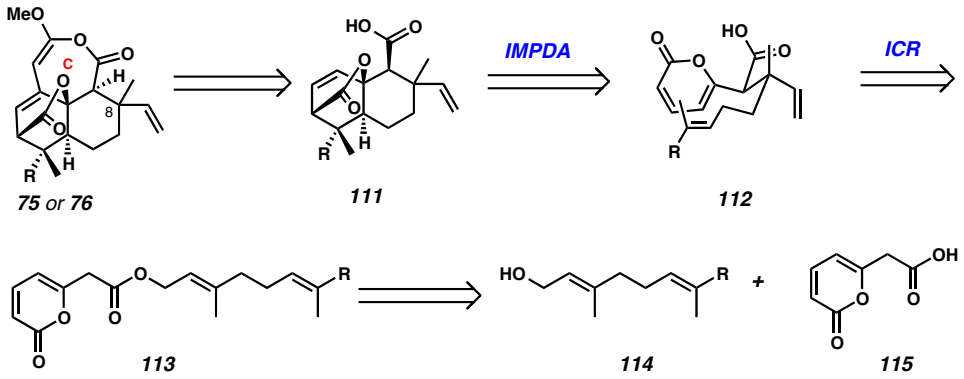

Scheme 2.7. Reasoning for late-stage oxepinone formation

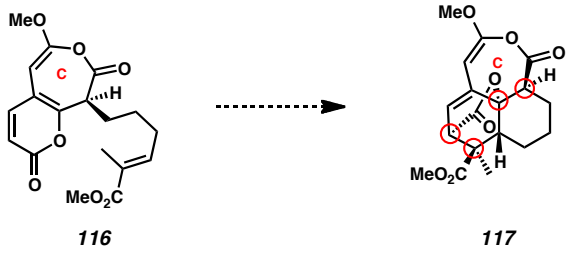

2.3 Model Studies

At the outset of the project, we sought to validate our retrosynthetic analysis *via* model studies. Of particular importance was the key IMPDA reaction, as this transformation constructs four of the six stereocenters in the natural product and two of its four rings in a single step. Furthermore, the well-documented propensity for thermal pyrone Diels–Alder cycloaddition products to undergo cycloreversion with extrusion of CO_2 threatened our approach.[15] Additionally confounding our synthetic proposal was the lack of precedence for ICRs with a pendant electron-withdrawing group, such as molecule **113**. Similar systems, such as those employed in the Carroll rearrangement, are also known to undergo thermal decarboxylation.[16]

2.3.1 Intramolecular Pyrone Diels–Alder Model System

We envisioned that a compound such as **117** might serve as an adequate model to probe the capacity of geraniol derivative **112** to undergo IMPDA under thermal or Lewis acidic conditions. We proposed that preparation of the IMPDA model system **112** could be achieved *via* alkylation of a malonate (**120**) with a pyrone electrophile such as **118** followed by an electrophilic dienophile fragment such as **119** (Scheme 2.8).

Scheme 2.8. Retrosynthetic analysis of IMPDA model system

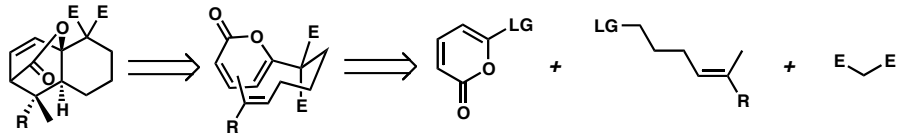

116 ***117*** ***118*** ***119*** ***120***

The preparation of **119** began with the partial reduction of γ-butyrolactone (**121**) to the corresponding lactol, which was immediately treated with stabilized ylide **122**[17] to afford hydroxyenoate **123** (Scheme 2.9). Alcohol **123** was converted to iodide **119a** by treatment with iodine, imidazole, and PPh_3.

Scheme 2.9. Synthesis of dienophile fragment

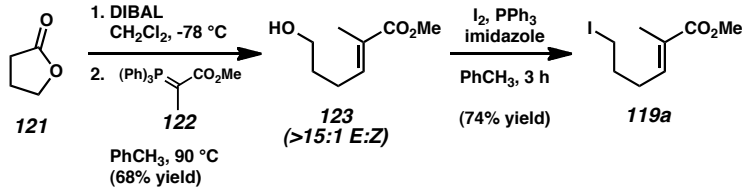

121 ***122*** ***123*** ***(>15:1 E:Z)*** ***119a***

In parallel, pyrone **124** was assembled by substitution reaction of chloride **118a** with the anion of dimethyl malonate (**120a**, Scheme 2.10). Coupling of pyrone **124** to alkyl iodide **119a** furnished the IMPDA substrate **117a** in 83% yield.

Unfortunately, upon exposure of pyrone **117a** to thermal or Lewis acid catalyzed

reaction conditions, we were unable to obtain the desired IMPDA product **116a**.[18] In accord with literature precedent,[19] we found that higher temperatures were required to obtain noticeable production of a Diels-Alder adduct. Furthermore, at these temperatures (≥120 °C) the decarboxylated product (**125**) was formed as the predominant product in 62% yield.

Scheme 2.10. Initial IMPDA attempts

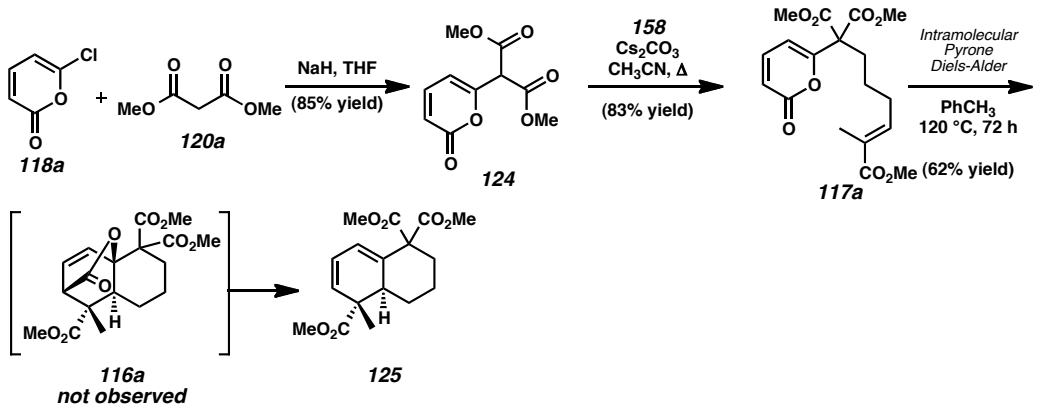

Given the lack of desired reactivity in our model compound **117a**, we turned our attention toward brominated derivative **117b** (Scheme 2.11). Posner and others have demonstrated that halogen substitution at the *3*- and/or *5*-position of pyrone rings activates them toward electron-poor and electron-rich dienophiles, allowing for lower-temperature non-decarboxylative cycloadditions.[20] Although direct mono-bromination of **117a** proved challenging due to competing bromination of the enoate moiety, we were delighted to find that treatment of pyrone **124** with bromine yielded bromopyrone **126** and dibrominated pyrone **127** in 48% and 32% yield, respectively (Scheme 2.11). Additionally, dibromide **127** could be smoothly monodehalogenated by exposure to Zn dust and acetic acid, providing bromopyrone **126** in an overall 74% yield from pyrone **124**. The alkylative coupling of **126** with **119a** was achieved using a carbonate base to

provide IMPDA substrate **117b** in 58% yield. Importantly, upon heating bromide **117b** in a sealed tube at 90 °C, smooth cycloaddition occurred to produce tricycle **116b** as a single diastereomer in 76% yield.[21] The structure and relative stereochemistry of endo Diels–Alder adduct **116b** was unambiguously established by single crystal X-ray diffraction (Scheme 2.12).[22] Treatment of the IMPDA product **116b** with tributyltin hydride and AIBN allowed for removal of the bridgehead bromine to provide **116a** in 50% yield.[20b]

Scheme 2.11. Implementation of the Posner modification

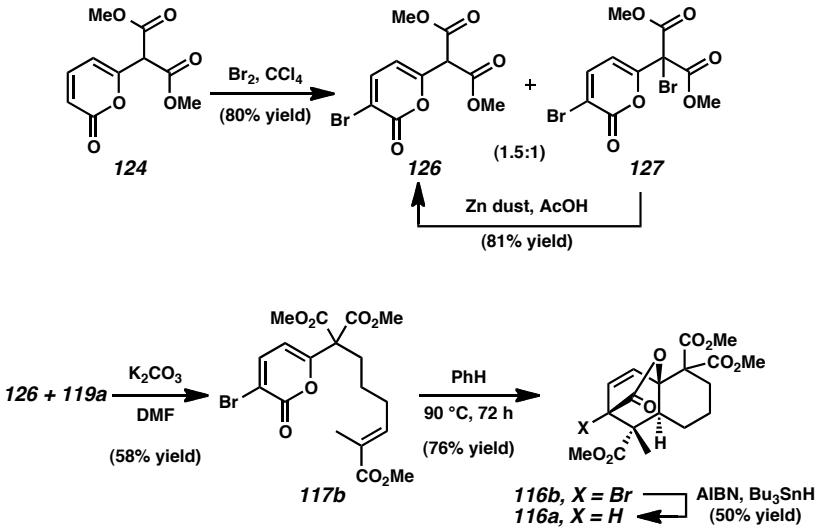

*Scheme 2.12. X-ray crystal structure of **116b***

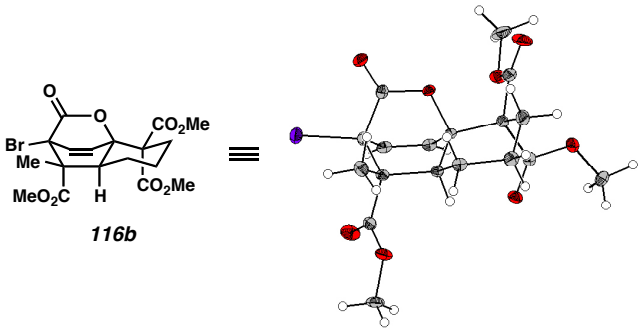

Following our initial report, several other groups reported IMPDA approaches to the transtaganolide/basiliolide natural products. Dudley and co-workers demonstrated that *5*-iodopyrone **128** undergoes facile IMPDA to yield tricycle **129** when heated to 100 °C for 3 days (Scheme 2.13).[23] Notably, his *5*-iodo substitution of the pyrone allows for possible elaboration to the C-ring of basiliolide B.

Scheme 2.13. Dudley's approach to the core of basiliolide B

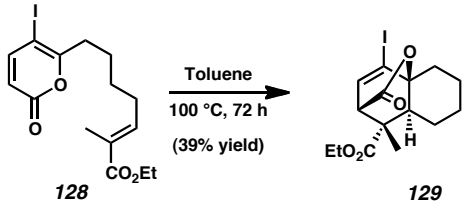

128 *129*

Lee and co-workers reported an elegant approach to the core that relied on the use of base catalysis.[24] Oxidation of dihydropyrone **130** with Jones' reagent formed an intermediate *5*-hydroxypyrone that under basic conditions underwent facile normal-demand IMPDA to yield ketone **131**. Notably, Lee's system is also appropriately substituted for elaboration of the C-ring and advancement to the natural product targets.

Scheme 2.14. Lee's approach to the core of basiliolide B

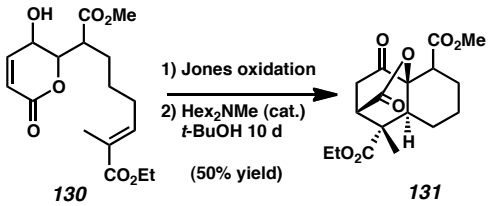

130 *131*

2.4 Conclusion

In conclusion, we have proposed a highly modular route to the transtaganolides. This route is strongly supported by extensive model study work. An intramolecular pyrone

Diels–Alder (IMPDA) model system was constructed and used to forge the tricyclic core of the natural product targets.

2.5 Experimental Section

2.5.1 Comments on IMPDA

As stated in the text, heating of **117a** to reflux in benzene results in low conversion to **116a**. Shown below is a ^{1}H NMR spectra taken after 86 hours. For comparison, the spectra of pure **116a** (prepared by radical dehalogenation of **116b**), and the spectra of **117a** are shown.

Figure 2.1. IMPDA reaction

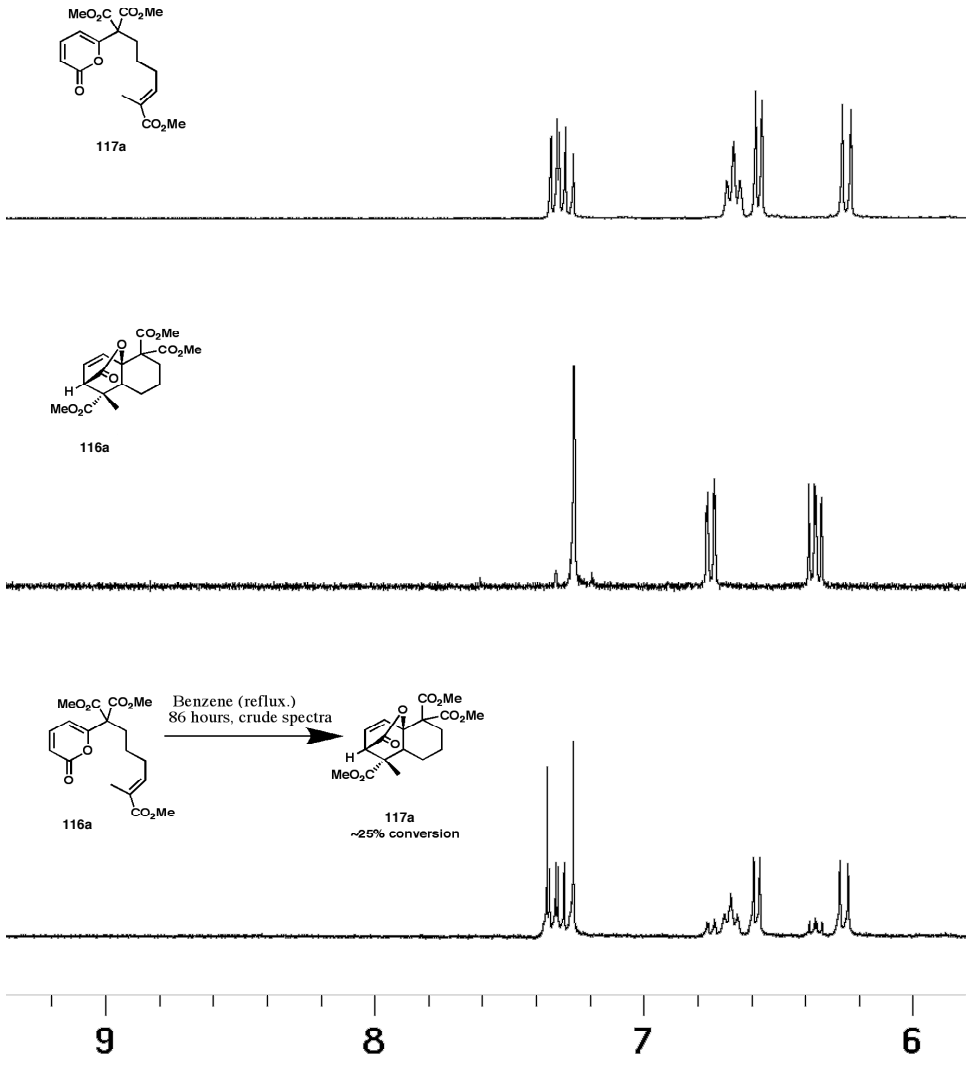

2.5.2 Materials and Methods

Unless otherwise stated, reactions were performed in flame-dried glassware under an argon or nitrogen atmosphere using dry deoxygenated solvents. Solvents were dried by passage through an activated alumina column under argon. 6-Chloro-2*H*-pyran-2-one was purchased from Sigma-Aldrich Chemical Company and used as received. 1-Methoxycarbonylethylidenetriphenylphosphorane was prepared using known methods[1]. Thin-layer chromatography (TLC), both preparatory and analytical, were performed using E. Merck silica gel 60 F254 pre-coated plates (0.25 mm) and visualized by UV fluorescence quenching, p-anisaldehyde, I_2, or $KMnO_4$ staining. ICN Silica gel (particle size 0.032–0.063 mm) was used for flash chromatography. ^{1}H NMR, and ^{13}C NMR spectra were recorded on a Varian Mercury 300 (at 300 MHz) or on a Varian Unity Inova 500 (at 500 MHz). ^{1}H NMR spectra are reported relative to $CDCl_3$ (7.26 ppm). Data for ^{1}H NMR spectra are reported as follows: chemical shift, multiplicity, coupling constant (Hz), integration. Multiplicities are reported as follows: s = singlet, d = doublet, t = triplet, q = quartet, sept. = septet, m= multiplet, comp. m = complex multiplet, app. = apparent, bs = broad singlet. ^{13}C NMR were reported relative to $CDCl_3$ (77.0 ppm). FTIR spectra were recorded on a Perkin Elmer SpectrumBX spectrometer and are reported in frequency of absorption (cm^{-1}). High resolution mass spectra were obtained from the Caltech Mass Spectral Facility. Crystallographic data were obtained from the Caltech X-ray Diffraction Facility.

2.5.3 Experimental Procedures

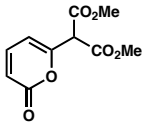

Dimethyl 2-(2-oxo-2*H*-pyran-6-yl)propanedioate (124). To a suspension of Sodium hydride (60% in mineral oil) (399 mg, 16.6 mmol, 1.9 equiv) in tetrahydrofuran (75 ml) at 0 °C was added dimethyl malonate (2 ml, 17.5 mmol, 2 equiv) over 5 minutes. The mixture was warmed to ambient temperature and stirred for 20 minutes. The solution was then cooled to 0 °C, and a solution of 6-chloro-2*H*-pyran-2-one (1.1 g, 8.8 mmol, 1 equiv) in tetrahydrofuran (5 ml) was added dropwise over 5 minutes. The reaction was allowed to come to ambient temperature, then stirred for an additional hour. The reaction mixture was acidified to pH 5 by the addition of 3N HCl(aq). Water was then added (50 mL), and the reaction mixture was extracted with CH_2Cl_2 (3 x 200 ml). The combined organic extracts were dried over Na_2SO_4(anhydrous) and concentrated by rotary evaporation. The resulting residue was chromatographed (50%⇒100% diethyl ether in petroleum ether on SiO_2) to yield 1.7 g of **124** as a yellow oil (84.5%). ^{1}H NMR (300 MHz, $CDCl_3$) δ 7.31 (dd, J = 9.5, 6.8 Hz, 1H), 6.34 (d, J = 6.6 Hz, 1H), 6.26 (d, J = 9.3 Hz, 1H), 4.52 (s, 1H), 3.78 (s, 6H); ^{13}C NMR (75 MHz, $CDCl_3$) δ 165.5, 161.4, 155.6, 143.3, 116.0, 105.9, 56.2, 53.8; FTIR (Neat Film NaCl) 1740, 1640, 1559, 1437, 1277, 1241, 1201, 1155, 1099, 1027, 808 cm^{-1} ; HRMS (EI) m/z calc'd for $C_{10}H_{10}O_6$ [M^+]: 226.0477, found 226.0479.

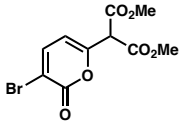

Dimethyl 2-(3-bromo-2-oxo-2*H*-pyran-6-yl)propanedioate (126). To a solution of **124** (283.0 mg, 1.2 mmol, 1.0 equiv) in CCl_4 (10 mL) was added bromine (312 mg, 100 μL , 1.9 mmol, 1.6 equiv). The reaction mixture was stirred at ambient temperatures for 72 hours then quenched by the addition of 20 mL of 20% Na_2SO_4(aq). The solution was extracted with CH_2Cl_2 (3 x 40 mL) and the combined organic layers were collected and dried over Na_2SO_4(anhydrous). After concentration by rotary evaporation, the crude residue was chromatographed (50% diethyl ether in petroleum ether on SiO_2) to yield **126** as a white powder (181 mg, 48%) and **127** as a yellow powder (152 mg, 32%).

To a flame-dried flask charged with **127** (28.0 mg, 0.07 mmol, 1 equiv), Zn dust (10 mg, 0.15, 2 equiv), and tetrahydrofuran (0.50 mL) was added glacial acetic acid (0.25 mL). The reaction was stirred at ambient temperatures for 30 minutes, filtered through Celite, and then extracted with CH_2Cl_2 (2 x 1 mL). The combined organic layers were washed with brine. After drying over Na_2SO_4(anhydrous) and concentration by rotary evaporation, the crude residue was chromatographed (50% diethyl ether in petroleum ether on SiO_2) to yield **126** (18 mg, 81%) as a white powder.

126: ^{1}H NMR (300 MHz, $CDCl_3$) δ 7.68 (d, J = 7.2, 1H), 6.30 (d, J = 7.2 Hz, 1H), 4.55 (s, 1H), 3.79 (s, 6H); ^{13}C NMR (75 MHz, $CDCl_3$) δ 164.1, 157.9, 154.9, 144.4, 112.1, 106.6, 55.8, 53.9 ; FTIR (Neat Film NaCl) 1743, 1642, 1542, 1436, 1313, 1240, 1201,

1153, 1100, 1027, 978, 750 cm^{-1} ; HRMS (EI) m/z calc'd for $C_{10}H_9BrO_6$ $[M^+]$:300 .9582, found 303.9587.

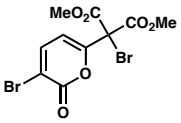

Dimethyl 2-bromo-2-(3-bromo-2-oxo-2H-pyran-6-yl)propanedioate (127). See preparation of **126** for experimental details. ^1H NMR (300 MHz, $CDCl_3$) δ 7.69 (d, J = 7.2, 1H), 6.70 (d, J = 7.2 Hz, 1H), 3.90 (s, 6H); ^{13}C NMR (75 MHz, $CDCl_3$) δ 164.1, 156.8, 155.4, 143.8, 113.4, 106.4, 57.1, 55.2; FTIR (Neat Film NaCl) 1748, 1634, 1541, 1436, 1336, 1265, 1228, 1102, 1052, 1020, 979, 772, 748 cm^{-1} ; HRMS (EI) m/z calc'd for $C_{10}H_9BrO_6$ $[M^+]$: 383.8667, found 383.8657.

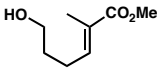

(*E*)-Methyl 6-hydroxy-2-methylhex-2-enoate (123). To a flame-dried flask charged with CH_2Cl_2 (60 mL) was added γ-butyrolactone (**121**) (1.1 g, 13.0 mmol, 1 equiv). The reaction was cooled to -78° C, and a solution of DIBAL-H (2.0 g, 14.3 mmol, 1.1 equiv) in dry hexanes (11.5 ml) was added over 15 minutes. The reaction was stirred for two hours then diluted with ethyl acetate (50 mL), and a saturated solution of sodium/potassium tartrate (50 mL) was then added. After separation, the aqueous layer was further extracted with ethyl acetate (2 x 50 mL). The combined organics were combined, dried over $MgSO_4$(anhydrous), and concentrated by rotary evaporation. The

crude oil was dissolved in benzene (50 mL) and added to a flask charged with stabilized ylide **122** (4.3 g, 12.3 mmol, 1.2 equiv) and the reaction was heated to reflux and stirred for 12 hours. The reaction was cooled to ambient temperatures then diluted with diethyl ether (50 ml) and saturated brine solution (50 mL). After separation the aqueous layers were further extracted with ether, and the combined organics were dried over $MgSO_4$(anhydrous) and concentrated by rotary evaporation. The crude oil was chromatographed (0⇒100% ether in petroleum ether on SiO_2) to yield 1.4 g (68%) of **123** as a clear colorless oil. ^{1}H NMR (300 MHz, $CDCl_3$) δ 6.70 (t, J = 7.5, 1H), 3.66 (s, 3H), 3.58 (t, J = 6.3 Hz, 3H), 2.64 (br s, 1H), 2.20 (m, 2H), 1.78(s, 3H), 1.64 (m, 2H); ^{13}C NMR (75 MHz, $CDCl_3$) δ 169.0, 142.2, 128.1, 62.1, 51.9, 31.6, 25.2, 12.5; FTIR (Neat Film NaCl) 3404, 1714, 1649, 1438, 1268.81196, 1129, 1059, 747 cm^{-1} ; HRMS (EI) m/z calc'd for $C_8H_{14}O_3$ [M^+]: 158.0943, found 158.0943.

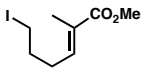

(*E*)-Methyl 6-iodo-2-methylhex-2-enoate (119a). To a flame-dried flask was added (*E*)-Methyl 6-hydroxy-2-methylhex-2-enoate (**123**) (700 mg, 4.4 mmol, 1 equiv), iodine chips (2.0 g, 7.9 mmol, 1.8 equiv), imidazole (897 mg, 13.2 mmol, 3 equiv), triphenylphosphine (1.9 g, 7.0 mmol, 1.6 equiv), and toluene (45 mL). The reaction was stirred at room temperature for 2 hours then diluted with saturated $NaHCO_3$ (aq) (20 mL) and saturated $Na_2S_2O_3$(aq)(5 mL). It was then extracted with Ethyl Acetate (3 x 20 mL). The combined organic extracts were washed with brine, dried over anhydrous $MgSO_4$, and concentrated by rotary evaporation. The crude oil was chromatographed (

hexanes in ethyl acetate 10:1 ⇒ 3:1 on SiO_2) to give iodide **119a** as a yellow oil (873 mg, 74%).^{1}H NMR (300 MHz, $CDCl_3$) δ 6.65 (t, J = 7.5, 1H), 3.70 (s, 3H), 3.16 (t, J = 6.7 Hz, 2H), 2.26 (m, 2H), 1.92 (m, 2H), 1.84 (s, 3H); ^{13}C NMR (75 MHz, $CDCl_3$) δ 168.5, 140.1, 129.2, 52.0, 32.4, 29.5, 12.8, 6.2; FTIR (Neat Film NaCl) 1715, 1651, 1435, 1282, 1260, 1219, 1167, 1107 cm^{-1} ; HRMS (EI) m/z calc'd for $C_8H_{13}O_2I$ [M^+]: 267.9961, found 267.9967.

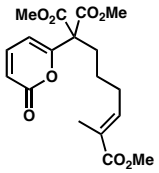

(*E*)-Trimethyl 1-(2-oxo-2*H*-pyran-6-yl)hex-4-ene-1,1,5-tricarboxylate (117a). To an ice cold mixture of acetonitrile (1 mL) and Cs_2CO_3 (132.0 mg, 0.4 mmol, 1.1 equiv) was added a solution of **124** (100.0 mg, 0.442 mmol, 1.2 equiv) in acetonitrile (0.5 mL)**.** The reaction was brought to ambient temperature and stirred for 10 minutes, then cooled to 0° C. A solution of **119a** (99.0 mg, .4 mmol, 1 equiv) in acetonitrile (0.5 mL) was then added over 5 minutes. The reaction was allowed to warm to ambient temperature, then brought to reflux and stirred for 15 hours. The reaction was then cooled to room temperature and diluted with saturated NH_4Cl(aq) (2 mL) and extracted with ethyl acetate (3 x 2 mL). The combined organics were dried over Na_2SO_4 (anhydrous) and concentrated by rotary evaporation. The crude oil was chromatographed (ethyl acetate in hexanes gradient 0⇒100% on SiO_2) to yield 111 mg (83%) of yellow oil. ^{1}H NMR (300 MHz, $CDCl_3$) δ 7.32 (dd, J = 6.3, 6.9 Hz , 1H), 6.66 (t, J=7.4 Hz, 1H), 6.58 (d, J = 6.6 Hz, 1H), 6.25 (d, J = 6.3 Hz, 1H) , 3.78 (s, 6H), 3.72 (s, 3H), 2.22 (m, 4H),

1.80 (s, 3H), 1.43 (m, 3H); ^{13}C NMR (75 MHz, $CDCl_3$) δ 168.7, 168.0, 161.3, 159.3, 143.3, 141.2, 128.6, 115.5, 105.5, 62.6, 53.6, 52.0, 34.0, 28.7, 24.1, 12.7; FTIR (Neat Film NaCl) 1741, 1636, 1556, 1436, 1240, 1093, 807 cm^{-1} ; HRMS (EI) m/z calc'd for $C_8H_{13}O_2I$ [M^+]: 366.1314, found 366.1330.

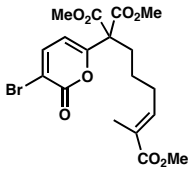

(*E*)-Trimethyl 1-(3-bromo-2-oxo-2*H*-pyran-6-yl)hex-4-ene-1,1,5-tricarboxylate (117b). To a mixture of dimethylformamide (3 mL) and K_2CO_3 (64.7 mg, 0.5 mmol, 1.1 equiv) at 0° C was added a solution of **126** (130.2 mg, 0.4 mmol, 1.0 equiv) in dimethylformamide (0.5 mL) and **119a** (342.10 mg, 1.28 mmol, 3.0 equiv) in dimethylformamide (0.5 mL)**.** The reaction mix was brought to room temperature and stirred for 10 minutes, then heated to 50° C for 5 hours. The reaction was then cooled to room temperature and diluted with saturated aqueous NH_4Cl (20 mL) and extracted with ethyl acetate (3 x 10 mL). The combined organic extracts were washed with brine (6 x 10 mL), dried over Na_2SO_4(anhydrous) and concentrated by rotary evaporation. The crude oil was chromatographed (diethyl ether in petroleum ether gradient 50⇒100% on SiO_2) to yield 110 mg (58%) of **117b** as a yellow powder. Furthermore, 170 mg of **119a** was recovered as a clear oil. ^{1}H NMR (300 MHz, $CDCl_3$) δ 7.66 (d, J = 6.6 Hz, 1H), 6.66 (t, J=7.4 Hz, 1H), 6.54 (d, J = 6.6 Hz, 1H), 3.79 (s, 6H), 3.72 (s, 3H), 2.22 (m, 4H), 1.81 (s, 3H), 1.4 (m, 2H); ^{13}C NMR (75 MHz, $CDCl_3$) δ 168.5, 167.6, 158.7, 157.6, 144.4, 141.0, 128.7, 111.2, 106.0, 62.3, 53.8, 52.0, 33.9, 28.6, 24.0, 12.7;

FTIR (Neat Film NaCl) 1742, 1714, 1634, 1542, 1436, 1242, 1073, 974, 749 cm^{-1} ; HRMS (EI) m/z calc'd for $C_{18}H_{21}O_8{}^{81}Br$ [M^+H]: 447.0477, found 447.0461.

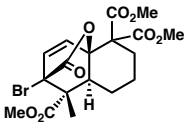

Tricycle 116b

A solution of **117b** (63.0 mg, 0.15 mmol, 1.0 equiv) in benzene (10 mL), was sealed in a scintillation vial and heated to reflux for 72 hours. The reaction mixture was cooled to room temperature, the solvent removed by rotary evaporation, and the crude residue chromatographed (chloroform/diethyl ether/n-heptane, 1:1:1 on SiO_2) to yield **117b** as 48 mg (76%) of white powder. ^1H NMR (500 MHz), $CDCl_3$ δ 6.61 (d, J = 8.1 Hz, 1H), 6.59 (d, J=8.1 Hz, 1H), 3.77 (s, 1H) , 3.74 (s, 3H), 3.73 (s, 3H), 2.85 (dd, J= 15.0 Hz, 5.5 Hz, 1H), 2.23 (m, 2H), 1.8 (m, 2H), 1.4 (m, 1H), 1.38 (s, 3H), 1.2 (m, 1H); ^{13}C NMR (75 MHz, $CDCl_3$) δ 172.6, 169.3, 168.3, 166.7, 134.8, 133.3, 82.9, 66.0, 59.5, 53.1, 53.0, 52.8, 52.6, 46.1, 27.9, 24.8, 20.3, 19.1; FTIR (Neat Film NaCl) 1773, 1734, 1435, 1304, 1255, 1208, 1173, 1158, 1124, 1022, 945 cm^{-1} ; HRMS (EI) m/z calc'd for $C_{18}H_{21}O_8Br$ [M^+]: 444.0420, found 444.0411. Crystals were grown from dichloromethane/Hexanes. MP: 156–170° C (at these temperatures decarboxylation is thought to occur, as the crystal and the resulting liquid were vigorously bubbling, thus it is unclear whether thermal decomposition precluded state change).

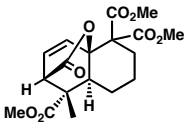

Tricycle 116a

116b (18 mg, 0.04 mmol, 1.0 equiv), Bu_3SnH (18 mg, 0.06 mmol, 1.5 equiv), AIBN (1.5 mg, 0.009 mmol, 0.2 equiv) and benzene (0.40 mL) were combined in a 1 dm vial, and stirred at reflux for 3 hours. The reaction was cooled to ambient temperature, concentrated by rotary evaporation, diluted with wet diethyl ether (1 mL), and 1,8-diazabicyclo[5.4.0]undec-7-ene (DBU) (10.5 mg, .07 mmol, 1.7 equiv) was added. The resulting white suspension was stirred for 15 minutes, then filtered through Celite. The solvent was removed under vacuum, and the crude residue was purified by preparatory thin-layer chromatography (chloroform/diethyl ether/n-heptane, 1:1:1) to yield 7.5 mg (50%) of **116a** as a white residue. ^{1}H NMR (500 MHz $CDCl_3$) δ 6.75 (d, J = 8.0 Hz, 1H), 6.36 (dd, J= 8.0, 6.0 Hz, 1H), 3.77 (s, 1H) , 3.73 (s, 3H), 3.70 (s, 3H), 3.56 (d, J= 6.0 Hz, 1H), 3.01 (dd, J=13 HZ, 6 HZ, 1H), 2.3 (m, 2H), 1.8 (m, 2H), 1.36 (m, 2H), 1.27 (s, 3H); ^{13}C NMR (75 MHz, $CDCl_3$) δ 175.4, 171.5, 169.5, 168.8, 136.2, 128.304, 83.5, 59.4, 53.0, 52.9, 52.7, 49.3, 48.0, 42.2, 28.1, 24.0, 21.4, 20.6; FTIR (Neat Film NaCl) 1761, 1734, 1626, 1542, 1434, 1255, 1203, 1160, 1108, 1019, 689 cm^{-1} ; HRMS (EI) m/z calc'd for $C_{18}H_{22}O_8$ $[M+H]^+$: 367.1393, found 367.1392.

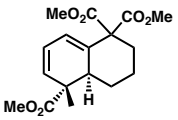

Diene 125

A solution of **117a** (63.0 mg, 0.15 mmol, 1.0 equiv) in toluene (10 mL) was sealed in a scintillation vial and heated to reflux for 72 hours. The reaction mixture was cooled to room temperature, the solvent removed by rotary evaporation, and the crude residue was purified by preparatory thin-layer chromatography (30% ethyl acetate in hexanes) to yield **125** as 6.8 mg (62%) of white residue. ^{1}H NMR (500 MHz), $CDCl_3$ δ 5.91 (dd, J = 9.0, 5.5 Hz, 1H), 5.67 (d, J= 5.5 Hz, 1H), 5.61 (d, J = 9.0 Hz, 1H) , 3.78 (s, 3H), 3.76 (s, 3H), 3.71 (s, 3H), 3.00 (dd, J= 6.0 Hz, 1H), 3.01 (dd, J = 13, 4.5 Hz, 1H), 2.44 (d, J = 13.5 Hz 1H), 1.82 (m, 1H), 1.62 (m, 1H), 1.38 (m, 2H), 1.26 (s, 1H), 1.19, (s, 2H); ^{13}C NMR (75 MHz, $CDCl_3$) δ 177.2, 171.2, 170.9, 136.6, 129.7, 122.5, 119.5, 62.3, 52.8, 52.7, 52.4, 46.7, 41.1, 33.3, 29.7, 25.3, 21.6, 18.5; FTIR (Neat Film NaCl) 1731, 1435, 1255, 1139, 801 cm^{-1} ; HRMS (EI) m/z calc'd for $C_{17}H_{22}O_7$ $[M+H]^+$: 323.1495, found 323.1485.

2.6 References and Notes

Note: Portions of this chapter have been published, see: Nelson, H. M.; Stoltz, B. M. *Org. Lett.* **2007**, *10*, 25–28.

1) Christensen, S.B.; Andersen, A.; Smitt, U.W. *Prog. Chem. Org. Nat. Prod* **1997**, *71*, 130–167.

2) Christensen, S. B.; Larsen, I. K.; Rasmussen, U.; Christophersen, C. *J. Org. Chem.* **1982**, *47,* 649–652.

3) Perchellet, E. M.; Gali, H. U.; Gao, X. M.; Perchellet, J. *Int. J. Cancer* **2006**, *55,* 1036–1043.

4) Lytton, J.; Westlin, M.; Hanley, M. R. *J. Biol. Chem.* **1991**, *26*, 17067–17071.

5) Treiman, T.; Caspersen, C.; Christensen, S. B. *Trends Pharma. Sciences* **1998**, *19*, 131–135.

6) At that time of this publication Sigma-Aldrich lists TG at $57.00 per 0.5 mg. However there has recently been an improvement made to TG's isolation procedure, see: Pagani, A.; Pollastro, F.; Spera, S.; Ballero, M.; Sterner, O.; Appendino, G. *Nat. Prod. Commun.* **2007**, *2*, 637–642.

7) a) Abderrahmane, A.; Guerra, F. M.; Rubal J. J.; Moreno-Durado, F. J.; Akssira, M.; Mellouki, F.; Lopez, M.; Pujadas, A. J.; Jorge, Z. D.; Massanet, G. M. *Org. Lett.* **2005**, *5,* 881–884. b) Appendino, G.; Properini, S.; Valdivia, C.; Ballero, M.; Colombano, G.; Billington, R. A.; Genazzani, A. A.; Sterner, O. *J. Nat. Prod.* **2005**, *68*, 1213–1217.

8) Navarette, C.; Sancho, R.; Caballero, F. J.; Pollastro, F.; Fiebich, B. L.; Sterner, O.; Appendino, G.; Muñoz, E. *J. Pharmacol. Exp. Ther.* **2006**, *319*, 422–430

9) a)Yamaguchi, H.; Bhalla, K.; Wang, H.-G. *Cancer Res*. **2003**, *63*, 1483–1489. b) Futami, T.; Miyagishi, M.; Taira, K. *J*. *Biol*. *Chem*. **2005**, *280*, 826–831.

10) a) Oguri, H.; Yamagishi, Y.; Hiruma, T.; Oikawa, H. *Org. Lett.* **2008,** *11*, 601–604. b) Mizoguchi, H.; Oguri, H.; Tsuge, K.; Oikawa, H. *Org. Lett.* **2009,** *11*, 3016–3019.

11) Oguri, H.; Hiruma, T.; Yamagishi, Y.; Oikawa, H.; Ishiyama, A.; Otoguro, K.; Yamada, H.; Omura, S. *J. Am. Chem. Soc.* **2011,** *133*, 7096–7105.

12) Breitmaier, E. *Terpenes: Flavors, Fragrances, Pharmaca, Phermones*; WILEY-VCH: New York, 2006

13) Rubal, J. J.; Moreno-Dorado, F. J.; Guerra, F. M.; Jorge, Z. a. D.; Saouf, A.; Akssira, M.; Mellouki, F.; Romero-Garrido, R. l.; Massanet, G. M. *Phytochem.* **2007,** *68*, 2480–2486.

14) Larsson, R.; Sterner, O.; Johansson, M. *Org. Lett.* **2009,** *11*, 657–660.

15) For a review of the subject, see: Afarinkia, K.; Vinader, V.; Nelson, T. D.; Posner, G. H. *Tetrahedron* **1992**, *48*, 9111–9171.

16) Carroll, M. F. *J. Chem. Soc. (Resumed)* **1940**, 704–706.

17) Werkhoven, T. M.; van Nipsen, R.; Lugtenburg *J. Eur. J. Org. Chem*. **1999**, *11*, 2909–2914.

18) Treatment of **117a** with a number of Lewis acids did not afford observable conversion to **113a** Furthermore, heating of **117a** to 90 °C for 86 h led to minimal conversion to **113a**. See experimental section for details.

19) For a review of the subject, see: Afarinkia, K.; Vinader, V.; Nelson, T. D.; Posner, G. H. *Tetrahedron* **1992**, *48*, 9111–9171.

20) a) Posner, G. H.; Nelson, T. D.; Kinter, C. M.; Afarankia, K. *Tetrahedron Lett.* **1991**, *32*, 5295–5298. b) Posner, G. H.; Dai, H.; Afarankia, K.; Murthy, N. N.; Guyton, K. Z.; Kensler, T. W. *J. Org. Chem.* **1993**, *58,* 7209–7215. c) For a theoretical discussion and computational models, see: Afarinkia, K; Bearpark, M. J.; Ndibwami, A. *J. Org. Chem.* **2005**, *70,* 1122–1133.

21) The Diels-Alder product can be directly isolated from the alkylation reaction. However, better yields are obtained if the alkylation product is purified prior to cycloaddition.

22) Crystallographic data have been deposited at the CCDC, 12 Union Road, Cambridge CB2 1EZ, UK, and copies can be obtained on request, free of charge, by quoting the publication citation and the deposition number 656115.

23) Kozytska, M. V.; Dudley, G. B. *Tetrahedron Lett.* **2008**, *49*, 2899–2901.

24) Zhou, X.; Wu, W.; Liu, X.; Lee, C.-s. *Org. Lett.* **2008,** *10*, 5525–5528.

APPENDIX 1

Spectra Relevant to Chapter 2: Model Studies Aimed at The Total Syntheses of The Transtaganolide Natural Products

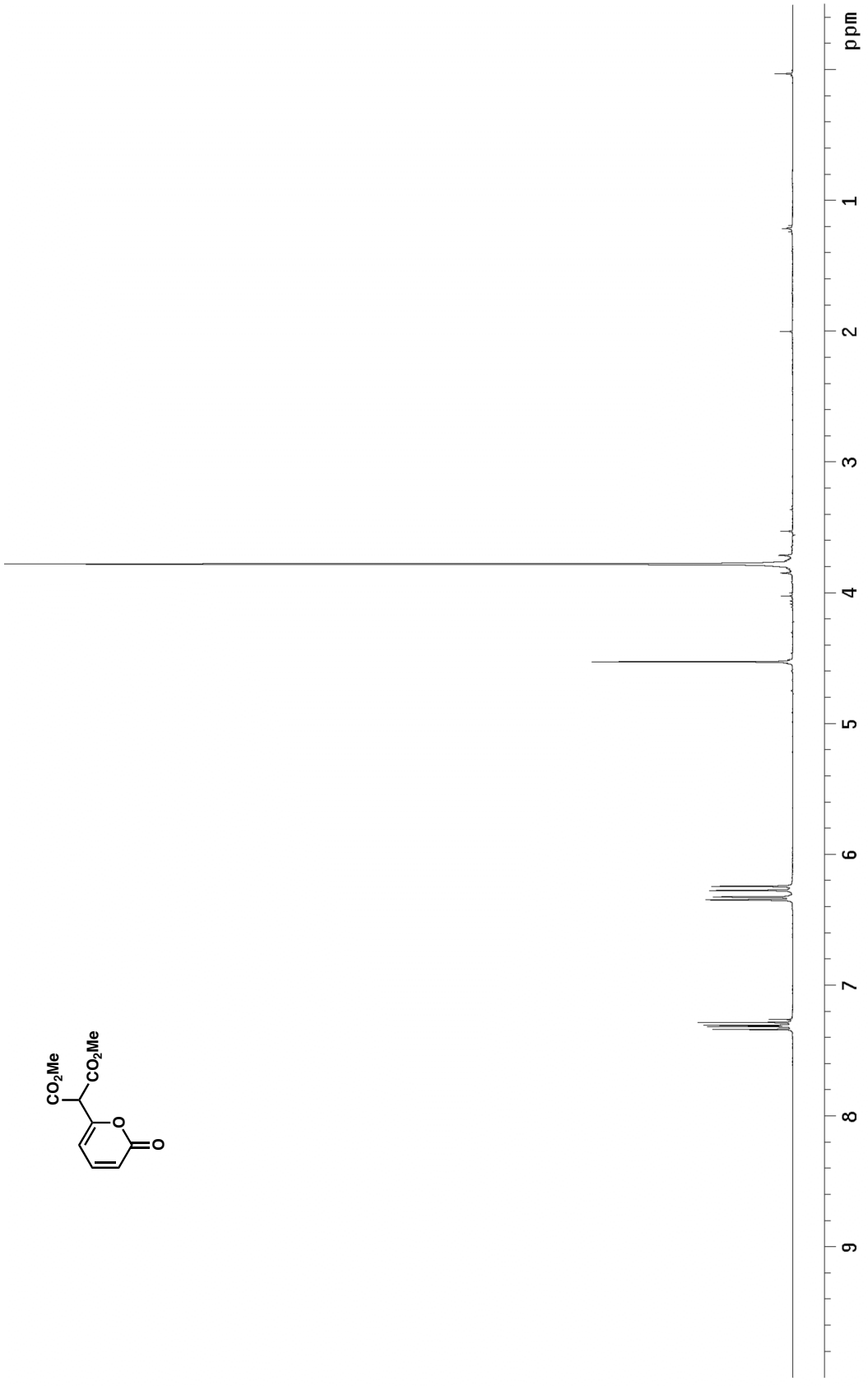

Figure A1.1.1 ^{1}H NMR (500 MHz, $CDCl_3$) of compound **124**

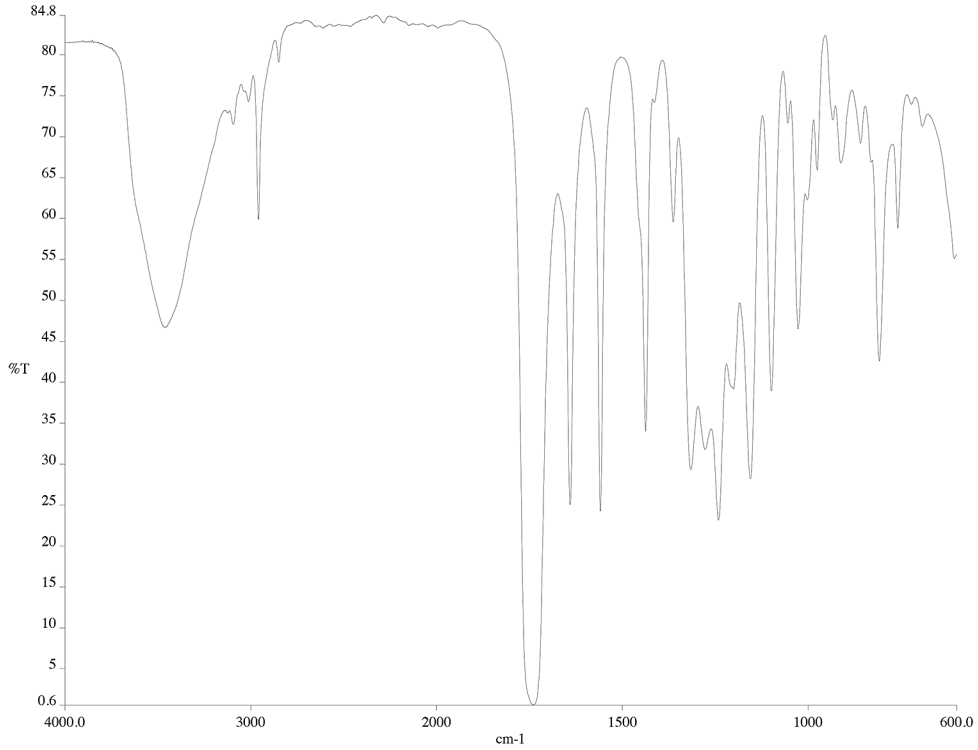

Figure A1.1.2 Infrared spectrum (thin film/NaCl) of compound **124**

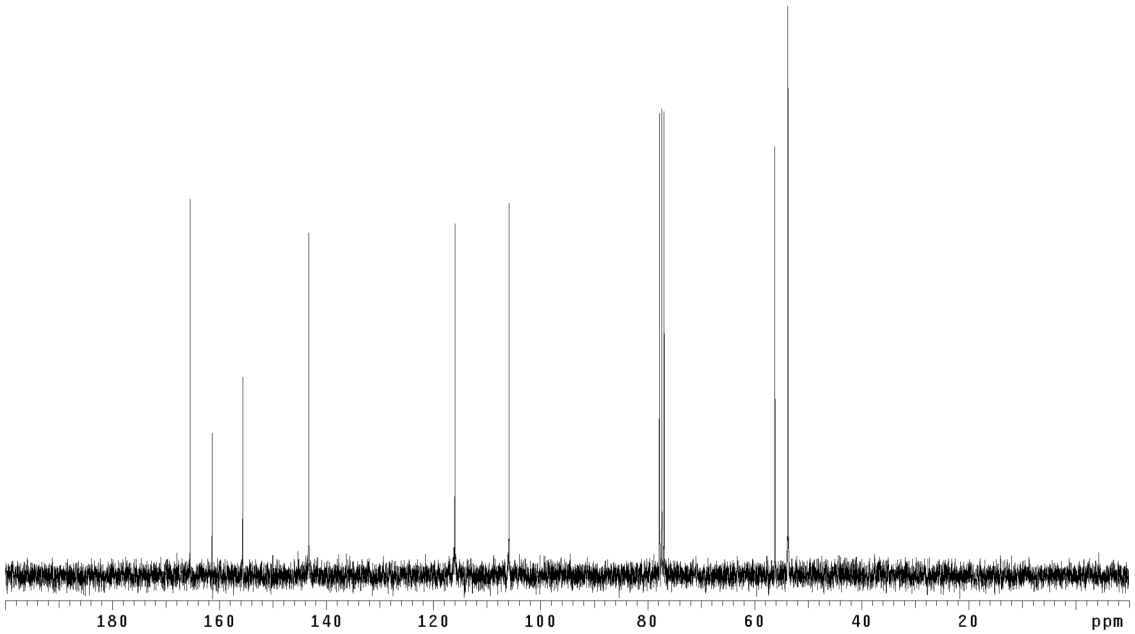

Figure A1.1.3 ^{13}C NMR (125 MHz, $CDCl_3$) of compound **124**

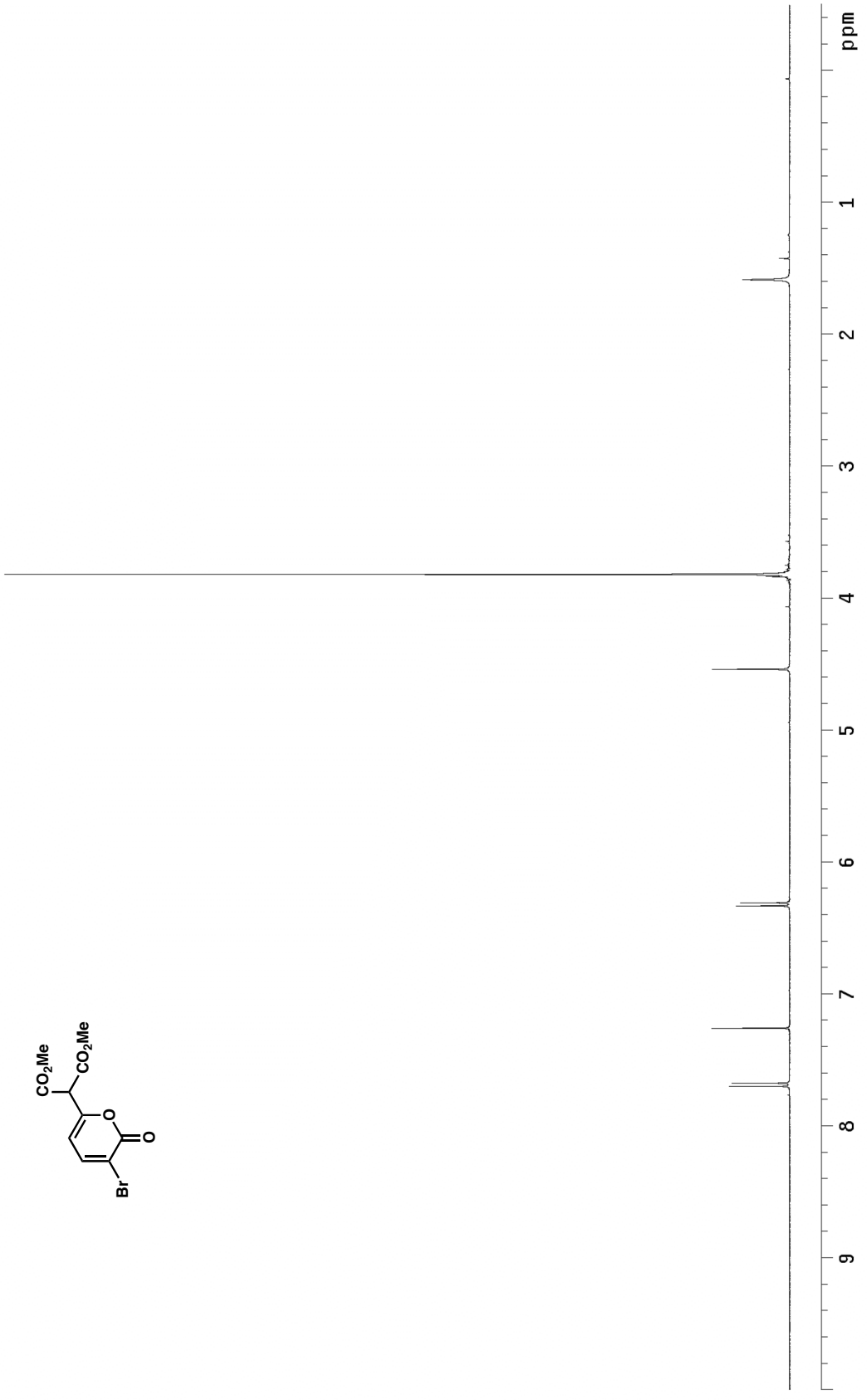

Figure A1.2.1 ^{1}H NMR (500 MHz, $CDCl_3$) of compound **126**

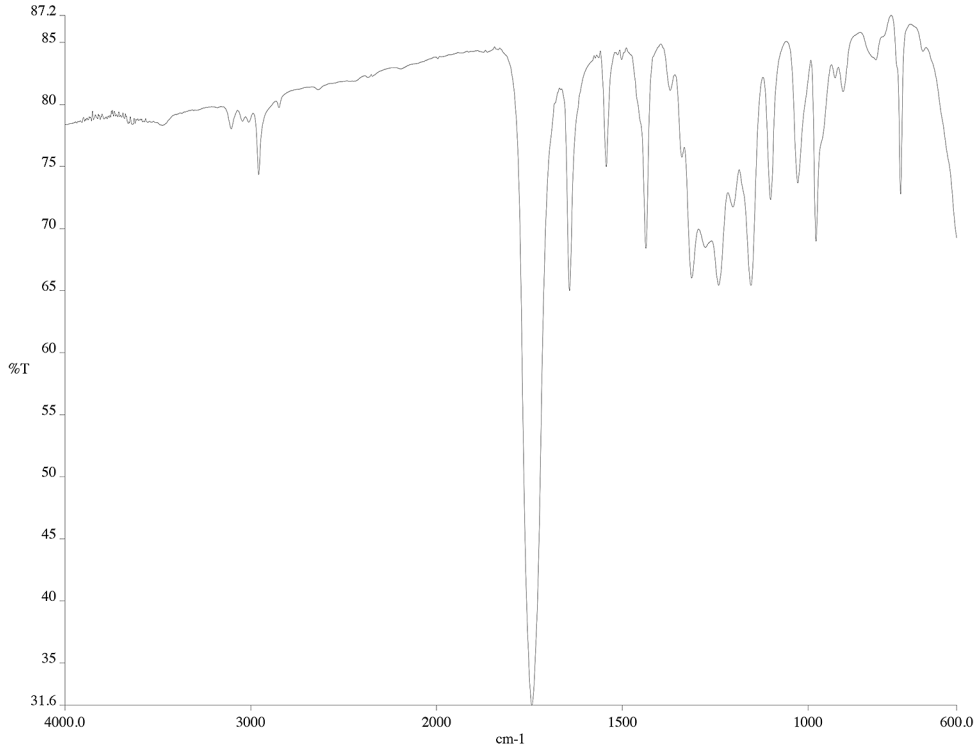

Figure A1.2.2 Infrared spectrum (thin film/NaCl) of compound **126**

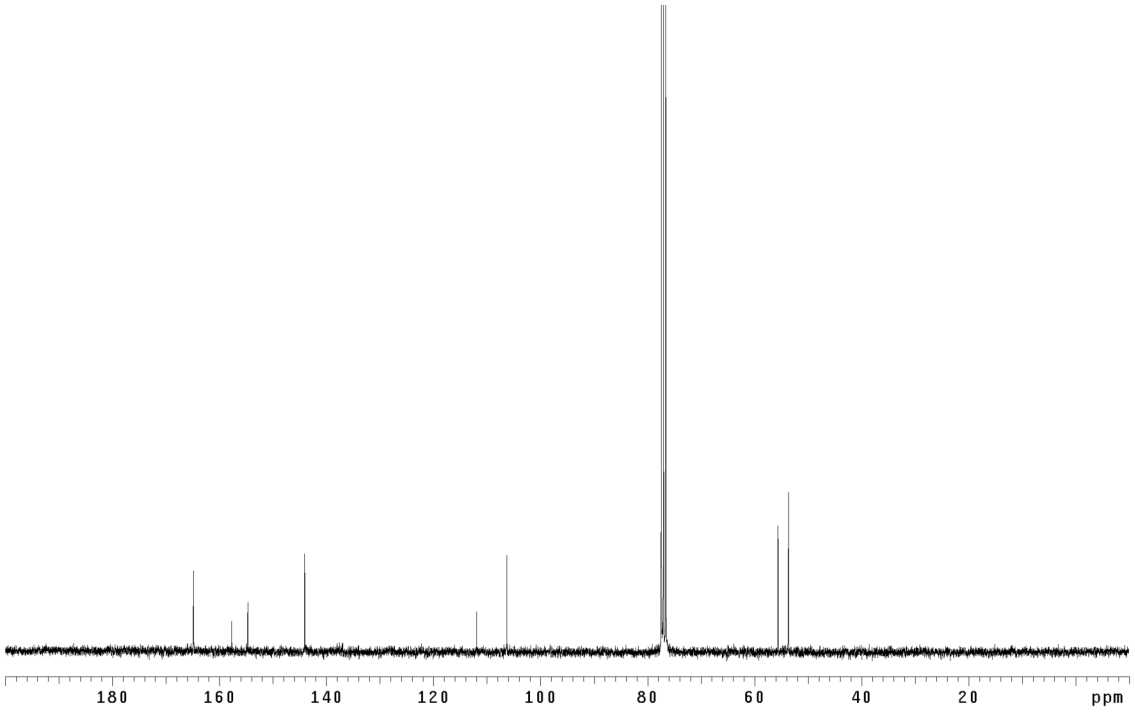

Figure A1.2.3 ^{13}C NMR (125 MHz, $CDCl_3$) of compound **126**

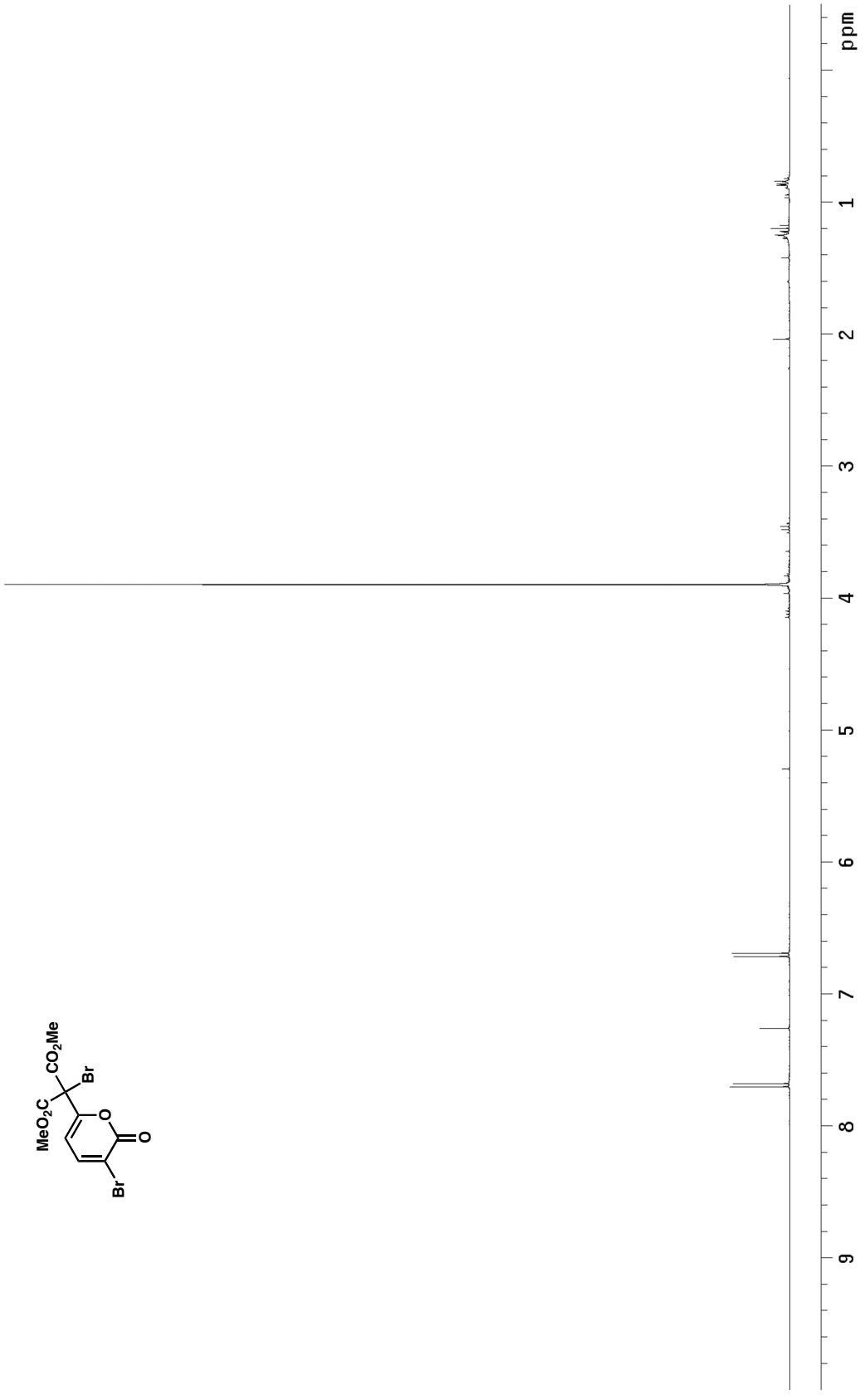

Figure A1.3.1 ^{1}H NMR (500 MHz, $CDCl_3$) of compound **127**

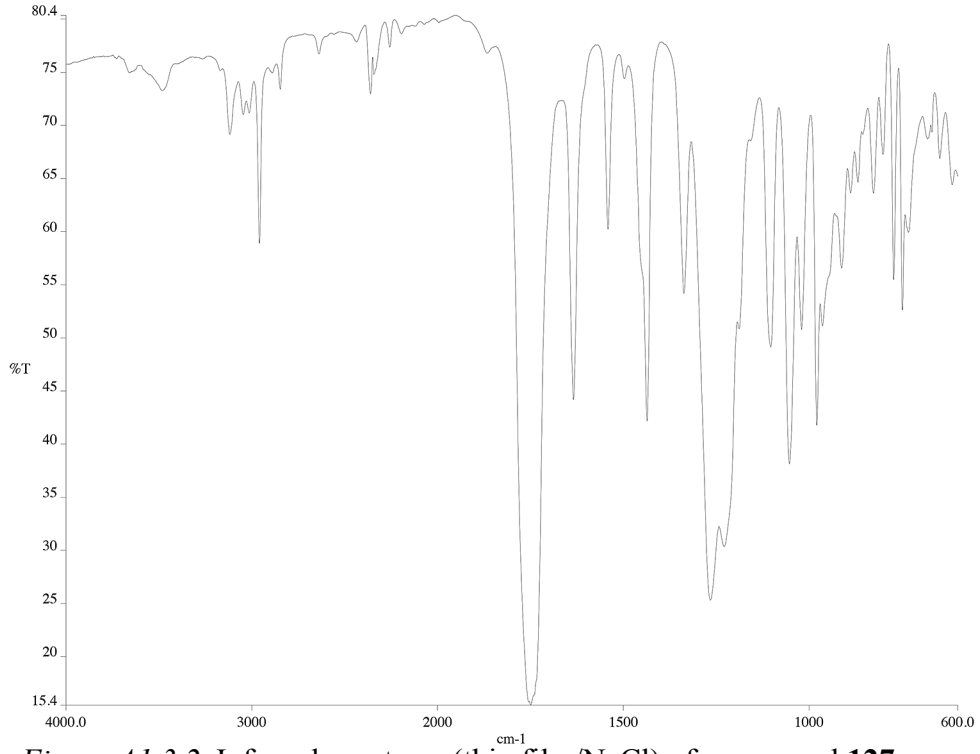

Figure A1.3.2 Infrared spectrum (thin film/NaCl) of compound **127**

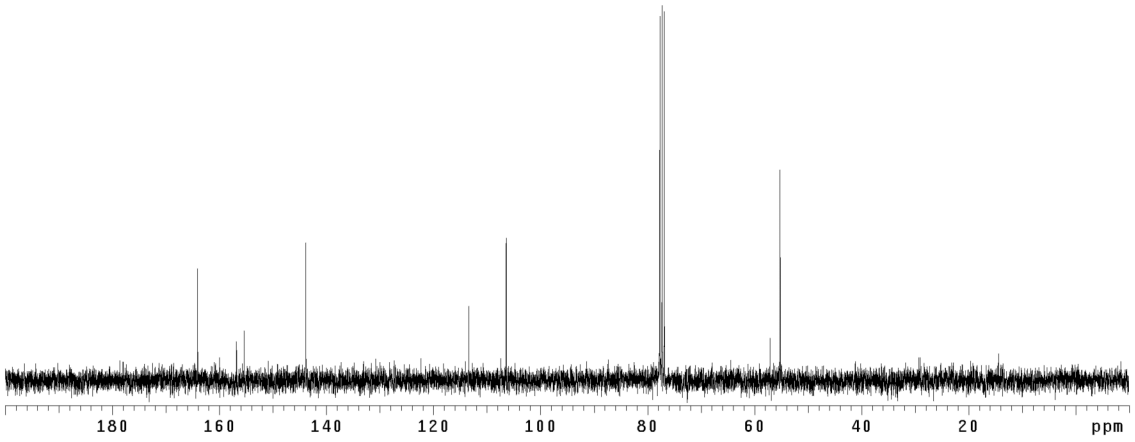

Figure A1.3.3 ^{13}C NMR (125 MHz, $CDCl_3$) of compound **127**

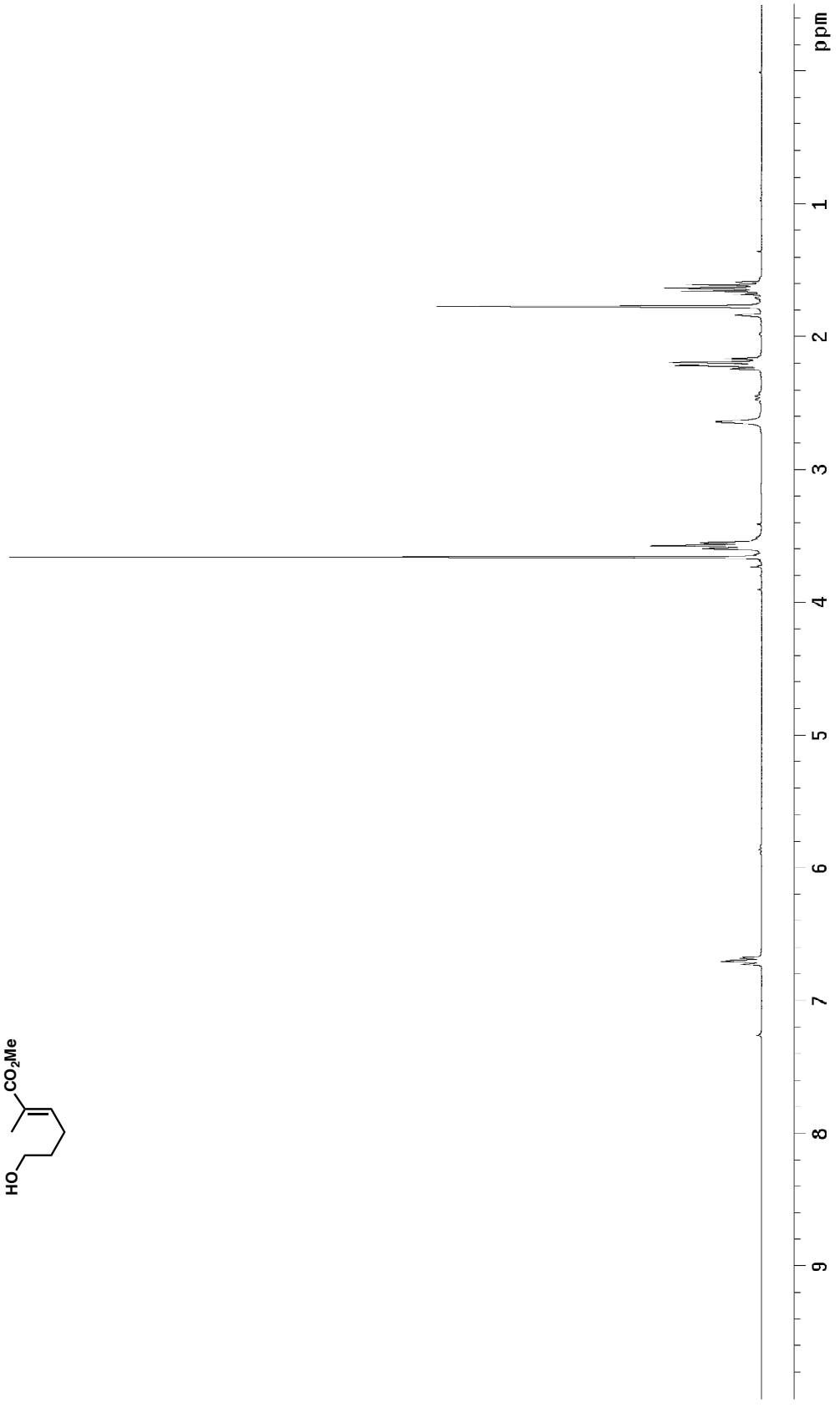

Figure A1.4.1 ^{1}H NMR (500 MHz, $CDCl_3$) of compound **123**

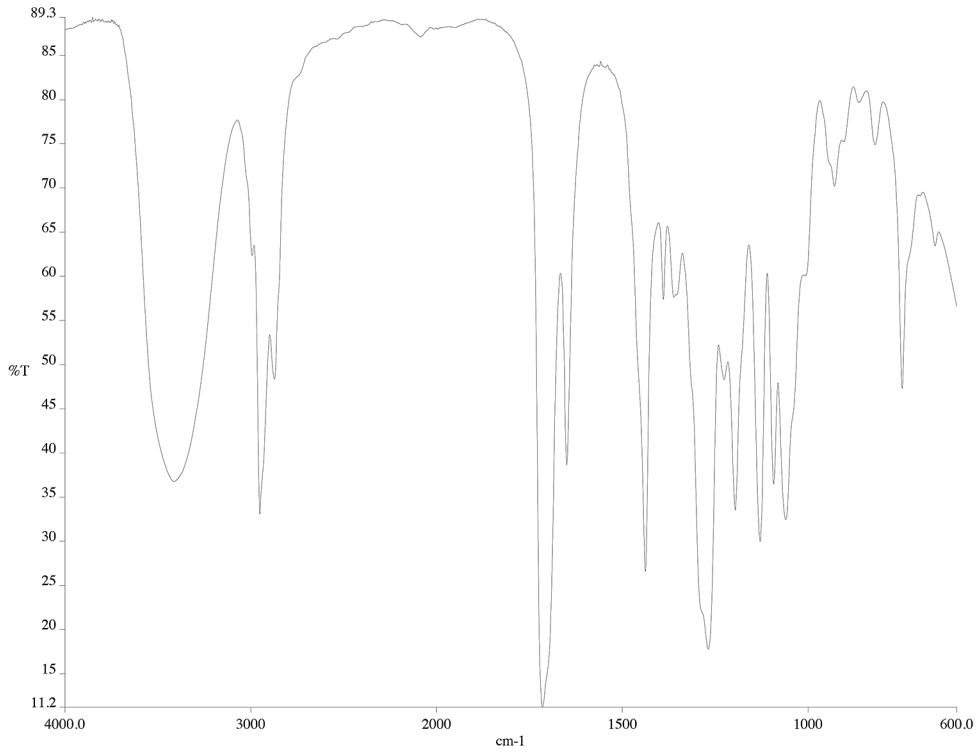

Figure A1.4.2 Infrared spectrum (thin film/NaCl) of compound **123**

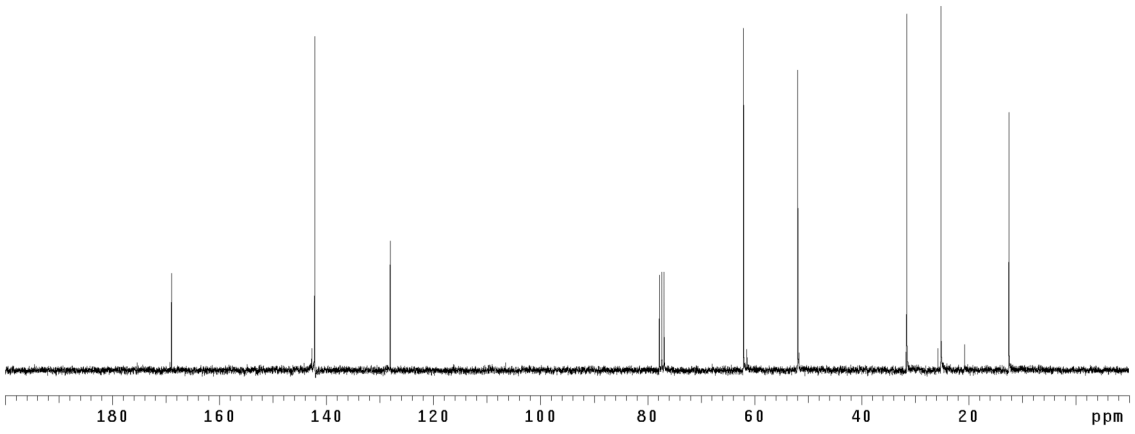

Figure A1.4.3 ^{13}C NMR (125 MHz, $CDCl_3$) of compound **123**

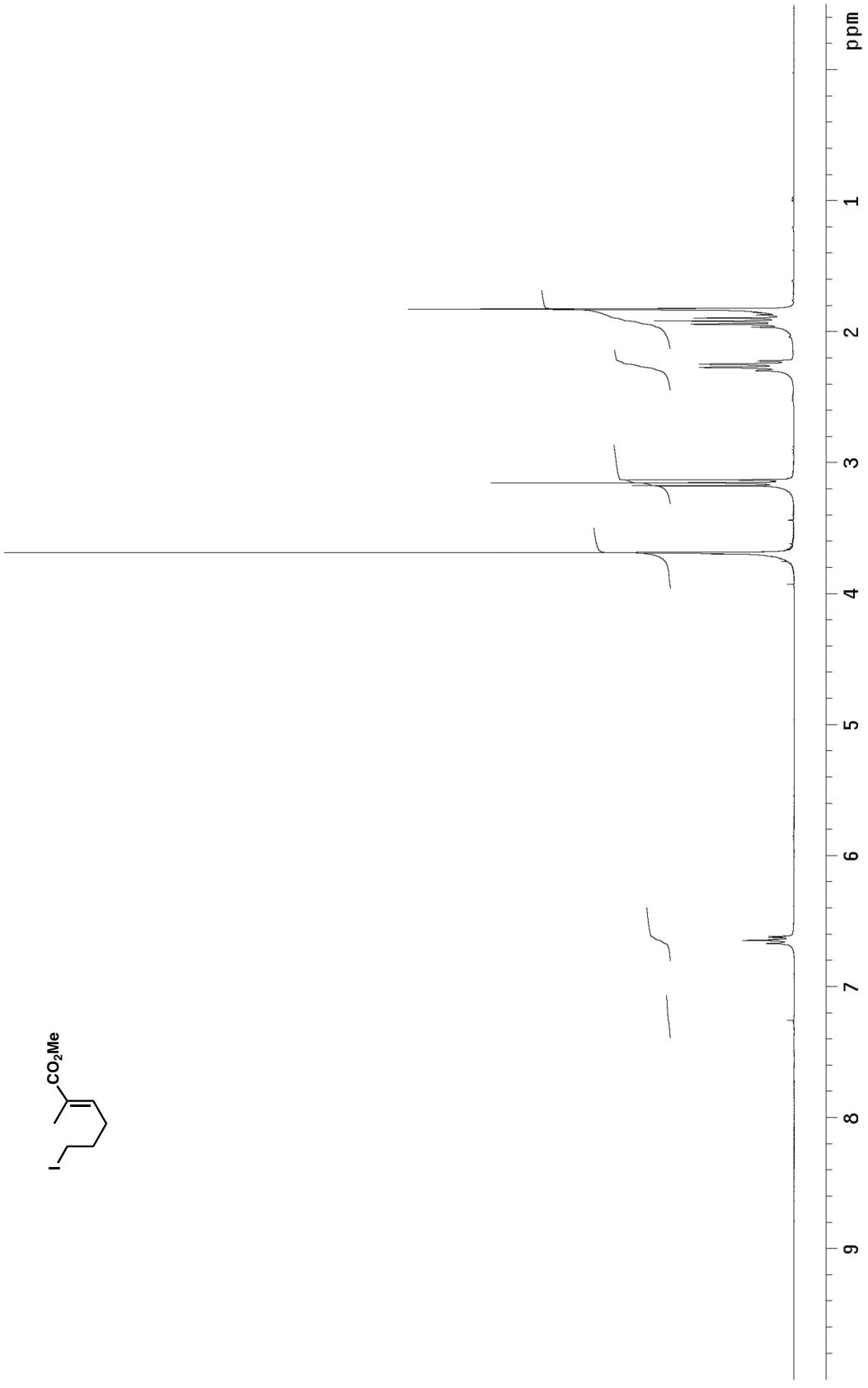

Figure A1.5.1 ^{1}H NMR (500 MHz, $CDCl_3$) of compound **119a**

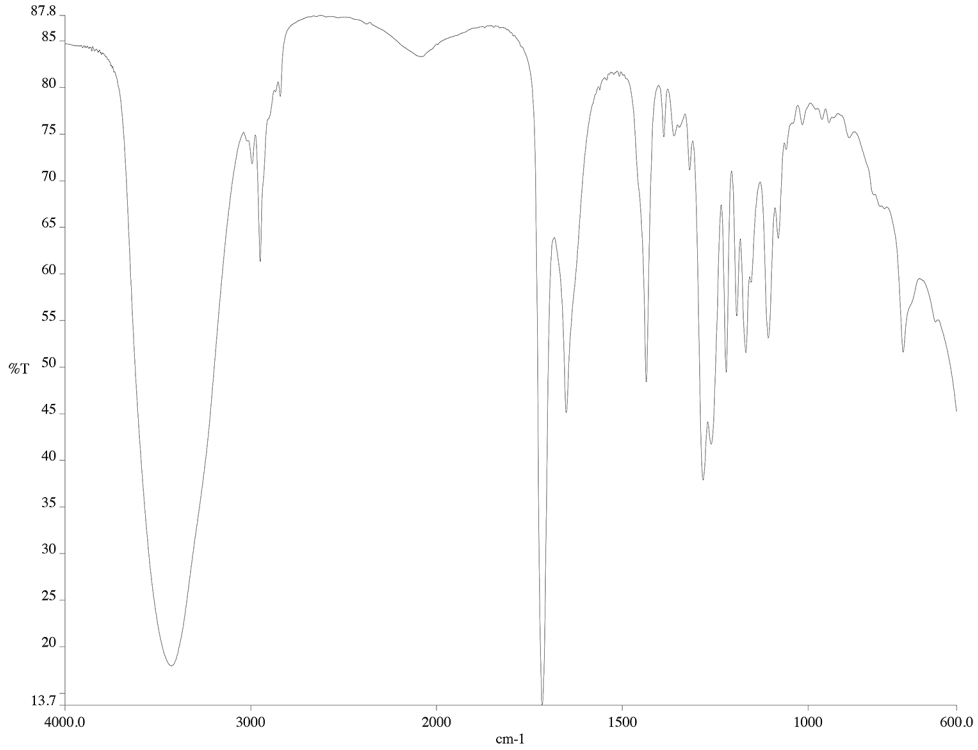

Figure A1.5.2 Infrared spectrum (thin film/NaCl) of compound **119a**

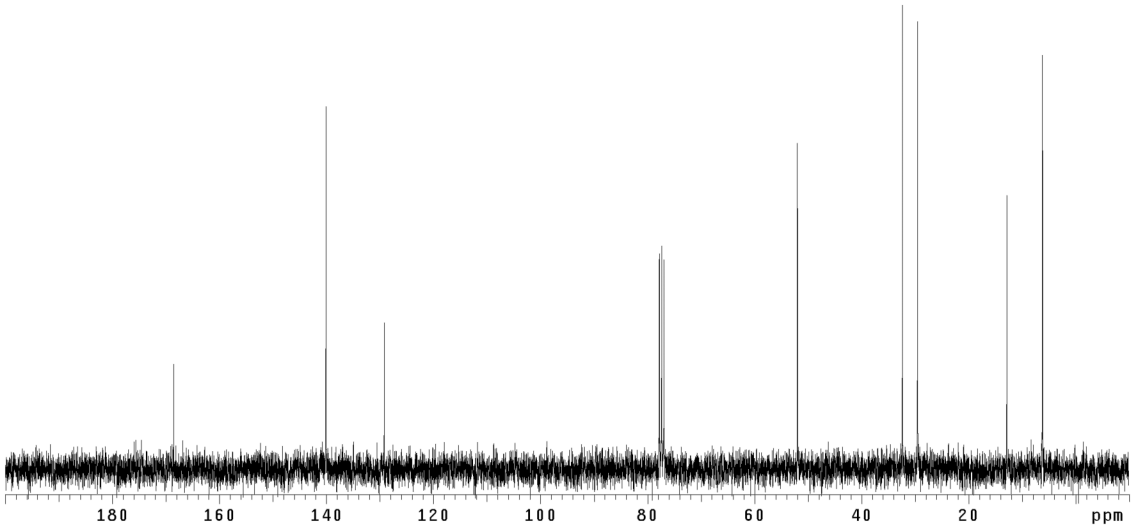

Figure A1.5.3 ^{13}C NMR (125 MHz, $CDCl_3$) of compound **119a**

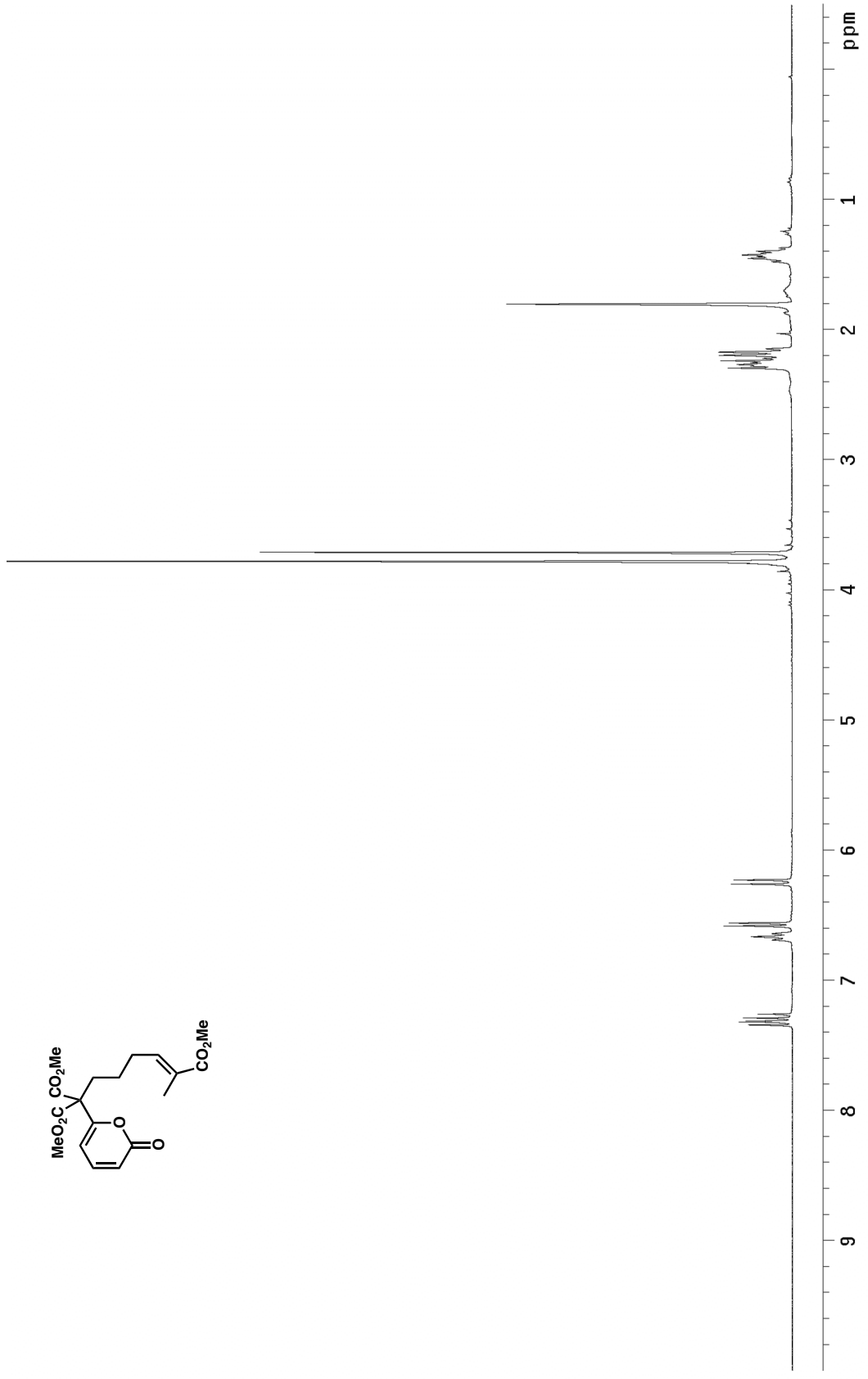

Figure A1.6.1 ^{1}H NMR (500 MHz, $CDCl_3$) of compound **117a**

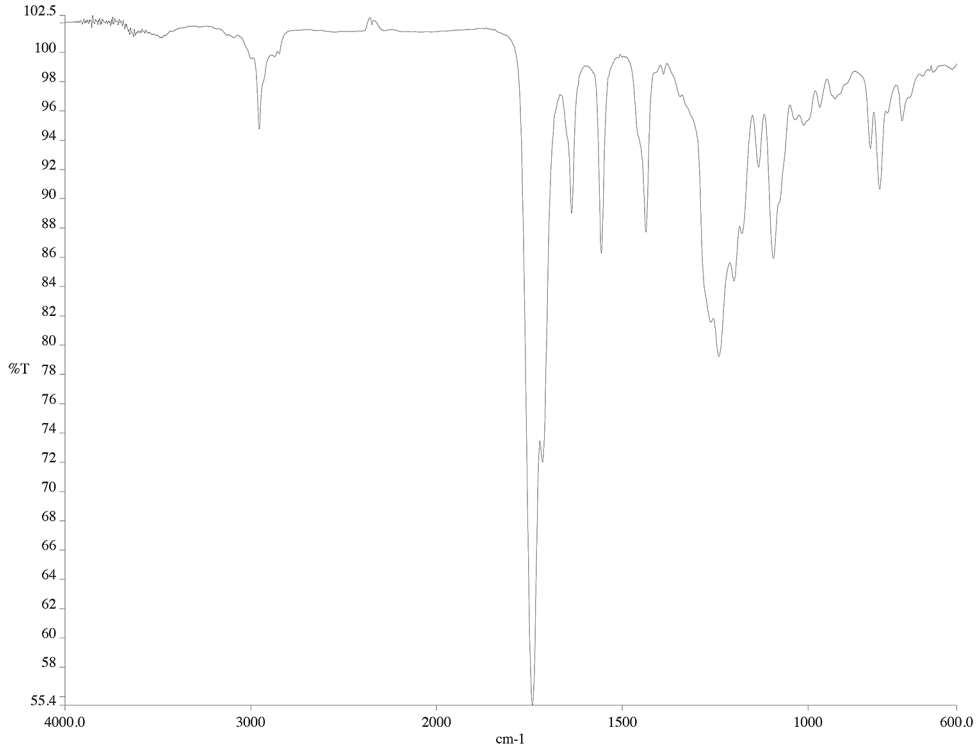

Figure A1.6.2 Infrared spectrum (thin film/NaCl) of compound **117a**

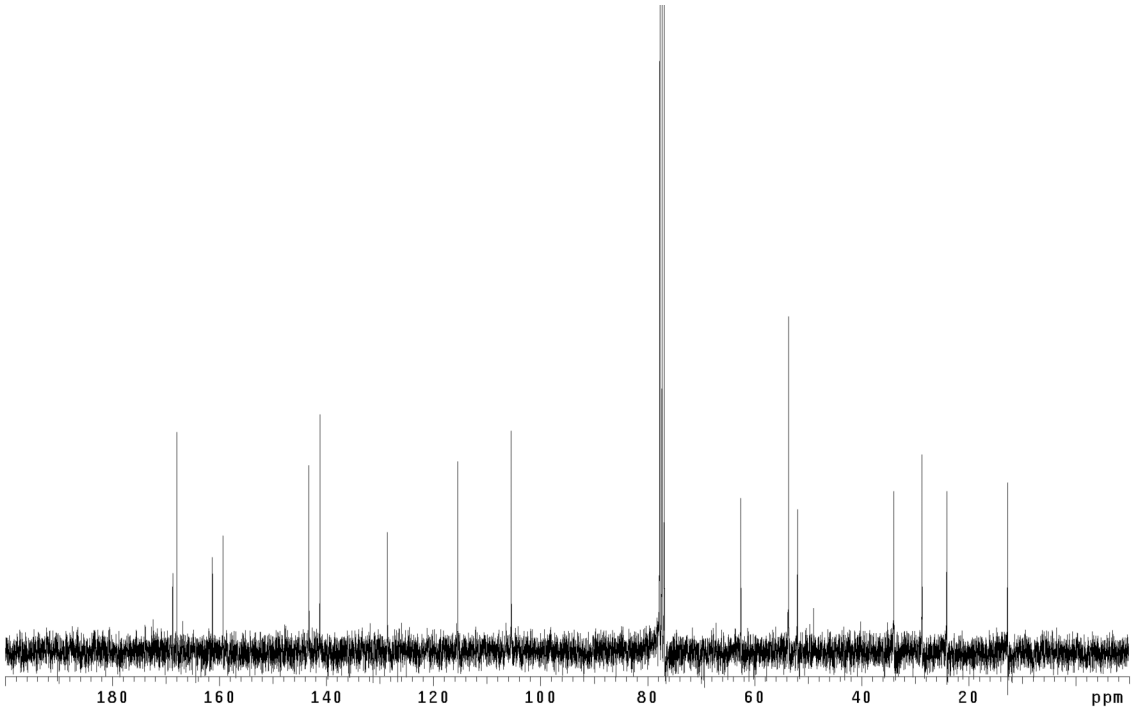

Figure A1.6.3 ^{13}C NMR (125 MHz, $CDCl_3$) of compound **117a**

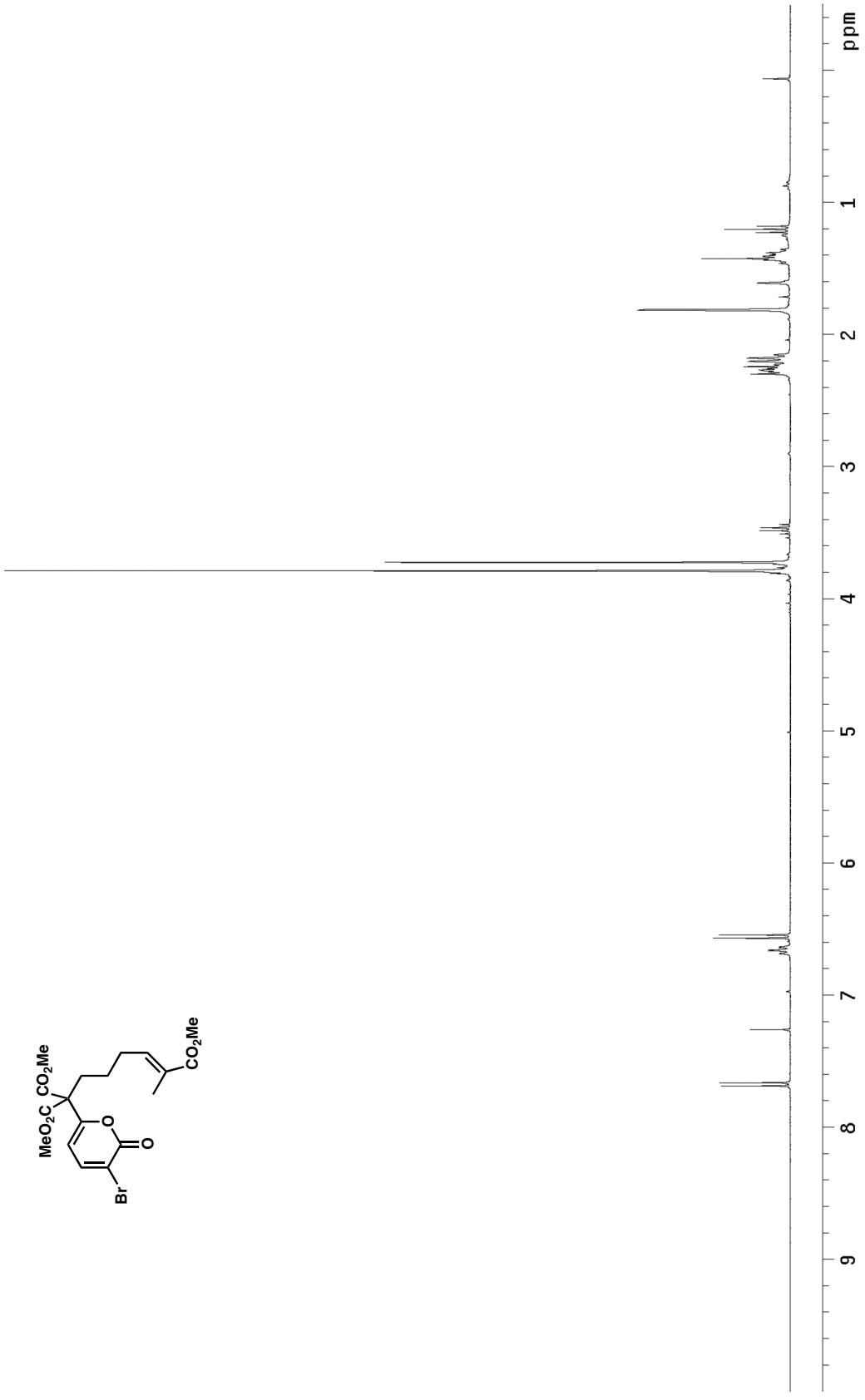

Figure A1.7.1 ^{1}H NMR (500 MHz, $CDCl_3$) of compound **117b**

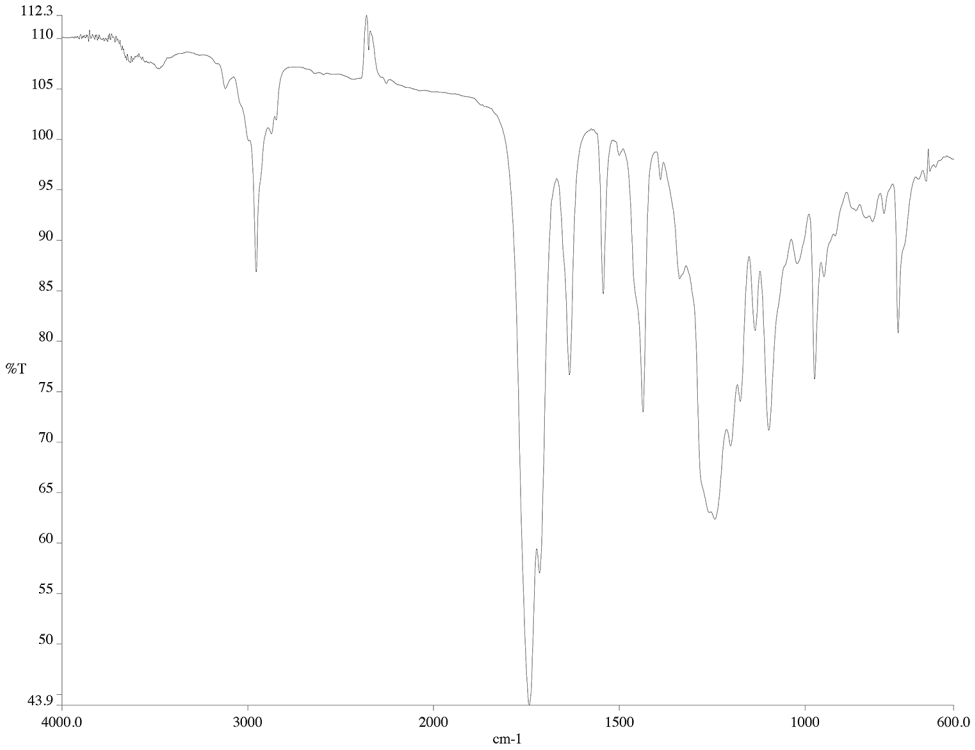

Figure A1.7.2 Infrared spectrum (thin film/NaCl) of compound **117b**

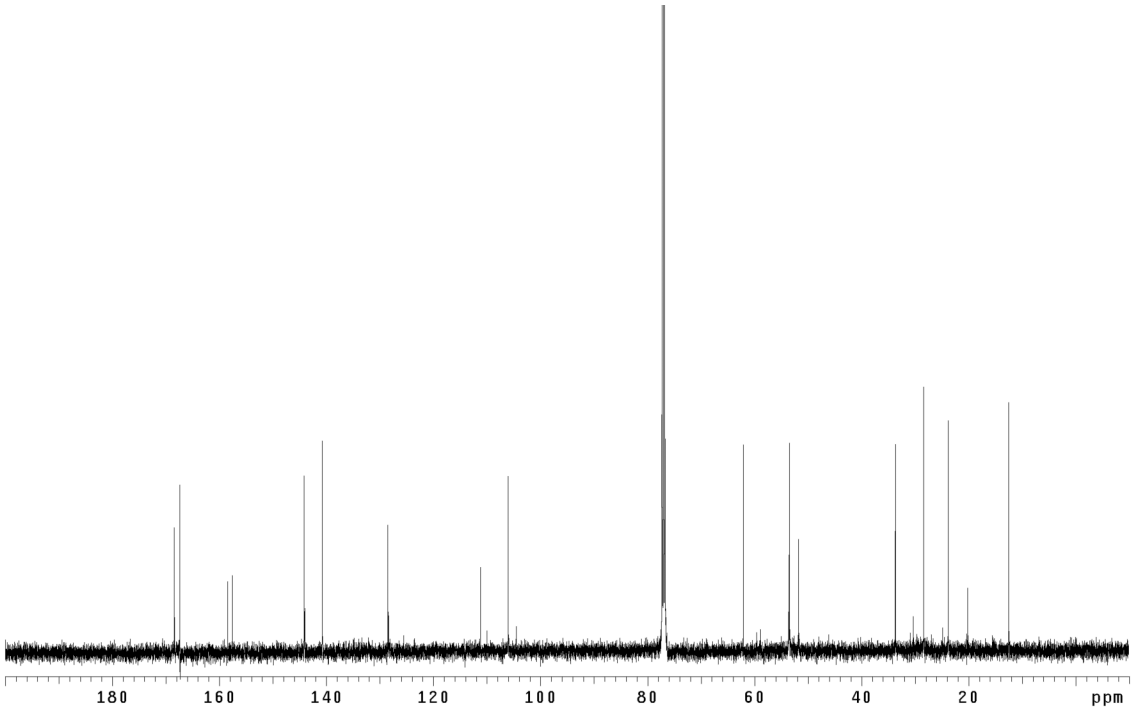

Figure A1.7.3 ^{13}C NMR (125 MHz, $CDCl_3$) of compound **117b**

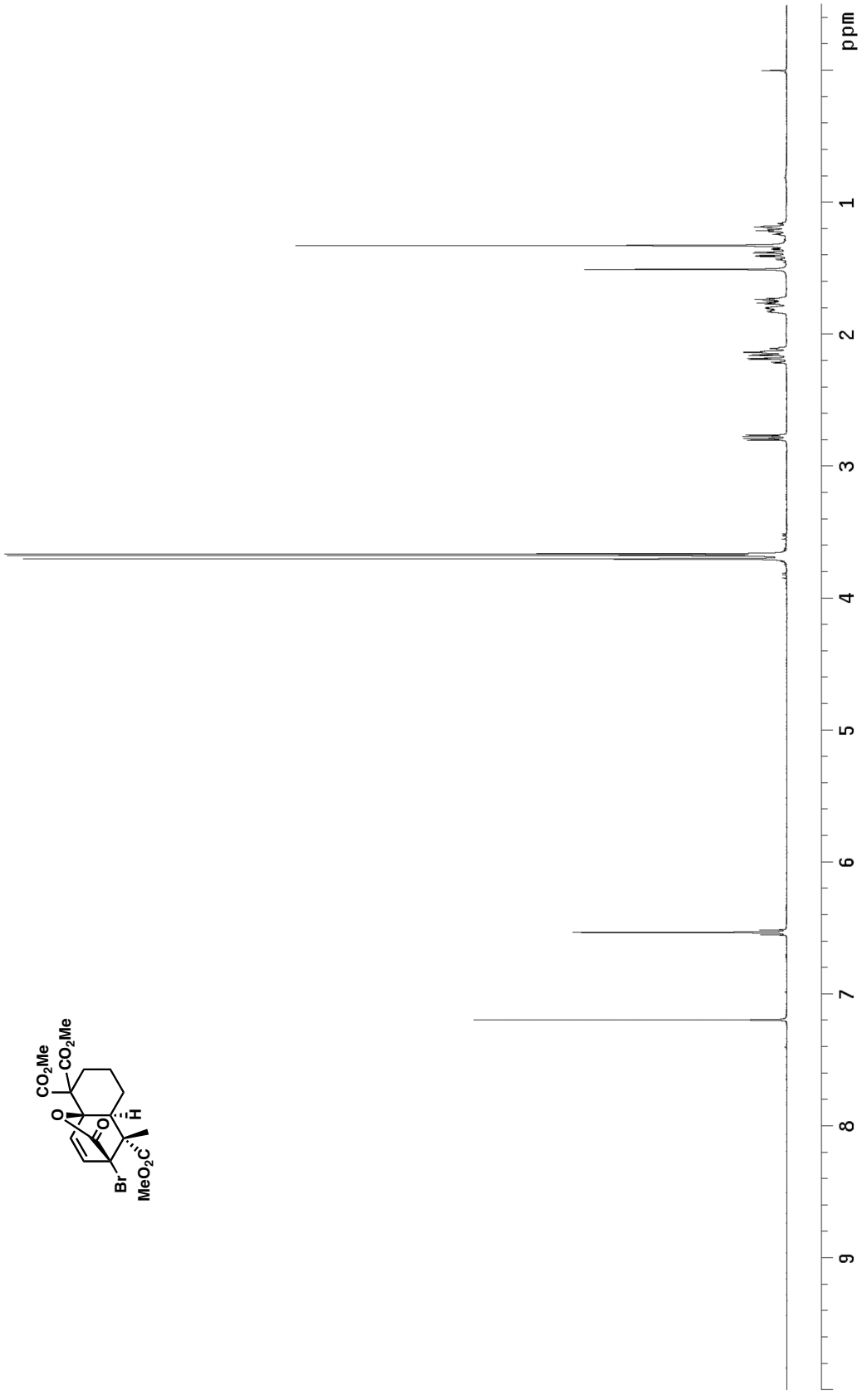

Figure A1.8.1 ^{1}H NMR (500 MHz, $CDCl_3$) of compound **116b**

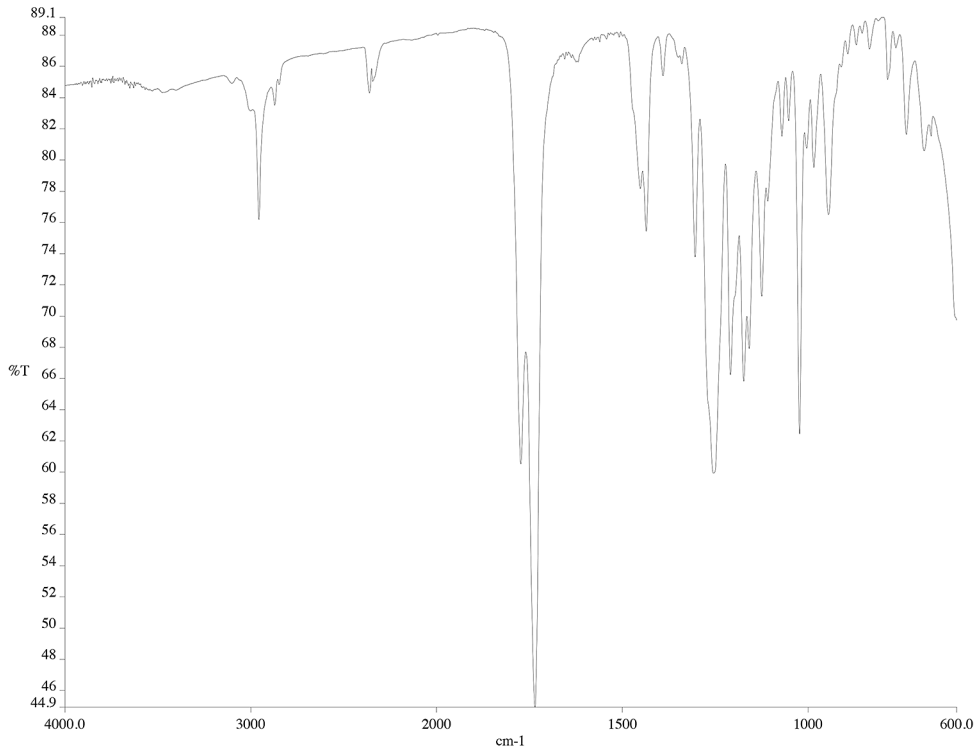

Figure A1.8.2 Infrared spectrum (thin film/NaCl) of compound **116b**

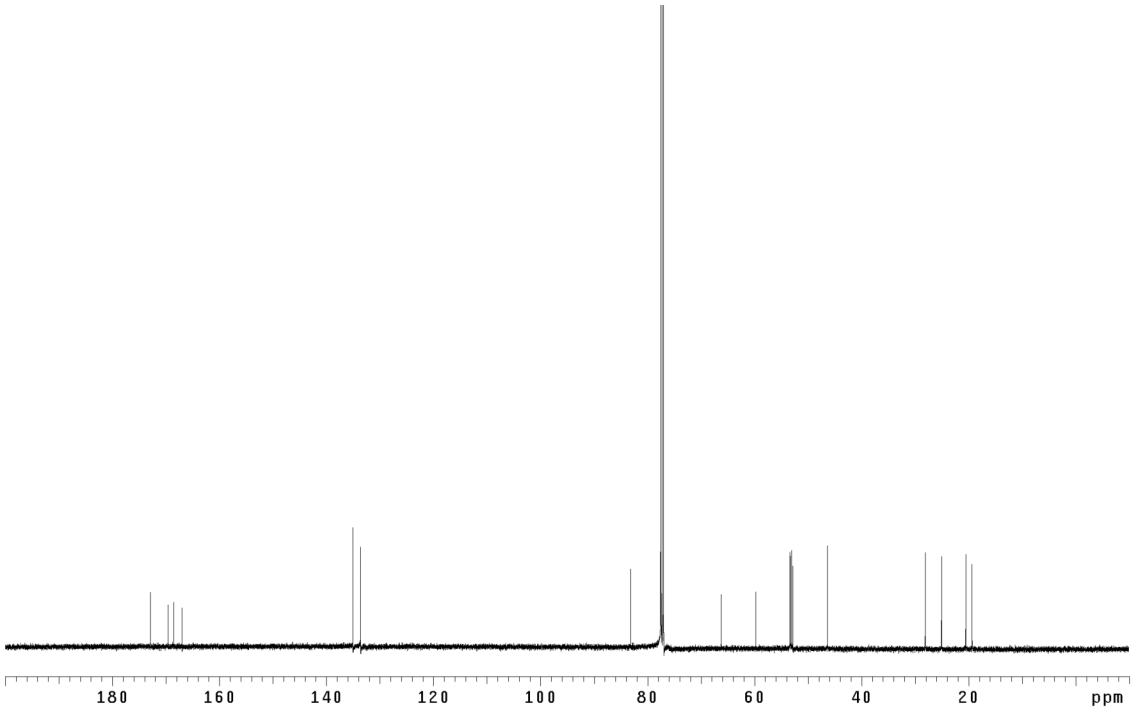

Figure A1.8.3 ^{13}C NMR (125 MHz, $CDCl_3$) of compound **116b**

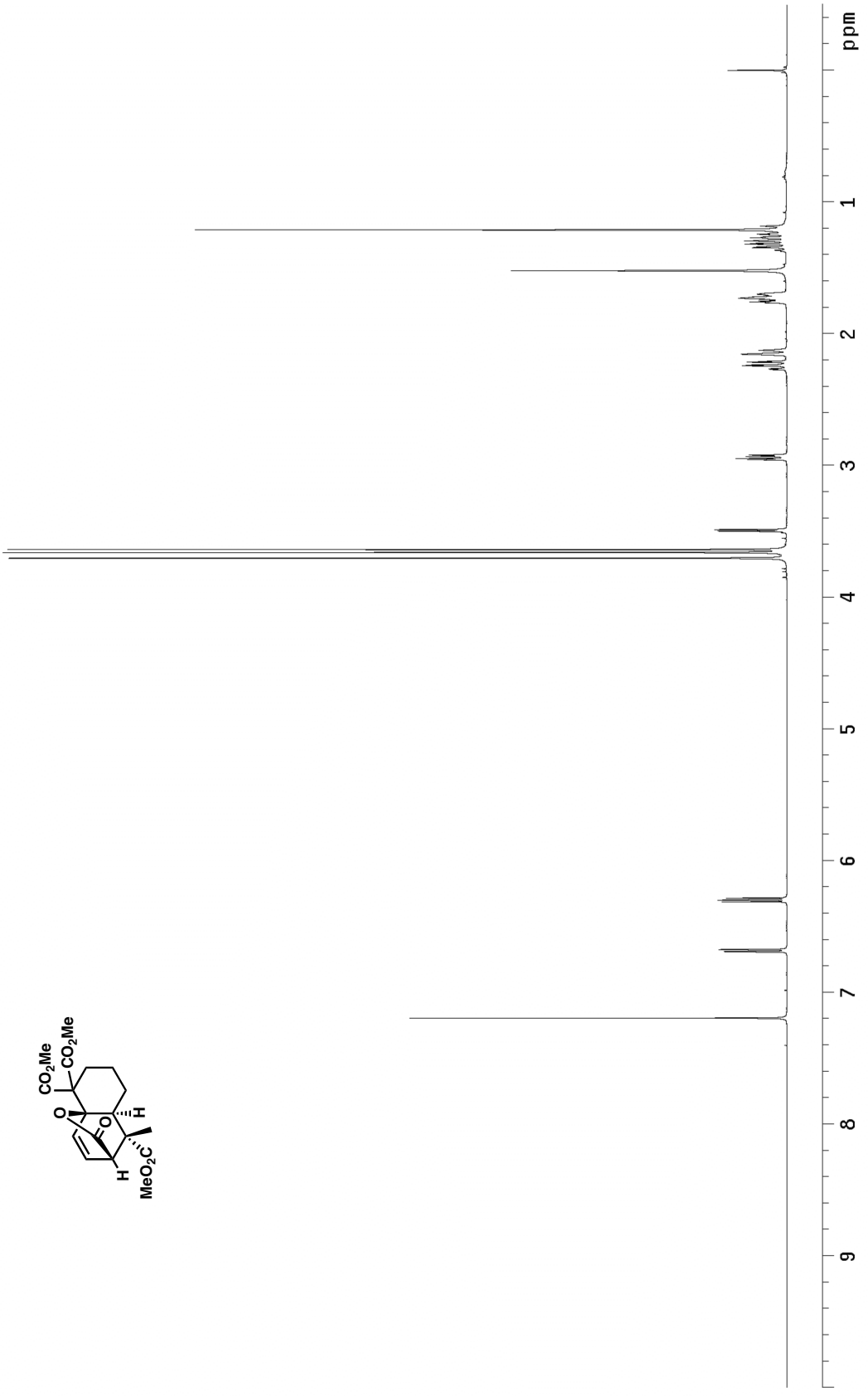

Figure A1.9.1 ^{1}H NMR (500 MHz, $CDCl_3$) of compound **116a**

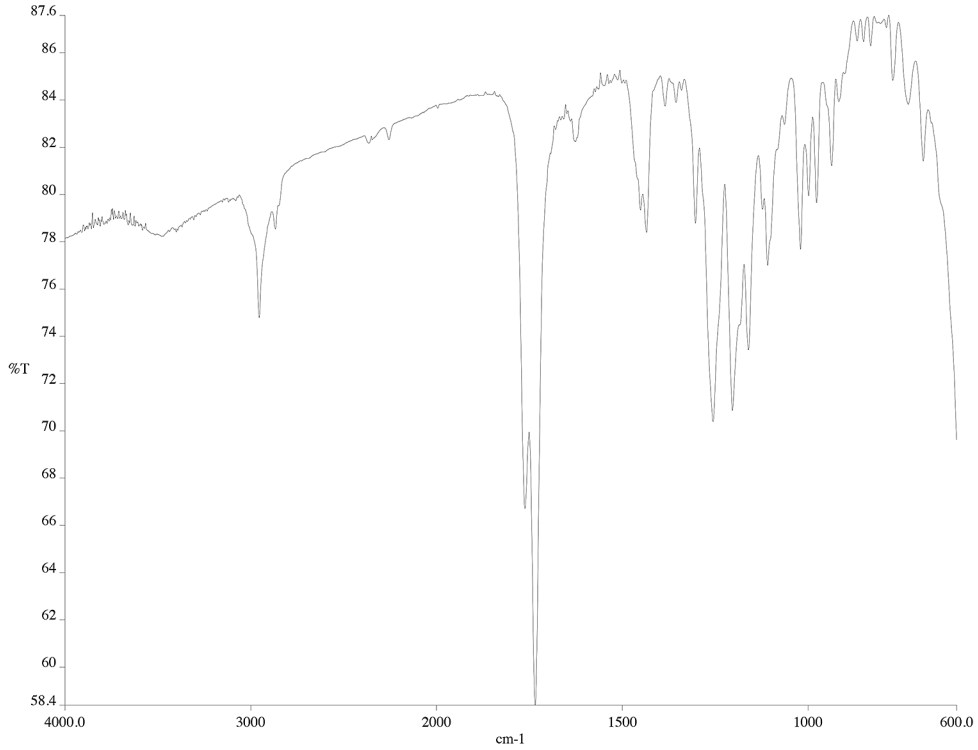

Figure A1.9.2 Infrared spectrum (thin film/NaCl) of compound **116a**

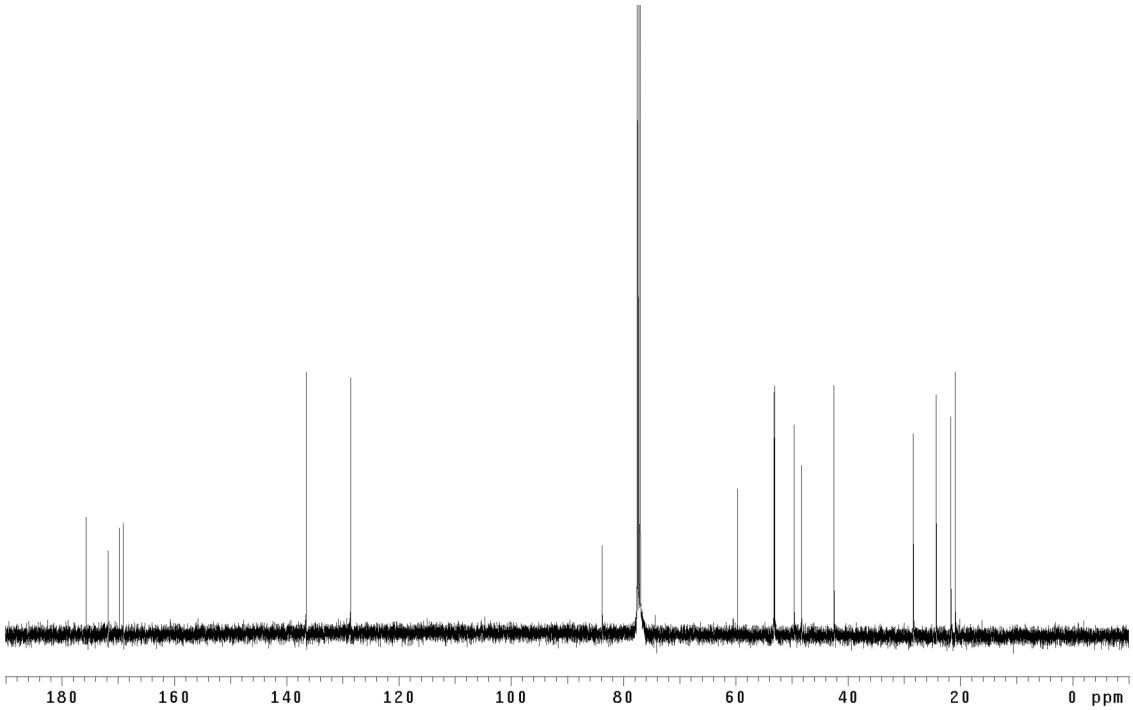

Figure A1.9.3 ^{13}C NMR (125 MHz, $CDCl_3$) of compound **116a**

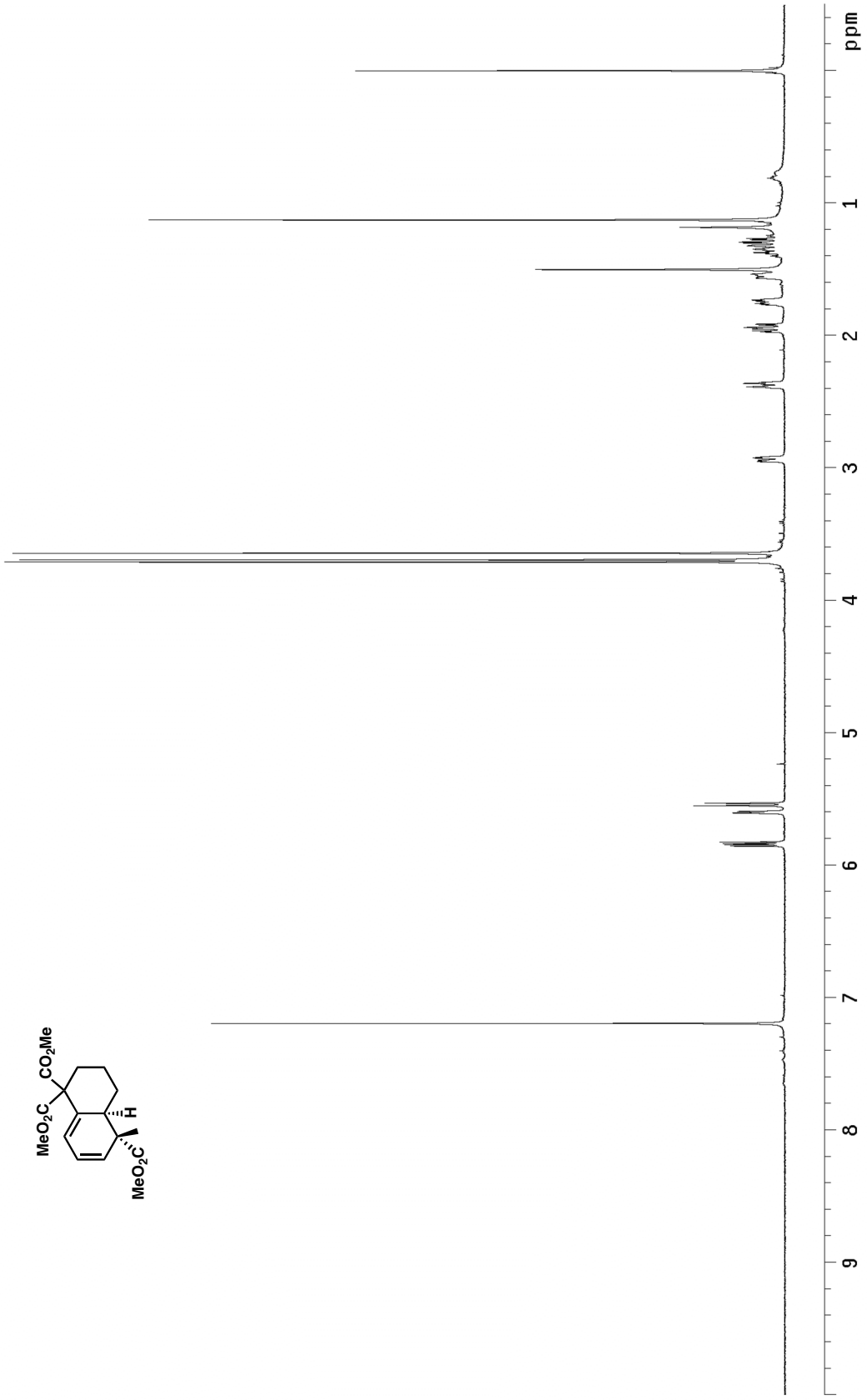

Figure A1.10.1 ^{1}H NMR (500 MHz, $CDCl_3$) of compound **125**

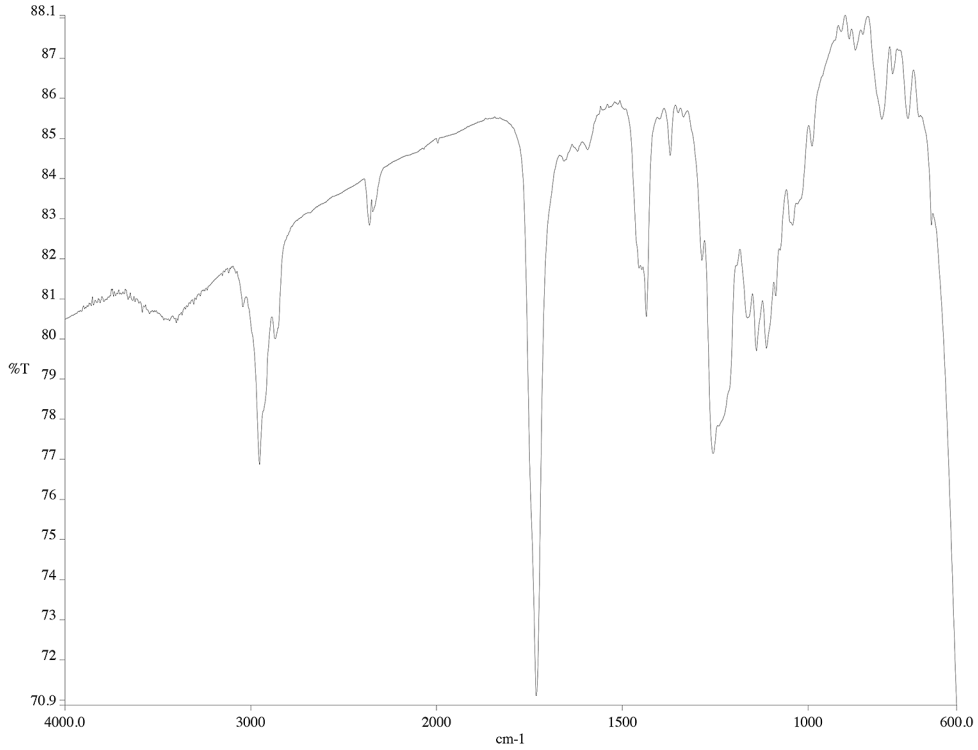

Figure A1.10.2 Infrared spectrum (thin film/NaCl) of compound **125**

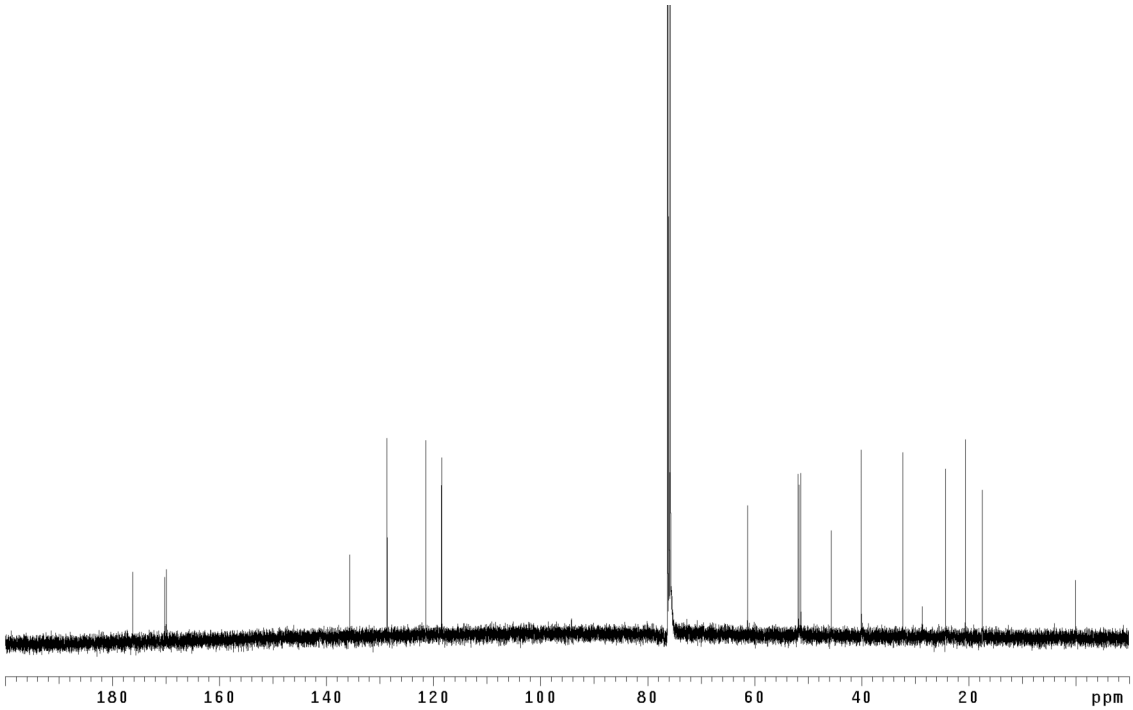

Figure A1.10.3 ^{13}C NMR (125 MHz, $CDCl_3$) of compound **125**

APPENDIX 2

X-Ray Data Relevant to Chapter 2: Model Studies Aimed at The Total Syntheses of The Transtaganolide Natural Products

Figure A2.1. ORTEP diagram of ***116a****. Shown at 50% probabilities The crystallographic data have been deposited in the Cambridge Database (CCDC) and has been placed on hold pending further instructions from me. The deposition number is 656115. Ideally the CCDC would like the publication to contain a footnote of the type: "Crystallographic data have been deposited at the CCDC, 12 Union Road, Cambridge CB2 1EZ, UK and copies can be obtained on request, free of charge, by quoting the publication citation and the deposition number 656115."*

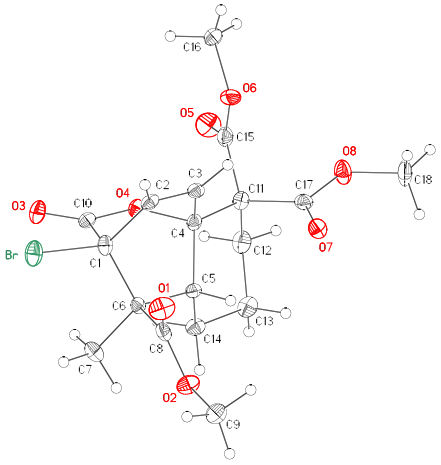

116a

Table A2.1. Crystal data and structure refinement for HMN01 (CCDC 656115).

Empirical formula	$C_{18}H_{21}O_8Br$
Formula weight	445.26
Crystallization Solvent	Dichloromethane/hexanes
Crystal Habit	Fragment
Crystal size	0.30 x 0.15 x 0.05 mm^3
Crystal color	Colorless
Data Collection	
Type of diffractometer	Bruker SMART 1000
Wavelength	0.71073 Å MoKα
Data Collection Temperature	100(2) K
θ range for 4422 reflections used in lattice determination	2.50 to 30.90°
Unit cell dimensions	a = 6.6117(3) Å b = 19.4403(16) Å β= 101.003(3)° c = 14.6195(13) Å
Volume	1844.6(2) $Å^3$

Z	4
Crystal system	Monoclinic
Space group	$P2_1/c$
Density (calculated)	1.603 Mg/m^3
F(000)	912
Data collection program	Bruker SMART v5.630
θ range for data collection	1.76 to 33.90°
Completeness to θ = 33.90°	89.1 %
Index ranges	$-10 \leq h \leq 9$, $0 \leq k \leq 29$, $0 \leq l \leq 22$
Data collection scan type	ω scans at 5 ϕ settings
Data reduction program	Bruker SAINT v6.45A
Reflections collected	11273
Independent reflections	11273 [R_{int}= 0.0000]
Absorption coefficient	2.273 mm^{-1}
Absorption correction	TWINABS
Max. and min. transmission	0.7466 and 0.5283

Structure Solution and Refinement

Structure solution program	SHELXS-97 (Sheldrick, 1990)
Primary solution method	Direct methods
Secondary solution method	Difference Fourier map
Hydrogen placement	Geometric positions
Structure refinement program	SHELXL-97 (Sheldrick, 1997)
Refinement method	Full matrix least-squares on F^2
Data / restraints / parameters	11273 / 0 / 249
Treatment of hydrogen atoms	Riding
Goodness-of-fit on F^2	1.437
Final R indices [I>2σ(I), 7706 reflections]	R1 = 0.0691, *w*R2 = 0.1161
R indices (all data)	R1 = 0.1128, *w*R2 = 0.1245
Type of weighting scheme used	Sigma
Weighting scheme used	$w=1/\sigma^2(Fo^2)$
Max shift/error	0.001
Average shift/error	0.000
Largest diff. peak and hole	1.261 and -0.700 $e.Å^{-3}$

Special Refinement Details

The crystal is twinned. CELL_NOW was used to establish the following relationship between domains. Domain 2 is rotated from first domain by 180.0 degrees about reciprocal axis -0.001 0.000 1.000 and real axis 0.425 -0.001 1.000. Of 999 reflections, 869 reflections within 0.250 of an integer index are assigned to domain 1 (130 reflections not yet assigned to a domain), 646 reflections within 0.250 of an integer index are assigned to domain 2, 121 of them exclusively.

The data were integrated with SAINT to give the following; (R_{int} all scans = 0.1057)

8959 data (2726 unique) involve domain 1 only, mean I/sigma 4.1

8923 data (2744 unique) involve domain 2 only, mean I/sigma 2.7

19687 data (6016 unique) involve 2 domains, mean I/sigma 4.2

Refinement of F^2 against ALL reflections. The weighted R-factor (*w*R) and goodness of fit (S) are based on F^2, conventional R-factors (R) are based on F, with F set to zero for negative F^2. The threshold expression of $F^2 > 2\sigma(F^2)$ is used only for calculating R-factors(gt) etc. and is not relevant to the choice of reflections for refinement. R-factors based on F^2 are statistically about twice as large as those based on F, and R-factors based on ALL data will be even larger.

All esds (except the esd in the dihedral angle between two l.s. planes) are estimated using the full covariance matrix. The cell esds are taken into account individually in the estimation of esds in distances, angles and torsion angles; correlations between esds in cell parameters are only used when they are defined by crystal symmetry. An approximate (isotropic) treatment of cell esds is used for estimating esds involving l.s. planes.

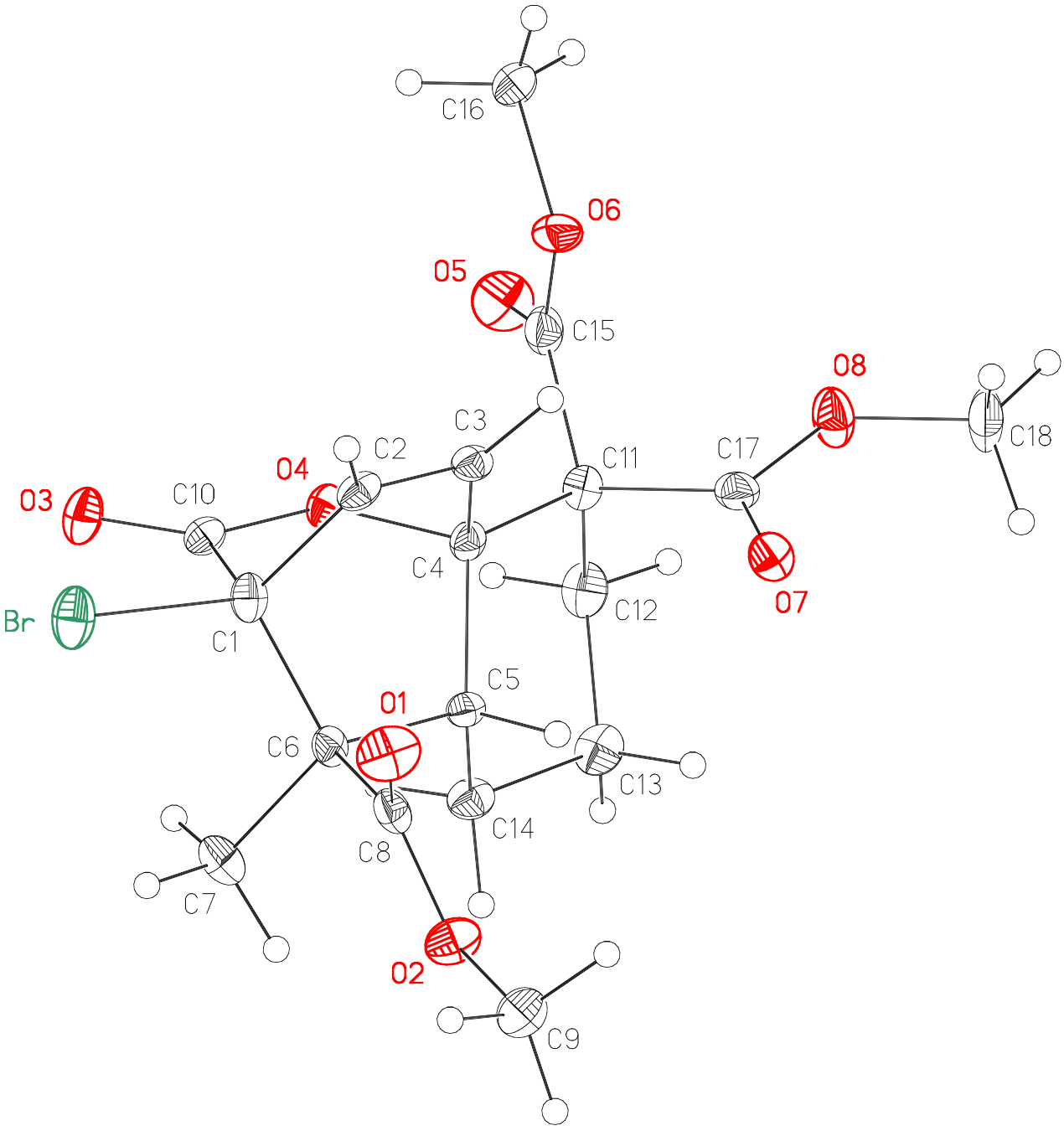
C16
O6
O5
C15
O8
C18
C3
C2
C11
C17
O4
O3
C10
C4
O7
C12
Br
C1
C5
O1
C6
C13
C14
C8
C7
O2
C9

Table A2.2. Atomic coordinates (x 10^4) and equivalent isotropic displacement parameters (Å^{2}x 10^3) for ***116a*** *(CCDC 656115). U(eq) is defined as the trace of the orthogonalized U^{ij} tensor.*

	x	y	z	U_{eq}
Br	2249(1)	6847(1)	71(1)	23(1)
O(1)	184(3)	6893(1)	1925(1)	25(1)
O(2)	2607(3)	6719(1)	3196(1)	20(1)
O(3)	5675(3)	7904(1)	152(1)	20(1)
O(4)	5019(3)	8586(1)	1275(1)	13(1)
O(5)	5955(3)	10171(1)	1567(2)	28(1)
O(6)	2525(3)	10033(1)	1213(2)	20(1)
O(7)	1630(3)	9172(1)	3348(1)	17(1)
O(8)	3101(3)	10212(1)	3340(2)	23(1)
C(1)	2879(4)	7589(1)	969(2)	15(1)
C(2)	1050(4)	8065(1)	944(2)	14(1)
C(3)	1473(4)	8608(1)	1471(2)	13(1)
C(4)	3680(4)	8651(1)	1978(2)	13(1)
C(5)	4156(4)	8012(1)	2618(2)	12(1)
C(6)	3644(4)	7343(1)	1997(2)	13(1)
C(7)	5477(4)	6843(2)	2057(2)	19(1)
C(8)	1915(4)	6963(1)	2347(2)	15(1)
C(9)	1088(4)	6368(2)	3626(2)	22(1)
C(10)	4658(4)	8021(1)	728(2)	14(1)
C(11)	4347(4)	9350(1)	2453(2)	13(1)
C(12)	6527(4)	9303(2)	3073(2)	20(1)
C(13)	6723(4)	8703(1)	3736(2)	19(1)
C(14)	6345(4)	8030(1)	3211(2)	16(1)
C(15)	4393(5)	9904(1)	1703(2)	18(1)
C(16)	2494(5)	10525(2)	463(2)	29(1)
C(17)	2832(4)	9553(1)	3078(2)	16(1)
C(18)	1813(5)	10453(2)	3980(2)	27(1)

Table A2.3. Bond lengths [Å] and angles [°] for **116a** (CCDC 656115)

Br-C(1)	1.940(3)	C(3)-C(4)-C(5)	108.6(2)
O(1)-C(8)	1.200(3)	O(4)-C(4)-C(11)	103.18(19)
O(2)-C(8)	1.325(3)	C(3)-C(4)-C(11)	115.7(2)
O(2)-C(9)	1.453(3)	C(5)-C(4)-C(11)	115.1(2)
O(3)-C(10)	1.196(3)	C(14)-C(5)-C(4)	112.5(2)
O(4)-C(10)	1.352(3)	C(14)-C(5)-C(6)	114.6(2)
O(4)-C(4)	1.484(3)	C(4)-C(5)-C(6)	108.3(2)
O(5)-C(15)	1.206(3)	C(8)-C(6)-C(7)	107.8(2)
O(6)-C(15)	1.328(3)	C(8)-C(6)-C(1)	110.1(2)
O(6)-C(16)	1.451(3)	C(7)-C(6)-C(1)	110.7(2)
O(7)-C(17)	1.206(3)	C(8)-C(6)-C(5)	107.2(2)
O(8)-C(17)	1.339(3)	C(7)-C(6)-C(5)	113.9(2)
O(8)-C(18)	1.457(3)	C(1)-C(6)-C(5)	107.2(2)
C(1)-C(2)	1.517(4)	O(1)-C(8)-O(2)	124.4(2)
C(1)-C(10)	1.541(4)	O(1)-C(8)-C(6)	125.7(3)
C(1)-C(6)	1.565(4)	O(2)-C(8)-C(6)	109.9(2)
C(2)-C(3)	1.307(4)	O(3)-C(10)-O(4)	120.8(2)
C(3)-C(4)	1.508(4)	O(3)-C(10)-C(1)	127.9(2)
C(4)-C(5)	1.551(4)	O(4)-C(10)-C(1)	111.3(2)
C(4)-C(11)	1.551(4)	C(17)-C(11)-C(15)	110.3(2)
C(5)-C(14)	1.539(4)	C(17)-C(11)-C(12)	107.9(2)
C(5)-C(6)	1.584(4)	C(15)-C(11)-C(12)	108.3(2)
(6)-C(8)	1.529(4)	C(17)-C(11)-C(4)	109.3(2)
C(6)-C(7)	1.543(4)	C(15)-C(11)-C(4)	109.7(2)
C(11)-C(17)	1.531(4)	C(12)-C(11)-C(4)	111.3(2)
C(11)-C(15)	1.542(4)	C(13)-C(12)-C(11)	112.2(2)
C(11)-C(12)	1.553(4)	C(12)-C(13)-C(14)	111.0(2)
C(12)-C(13)	1.506(4)	C(13)-C(14)-C(5)	110.6(2)
C(13)-C(14)	1.514(4)	O(5)-C(15)-O(6)	124.6(3)
		O(5)-C(15)-C(11)	123.5(3)
C(8)-O(2)-C(9)	115.5(2)	O(6)-C(15)-C(11)	111.9(2)
C(10)-O(4)-C(4)	114.65(19)	O(7)-C(17)-O(8)	123.6(3)
C(15)-O(6)-C(16)	114.2(2)	O(7)-C(17)-C(11)	125.7(2)
C(17)-O(8)-C(18)	115.4(2)	O(8)-C(17)-C(11)	110.6(2)
C(2)-C(1)-C(10)	107.5(2)		
C(2)-C(1)-C(6)	108.6(2)		
C(10)-C(1)-C(6)	105.4(2)		
C(2)-C(1)-Br	111.65(18)		
C(10)-C(1)-Br	108.98(18)		
C(6)-C(1)-Br	114.29(17)		
C(3)-C(2)-C(1)	113.5(2)		
C(2)-C(3)-C(4)	114.3(2)		
O(4)-C(4)-C(3)	107.7(2)		
O(4)-C(4)-C(5)	105.71(19)		

*Table A2.4. Anisotropic displacement parameters ($Å^2 x\ 10^4$) for **116a** (CCDC 656115). The anisotropic displacement factor exponent takes the form: $-2\pi^2 [h^2 a^{*2} U^{11} + ... + 2 h k a^* b^* U^{12}]$.*

	U^{11}	U^{22}	U^{33}	U^{23}	U^{13}	U^{12}
Br	227(2)	246(1)	214(2)	-91(1)	69(1)	-62(1)
O(1)	142(10)	318(12)	278(12)	49(10)	22(9)	-55(10)
O(2)	184(11)	222(11)	209(12)	53(8)	57(9)	-57(8)
O(3)	211(11)	248(11)	174(11)	-37(8)	99(9)	-33(8)
O(4)	111(10)	171(9)	116(10)	-7(8)	47(8)	-12(7)
O(5)	227(13)	270(11)	388(14)	65(10)	169(10)	-56(9)
O(6)	258(12)	163(10)	205(12)	73(8)	79(10)	34(8)
O(7)	153(10)	159(10)	229(12)	3(8)	86(9)	-23(8)
O(8)	309(13)	156(10)	277(13)	-61(9)	155(10)	-50(9)
C(1)	131(15)	166(13)	164(15)	-44(11)	50(12)	-27(11)
C(2)	98(13)	209(14)	112(14)	30(11)	11(11)	-4(11)
C(3)	106(13)	164(13)	134(15)	32(11)	25(11)	20(11)
C(4)	129(14)	139(12)	123(14)	3(10)	52(12)	-9(11)
C(5)	116(14)	133(13)	114(14)	18(10)	18(11)	4(10)
C(6)	105(13)	133(12)	152(15)	3(10)	61(12)	3(10)
C(7)	161(14)	153(12)	270(16)	-18(13)	57(12)	18(12)
C(8)	147(15)	116(14)	208(16)	-11(11)	86(12)	4(11)
C(9)	236(17)	225(15)	245(18)	57(13)	142(14)	-24(13)
C(10)	133(13)	166(14)	98(14)	-6(10)	-22(11)	3(11)
C(11)	110(13)	148(13)	143(15)	-20(11)	31(12)	-40(11)
C(12)	180(16)	219(14)	200(16)	-51(12)	37(13)	-52(12)
C(13)	129(14)	255(15)	170(16)	-21(12)	-10(13)	-29(12)
C(14)	116(13)	208(15)	160(15)	27(11)	9(12)	10(11)
C(15)	226(16)	162(14)	189(17)	-12(12)	106(14)	-1(12)
C(16)	470(20)	234(16)	214(17)	93(13)	207(16)	111(14)
C(17)	195(15)	140(13)	142(16)	3(11)	-10(12)	16(11)
C(18)	384(19)	211(15)	260(18)	-82(13)	205(16)	-32(14)

APPENDIX 3

Ireland–Claisen Model Studies

A3.1 Ireland–Claisen Model Studies

Having successfully established proof of concept for the key intramolecular pyrone Diels–Alder cycloaddition, we sought to model the proposed Ireland–Claisen rearrangement (ICR). Our initial plan was to prepare prenylated pyrone **132** by coupling of pyrone acid **133** with geraniol. Pyrone acid **133** would in turn be prepared from saponification and decarboxylation of malonates **124** or **125** (Scheme A3.1).

Scheme A3.1. Retrosynthetic analysis of ICR model system

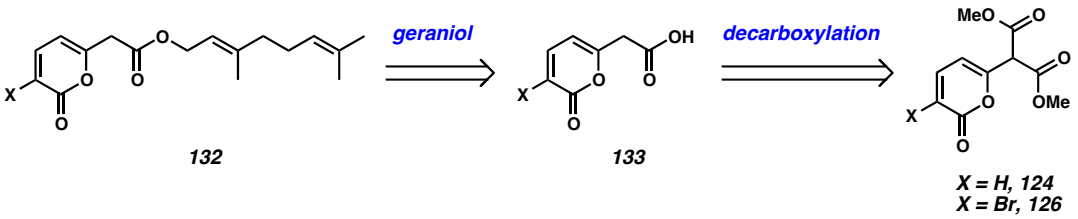

However, in practice, treatment of malonates **124** or **126** with acidic or basic aqueous conditions led to complex mixtures of decomposition products. Furthermore, under a variety of Krapcho's decarboxylation conditions, non-productive decomposition of the pyrone was also observed (Scheme A3.2).

Scheme A3.2. Initial attempts of saponification/decarboxylation

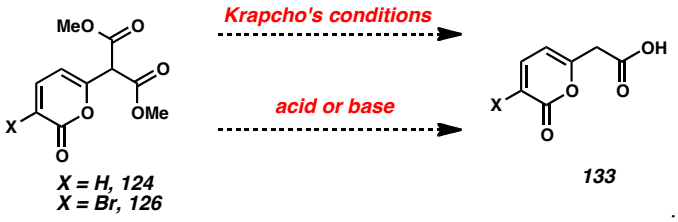

We hypothesized that hydrolysis of the pyrone moiety was the cause of decomposition.[1] In light of this hypothesis, our attention turned to a milder, nonaqueous,

decarboxylative method (Scheme A3.3). We envisioned that substrate **113a** could be derived from the Pd-catalyzed decarboxylative protonation of allyl ester **134**.

Scheme A3.3. Revised retrosynthetic analysis of ICR model system

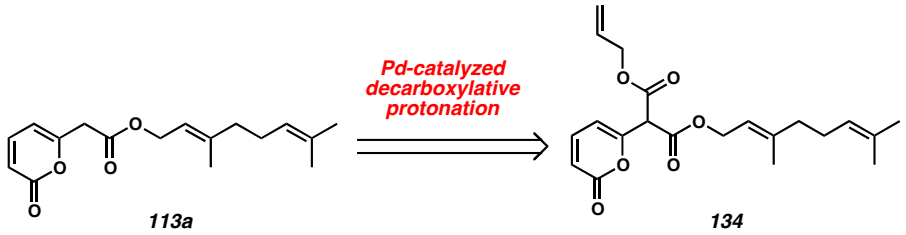

The construction of desired pyrone ester **113a** is shown in Scheme A3.4. Heating of Meldrum's acid (**135**) with a stoichiometric amount of geraniol provided smooth conversion to half-acid **136**. Treatment of **136** with allyl bromide and K_2CO_3 gave the mixed malonate **137** in excellent yield. Exposure of mixed malonate **137** to *6*-choloro-*2*-pyrone and NaH yielded pyrone malonate **134**. Gratifyingly, treatment of **134** with $Pd(PPh_3)_4$, NEt_3, and formic acid yielded the desired ester **113a**. Although the Pd-catalyzed, decarboxylative protonation gave variable yields (0–82%) of the desired ester, sufficient material for our Ireland–Claisen model studies were prepared. No attempts were made to optimize this reaction, but in the best case the desired protonation product (**113a**) was made exclusively. In the lower yielding cases, allylation was identified as the competing process.

Scheme A3.4. Construction of the ICR model compound

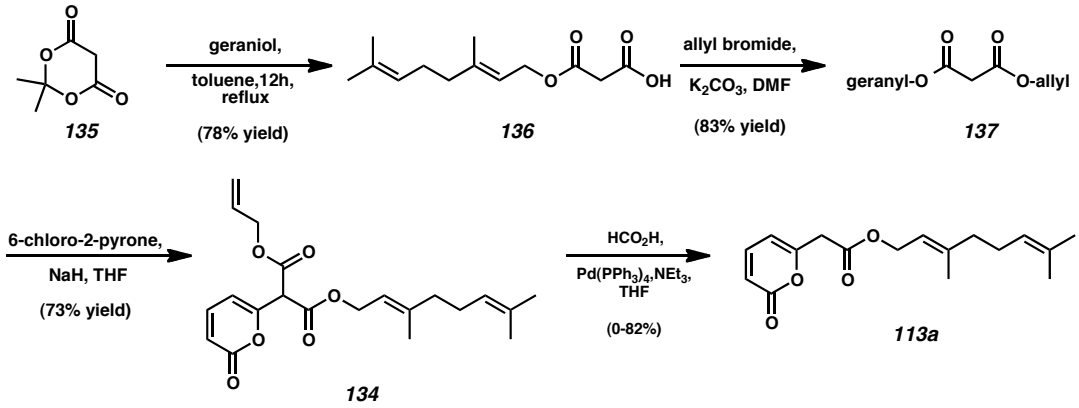

Importantly, treatment of ester **113a** with LDA and TMSCl at low temperatures allowed for smooth [3,3] sigmatropic rearrangement to desired ICR product **112a**. While initial efforts used THF as solvent, it was found that the use of HMPA as a co-solvent increased the reaction rate and improved the diastereoselectivity from 1.5:1 to 5:1 (Scheme A3.5). Much to our disappointment, attempts to directly cyclize ICR product **111a** *via* IMPDA were unsuccessful.

The relative stereochemistry of the Ireland–Claisen rearrangement product has not yet been established. However, control over E/Z selectivity in enolate formation, as well as the use of geraniol and its olefin isomer nerol are envisioned to allow for sufficient stereochemical modularity to prepare most of the transtaganolides, many of which are epimers at C8 (Scheme 2.2).

Scheme A3.5. Completion of ICR model study

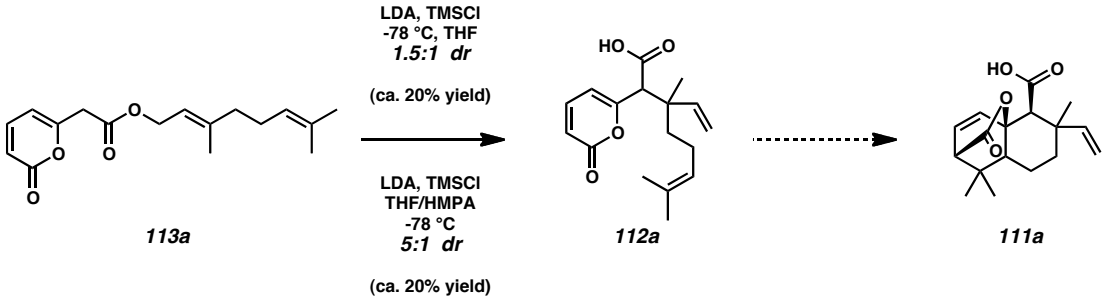

A3.2 Conclusion

In conclusion, we have proposed a highly modular route to the transtaganolides. This route is strongly supported by extensive model study work. An intramolecular pyrone Diels–Alder (IMPDA) model system was constructed and used to forge the tricyclic core of the natural product targets. Furthermore, an Ireland–Claisen model system was prepared and utilized in the construction of the C8 quaternary stereocenter.

---

1) Eicher, T.; Hauptmann, S.; 6.3 *2H*-Pyran-*2*-one. The Chemistry of Heterocycles, 2nd edition. Wiley-VCH: New York, 2003; pp 233–256.

Chapter 3

The Total Syntheses of (±)-Transtaganolide C, (±)-Transtaganolide D, (±)-Basiliolide B, and (±)-epi-8-Basiliolide B

3.1 Introduction

Owing to their interesting biological activity and striking architectures, the transtaganolides (**75** and **85**) and basiliolides (**76**) have inspired significant interest from the synthetic community (Scheme 2.2). Initial synthetic efforts from our own group,[1] as well as those of Dudley[2] and Lee,[3] have utilized an intramolecular pyrone Diels–Alder (IMPDA) cycloaddition to construct the oxabicyclo[2.2.2]octene moiety constituting the ABD ring system of **75**, **76** and **85**. However, these studies failed to install the C8 quaternary center present in all of the transtaganolides and basiliolides (Scheme 2.2).

Unpublished model studies from our group demonstrated the propensity of prenylated pyrones such as **113a** to undergo facile Ireland–Claisen rearrangements (ICR) (Scheme 2.16). However, initial efforts to coax that ICR product **113a** to cyclize *via* IMPDA were unsuccessful. As evidenced by our own IMPDA work, and extensive literature precedent, activation of the pyrone moiety by halogenation was needed to allow

IMPDA to proceed.[4] Furthermore, we posited that halogenation of the *5*–position would have the additional benefit of allowing for elaboration of the core to the natural product targets.

3.2 Retrosynthetic Analysis

Retrosynthetically, we envisioned that transtaganolide C (**75a**), transtaganolide D (**75b**) basiliolide B (**76a**), and *epi*-8-basiliolide B (**76b**) could be prepared in the laboratory via an Ireland–Claisen rearrangement (ICR)/intramolecular pyrone Diels–Alder (IMPDA) sequence (Scheme 3.1). We proposed that intermediate **138** could arise from pyrone **139** *via* an IMPDA. Furthermore, we reasoned that IMPDA substrate **139** could be derived from the Ireland–Claisen rearrangement of pyrone ester **140**. The ICR substrate (**140**) was to arise from the coupling of a geraniol derivative (**141**) to pyrone acid **142**, which possesses the requisite halogenation.

Scheme 3.1. Retrosynthetic analysis

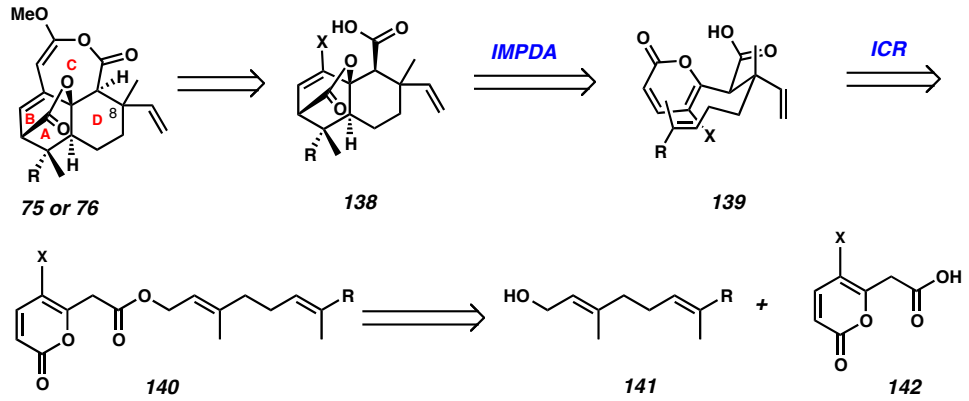

3.3 Synthesis of Halogenated Substrate

The synthesis began with the palladium catalyzed coupling of known (*Z*)-methyl iodoacrylate **143**[5] with commercially available 3-butyn-1-ol to provide methylester **144** in

good yield (Scheme 3.2). Heating of ester **144** with $CuBr_2$ in the presence of a catalytic amount of dicyclohexylamine hydrobromide led to the formation of bromopyrone **145**.[9] Jones oxidation of the resulting primary alcohol **145** yielded the desired pyrone acid **142a** in moderate yield. Direct DCC coupling of the pyrone acid **142a** to geraniol cleanly provided Ireland–Claisen substrate **140a**. We were delighted to find that a slow addition of a NaHMDS solution to a cold mixture of pyrone ester **140a** and TMSCl promoted a high yielding Ireland–Claisen rearrangement. After removal of volatiles from the crude ICR reaction,[6] prolonged heating in a sealed tube charged with benzene and argon smoothly afforded the IMPDA product **138d** in 87% yield from **140**a as a mixture of C(8) diastereomers (~2:1 dr).

Scheme 3.2. Synthesis of the functionalized core

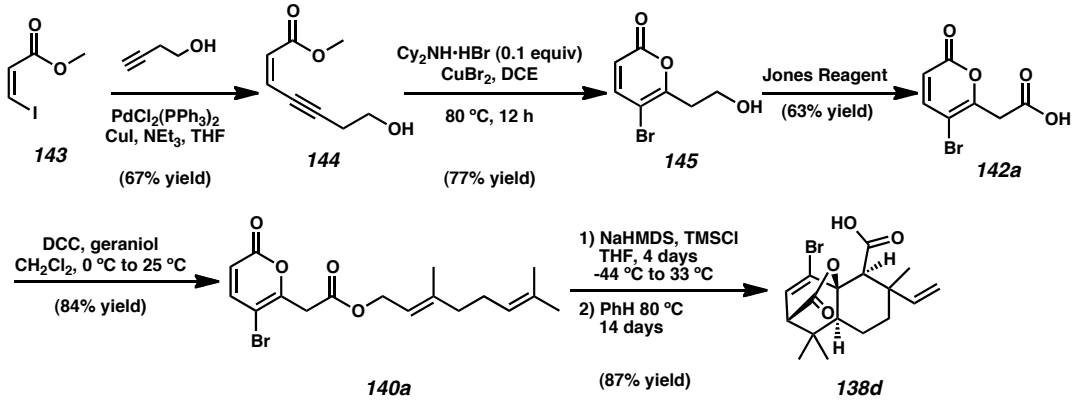

3.4 Larsson's ICR Conditions and Our Development of an ICR/IMPDA Cascade

Shortly after our preparation of brominated tricycle **138d**, Larsson and co-workers reported a nearly identical strategy for the synthesis of the cores of the transtaganolides (Scheme 3.3).[6] Notable in their strategy was the catalytic use of a mild base to induce the ICR. Furthermore, they demonstrated that tricycle **147** was a competent cross-coupling

partner, as **148** could be prepared by treatment with TMS-acetylene employing Sonagashira's conditions.

Scheme 3.3. Larsson's partial synthesis

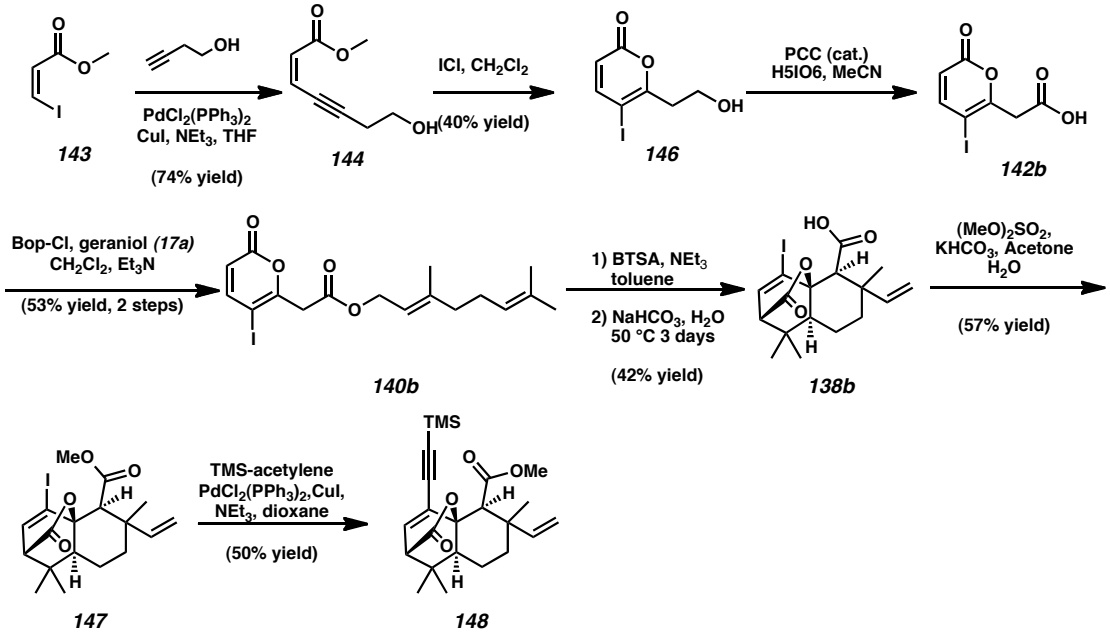

While the authors specifically stated that the IMPDA did not proceed under their ICR conditions due to substrate decomposition, we knew from our work that if the intermediate TMS-ester was not hydrolyzed, the ICR product could be used directly in the IMPDA reaction. Capitalizing on Larsson's successful choice of reaction conditions, and experimental insight gained by our group, we were able to develop conditions for a one-pot ICR/IMPDA cascade reaction, preparing **138b** from **140b** in a single operation (Scheme 3.4).

Scheme 3.4. Development of the ICR/IMPDA cascade reaction

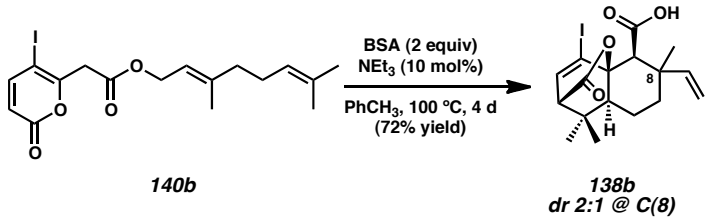

3.5 The Total Syntheses of Transtaganolides C and D

The challenge in advancing intermediates akin to tricycle **138b** (Scheme 3.4) to the natural products lies in the formation of the unusual *7*-methoxy-*4*,*5*-dihydrooxepin-*2*(*3H*)-one ring (ring C, Scheme 3.5).[7] Embedded within this ring is an acyl ketene acetal that is potentially labile to both acid and base, as evidenced by the co-isolation of seco acid derivatives (**90** and **91**, Scheme 2.2) from *Thapsia* sp.[8] Retrosynthetically, we envisioned that the C-ring could be prepared by a formal [5+2] annulation process of advanced tricycle **138b** and methoxyacetylene, or a suitable derivative, leading directly to the natural products (Scheme 3.5). Tricycle **138** would be prepared from the tandem Claisen/Diels-Alder sequence of ester **140**. Importantly, with an available late stage construction of ring C, variants of this ester (e.g., **140b** and **140c**) prepared from geraniol derivatives could provide rapid access to a number of basiliolide and transtaganolide natural products.

Scheme 3.5. Retrosynthetic analysis of end-game strategy

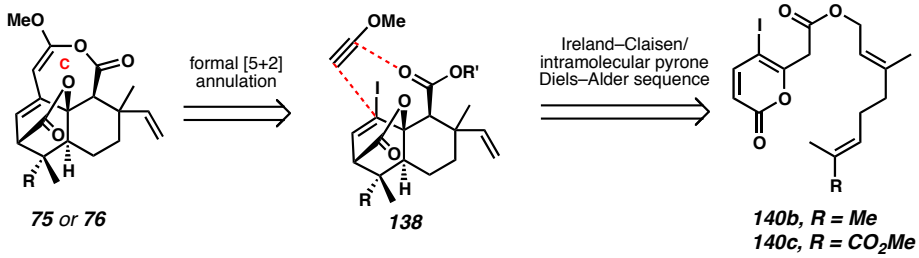

At the outset of our studies to build the C-ring, we attempted a variety of inter- and intramolecular annulation strategies but were unable to affect formation of the daunting C-ring. Having few remaining options, we turned our attention to approaches involving palladium-mediated cross-coupling reactions.[9] In addition to the possible steric hindrance of vinyl halide **138**, no successful cross-coupling reactions of methoxyacetylene or derivatives thereof have been reported to any vinyl or aryl halide. Nonetheless, limited reports of tin and zinc derivatives of commercial ethoxyacetylene in palladium-catalyzed cross-couplings have been published and provided some precedent for the coupling.[10,11] Hence, efforts turned to the preparation of stannane **151** (Scheme 3.6). We were pleased to find, that when exposed to $LiNEt_2$, 1,1-dimethoxy-2-chloro-acetaldehyde (**149**) was transformed into lithium acetylide **150**,[12] which could be quenched with tributyltin chloride to safely[13] afford stannane **151** in 78% yield in a single operation.

Scheme 3.6. Synthesis of methoxyacetylene reagent

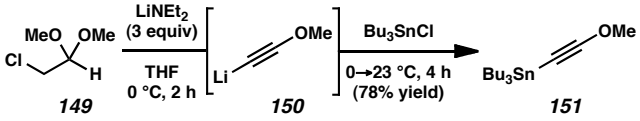

Attempts to directly couple stannane **151** to iodoacid **138b** (prepared from **140b**) were unsuccessful under standard cross-coupling conditions. We attributed the lack of desired reactivity to acid-mediated decomposition of stannane **151**.[14] Therefore, extensive efforts were undertaken to devise a suitable protecting group strategy for the carboxylic acid moiety. Ultimately, acid **138b** was transformed into *tert*-butyl

dimethylsilyl ester **152**[15] by treatment with TBSCl and imidazole.[16] Exposure of silyl ester **152** and stannane **151** to $Pd(PPh_3)_4$ or Fu's $Pd(Pt\text{-}Bu_3)_2$[17] led to transient formation of enyne **153**. While observable by mass spectrometry and 1H NMR analysis, direct isolation of methoxyenyne **153** proved difficult. After optimization of the reaction conditions, we found that aqueous work-up effected an situ desilylation and cyclization to afford a separable mixture of transtaganolide C (**75a**) and transtaganolide D (**75b**) in 21% and 10% yield, respectively (19% and 10% with Fu's catalyst). The relative stereochemistry of synthetic transtaganolide C (**75a**) was unambiguously confirmed by X-ray crystallography,[18] and synthetic transtaganolides C and D were spectroscopically indistinguishable from the naturally occurring isolates.[19]

Scheme 3.7. Total synthesis of transtaganolides C and D and X-ray crystal structure

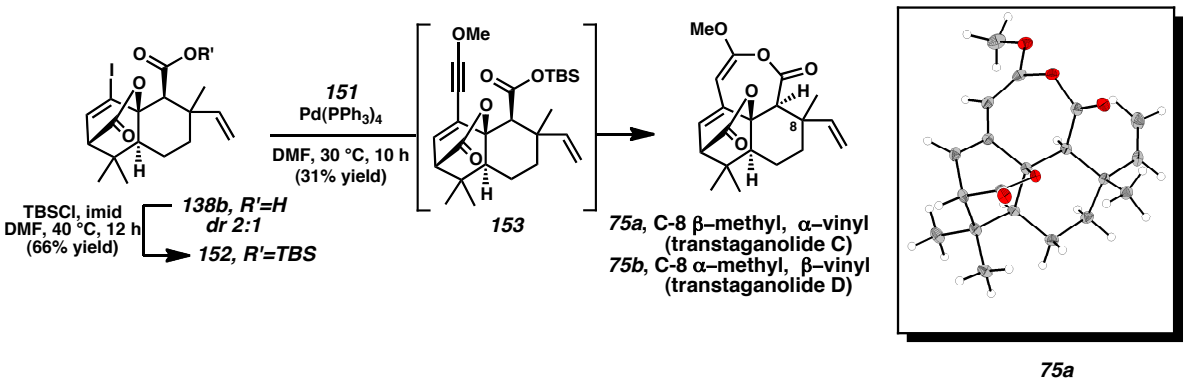

3.6 The Total Syntheses of Basiliolide B and *Epi*-8-Basiliolide B

With the syntheses of transtaganolide C (**75a**) and transtaganolide D (**75b**) serving as a proof of concept, we sought to extend our approach to the rapid total synthesis of more complex members of this family. Our efforts to prepare basiliolide B (**76a**) were undertaken by preparation of known geraniol derivative **141a** (available in 3

steps)[20] and coupling to iodopyrone acid **142b** producing ester **140c** in excellent yield (Scheme 3.8).

We were pleased to find that treatment of ester **140c** with *N,O*-bis(trimethylsilyl)acetamide (BSA) and triethylamine resulted in a Claisen/Diels-Alder cascade to yield the resulting acid **138c** in a single operation and in 67% yield as a 2:1 mixture of diastereomers (Scheme 3.8). This represents a significant improvement over previous, two-step procedures that required isolation and/or manipulation of the Claisen products (see Schemes 3.2–3.4), and is the first example in this area that utilizes a more functionalized dienophile. Following silylation of the free acid (**138c→154**),[21] the resulting silyl ester **154** was exposed to our methoxyalkynylation conditions comprised of stannane **151** and $Pd(Pt\text{-}Bu_3)_2$. Gratifyingly, cross-coupling and treatment of the crude product mixture with H_2O resulted in the production and isolation of basiliolide B (**76a**)[22] and previously unreported *epi*-8-basiliolide B (**76b**) in 5% and 14% yields, respectively (6% and 12% with $Pd(PPh_3)_4$).

Scheme 3.8. Synthesis of basiliolide B and epi-8-basiliolide B

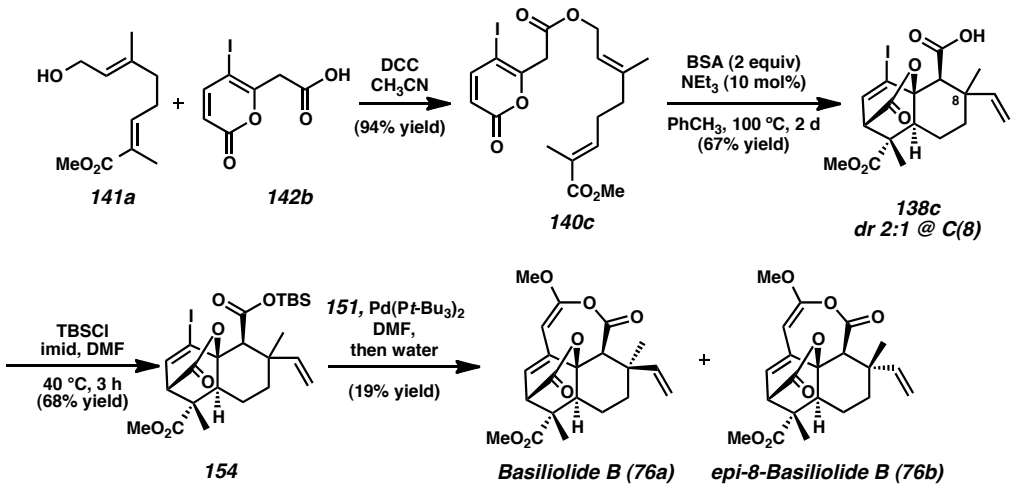

3.7 Conclusion

A rapid, modular, and convergent strategy for the synthesis of the basiliolides and transtaganolides has been described. Basiliolide B (**76a**), *epi*-8-basiliolide B (**76b**), transtaganolide C (**75a**) and transtaganolide D (**75b**) were each prepared in only seven steps (longest linear sequence) from commercially available materials. Critical to the success of this effort was the development of an effective preparation of, and cross-coupling protocol for, methoxyacetylide **151**. Remarkably, the disclosed end-game procedure transforms simple, monocyclic, achiral precursors to the stereochemically rich, tetracyclic natural products in three steps (e.g., **140c→76a**).

3.8 Experimental Section

3.8.1 Materials and Methods

Unless otherwise stated, reactions were performed in flame-dried glassware under an argon or nitrogen atmosphere using dry deoxygenated solvents. Solvents were dried by passage through an activated alumina column under argon. $Pd(t\text{-}Bu_3P)_2$, *N,N'*-dicyclohexylcarbodiimide, 1,1-dimethoxy-2-chloro-acetaldehyde, *N,O*-bis(trimethylsilyl)acetamide, *N*-methyl-*N*-(*tert*-butyldimethylsilyl)trifluoroacetamide, and imidazole were purchased from Sigma-Aldrich Chemical Company and used as received. $Pd(PPh_3)_4$ was prepared using known methods. Thin-layer chromatography (TLC), both preparatory and analytical, were performed using E. Merck silica gel 60 F254 precoated plates (0.25 mm) and visualized by UV fluorescence quenching, *p*-anisaldehyde, I_2, or $KMnO_4$ staining. ICN Silica gel (particle size 0.032–0.063 mm) was used for flash chromatography. ^1H NMR, and ^{13}C NMR spectra were recorded on a Varian Mercury 300 (at 300 MHz) or on a Varian Unity Inova 500 (at 500 MHz). ^1H NMR spectra are reported relative to $CDCl_3$ (7.26 ppm). Data for ^1H NMR spectra are reported as follows: chemical shift, multiplicity, coupling constant (Hz), integration. Multiplicities are reported as follows: s = singlet, d = doublet, t = triplet, q = quartet, sept. = septet, m = multiplet, comp. m = complex multiplet, app. = apparent, bs = broad singlet. ^{13}C NMR spectra are reported relative to $CDCl_3$ (77.0 ppm). FTIR spectra were recorded on a Perkin Elmer SpectrumBX spectrometer and are reported in frequency of absorption (cm^{-1}). HRMS were acquired using an Agilent 6200 Series TOF with an Agilent G1978A Multimode source in electrospray ionization (ESI), atmospheric pressure chemical ionization (APCI) or multimode-ESI/APCI. Crystallographic data were obtained from the Caltech X-ray Diffraction Facility.

3.8.2 Experimental Procedures

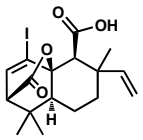

Iodoacid 138b. To a solution of **140b** (6.2 g, 15 mmol, 1.0 equiv) in toluene (75 mL) at 25 ˚C in a sealed tube was added *N,O*-bis(trimethylsilyl)acetamide (7.2 mL, 30 mmol 2.0 equiv). To the reaction mixture was then added triethylamine (0.41 mL, 3.0 mmol, 0.20 equiv). The reaction mixture was heated to 110 ˚C and stirred for 20 minutes. The mixture was cooled to 25 ˚C and diluted with toluene (750 mL). The reaction mixture was then re-heated to 100 ˚C and stirred for 4 days. The mixture was cooled to 25 ˚C and extracted with saturated aqueous $NaHCO_3$ (7 x 100 mL). To the combined aqueous extracts was added 1 M aqueous HCl until pH = 3. The aqueous layer was then extracted with ethyl acetate (3 x 100 mL). The combined organics were dried over Na_2SO_4, and concentrated by rotary evaporation to yield 3.2 g (51%) of **138a** as a tan foam.

Major: ^{1}H NMR (500 MHz, $CDCl_3$) δ 6.93 (d, *J* = 6.5 Hz, 1H), 6.01 (dd, *J* = 10.5, 17.5 Hz, 1H), 5.05–5.02 (m, 2H), 3.00–2.94 (m, 2H), 1.68–1.42 (m, 5H), 1.29 (s, 3H), 1.08 (s, 3H), 1.00 (s, 3H); ^{13}C NMR (125 MHz, $CDCl_3$) δ 172.7, 170.5, 148.0, 140.0, 111.5, 97.9, 84.7, 59.4, 56.5, 47.9, 39.8, 38.2, 36.8, 29.8, 24.5, 20.5, 18.4.

Minor: ^{1}H NMR (500 MHz, $CDCl_3$) δ 6.93 (d, *J* = 6.5 Hz, 1H), 6.35 (dd, *J* = 11.0, 17.5 Hz, 1H), 5.09 (d, *J* = 11.0 Hz, 1H), 5.05–5.02 (m, 1H), 3.00–2.94 (m, 2H), 1.92–1.90 (m, 1H), 1.68–1.42 (m, 4H), 1.26 (s, 3H), 1.08 (s, 3H), 1.00 (s, 3H); ^{13}C NMR (125 MHz,

$CDCl_3$) δ 172.7, 170.4, 140.4, 140.3, 113.7, 97.4, 84.8, 61.0, 56.6, 48.0, 39.3, 38.7, 37.0, 29.8, 29.5, 24.5, 20.6.

FTIR (Neat Film NaCl) 3082, 2967, 2931, 1754, 1741, 1738, 1732, 1708, 1414, 1396, 1219, 1175, 964, 916, 874, 797, 736 cm^{-1}; HRMS (Multimode-ESI/APCI) m/z calc'd for $C_{17}H_{21}O_4I$ $[M+H]^+$: 417.0557, found 417.0553.

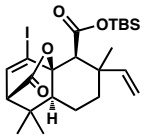

***tert*-Butyldimethylsilyl ester 152**. To a solution of **138a** (46 mg, 0.11 mmol, 1.0 equiv) in dimethylformamide (0.30 mL) were added *tert*-butyldimethylsilylchloride (84 mg, 0.56 mmol, 5.0 equiv) and imidazole (76 mg, 1.1 mmol, 10 equiv). The reaction was warmed to 40 ˚C and then stirred for 12 hours. The reaction mixture was then diluted with saturated aqueous NaCl (1 mL) and extracted with diethyl ether/hexane (1:1) (3 x 2 mL). The combined organic extracts were washed with saturated aqueous $KHSO_4$ (1 mL) and then with saturated aqueous NaCl (3 x 1 mL). The combined organics were dried over Na_2SO_4, and concentrated by rotary evaporation. The crude oil was chromatographed (ethyl acetate in hexane 10⇒50% on SiO_2) to yield 39 mg (66%) of **6b** as a white powder.

Procedure 2. To a solution of **138a** (180 mg, 0.43 mmol, 1.0 equiv) in acetonitrile (0.43 mL) was added *N*-methyl-*N*-(*tert*-butyldimethylsilyl)trifluoroacetamide (1.0 g, 4.3 mmol, 10 equiv) at 25 ºC and stirred for 15 minutes. The reaction mixture was diluted with

saturated aqueous NaCl (1 mL) and extracted with diethyl ether/hexane (1:1) (3 x 2 mL). The combined organic extracts were washed with saturated aqueous $KHSO_4$ (1 mL) and then with saturated aqueous NaCl (3 x 1 mL). The combined organics were dried over Na_2SO_4, and concentrated by rotary evaporator. The crude oil was chromatographed (ethyl acetate in hexane 10⇒50% on SiO_2) to yield 150 mg (64%) of **152** as a white powder.

Major: ^{1}H NMR (500 MHz, $CDCl_3$) δ 6.90 (d, *J* = 6.5 Hz, 1H), 6.03 (dd, *J* = 11.0, 17.5 Hz, 1H), 4.99 (d, *J* = 17.5 Hz, 1H), 4.99 (d, *J* = 11.0 Hz, 1H), 2.95 (s, 1H), 2.93 (d, *J* = 6.5 Hz, 1H), 1.66–1.39 (m, 4H), 1.32–1.29 (m, 1H), 1.26 (s, 3H), 1.07 (s, 3H), 0.99 (s, 3H), 0.91 (s, 9H), 0.29 (s, 3H), 0.27 (s, 3H); ^{13}C NMR (125 MHz, $CDCl_3$) δ 170.6, 169.1, 149.2, 139.7, 110.5, 98.7, 84.6, 60.4, 56.7, 48.2, 40.1, 38.7, 36.9, 29.8, 25.5, 24.5, 20.7, 18.1, 17.5, –4.8, –4.8**.**

Minor: ^{1}H NMR (500 MHz, $CDCl_3$) δ 6.90 (d, *J* = 6.5 Hz, 1H), 6.40 (dd, *J* = 11.0, 17.5 Hz, 1H), 5.05 (dd, *J* = 1.0, 11.0 Hz, 1H), 5.03–4.98 (m, 1H), 2.91 (d, *J* = 6.5 Hz, 1H), 2.86 (s, 1H), 1.85 (dt, J = 3.5, 13.5 Hz, 1H), 1.66–1.39 (m, 3H), 1.36 (s, 3H), 1.34–1.29 (m, 1H), 1.05 (s, 3H), 0.98 (s, 3H), 0.90 (s, 9H), 0.30 (s, 3H), 0.28 (s, 3H); ^{13}C NMR (125 MHz, $CDCl_3$) δ 170.6, 169.3, 141.3, 139.9, 112.9, 98.3, 84.7, 61.8, 56.8, 48.4, 39.6, 39.4, 37.2, 29.6, 25.6, 25.4, 24.4, 20.8, 17.5, –4.9, –4.9.

FTIR (Neat Film NaCl) 2959, 2929, 2857, 1760, 1716, 1708, 1471, 1284, 1250, 1173, 1022, 967, 840, 827, 789, 736 cm^{-1}; HRMS (Multimode-ESI/APCI) m/z calc'd for $C_{23}H_{36}O_4ISi$ $[M+H]^+$: 531.1422, found 531.1432.

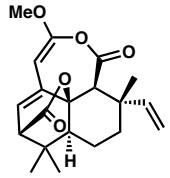

75a **Transtaganolide C**
(*aka Basiliolide A2*)

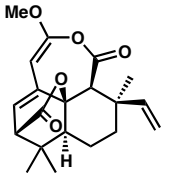

75b **Transtaganolide D**
(*aka Basiliolide A1*)

Transtaganolides (**75**). In a nitrogen filled glovebox, to a solution of **152** (16 mg, 0.030 mmol, 1.0 equiv) and $Pd(PPh_3)_4$ (35 mg, 0.030 mmol, 1 equiv) in dimethylformamide (0.30 mL, 0.10 M) was added tributyl(2-methoxyethynyl)stananne (**151**) (32 mg, 0.090 mmol, 3.0 equiv). The reaction was stirred at 31 ˚C for 16 h. The reaction mixture was then treated with water (30 μL) and stirred at room temperature for 1 hour. The mixture was diluted with ethyl acetate (1 mL) and washed with water (4 x 0.5 mL) and concentrated by rotary evaporation. The crude oil was purified by normal phase HPLC to yield 2.1 mg (21%) of transtaganolide C (**75a**) and 1.1 mg (10%) of transtaganolide D (**75b**) as white powders. Crystals were grown by slow evaporation from acetonitrile.

Procedure 2. In a nitrogen filled glovebox, to a solution of **152** (16 mg, 0.030 mmol, 1.0 equiv) and Pd(*t*-$Bu_3P)_2$ (15 mg, 0.030 mmol, 1.0 equiv) in dimethylformamide (0.30 mL, 0.10 M) was added tributyl(2-methoxyethynyl)stannane (**10**) (32 mg, 0.090 mmol, 3.0 equiv). The reaction was stirred at 31 ºC for 10 hours. The reaction mixture was then treated with water (30 μL) and stirred at room temperature for 1 hour. The mixture was diluted with ethyl acetate (1 mL) and washed with water (4 x 0.5 mL) and concentrated by rotary evaporation. The crude oil was purified by normal phase HPLC to yield 2.0 mg (19%) of transtaganolide C (**75a**) and 1.0 mg (10%) of transtaganolide D (**75b**) as white powders.

Transtaganolide C (75a).

^{1}H NMR (500 MHz, $CDCl_3$) δ6.07 (dd, *J* = 1.5, 6.5 Hz, 1H), 5.80 (dd, *J* = 11.0, 17.5 Hz, 1H), 5.07 (d, J = 17.5 Hz, 1H), 5.03 (d, *J* = 11.0 Hz, 1H), 5.00 (d, *J* = 1.5 Hz, 1H), 3.71 (s, 3H), 3.23 (s, 1H), 3.06 (d, *J* = 6.5 Hz, 1H), 1.71–1.63 (m, 3H), 1.60 (s, 3H), 1.44 (m, 1H), 1.30 (m, 1H), 1.08 (s, 3H), 0.97 (s, 3H); ^{13}C NMR (125 MHz, $CDCl_3$) δ 171.8, 162.3, 156.7, 146.5, 138.0, 123.6, 112.8, 87.3, 79.3, 56.3, 53.8, 50.6, 48.1, 38.4, 38.3, 33.3, 29.9, 24.8, 19.9, 19.2; FTIR (Neat Film NaCl) 2965, 2928, 2872, 1791, 1761, 1668, 1619, 1456, 1334, 1267, 1233, 1178, 1115, 970, 954, 828 cm^{-1}; HRMS (Multimode-ESI/APCI) m/z calc'd for $C_{20}H_{24}O_5$ $[M+H]^+$: 345.1697, found 345.1703; MP: 135–160 ºC (at these temperatures decarboxylation is thought to occur, as the crystalline sample and the resulting liquid were vigorously bubbling throughout the measurement; thus it is unclear whether thermal decomposition precluded state change).

Transtaganolide D (75b).

^{1}H NMR (500 MHz, $CDCl_3$) δ 7.00 (dd, *J* = 11.0, 17.5 Hz, 1H), 6.09 (dd, *J* = 1.0, 6.5 Hz, 1H), 5.15 (dd, *J* = 1.0, 11.0 Hz, 1H), 5.05 (dd, *J* = 1.0, 17.5 Hz, 1H), 5.02 (d, *J* = 1.0 Hz, 1H), 3.73 (s, 3H), 3.13 (s, 1H), 3.06 (d, *J* = 6.5 Hz, 1H), 1.91 (dt, *J* = 3.5, 13.5 Hz, 1H), 1.64 (dquint, *J* = 3.0, 13.5 Hz, 1H), 1.58 (m, 1H), 1.39 (dt, *J* = 3.5, 13.5 Hz, 1H), 1.33 (dd, *J* = 4.5, 13.5 Hz, 1H), 1.22 (s, 3H), 1.04 (s, 3H), 0.97 (s, 3H); ^{13}C NMR (125 MHz, $CDCl_3$) δ 171.7, 162.6, 156.7, 142.9, 137.7, 123.9, 112.1, 87.3, 79.4, 56.3, 54.0, 53.3, 48.4, 40.5, 38.4, 33.3, 29.9, 28.5, 24.8, 20.5; FTIR (Neat Film NaCl) 2964, 2929, 2872, 1764, 1760, 1738, 1667, 1620, 1467, 1334, 1267, 1235, 1195, 1177, 1106, 1009, 954, 827 cm^{-1}; HRMS (Multimode-ESI/APCI) m/z calc'd for $C_{20}H_{24}O_5$ $[M+H]^+$: 345.1697, found 345.1698; MP: 135–160 ºC (at these temperatures decarboxylation is thought to occur, as

the crystalline sample and the resulting liquid were vigorously bubbling throughout the measurement; thus it is unclear whether thermal decomposition precluded state change).

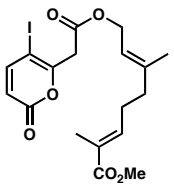

Ester 140c. To a solution of **12** (140 mg, 0.70 mmol, 1.0 equiv) and **13** (210 mg, 0.70 mmol, 1.0 equiv) in acetonitrile (7.0 mL) was added *N*,*N*'-dicyclohexylcarbodiimide (190 mg, 0.91 mmol, 1.3 equiv) at 0 ˚C. The reaction was warmed to 25 ºC and stirred for seven additional hours. The reaction mixture was then filtered through a pad of Celite, and then concentrated by rotary evaporation. The crude reaction mixture was then chromatographed (ethyl acetate in hexane 0⇒30% on SiO_2) to give 300 mg (94%) of **7b** as a pale yellow oil. ^{1}H NMR (500 MHz, $CDCl_3$) δ7.45 (d, *J* = 10.0 Hz, 1H), 6.70 (tq, *J* = 1.5, 7.5 Hz, 1H), 6.06 (d, *J* = 10.0 Hz, 1H), 5.35 (tq, *J* = 1.5, 7.0 Hz, 1H), 4.67 (d, *J* = 7.0 Hz, 2H), 3.77 (s, 2H), 3.72 (s, 3H), 2.30 (q, *J* = 7.5 Hz, 2H), 2.16 (t, *J* = 7.5 Hz, 2H), 1.83 (q, *J* = 1.5 Hz, 3H), 1.72 (q, *J* = 1.5 Hz, 3H); ^{13}C NMR (125 MHz, $CDCl_3$) δ 168.5, 166.6, 160.3, 157.9, 151.2, 142.0, 141.3, 128.0, 118.3, 116.1, 70.6, 62.5, 51.7, 42.6, 38.0, 26.8, 16.5, 12.4; FTIR (Neat Film NaCl) 2988, 2950, 1738, 1714, 1438, 1366, 1268, 1232, 1126, 1082, 1023, 955, 745 cm^{-1}; HRMS (Multimode-ESI/APCI) m/z calc'd for $C_{18}H_{25}NO_6I$ $[M+NH_4]^+$:478.0721, found 478.0725.

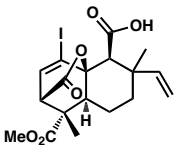

Iodoacid 138c. To a solution of **140c** (96 mg, 0.21 mmol, 1.0 equiv) in toluene (1.1 mL) in a sealed tube were successively added triethylamine (6.0 μL, 0.042 mmol, 0.20 equiv) and *N,O*-bis(trimethylsilyl)acetamide (100 μL, 0.42 mmol, 2.0 equiv). The reaction mixture was heated to 110 ˚C and stirred for 20 minutes, then cooled to 25 ˚C. The reaction mixture was diluted with toluene (250 mL) and heated to 100 ˚C for 48 hours. The reaction was then cooled to 25 ˚C, the solvent removed by rotary evaporation, and the crude residue chromatographed (hexane/ethyl acetate/acetic acid, 1:1:0.01 on SiO_2) to give 64 mg (67%) of **138c** as a colorless foam.

Major: ^{1}H NMR (500 MHz, $CDCl_3$) δ 6.93 (d, *J* = 6.5 Hz, 1H), 6.02 (dd, *J* = 10.5, 17.5 Hz, 1H), 5.07–5.03 (m, 2H), 3.72 (s, 3H), 3.56–3.53 (m, 1H), 3.03 (s, 1H), 2.40–2.33 (m, 1H), 1.77–1.56 (m, 4H), 1.32 (s, 3H), 1.30 (s, 3H); ^{13}C NMR (125 MHz, $CDCl_3$) δ 147.9, 139.7, 111.6, 99.2, 84.2, 59.2, 53.0, 52.6, 47.8, 44.5, 40.0, 38.1, 20.8, 18.4.

Minor: ^{1}H NMR (500 MHz, $CDCl_3$) δ 6.93 (d, *J* = 6.5 Hz, 1H), 6.33 (dd, *J* = 11.0, 17.5 Hz, 1H), 5.10 (d, *J* = 11.0 Hz, 1H), 5.07–5.03 (m, 1H), 3.72 (s, 3H), 3.56–3.53 (m, 1H), 2.97 (s, 1H), 2.40–2.33 (m, 1H), 1.98–1.95 (m, 1H), 1.77–1.56 (m, 3H), 1.38 (s, 3H), 1.30 (s, 3H); ^{13}C NMR (125 MHz, $CDCl_3$) δ 169.1, 169.0, 140.4, 140.0, 113.5, 98.8, 84.3, 60.6, 52.7, 48.0, 39.45, 38.5, 29.8, 20.8, 20.8, 20.8.

FTIR (Neat Film NaCl) 3080, 2951, 1756, 1739, 1734, 1700, 1559, 1506, 1457, 1211, 911, 756 cm^{-1}; HRMS (Multimode-ESI/APCI) m/z calc'd for $C_{18}H_{22}O_6I$ $[M+H]^+$: 461.0456, found 461.0460.

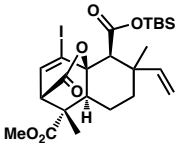

***tert*-Butyldimethylsilyl ester 154**. To a solution of **138c** (89 mg, 0.11 mmol, 1.0 equiv) in dimethylformamide (0.52 mL) were added *tert*-butyldimethylsilylchloride (150 mg, 0.97 mmol, 5.0 equiv) and imidazole (130 mg, 1.9 mmol, 10 equiv). The reaction mixture was warmed to 40 ˚C and stirred for 3 hours. The crude mixture was then diluted with saturated aqueous NaCl (1 mL) and extracted with diethyl ether/hexane (1:1) (3 x 2 mL). The combined organic extracts were washed with saturated aqueous NaCl (3 x 1 mL), dried over Na_2SO_4, and concentrated by rotary evaporation to yield 76 mg (68%) of **154** as a pale yellow powder.

Procedure 2. To a solution of **138c** (61 mg, 0.13 mmol, 1 equiv) in acetonitrile (0.13 mL, 1.0 M) was added *N*-methyl-*N*-(*tert*-butyldimethylsilyl)trifluoroacetamide (320 mg, 1.3 mmol, 10 equiv) at 25 ˚C and stirred for 15 minutes. The reaction mixture was diluted with saturated aqueous NaCl (1 mL) and extracted with diethyl ether/hexane (1:1) (3 x 2 mL). The combined organic extracts were washed with saturated aqueous $KHSO_4$ (1 mL) and then with saturated aqueous NaCl (3 x 1 mL). The combined organics were dried over Na_2SO_4, and concentrated by rotary evaporator. The crude oil was chromatographed (ethyl acetate in hexane 10⇒50% on SiO_2) to yield 51 mg (66%) of **154** as a white powder.

Major: ^{1}H NMR (500 MHz, $CDCl_3$) ẟ6.92 (d, *J* = 6.5 Hz, 1H), 6.04 (dd, *J* = 10.5, 17.5 Hz, 1H), 5.01 (d, *J* = 10.5 Hz, 1H), 5.01 (d, *J* = 17.5 Hz, 1H), 3.72 (s, 3H), 3.53 (d, *J* = 6.5 Hz, 1H), 2.98 (s, 1H), 2.38–2.31 (m, 1H), 1.76–1.54 (m, 4H), 1.31 (s, 3H), 1.27 (s, 3H), 0.90 (s, 9H), 0.29 (s, 3H), 0.26 (s, 3H)**;** ^{13}C NMR (125 MHz, $CDCl_3$)

Minor: ^{1}H NMR (500 MHz, $CDCl_3$) δ 6.92 (d, *J* = 6.5 Hz, 1H), 6.37 (dd, *J* = 11.0, 17.5 Hz, 1H), 5.06 (d, *J* = 11.0 Hz, 1H), 5.03–4.99 (m, 1H), 3.72 (s, 3H), 3.51 (d, *J* = 6.5 Hz, 1H), 2.90 (s, 1H), 2.38–2.31 (m, 1H), 1.92–1.88 (m, 1H), 1.76–1.54 (m, 3H), 1.38 (s, 3H), 1.29 (s, 3H), 0.89 (s, 9H), 0.29 (s, 3H), 0.28 (s, 3H); ^{13}C NMR (125 MHz, $CDCl_3$) δ 174.9, 169.1, 169.1, 141.0, 139.7, 113.0, 99.5, 84.3, 61.8, 52.9, 52.9, 48.3, 39.6, 39.0, 29.7, 25.3, 20.9, 20.8, 17.5, –4.90, –4.90.

FTIR (Neat Film NaCl) 2951, 2928, 2856, 1767, 1733, 1717, 1447, 1274, 1251, 1215, 1191, 968, 843, 828, 792, 736 cm^{-1}; HRMS (Multimode-ESI/APCI) m/z calc'd for $C_{24}H_{36}O_6ISi$ $[M+H]^+$: 575.1320, found 575.1317.

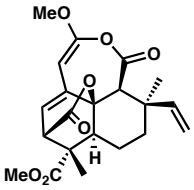

76a **Basiliolide B**

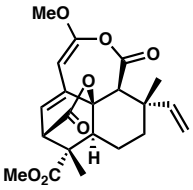

***76b epi*-8-Basiliolide B**

Basiliolides (**76a**, **76b**). In a nitrogen filled glovebox, to a solution of **154** (15 mg, 0.030 mmol, 1.0 equiv) and $Pd(PPh_3)_4$ (35 mg, 0.030 mmol, 1.0 equiv) in dimethylformamide (0.30 mL, 0.10 M) was added tributyl(2-methoxyethynyl)stananne (**151**) (53 mg, 0.050 mmol, 5.0 equiv). The reaction was stirred at 30 ˚C for 16 hours, then treated with water

(30 μL) and stirred at 25 ˚C for an additional 1 hour. The mixture was then diluted with ethyl acetate (1 mL) and washed with water (4 x 0.5 mL) and concentrated by rotary evaporation. The crude oil was purified by normal phase HPLC to yield 0.6 mg (6%) of basiliolide B (**76a**) and 1.2 mg (12%) of *epi*-8-basiliolide B (**76b**) as white powders.

Procedure 2. In a nitrogen filled glovebox, to a solution of **154** (16 mg, 0.030 mmol, 1.0 equiv) and Pd(*t*-$Bu_3P)_2$ (15 mg, 0.030 mmol, 1.0 equiv) in dimethylformamide (0.30 mL, 0.10 M) was added tributyl(2-methoxyethynyl)stananne (43 mg, 0.12 mmol, 4.0 equiv). The reaction was stirred at 30 ºC for 10 hours, and then an addition aliquot (22 mg, 0.060 mmol, 2.0 equiv) of stannane **151** was added and stirred for an additional two hours. The reaction was treated with water (30 μL) and stirred at 25 ˚C for an additional 1 hour. The crude reaction mixture was diluted with ethyl acetate (1 mL) and washed with water (4 x 0.5 mL) and concentrated by rotary evaporation. . The crude oil was purified by normal phase HPLC to yield 0.6 mg (5%) of basiliolide B (**76a**) and 1.6 mg (14%) of *epi*-8-basiliolide B (**76b**) as white powders.

Basiliolide B (76a).

^{1}H NMR (500 MHz, $CDCl_3$) δ 7.00 (dd, *J* = 11.5, 18 Hz, 1H), 6.08 (d, *J* = 5.5 Hz, 1H), 5.17 (d, *J* = 11.5 Hz, 1H), 5.06 (d, *J* = 18 Hz, 1H), 4.96 (s, 1H), 3.72 (s, 3H), 3.71 (s, 3H), 3.67 (d, *J* = 5.5 Hz, 1H), 3.17 (s, 1H), 2.29 (dd, *J* = 5.0, 12.5 Hz, 1H), 1.96 (dt, *J* = 3.0 Hz, 13.5 Hz, 1H), 1.74–1.65 (m, 2H), 1.54–1.48 (m, 1H), 1.30 (s, 3H), 1.24 (s, 3H); ^{13}C NMR (125 MHz, $CDCl_3$) δ 175.2, 170.1, 162.3, 156.7, 142.7, 139.2, 123.4, 112.3, 87.0, 79.2, 56.4, 53.3, 52.9, 50.0, 44.8, 44.7, 40.2, 38.5, 28.6, 21.0, 20.8; FTIR (Neat Film NaCl) 2951, 2875, 1791, 1761, 1771, 1767, 1733, 1668, 1663, 1456, 1334, 1262, 1230,

1213, 1180, 1107, 1011, 960, 908, 833, 736 cm^{-1}; HRMS (Multimode-ESI/APCI) m/z calc'd for $C_{21}H_{24}O_7$ $[M+H]^+$: 389.1595, found 389.1599.

***epi*-8-Basiliolide B (76b).**

^1H NMR (500 MHz, $CDCl_3$) δ 6.06 (d, *J* = 6.0 Hz, 1H), 5.80 (dd, *J* = 10.5, 17.5 Hz, 1H), 5.09 (d, *J* = 10.5 Hz, 1H), 5.05 (d, *J* = 17.5 Hz, 1H), 4.94 (s, 1H), 3.71 (s, 3H), 3.70 (s, 3H), 3.66 (d, *J* = 6.0 Hz, 1H), 3.26 (s, 1H), 2.25 (dd, *J* = 7.0, 12.0 Hz, 1H), 1.79–1.67 (m, 4H), 1.61 (s, 3H), 1.34 (s, 3H); ^{13}C NMR (125 MHz, $CDCl_3$) δ 175.1, 170.1, 162.0, 146.2, 139.5, 123.2, 113.0, 87.0, 79.0, 56.3, 52.9, 50.5, 49.9, 44.7, 44.6, 38.5, 38.2, 21.0, 20.3, 19.3; FTIR (Neat Film NaCl) 2980, 2951, 2929, 1770, 1767, 1761, 1732, 1668, 1619, 1442, 1335, 1261, 1219, 1182, 1106, 971, 960, 918, 834, 732 cm^{-1}; HRMS (Multimode-ESI/APCI) m/z calc'd for $C_{21}H_{24}O_7$ $[M+H]^+$: 389.1595, found 389.1604.

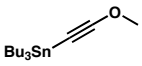

Tributyl(2-methoxyethynyl)stannane (151). To a solution of freshly distilled diethylamine (9.6 mL, 92 mmol, 3.9 equiv) in tetrahydrofuran (300 mL) at 0 ˚C was added *n*-butyllithium (2.5 M in hexanes, 32 mL, 80 mmol, 3.4 equiv). After stirring for 10 min, 1,1-dimethoxy-2-chloro-acetaldehyde (4.0 mL, 26 mmol, 1.1 equiv) was added dropwise to the reaction mixture. The reaction was stirred for 2 hours at 0 ˚C. Tributyltin chloride (6.2 mL, 24 mmol, 1.0 equiv) was then added to the reaction mixture. The reaction was warmed to 23 ºC over 1 hour and stirred for 8 hours. The volatiles were removed in *vacuo* and the reaction mixture was re-suspended in hexane (30 mL) and filtered through a glass frit under an argon atmosphere. The solution was then re-

concentrated by rotary evaporation and distilled by Kugelrohr to yield 6.4 g (78%) of **10** as a colorless oil. ^{1}H NMR (500 MHz, $CDCl_3$) δ 3.87 (s, 3H), 1.54 (m, 6H), 1.33 (sextet, J = 7.5 Hz, 6H), 0.94 (m, 6H), 0.90 (t, J = 7.5 Hz, 9H); ^{13}C NMR (125 MHz, $CDCl_3$) δ 114.7, 65.8, 31.5, 28.9, 27.0, 13.7, 11.2; FTIR (Neat Film NaCl) 2955, 2927, 2871, 2161, 1457, 1208, 1126, 910, 865 cm^{-1}; Elemental analysis found: C, 52.40%; H, 8.54%. Calc'd for $C_{15}H_{30}OSn$: C, 52.20%; H, 8.76%.

3.9 Notes and References.

Note: Portions of this chapter have been published, see: Nelson, H. M.; Murakami, K.; Virgil, S. C.; Stoltz, B. M. *Angew. Chem. Int. Ed.* **2011**, 50, 3688–3691.

1) Nelson, H. M.; Stoltz, B. M. *Org. Lett.* **2008**, *10*, 25–28.

2) a) Kozytska, M. V.; Dudley, G. B. *Tetrahedron Lett.* **2008**, *49*, 2899–2901. b) Kozytska, M. V.; Dudley, G. B. *Abstracts of Papers*, 234th National Meeting of the American Chemical Society, Boston, MA, Aug 19–23, **2007**; American Chemical Society; Washington, DC, **2007**; ORGN 1012. c) Kozytska, M. V. ; Dudley, G. B. *Abstracts of Papers*, 58th Southeast Regional Meeting of the American Chemical Society, Augusta, GA, Nov 1–4, **2006**; American Chemical Society; Washington, DC, **2006**; SRM06 011. d) Kozytska, M. V. *I. Siletanylmethyllithium, an ambiphilic siletane II. Synthetic approach to basiliolide B*. PhD Thesis, Florida State University College of Arts and Sciences: **2008**.

3) Zhou, X.; Wu, W.; Liu, X.; Lee, C.-s. *Org. Lett.* **2008**, *10*, 5525–5528.

4) For a review of the subject, see: Afarinkia, K.; Vinader, V.; Nelson, T. D.; Posner, G. H. *Tetrahedron* **1992**, *48*, 9111–9171.

5) Batsanov, A. S.; Knowles, J. P.; Whiting, A. *J. Org. Chem.* **2007**, *72*, 2525–2532.

6) As discussed by Johansson and coworkers, the immediate product of the Ireland–Claisen rearrangement is prone to thermal decomposition via a decarboxylative pathway. Use of the crude Ireland–Claisen product (presumably the silyl ester) under rigorously dry conditions allows for direct thermal cycloadditon.

7) At the time of submission, the authors have not been able to find any additional examples of such ring systems within naturally occurring compounds.

8) Rubal, J. J.; Moreno-Dorado, F. J. ; Guerra, F. M.; Jorge, Z. D.; Saouf, A.; Akssira, M.; Mellouki, F.; Romero-Garrido, R.; Massanet, G. M. *Phytochemistry* **2007**, *68*, 2480–2486.

9) Although simple cross-couplings of halide **178b** (X = Br or I, R = Me, R' = Me) with reagents such as vinyl tributylstannane were possible, neither Sonogashira-type reactions with alkoxyacetylenes nor other cross-coupling reactions with methoxyacetylide reagents were successful.

10) a) J. A. Marshall in *Organometallics in Synthesis: A Manual* (Ed.: M. Schlosser) John Wiley & Sons Ltd., West Sussex, **2002**, pp. 457.; b) Sakamoto, T.; Yasuhara, A.; Kondo, Y.; Yamanaka, H.; *Synlett* **1992**, *6*, 502; c) Sakamoto, T.; Yasuhara, A.; Kondo, Y.; Yamagishi, Y. *Chem. Pharm. Bull.* **1994**, *42*, 2032–2035; d) Löffler, A.; Himbert, G. *Synthesis* **1992**, *5*, 495–498.

11) Unpublished studies utilizing derivatives of commercially available ethoxyacetylene confirmed the effectiveness of analogous Stille couplings, while Negishi or Sonogashira-type couplings were non-productive in our hands

12) For an analogous preparation of the lithioethoxyacetylide, see: Raucher, S.; Bray, B. L. *J. Org. Chem.* **1987**, *52*, 2332–2333.

13) The hazards associated with the preparation of methoxyacetylene are well documented, see: a) Jones, E. R. H.; Eglington, G.; Whiting, M. C.; Shaw, B. L. *Org. Synth.* **1954**, *34*, 46–49. b) Wasserman, H. H.; Wharton, P. S. *J. Am. Chem. Soc.* **1960**, *82*, 661–665. c) Dombroski, J. R.; Schuerch, C. *Macromolecules (Washington, DC, U. S.)* **1970**, *3*, 257–260.

14) Wasserman, H. H.; Wharton, H. H. *J. Am. Chem. Soc.* **1960**, *82*, 661–665.

15) Silyl ester **152** could be prepared directly from ester **140b** under slightly modified reaction conditions, i.e., using *N*,*O*-bis(tert-butyldimethylsilyl)acetimide. However, the yield over three steps was significantly lower; ca. 10%.

16) Corey, E. J.; Venkateswarlu, A. *J. Am. Chem. Soc.* **1972**, *94*, 6190–6191.

17) Dai, C.; Fu, G. C. *J. Am. Chem. Soc.* **2001**, *122*, 2719–2724.

18) Crystallographic data have been deposited at the CCDC, 12 Union Road, Cambridge CB2 1EZ, UK, and copies can be obtained on request, free of charge, by quoting the publication citation and the deposition number 796908.

19) Saouf, A.; Guerra, F. M.; Rubal, J. J.; Moreno-Dorado, F. J.; Akssira, M.; Mellouki, F.; Lopez, M.; Pujadas, A. J.; Jorge, Z. D.; Massanet, G. M. *Org. Lett.* **2005**, *7*, 881–884.

20) Shibuya, H.; Ohashi, K.; Narita, N.; Ishida, T.; Kitigawa, I. *Chem*. *Pharm*. *Bull*. **1994**, *42*, 293–299.

21) Mawhinney, T. P.; Madson, M. A. *J. Org. Chem.* **1982**, *47*, 3336–3339.

22) Synthetic basiliolide B was spectroscopically indistinguishable from the natural product isolated from *Thapsia sp*.

APPENDIX 4

Synthetic Summary for (±)-Transtaganolide C, (±)-Transtaganolide D, (±)-Basiliolide B, and (±)-epi-8-Basiliolide B

Scheme A4.1. Development of the ICR/IMPDA cascade reaction

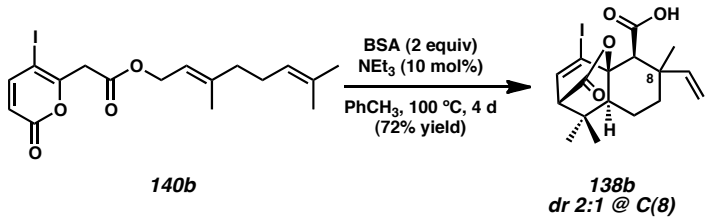

Scheme A4.2. Synthesis of methoxyacetylene reagent

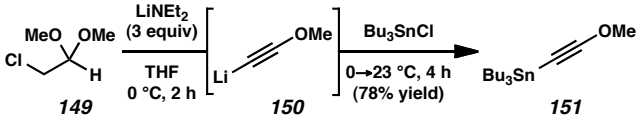

Scheme A4.3. Total synthesis of transtaganolides C and D and X-ray crystal structure

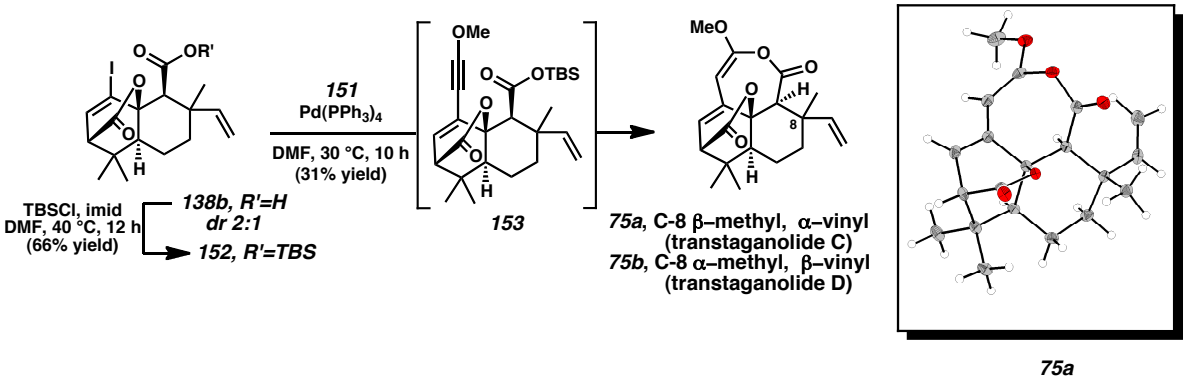

Scheme A4.4. Synthesis of basiliolide B and epi-8-basiliolide B

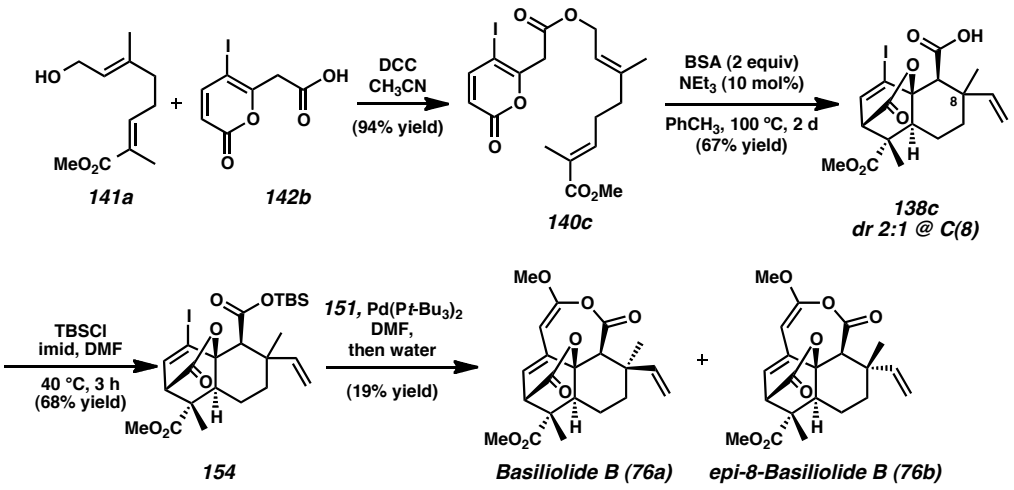

APPENDIX 5

Spectra Relevant to: The Total Syntheses of (±)-Transtaganolide C, (±)-Transtaganolide D, (±)-Basiliolide B, and (±)-epi-8-Basiliolide B

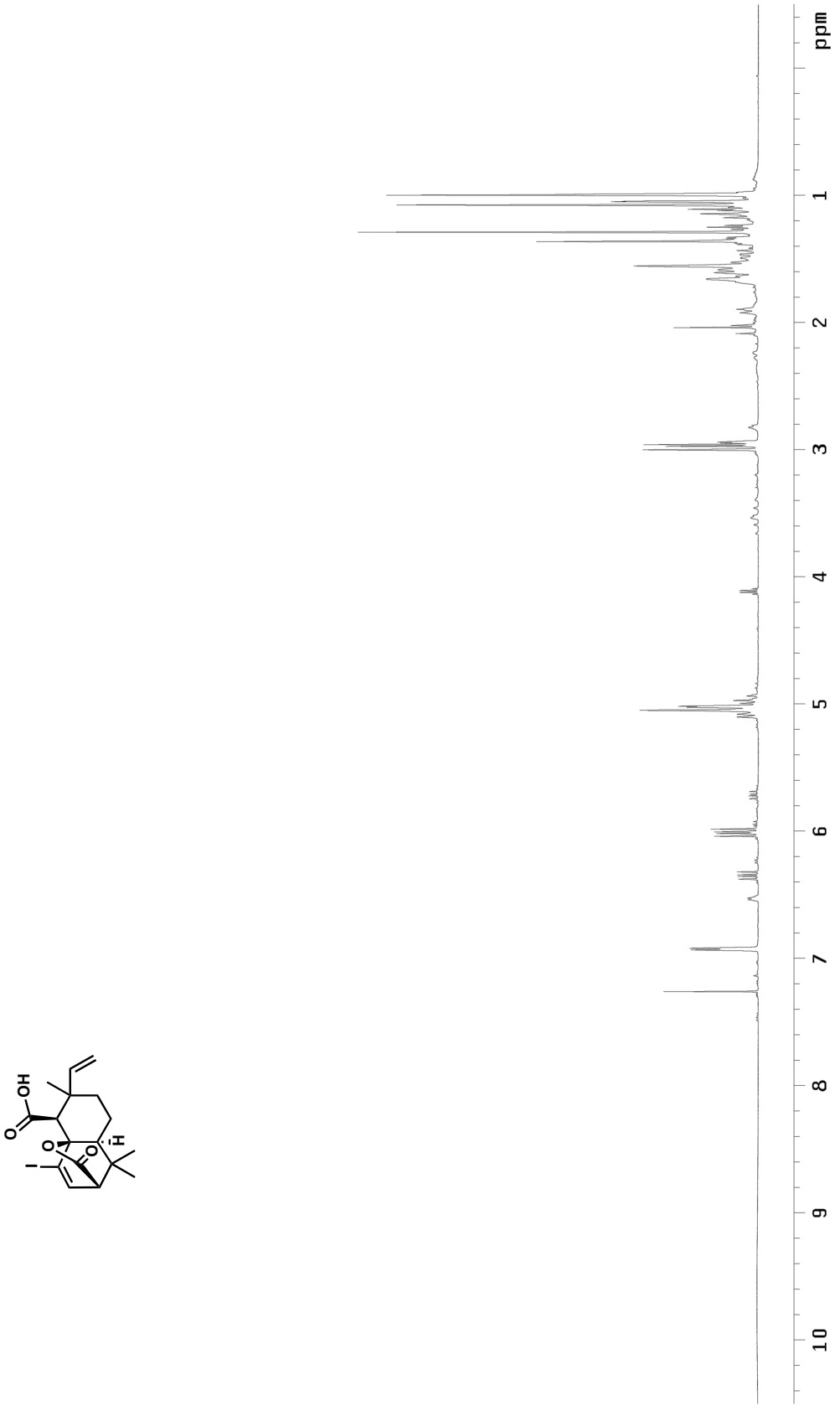

Figure A5.1.1 ^{1}H NMR (500 MHz, $CDCl_3$) of compound **138b**

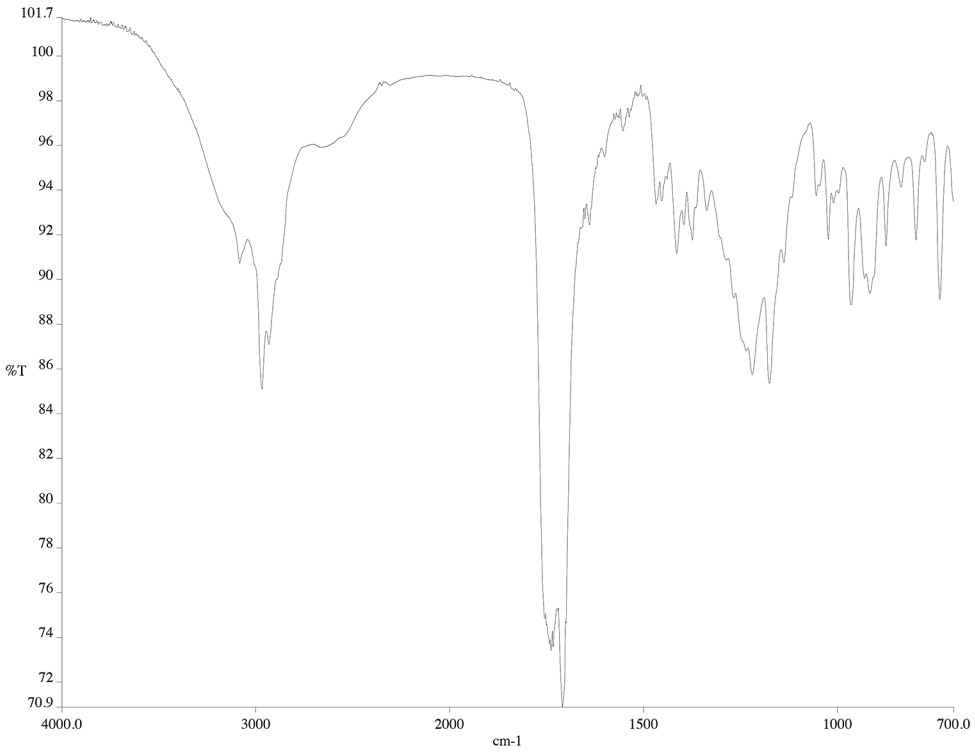

Figure A5.1.2 Infrared spectrum (thin film/NaCl) of compound **138b**

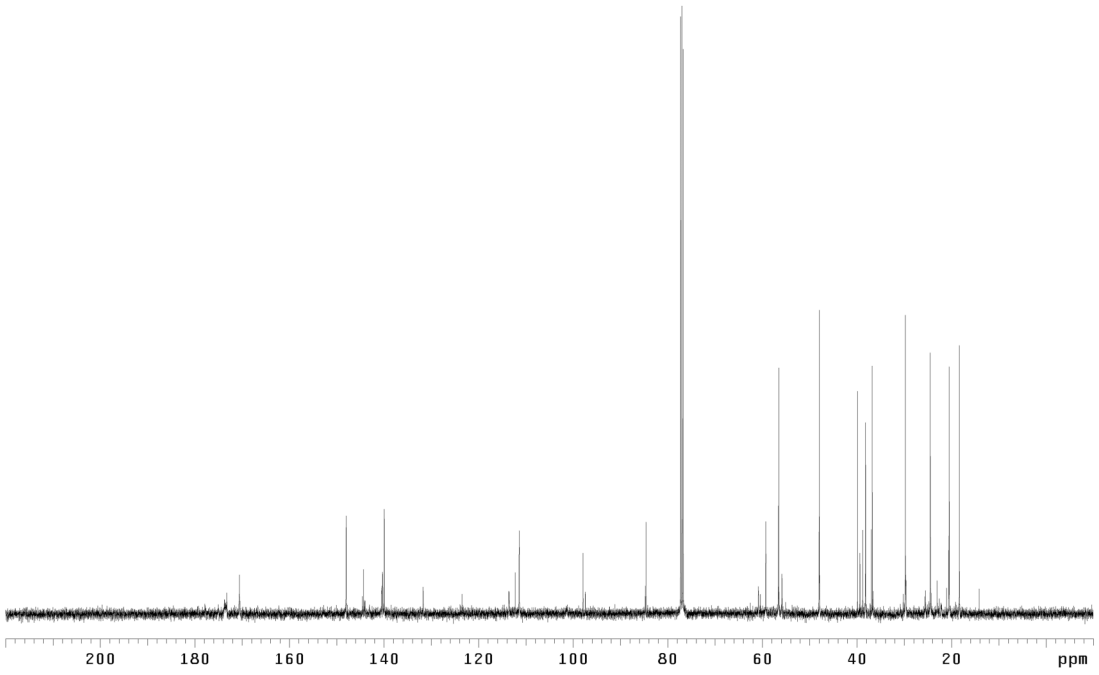

Figure A5.1.2 ^{13}C NMR (125 MHz, $CDCl_3$) of compound **138b**

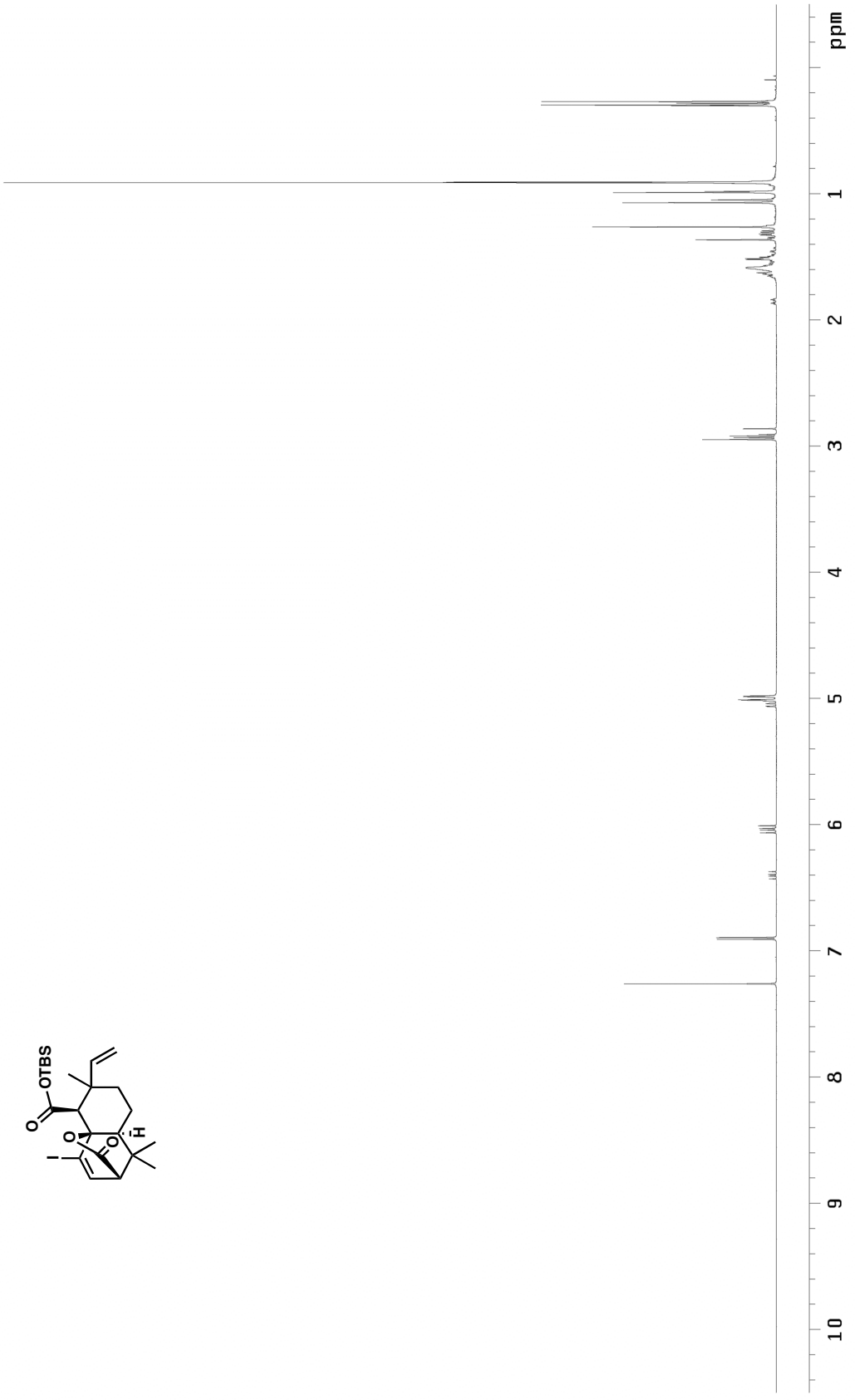

Figure A5.2.1 ^{1}H NMR (500 MHz, $CDCl_3$) of compound **152**

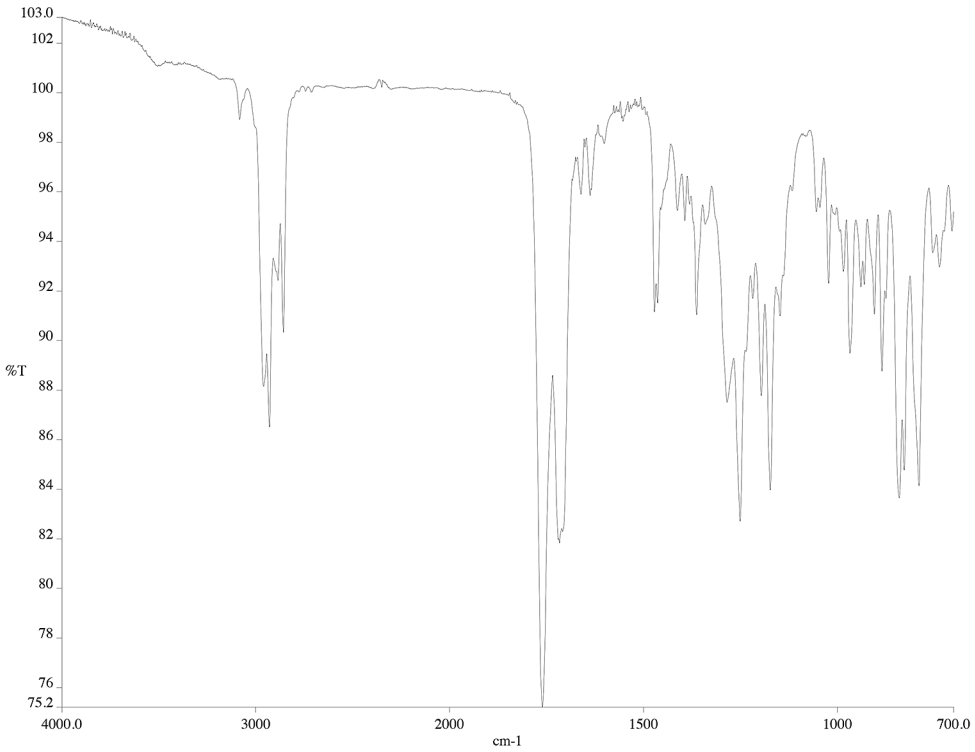

Figure A5.2.2 Infrared spectrum (thin film/NaCl) of compound **152**

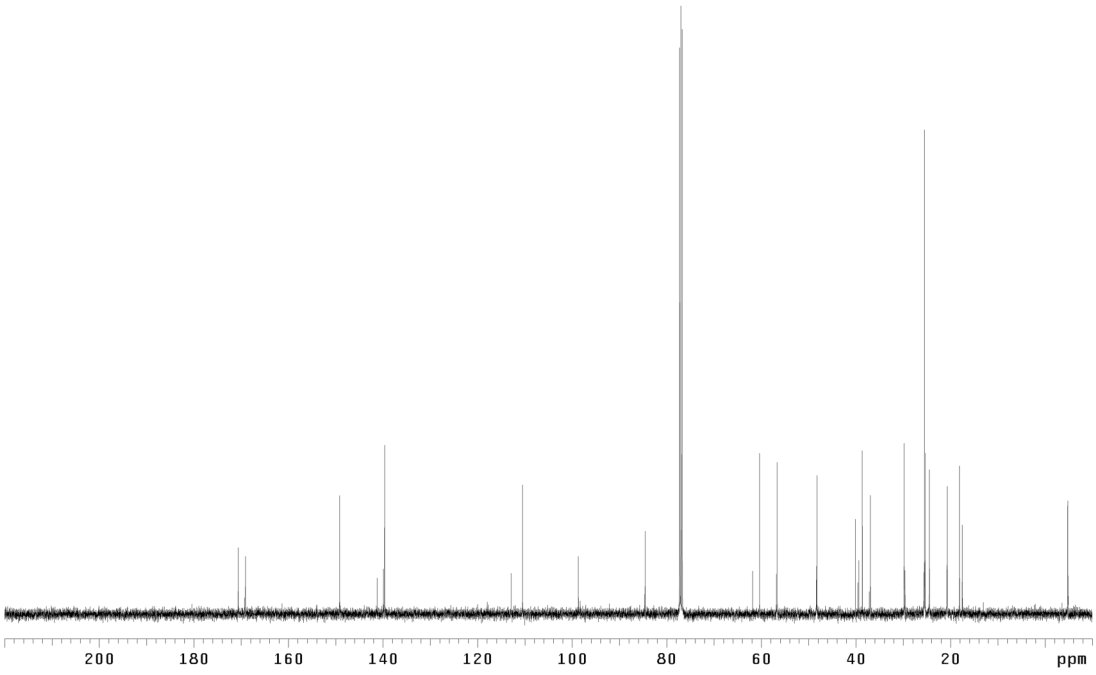

Figure A5.2.2 ^{13}C NMR (125 MHz, $CDCl_3$) of compound **152**

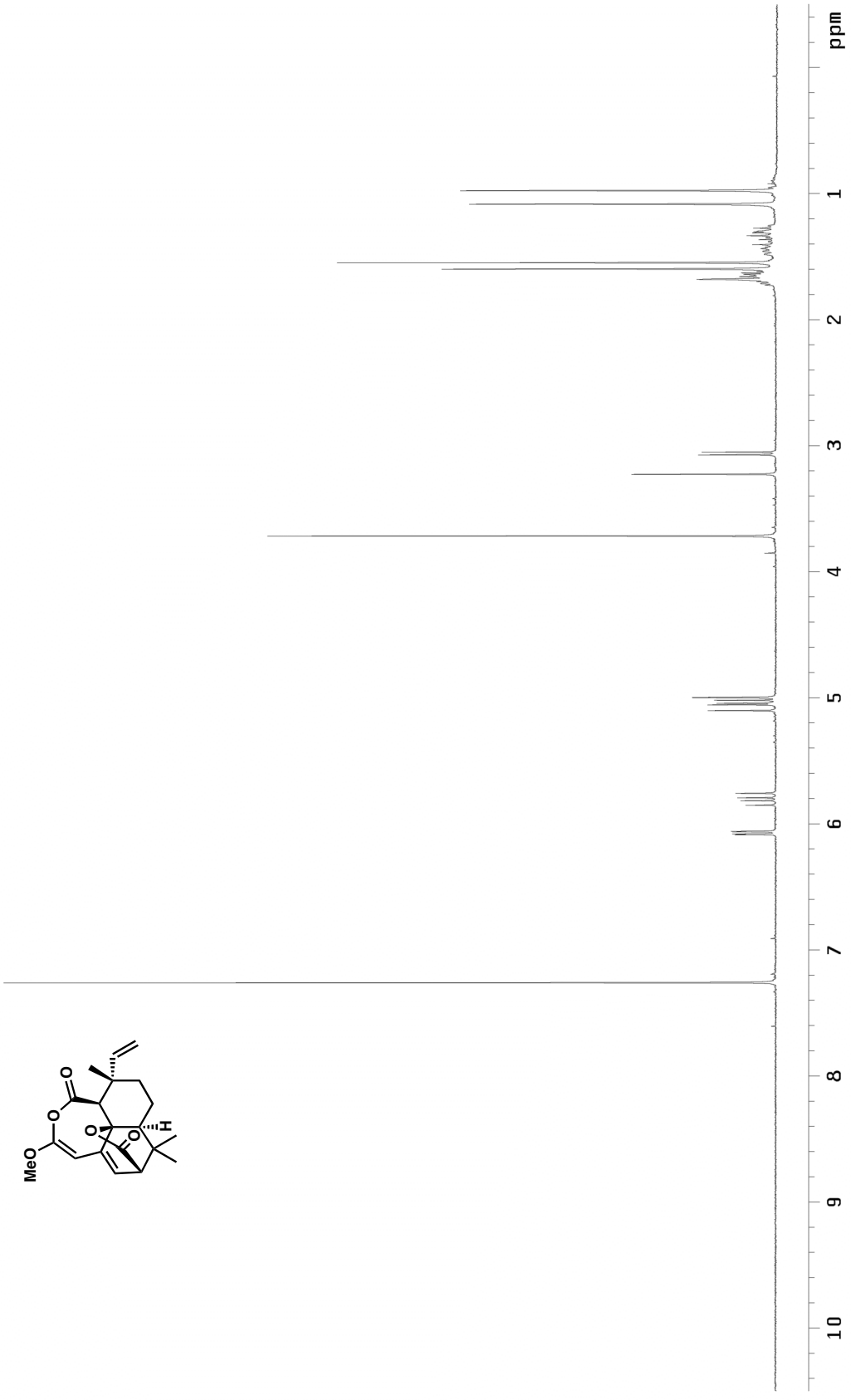

Figure A5.3.1 ^{1}H NMR (500 MHz, $CDCl_3$) of compound **75a**

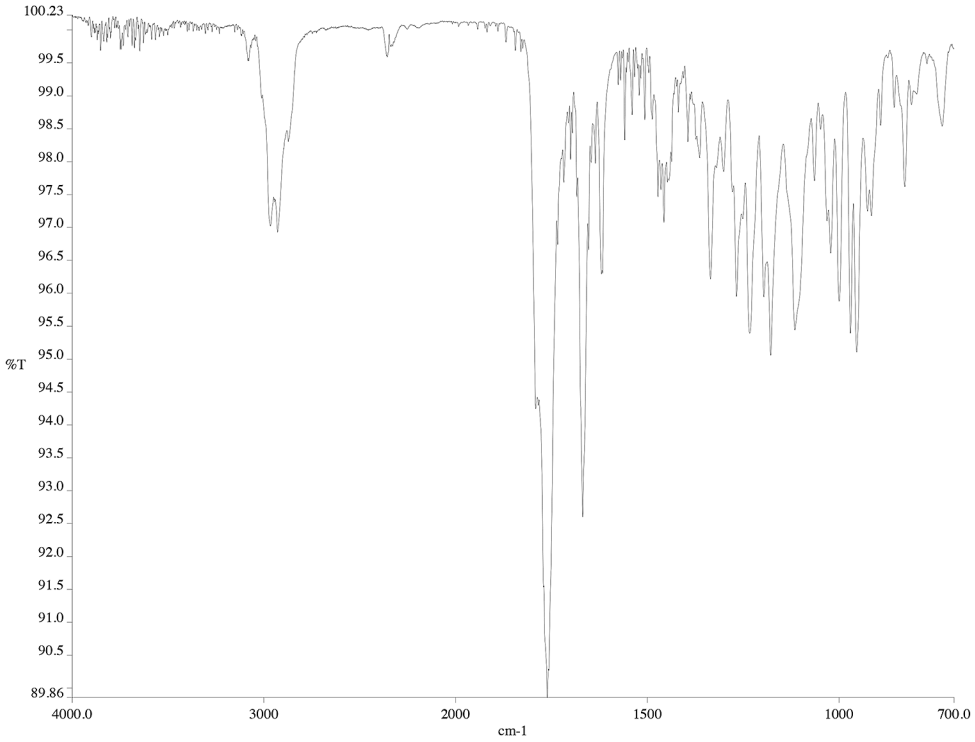

Figure A5.3.2 Infrared spectrum (thin film/NaCl) of compound **75a**

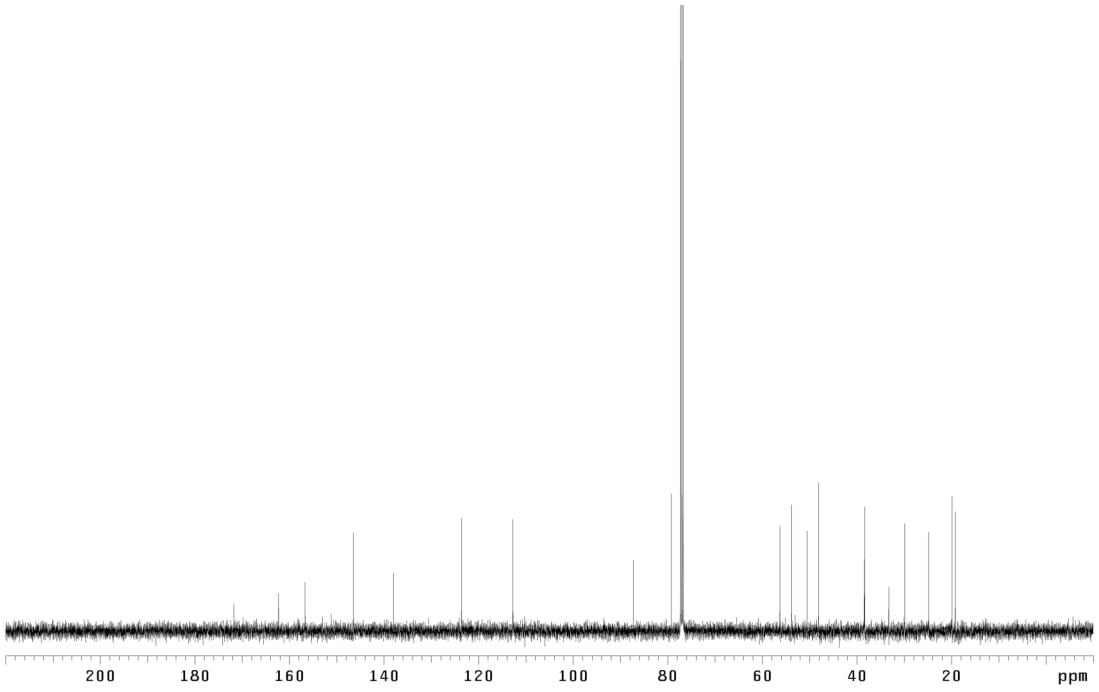

Figure A5.3.2 ^{13}C NMR (125 MHz, $CDCl_3$) of compound **75a**

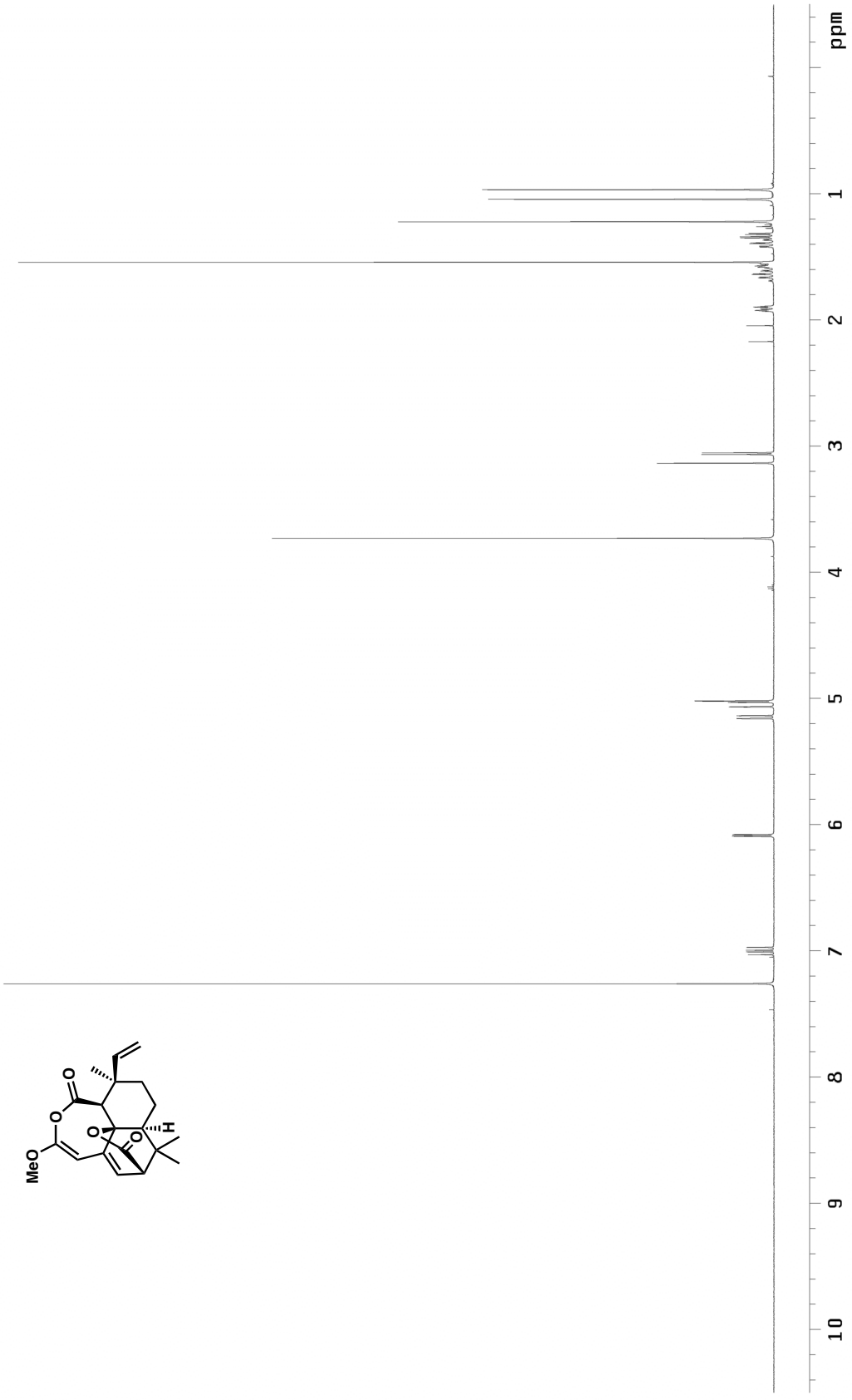

Figure A5.4.1 ^{1}H NMR (500 MHz, $CDCl_3$) of compound **75b**

Figure A5.4.2 Infrared spectrum (thin film/NaCl) of compound **75b**

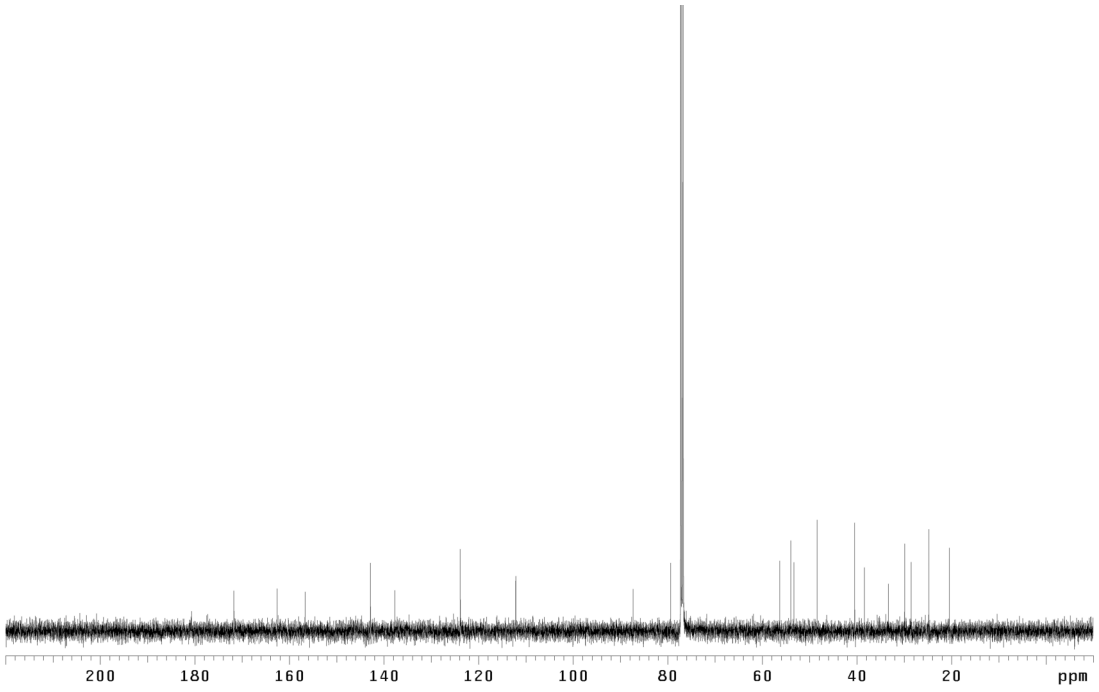

Figure A5.4.2 ^{13}C NMR (125 MHz, $CDCl_3$) of compound **75b**

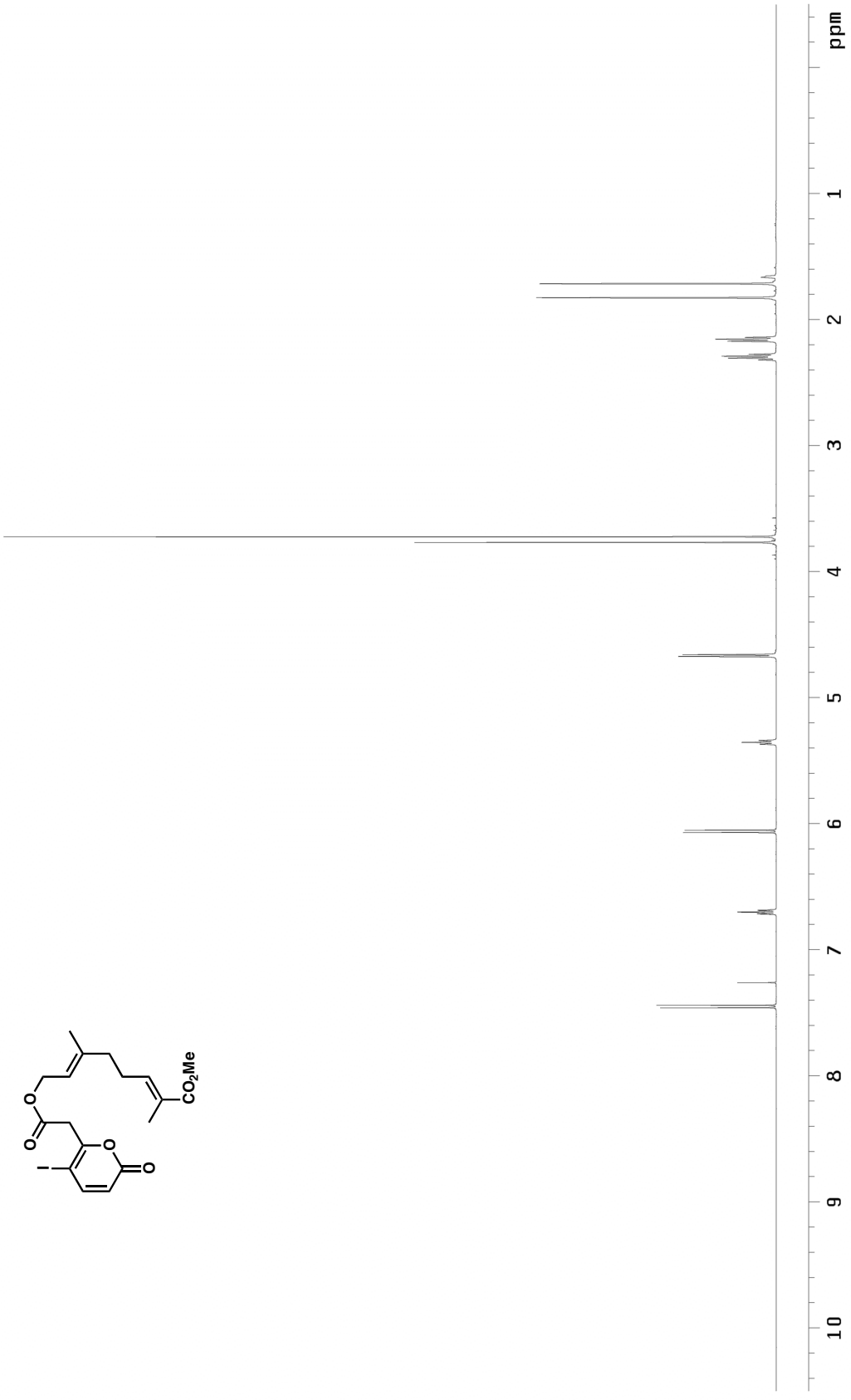

Figure A5.5.1 ^{1}H NMR (500 MHz, $CDCl_3$) of compound **140c**

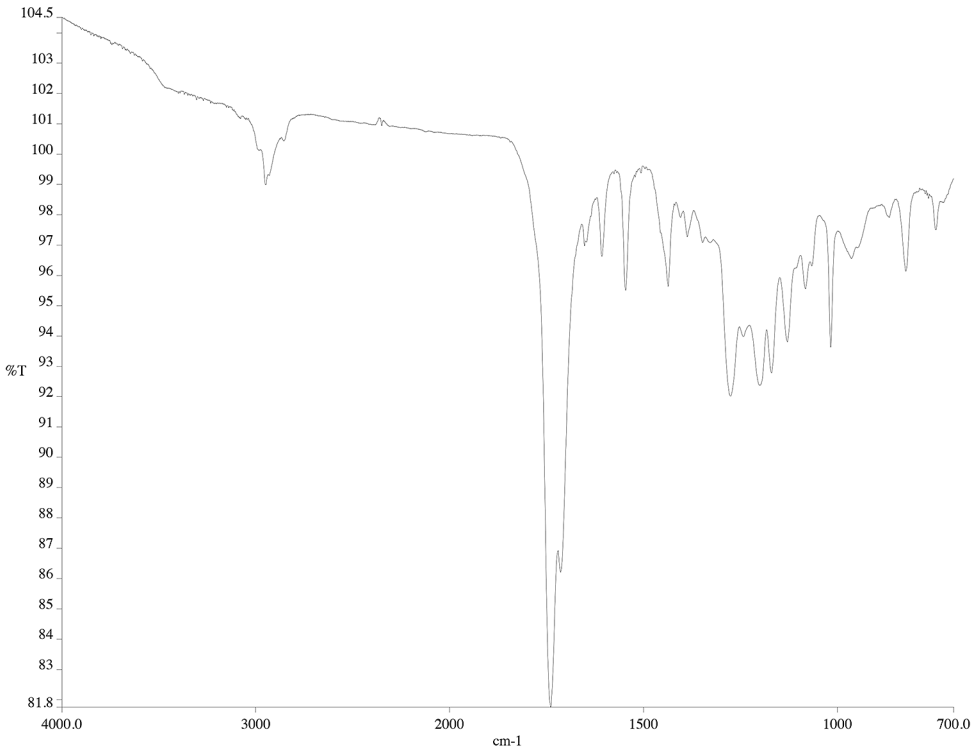

Figure A5.5.2 Infrared spectrum (thin film/NaCl) of compound **140c**

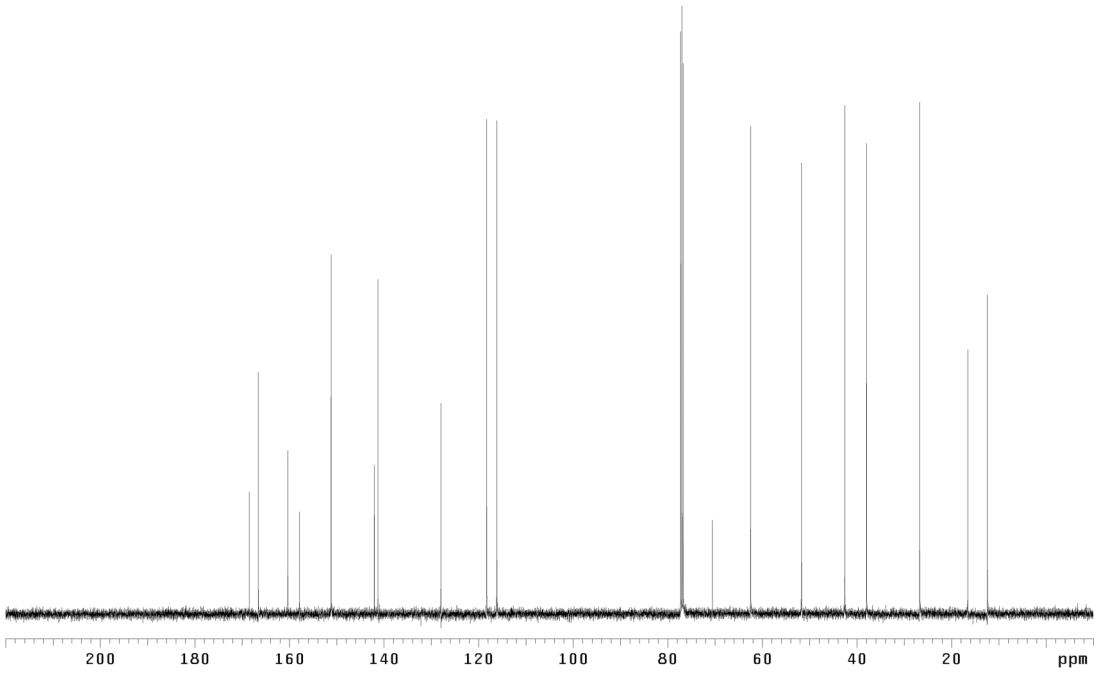

Figure A5.5.2 ^{13}C NMR (125 MHz, $CDCl_3$) of compound **140c**

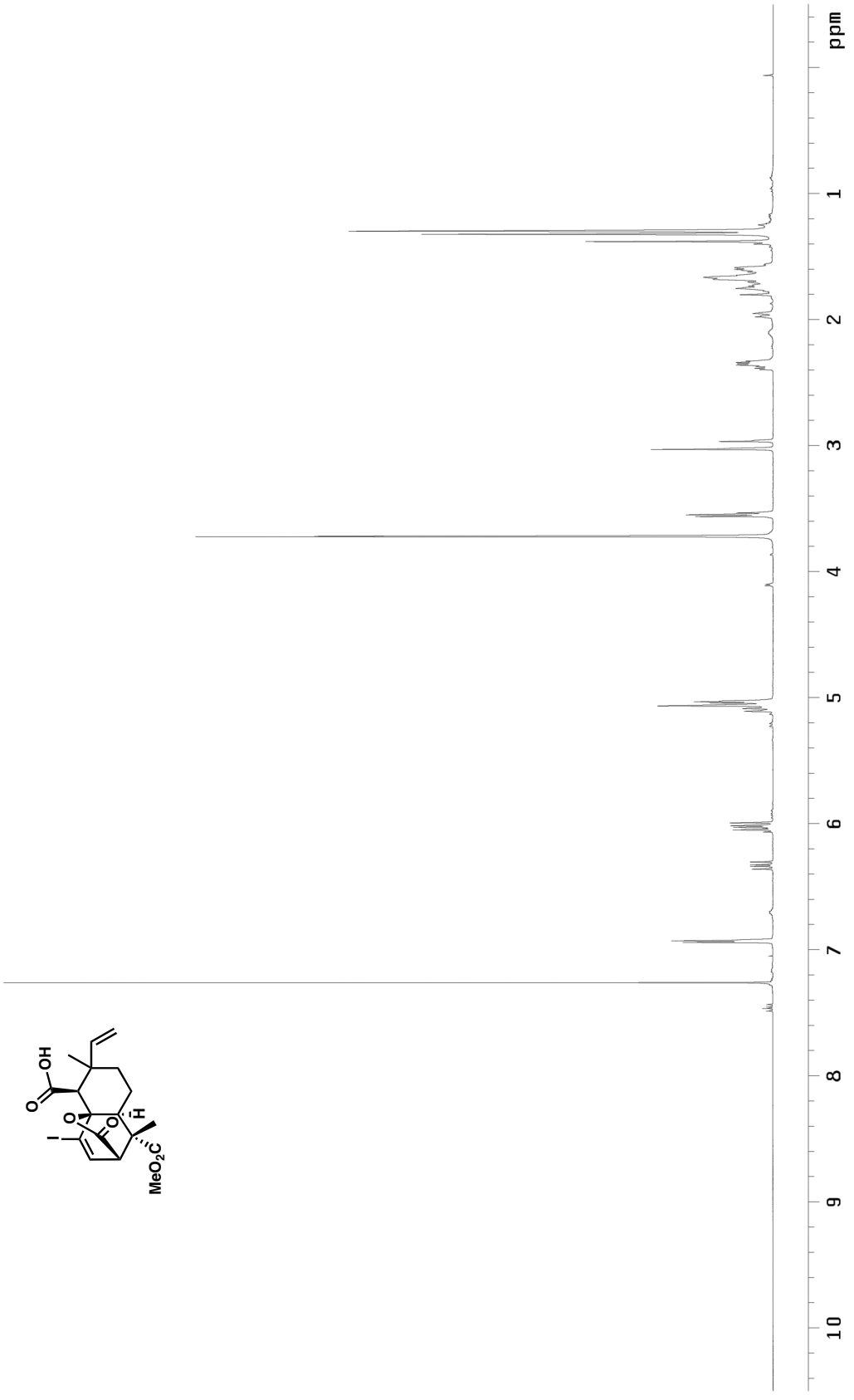

Figure A5.6.1 ^{1}H NMR (500 MHz, $CDCl_3$) of compound **138c**

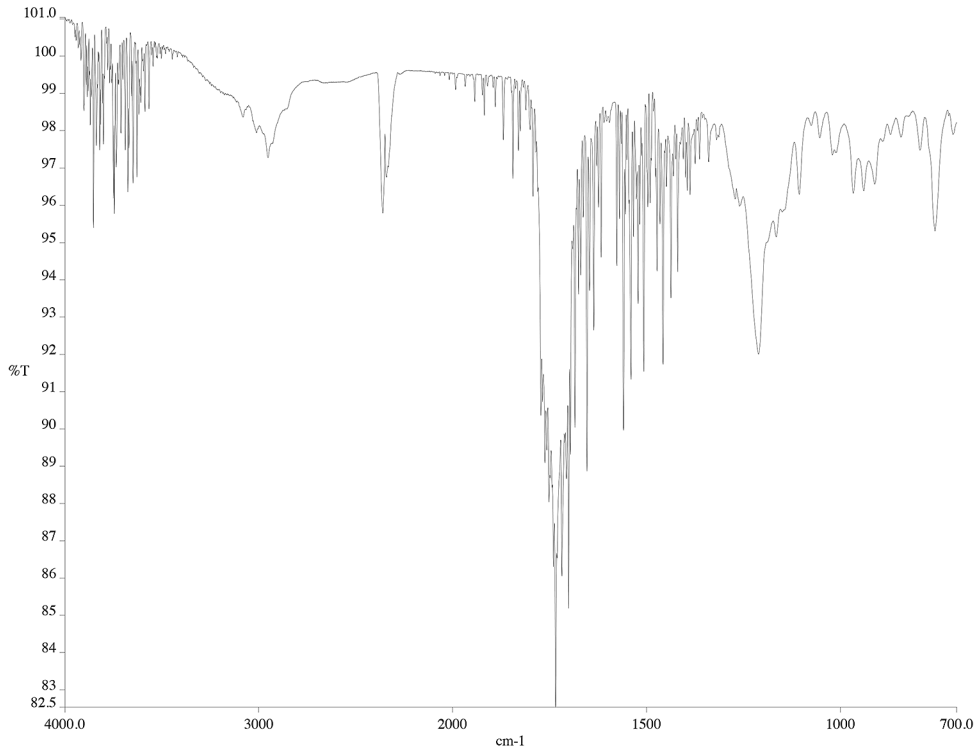

Figure A5.6.2 Infrared spectrum (thin film/NaCl) of compound **138c**

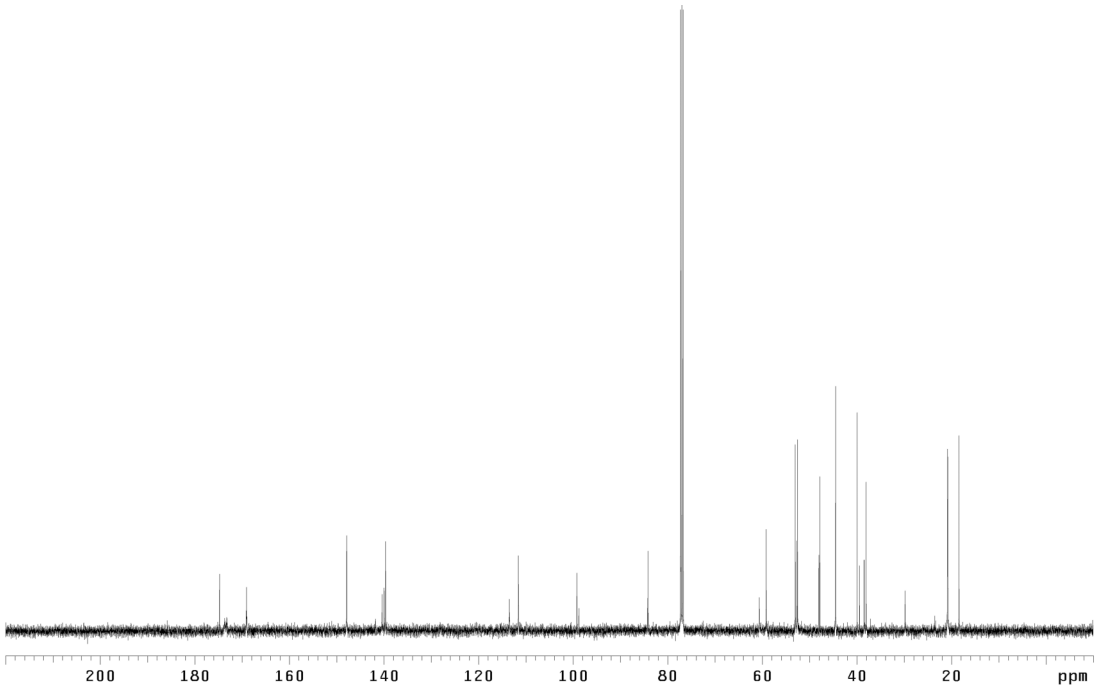

Figure A5.6.2 ^{13}C NMR (125 MHz, $CDCl_3$) of compound **138c**

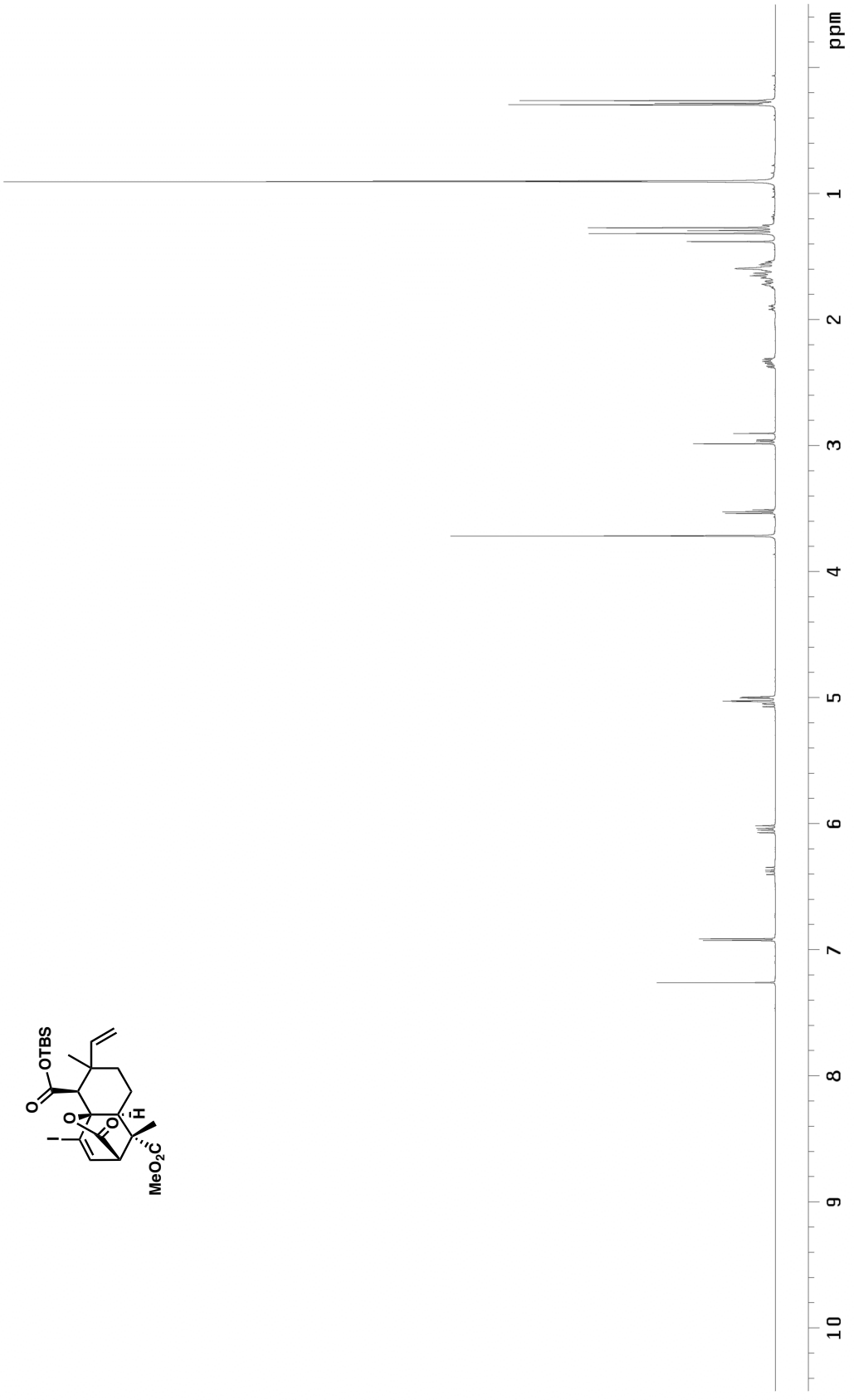

Figure A5.7.1 ^{1}H NMR (500 MHz, $CDCl_3$) of compound **154**

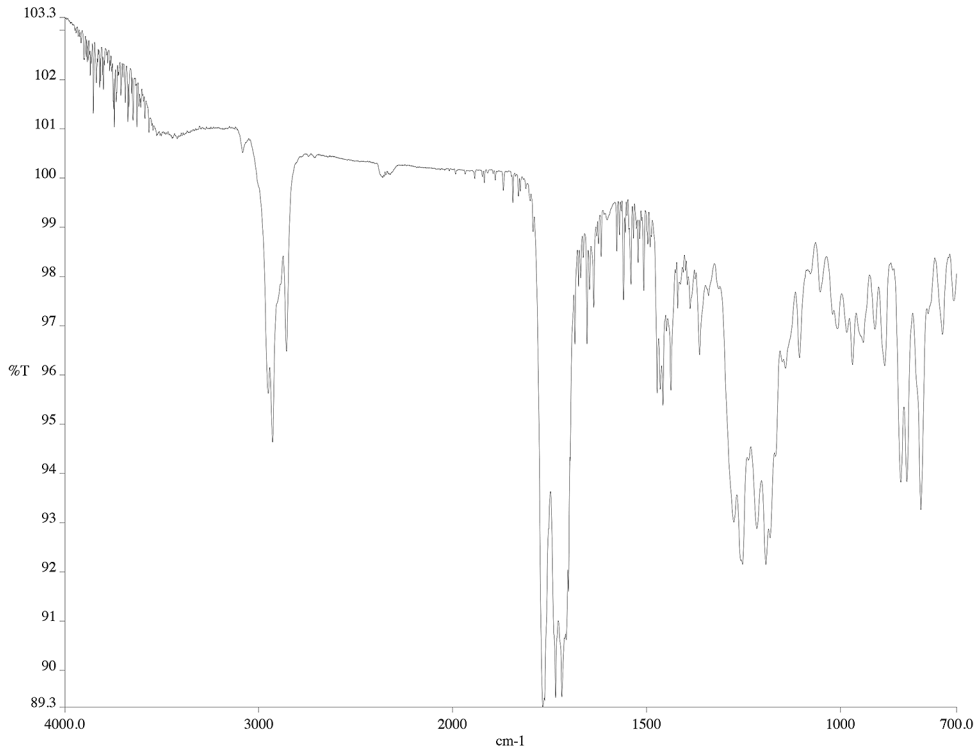

Figure A5.7.2 Infrared spectrum (thin film/NaCl) of compound **154**

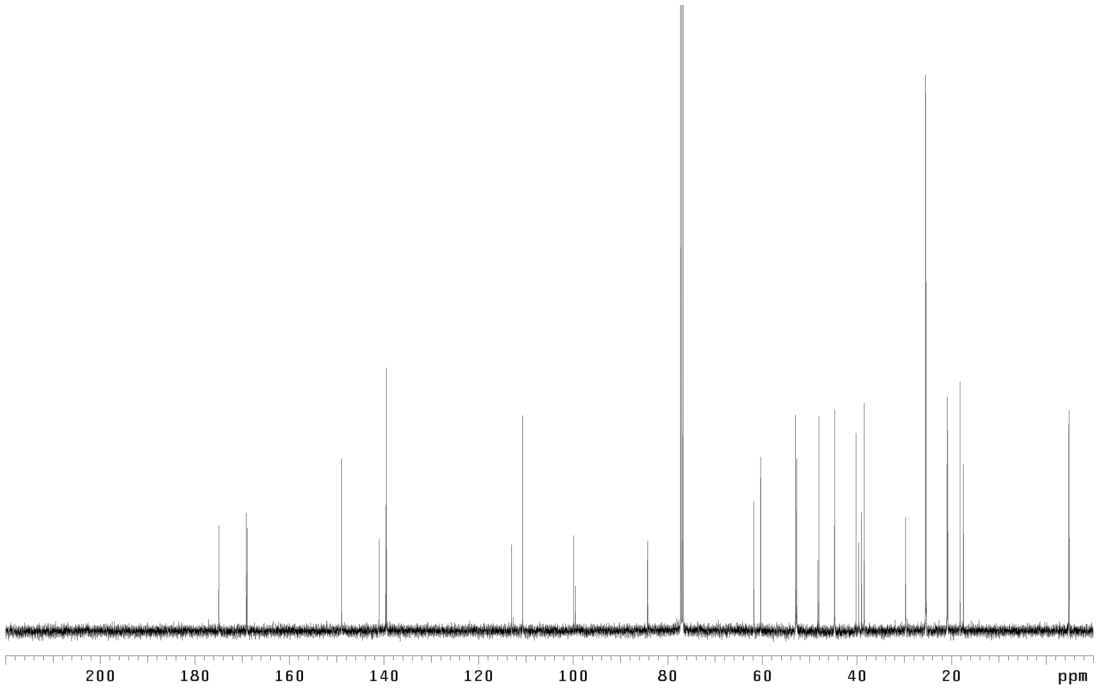

Figure A5.7.2 ^{13}C NMR (125 MHz, $CDCl_3$) of compound **154**

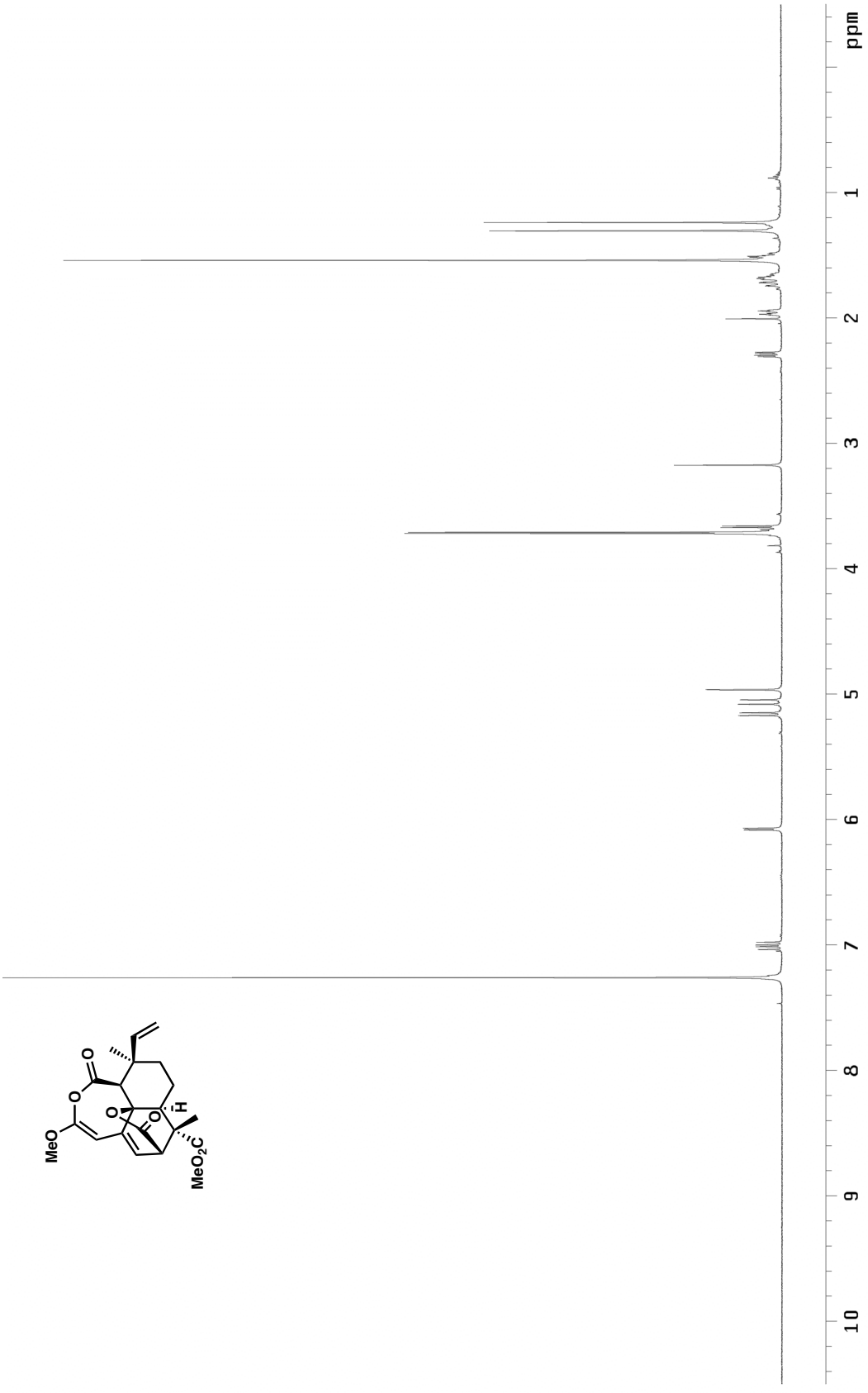

Figure A5.8.1 ^{1}H NMR (500 MHz, $CDCl_3$) of compound **76a**

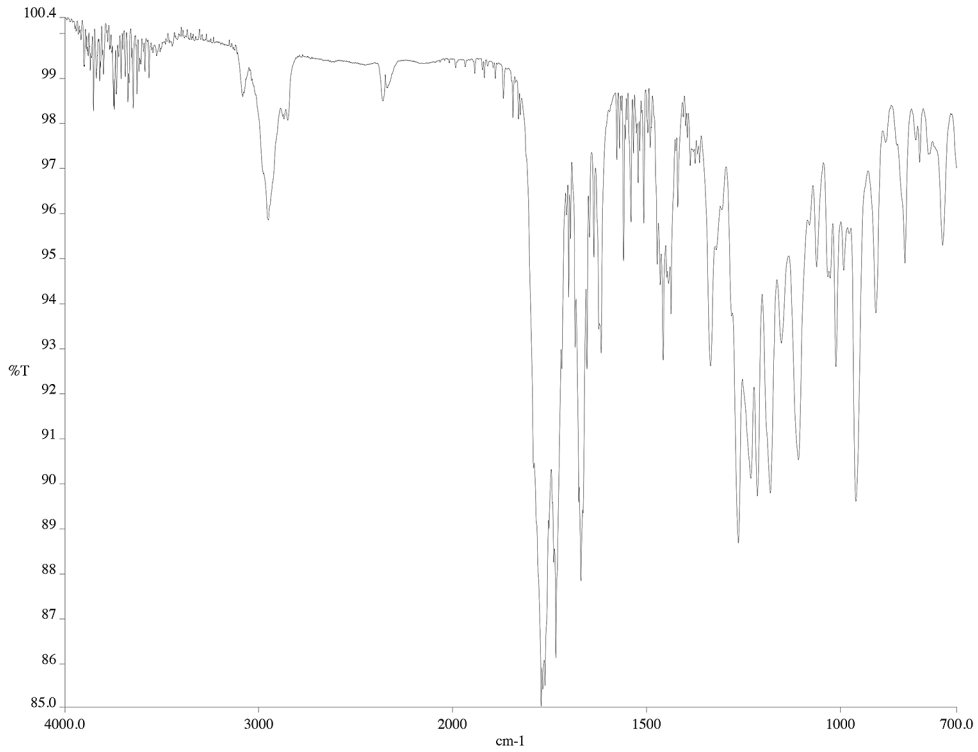

Figure A5.8.2 Infrared spectrum (thin film/NaCl) of compound **76a**

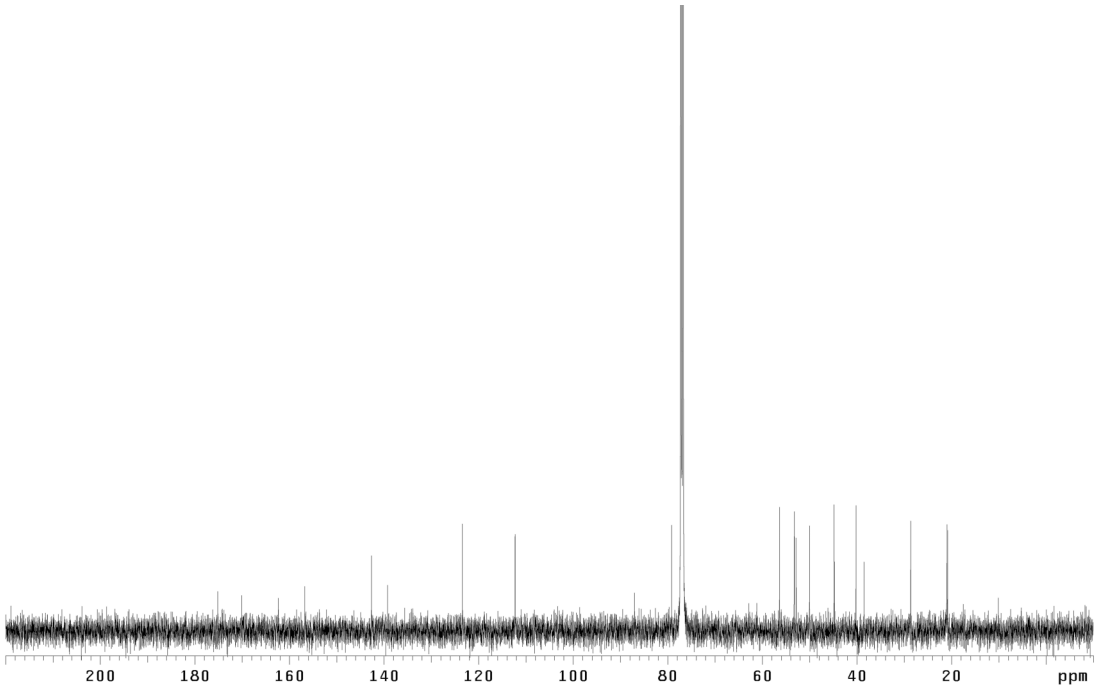

Figure A5.8.2 ^{13}C NMR (125 MHz, $CDCl_3$) of compound **76a**

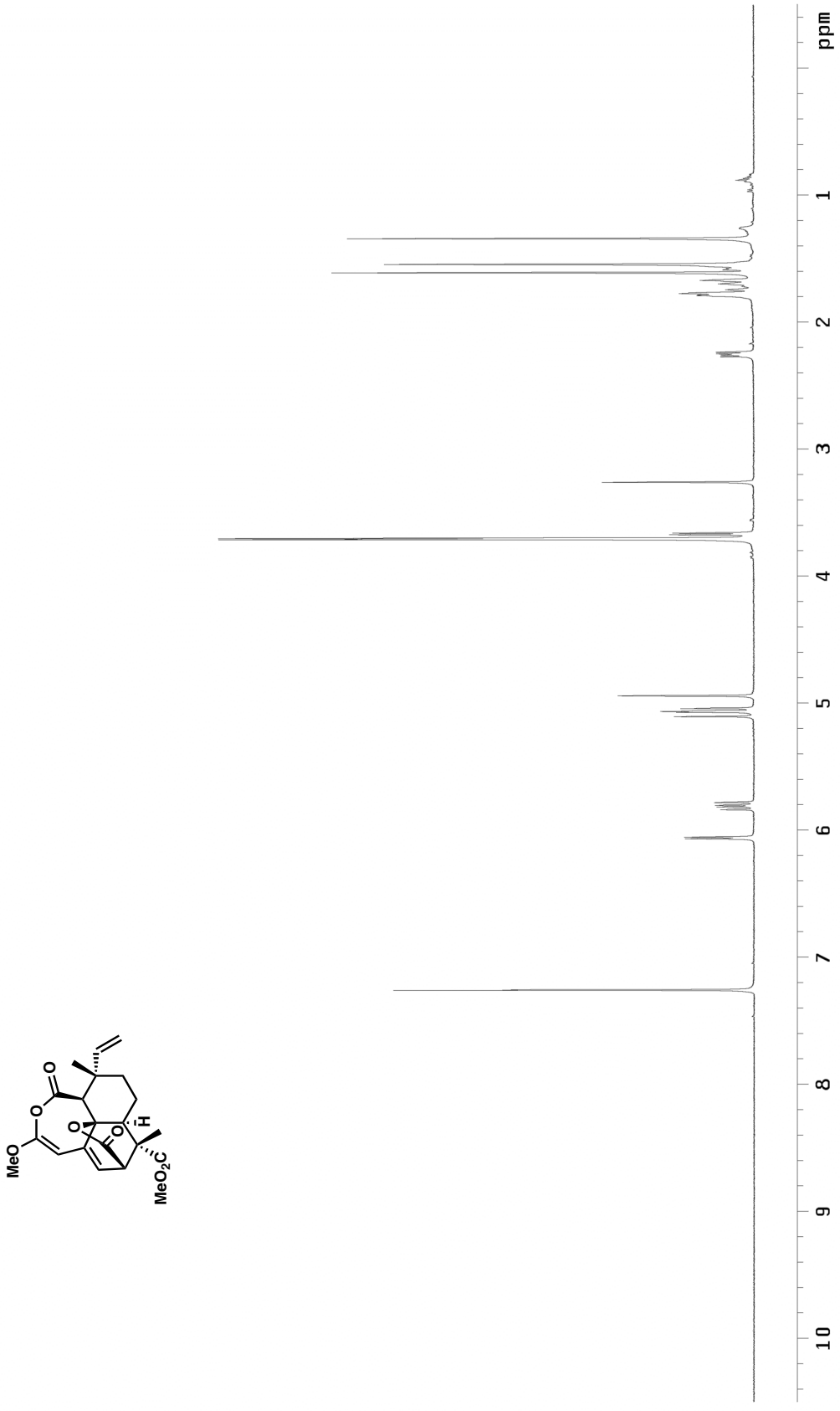

Figure A5.9.1 ^{1}H NMR (500 MHz, $CDCl_3$) of compound **76b**

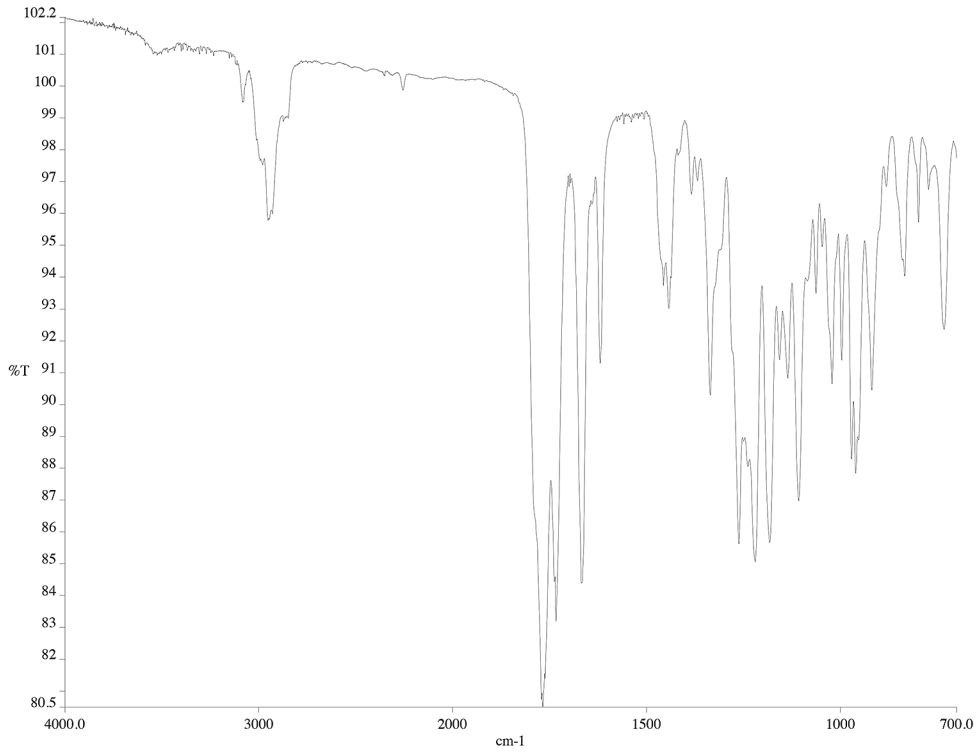

Figure A5.9.2 Infrared spectrum (thin film/NaCl) of compound **76b**

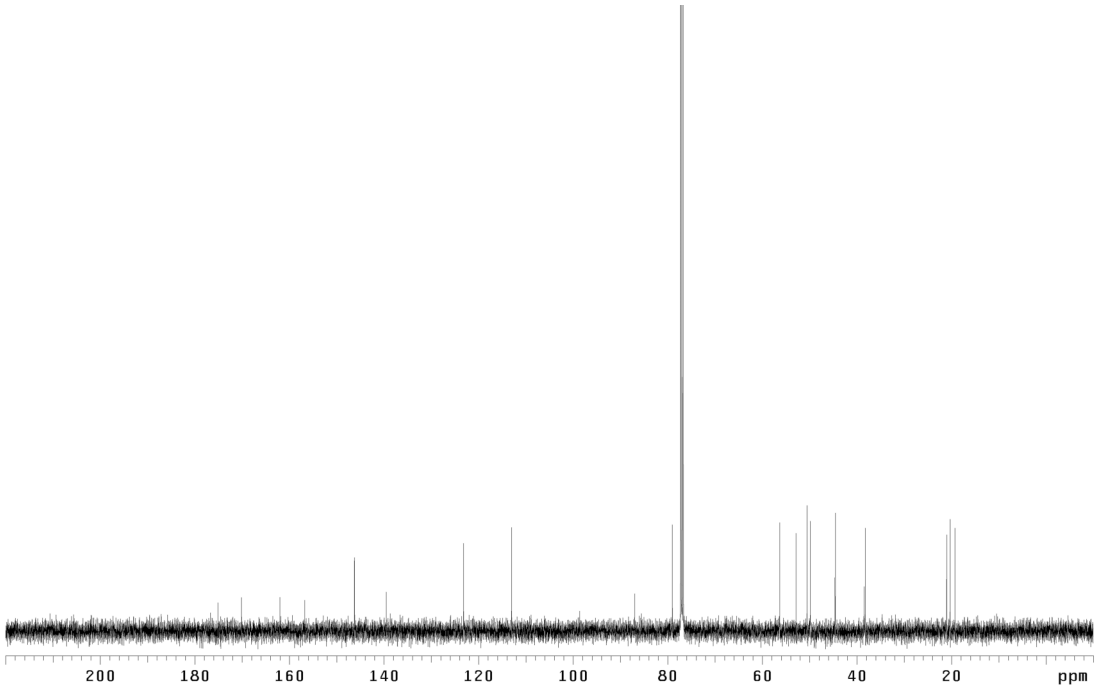

Figure A5.9.2 ^{13}C NMR (125 MHz, $CDCl_3$) of compound **76b**

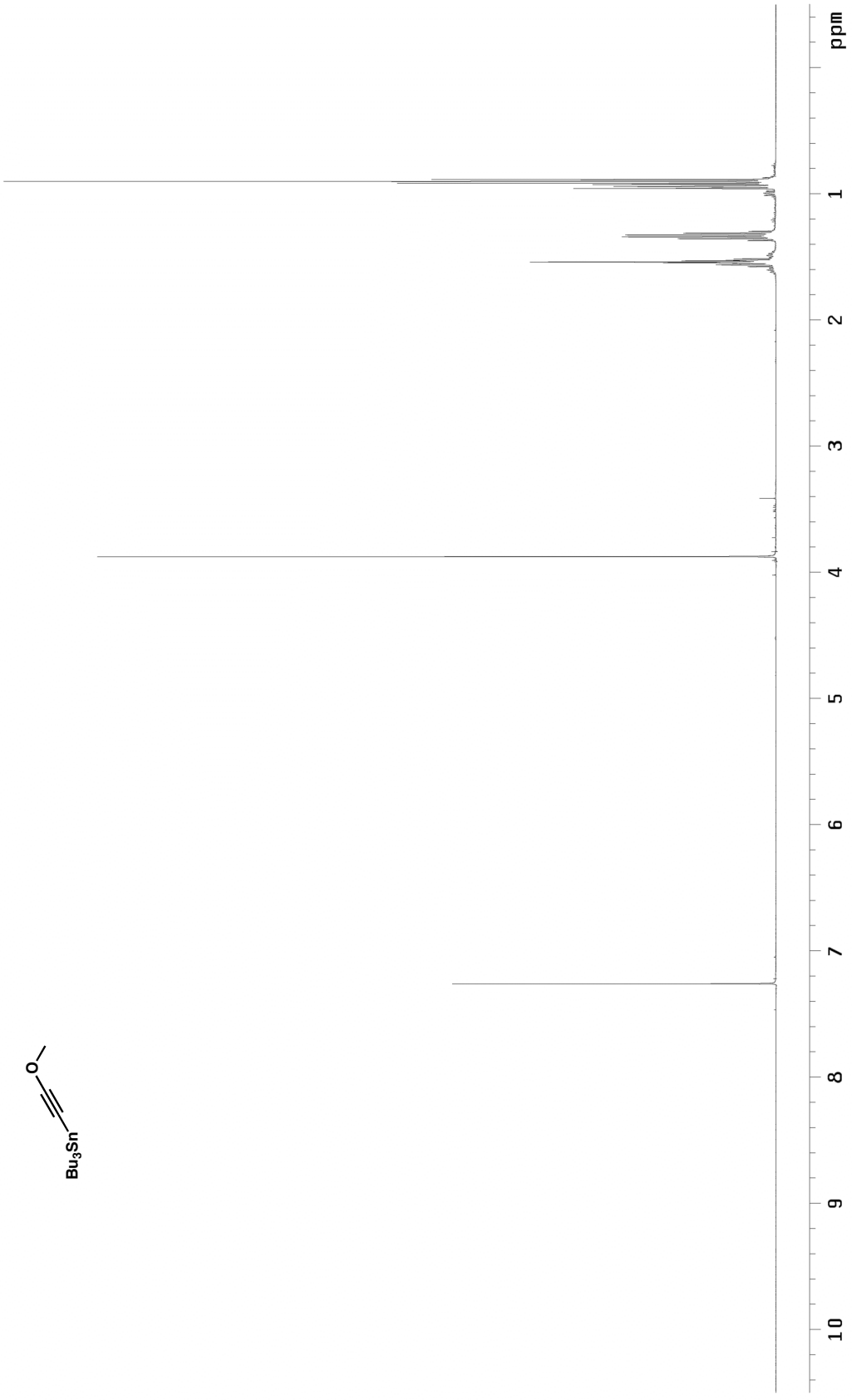

Figure A5.10.1 ^{1}H NMR (500 MHz, $CDCl_3$) of compound **151**

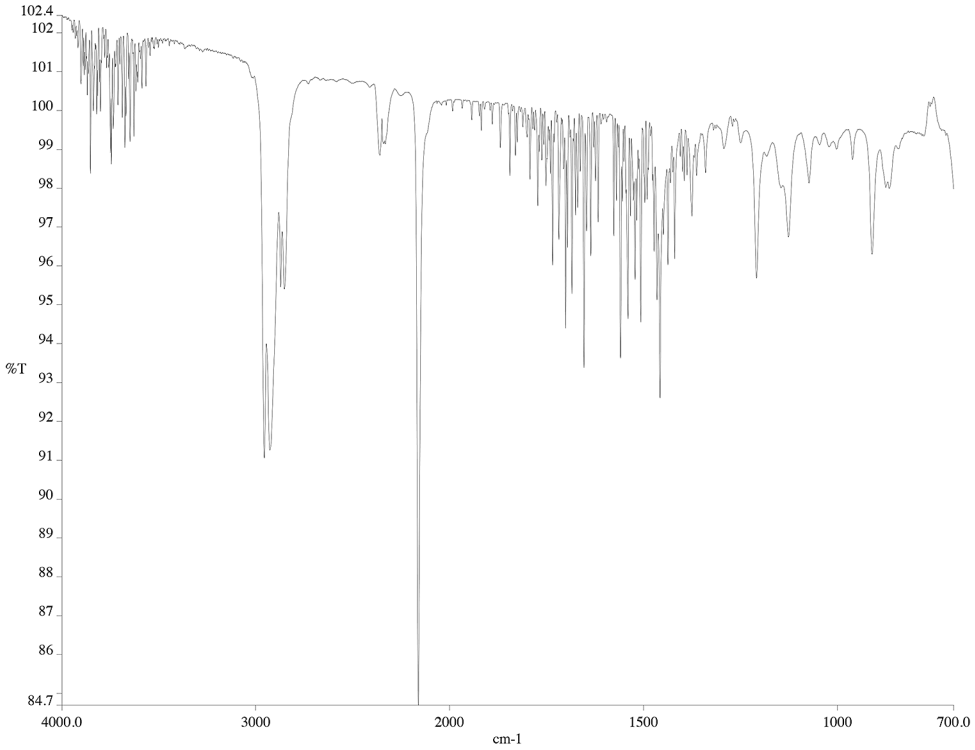

Figure A5.10.2 Infrared spectrum (thin film/NaCl) of compound **151**

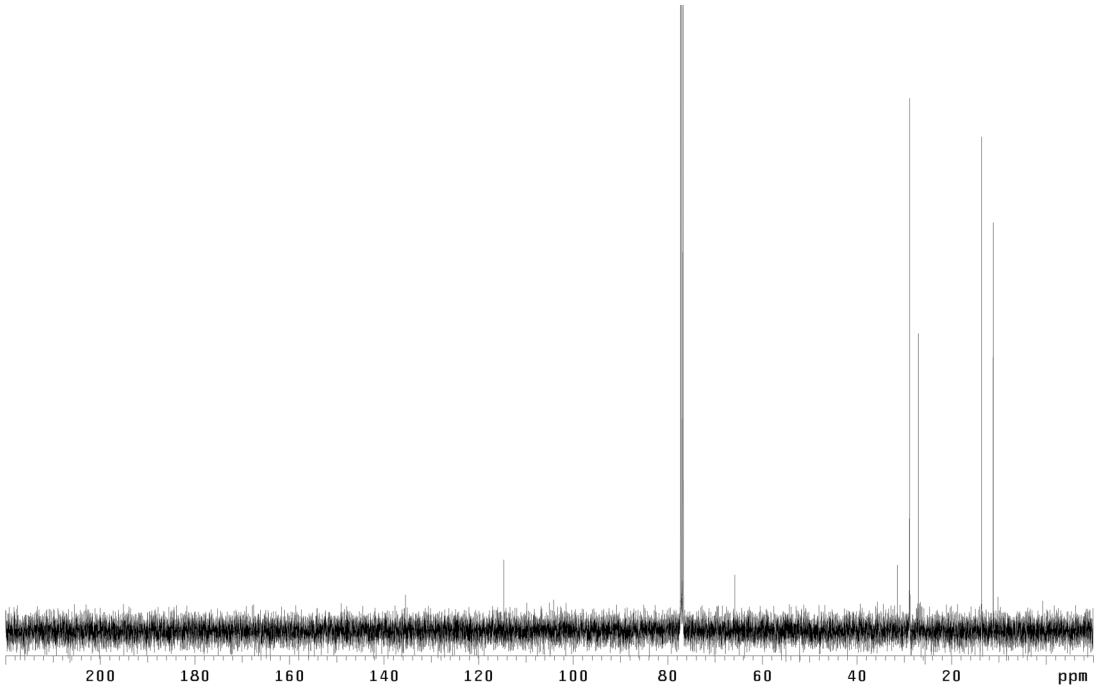

Figure A5.10.2 ^{13}C NMR (125 MHz, $CDCl_3$) of compound **151**

APPENDIX 6

X-Ray Data Relevant to Chapter 3

*Figure A6.1. Ortep diagram of **75a**. The crystallographic data have been deposited in the Cambridge Database (CCDC) and has been placed on hold pending further instructions from me. The deposition number is 796908. Ideally the CCDC would like the publication to contain a footnote of the type: "Crystallographic data have been deposited at the CCDC, 12 Union Road, Cambridge CB2 1EZ, UK and copies can be obtained on request, free of charge, by quoting the publication citation and the deposition number 796908."*

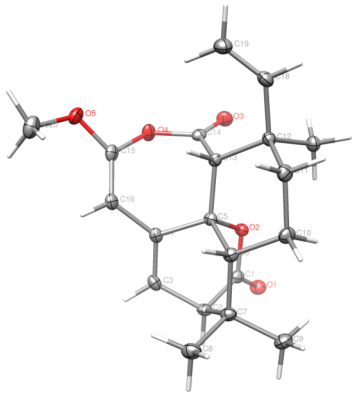

*Table A6.1 Crystal data and structure refinement for **75a** (CCDC 796908)*

Empirical formula	$C_{20}H_{24}O_5$
Formula weight	344.39
Crystallization Solvent	Acetonitrile
Crystal Habit	Plate
Crystal size	0.24 x 0.19 x 0.08 mm^3
Crystal color	Colorless

Data Collection

Type of diffractometer	Bruker KAPPA APEX II	
Wavelength	0.71073 Å MoKα	
Data Collection Temperature	100(2) K	
θ range for 9950 reflections used		
in lattice determination	2.46 to 31.12°	
Unit cell dimensions	a = 11.3376(4) Å	α= 90°

	b = 15.6613(5) Å	β= 90°
	c = 19.2798(7) Å	γ = 90°
Volume	3423.4(2) $Å^3$	
Z	8	
Crystal system	Orthorhombic	
Space group	P *bca*	
Density (calculated)	1.336 Mg/m^3	
F(000)	1472	
Data collection program	Bruker APEX2 v2009.7-0	
θ range for data collection	2.11 to 33.14°	
Completeness to θ = 33.14°	97.9 %	
Index ranges	$-17 \leq h \leq 17, -24 \leq k \leq 24, -28 \leq l \leq 28$	
Data collection scan type	ω scans; 8 settings	
Data reduction program	Bruker SAINT-Plus v7.66A	
Reflections collected	70734	
Independent reflections	6384 [R_{int}= 0.0712]	
Absorption coefficient	0.095 mm^{-1}	
Absorption correction	None	
Max. and min. transmission	0.9924 and 0.977	

Structure solution and Refinement

Structure solution program	SHELXS-97 (Sheldrick, 2008)
Primary solution method	Direct methods
Secondary solution method	Difference Fourier map
Hydrogen placement	Difference Fourier map
Structure refinement program	SHELXL-97 (Sheldrick, 2008)
Refinement method	Full matrix least-squares on F^2
Data / restraints / parameters	6384 / 0 / 322

Treatment of hydrogen atoms	Unrestrained
Goodness-of-fit on F^2	1.673
Final R indices [I>2σ(I), 4393 reflections]	R1 = 0.0432, *w*R2 = 0.0519
R indices (all data)	R1 = 0.0703, *w*R2 = 0.0533
Type of weighting scheme used	Sigma
Weighting scheme used	$w=1/\sigma^2(Fo^2)$
Max shift/error	0.001
Average shift/error	0.000
Largest diff. peak and hole	0.368 and -0.374 e.Å^{-3}

Special Refinement Details

Crystals were mounted on a glass fiber using Paratone oil then placed on the diffractometer under a nitrogen stream at 100K.

Refinement of F^2 against ALL reflections. The weighted R-factor (*w*R) and goodness of fit (S) are based on F^2, conventional R-factors (R) are based on F, with F set to zero for negative F^2. The threshold expression of $F^2 > 2\sigma(F^2)$ is used only for calculating R-factors(gt) etc. and is not relevant to the choice of reflections for refinement. R-factors based on F^2 are statistically about twice as large as those based on F, and R-factors based on ALL data will be even larger.

All esds (except the esd in the dihedral angle between two l.s. planes) are estimated using the full covariance matrix. The cell esds are taken into account individually in the estimation of esds in distances, angles and torsion angles; correlations between esds in cell parameters are only used when they are defined by crystal symmetry. An approximate (isotropic) treatment of cell esds is used for estimating esds involving l.s. planes.

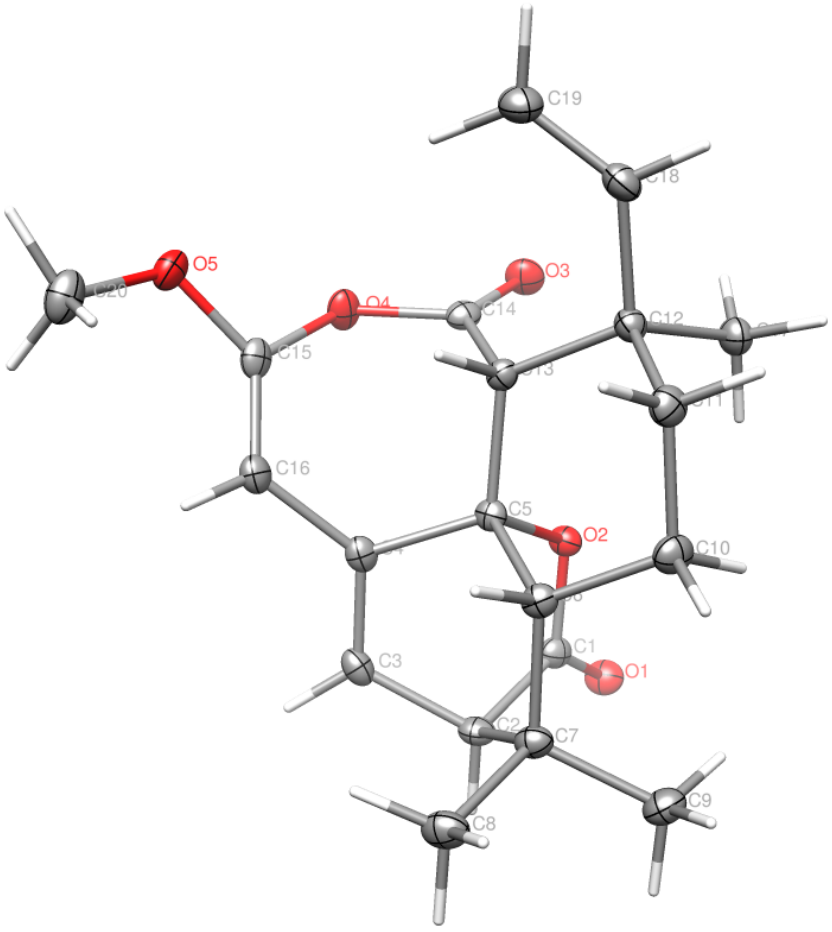
C19
C18
O5
O3
C20
O4
C14
C15
C12
C16
C5
O2
C10
C1
O1
C3
C2
C7
C9
C8

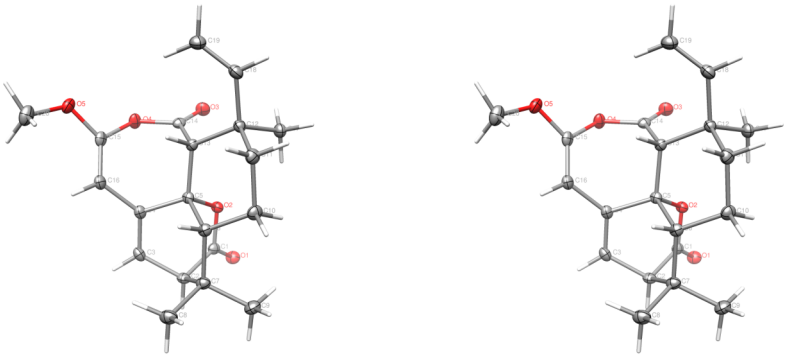

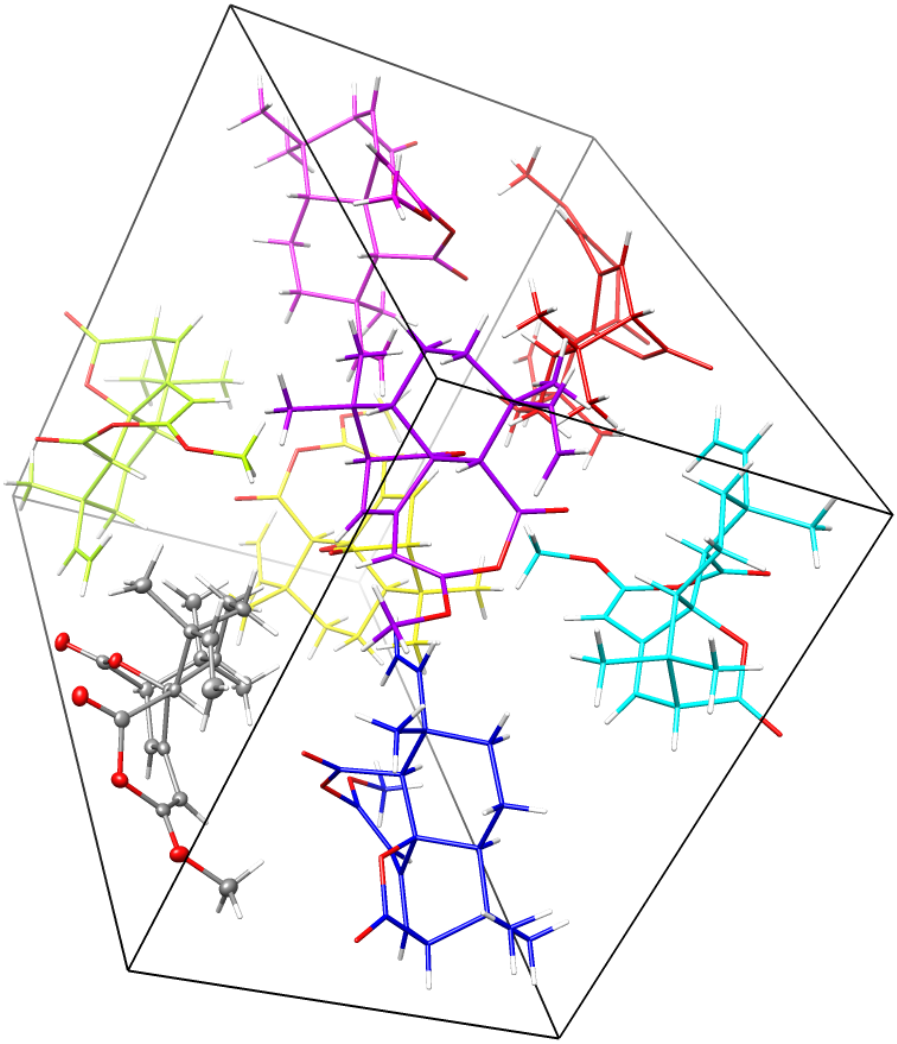

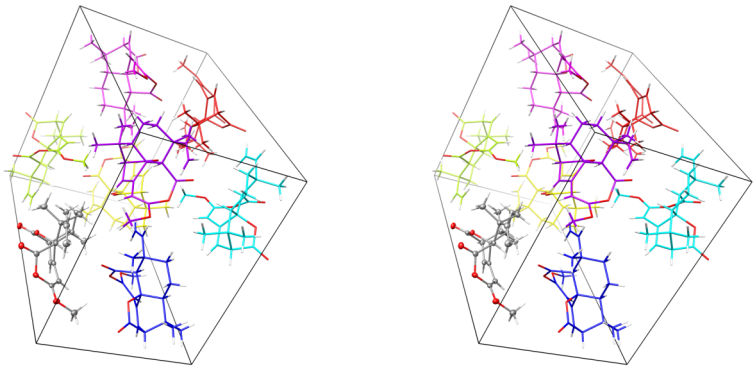

Table A6.2. Atomic coordinates (x 10^4) and equivalent isotropic displacement parameters (Å^{2}x 10^3) for **75a** (CCDC 796908). U(eq) is defined as the trace of the orthogonalized U^{ij} tensor.

	x	y	z	U_{eq}
O(1)	-665(1)	1162(1)	5055(1)	19(1)
O(2)	-56(1)	1806(1)	6020(1)	13(1)
O(3)	-1466(1)	2178(1)	7396(1)	19(1)
O(4)	-223(1)	1263(1)	7857(1)	18(1)
O(5)	1084(1)	850(1)	8621(1)	20(1)
C(1)	126(1)	1285(1)	5465(1)	15(1)
C(2)	1354(1)	928(1)	5448(1)	15(1)
C(3)	1520(1)	472(1)	6129(1)	16(1)
C(4)	1335(1)	957(1)	6685(1)	14(1)
C(5)	973(1)	1863(1)	6489(1)	12(1)
C(6)	2001(1)	2267(1)	6072(1)	14(1)
C(7)	2226(1)	1707(1)	5410(1)	16(1)
C(8)	3497(1)	1372(1)	5414(1)	21(1)
C(9)	2014(1)	2184(1)	4728(1)	20(1)
C(10)	1808(1)	3218(1)	5947(1)	18(1)
C(11)	1571(1)	3682(1)	6629(1)	17(1)
C(12)	439(1)	3369(1)	6992(1)	14(1)
C(13)	598(1)	2402(1)	7117(1)	12(1)
C(14)	-453(1)	1977(1)	7450(1)	15(1)
C(15)	908(1)	942(1)	7932(1)	16(1)
C(16)	1599(1)	731(1)	7407(1)	16(1)

C(17)	-637(1)	3614(1)	6545(1)	18(1)
C(18)	328(1)	3843(1)	7675(1)	18(1)
C(19)	333(1)	3540(1)	8312(1)	23(1)
C(20)	2259(1)	605(1)	8824(1)	26(1)

Table A6.3. Bond lengths [Å] and angles [°] for **75a**

O(1)-C(1)	1.2115(10)	C(9)-H(9A)	0.979(11)		
O(2)-C(1)	1.3627(10)	C(9)-H(9B)	1.006(10)		
O(2)-C(5)	1.4782(10)	C(9)-H(9C)	0.994(10)		
O(3)-C(14)	1.1951(11)	C(10)-C(11)	1.5253(14)		
O(4)-C(15)	1.3858(11)	C(10)-H(10A)	1.031(9)		
O(4)-C(14)	1.3896(11)	C(10)-H(10B)	0.987(10)		
O(5)-C(15)	1.3499(10)	C(11)-C(12)	1.5422(13)		
O(5)-C(20)	1.4414(13)	C(11)-H(11A)	0.999(10)		
C(1)-C(2)	1.5005(13)	C(11)-H(11B)	0.973(9)		
C(2)-C(3)	1.5072(14)	C(12)-C(18)	1.5159(13)		
C(2)-C(7)	1.5710(13)	C(12)-C(17)	1.5431(13)		
C(2)-H(2)	0.997(9)	C(12)-C(13)	1.5436(13)		
C(3)-C(4)	1.3298(13)	C(13)-C(14)	1.5082(13)		
C(3)-H(3)	0.955(10)	C(13)-H(13)	0.964(9)		
C(4)-C(16)	1.4684(13)	C(15)-C(16)	1.3220(13)		
C(4)-C(5)	1.5244(13)	C(16)-H(16)	0.924(9)		
C(5)-C(13)	1.5361(13)	C(17)-H(17A)	0.977(9)		
C(5)-C(6)	1.5512(13)	C(17)-H(17B)	0.979(9)		
C(6)-C(10)	1.5255(14)	C(17)-H(17C)	1.025(10)		
C(6)-C(7)	1.5685(13)	C(18)-C(19)	1.3158(14)		
C(6)-H(6)	0.968(9)	C(18)-H(18)	0.954(10)		
C(7)-C(8)	1.5328(13)	C(19)-H(19A)	1.017(11)		
C(7)-C(9)	1.5313(14)	C(19)-H(19B)	0.975(10)		
C(8)-H(8A)	1.013(10)	C(20)-H(20A)	1.000(11)		
C(8)-H(8B)	0.995(10)	C(20)-H(20B)	1.041(9)		
C(8)-H(8C)	0.985(10)	C(20)-H(20C)	0.973(11)		

		C(10)-C(6)-H(6)	107.0(6)
C(1)-O(2)-C(5)	113.39(7)	C(5)-C(6)-H(6)	104.9(5)
C(15)-O(4)-C(14)	121.69(7)	C(7)-C(6)-H(6)	107.8(5)
C(15)-O(5)-C(20)	115.58(8)	C(8)-C(7)-C(9)	108.55(8)
O(1)-C(1)-O(2)	119.71(9)	C(8)-C(7)-C(6)	109.91(8)
O(1)-C(1)-C(2)	127.90(9)	C(9)-C(7)-C(6)	113.58(9)
O(2)-C(1)-C(2)	112.39(8)	C(8)-C(7)-C(2)	109.02(9)
C(1)-C(2)-C(3)	105.85(8)	C(9)-C(7)-C(2)	108.60(8)
C(1)-C(2)-C(7)	107.22(8)	C(6)-C(7)-C(2)	107.10(8)
C(3)-C(2)-C(7)	109.24(8)	C(7)-C(8)-H(8A)	110.6(6)
C(1)-C(2)-H(2)	109.0(5)	C(7)-C(8)-H(8B)	111.9(6)
C(3)-C(2)-H(2)	112.7(5)	H(8A)-C(8)-H(8B)	108.6(8)
C(7)-C(2)-H(2)	112.4(5)	C(7)-C(8)-H(8C)	109.3(6)
C(4)-C(3)-C(2)	114.29(10)	H(8A)-C(8)-H(8C)	108.1(8)
C(4)-C(3)-H(3)	125.7(5)	H(8B)-C(8)-H(8C)	108.2(8)
C(2)-C(3)-H(3)	120.0(5)	C(7)-C(9)-H(9A)	111.7(5)
C(3)-C(4)-C(16)	126.43(9)	C(7)-C(9)-H(9B)	113.1(5)
C(3)-C(4)-C(5)	112.03(9)	H(9A)-C(9)-H(9B)	108.7(8)
C(16)-C(4)-C(5)	120.96(8)	C(7)-C(9)-H(9C)	110.0(6)
O(2)-C(5)-C(4)	107.93(7)	H(9A)-C(9)-H(9C)	106.6(8)
O(2)-C(5)-C(13)	107.24(7)	H(9B)-C(9)-H(9C)	106.5(7)
C(4)-C(5)-C(13)	113.04(8)	C(11)-C(10)-C(6)	110.82(8)
O(2)-C(5)-C(6)	107.49(7)	C(11)-C(10)-H(10A)	110.2(5)
C(4)-C(5)-C(6)	107.74(8)	C(6)-C(10)-H(10A)	110.6(5)
C(13)-C(5)-C(6)	113.15(8)	C(11)-C(10)-H(10B)	110.2(6)
C(10)-C(6)-C(5)	111.80(8)	C(6)-C(10)-H(10B)	109.4(6)
C(10)-C(6)-C(7)	116.19(8)	H(10A)-C(10)-H(10B)	105.5(7)
C(5)-C(6)-C(7)	108.44(8)	C(10)-C(11)-C(12)	112.75(9)

C(10)-C(11)-H(11A)	110.8(5)	H(17A)-C(17)-H(17B)	107.6(8)
C(12)-C(11)-H(11A)	107.9(5)	C(12)-C(17)-H(17C)	107.9(6)
C(10)-C(11)-H(11B)	111.0(5)	H(17A)-C(17)-H(17C)	109.8(8)
C(12)-C(11)-H(11B)	109.5(5)	H(17B)-C(17)-H(17C)	106.2(7)
H(11A)-C(11)-H(11B)	104.4(8)	C(19)-C(18)-C(12)	129.26(11)
C(18)-C(12)-C(17)	107.35(8)	C(19)-C(18)-H(18)	118.9(5)
C(18)-C(12)-C(11)	107.96(8)	C(12)-C(18)-H(18)	111.9(5)
C(17)-C(12)-C(11)	108.94(8)	C(18)-C(19)-H(19A)	122.3(5)
C(18)-C(12)-C(13)	110.78(8)	C(18)-C(19)-H(19B)	121.3(6)
C(17)-C(12)-C(13)	114.99(8)	H(19A)-C(19)-H(19B)	116.4(8)
C(11)-C(12)-C(13)	106.63(8)	O(5)-C(20)-H(20A)	111.9(6)
C(14)-C(13)-C(5)	108.18(8)	O(5)-C(20)-H(20B)	105.9(5)
C(14)-C(13)-C(12)	114.05(8)	H(20A)-C(20)-H(20B)	109.8(8)
C(5)-C(13)-C(12)	116.66(8)	O(5)-C(20)-H(20C)	111.0(6)
C(14)-C(13)-H(13)	107.4(5)	H(20A)-C(20)-H(20C)	109.4(9)
C(5)-C(13)-H(13)	104.0(5)	H(20B)-C(20)-H(20C)	108.8(8)
C(12)-C(13)-H(13)	105.6(6)		
O(3)-C(14)-O(4)	116.20(9)		
O(3)-C(14)-C(13)	127.22(9)		
O(4)-C(14)-C(13)	116.57(8)		
C(16)-C(15)-O(5)	129.76(10)		
C(16)-C(15)-O(4)	123.95(9)		
O(5)-C(15)-O(4)	106.16(8)		
C(15)-C(16)-C(4)	123.05(10)		
C(15)-C(16)-H(16)	118.4(6)		
C(4)-C(16)-H(16)	118.2(6)		
C(12)-C(17)-H(17A)	112.3(5)		
C(12)-C(17)-H(17B)	112.8(6)		

Table A6.4. Anisotropic displacement parameters ($Å^2 x\ 10^4$) for **75a**. The anisotropic displacement factor exponent takes the form: $-2\pi^2[\ h^2a^{*2}U^{11} + ... + 2\ h\ k\ a^*\ b^*\ U^{12}\ ]$

	U^{11}	U^{22}	U^{33}	U^{23}	U^{13}	U^{12}
O(1)	155(4)	237(4)	178(4)	-35(3)	-36(3)	-13(3)
O(2)	109(3)	152(4)	138(3)	-23(3)	-18(3)	2(3)
O(3)	133(4)	227(4)	216(4)	-8(3)	18(3)	0(3)
O(4)	148(4)	191(4)	209(4)	62(3)	18(3)	-6(3)
O(5)	237(4)	214(4)	149(4)	33(3)	-27(3)	-10(3)
C(1)	162(5)	133(5)	149(5)	8(4)	22(4)	-20(4)
C(2)	142(5)	172(5)	139(5)	-43(4)	4(4)	6(4)
C(3)	129(5)	143(5)	219(6)	-2(5)	-9(4)	20(4)
C(4)	109(5)	135(5)	178(5)	11(4)	-4(4)	-12(4)
C(5)	89(4)	143(5)	126(5)	-13(4)	-27(4)	-6(4)
C(6)	105(5)	168(5)	137(5)	-6(4)	-7(4)	-13(4)
C(7)	121(5)	202(6)	142(5)	-15(4)	6(4)	4(4)
C(8)	137(5)	301(7)	198(6)	-29(6)	14(5)	19(5)
C(9)	186(6)	256(6)	149(6)	-1(5)	8(5)	-13(5)
C(10)	184(6)	171(6)	170(6)	17(4)	29(5)	-35(5)
C(11)	194(6)	138(5)	183(6)	7(5)	-3(5)	-25(5)
C(12)	144(5)	125(5)	145(5)	-5(4)	-11(4)	5(4)
C(13)	103(5)	144(5)	120(5)	1(4)	-11(4)	-5(4)
C(14)	169(5)	145(5)	124(5)	-32(4)	-7(4)	-17(4)
C(15)	163(5)	129(5)	185(6)	33(4)	-35(4)	-32(4)
C(16)	147(5)	137(5)	191(6)	16(4)	-19(5)	0(4)

C(17)	185(6)	176(6)	177(6)	11(5)	-17(5)	27(5)
C(18)	179(5)	147(6)	207(6)	-34(5)	-20(4)	26(4)
C(19)	283(7)	227(6)	185(6)	-55(5)	-29(5)	36(5)
C(20)	251(7)	275(7)	246(7)	60(6)	-81(5)	-46(6)

Table A6.5. Hydrogen coordinates (x 10^4) and isotropic displacement parameters (Å^{2}x 10^3) for ***75a***

	x	y	z	U_{iso}
H(2)	1432(8)	540(6)	5040(4)	13(3)
H(3)	1765(8)	-111(6)	6135(4)	15(3)
H(6)	2683(8)	2213(6)	6371(4)	12(3)
H(8A)	3640(8)	988(7)	5000(5)	28(3)
H(8B)	3678(8)	1047(7)	5844(5)	27(3)
H(8C)	4047(9)	1858(7)	5384(5)	24(3)
H(9A)	2565(9)	2659(7)	4669(5)	22(3)
H(9B)	1186(9)	2407(6)	4683(4)	21(3)
H(9C)	2142(8)	1793(7)	4329(5)	26(3)
H(10A)	1119(8)	3314(6)	5607(4)	15(3)
H(10B)	2509(8)	3462(6)	5717(4)	21(3)
H(11A)	1493(8)	4310(7)	6551(4)	16(3)
H(11B)	2238(8)	3628(6)	6943(4)	13(3)
H(13)	1250(8)	2351(6)	7435(4)	11(3)
H(16)	2316(8)	476(6)	7503(4)	16(3)
H(17A)	-1382(8)	3537(6)	6793(4)	17(3)
H(17B)	-685(8)	3284(6)	6114(5)	21(3)
H(17C)	-544(9)	4240(7)	6401(4)	24(3)
H(18)	242(8)	4443(7)	7608(4)	21(3)
H(19A)	445(9)	2908(7)	8415(5)	31(3)
H(19B)	237(9)	3915(7)	8712(5)	30(3)
H(20A)	2450(8)	9(7)	8677(5)	24(3)
H(20B)	2279(8)	647(6)	9363(5)	28(3)

H(20C)	2843(9)	996(7)	8634(5)	35(3)

Chapter 4

The Enantioselective Total Syntheses of Transtaganolides A–D and the Biosynthetic Implications

4.1 Introduction

Recently our group disclosed a general strategy for the total syntheses of several transtaganolide natural products (**75** and **76**, Scheme 4.1).[1] In its simplest embodiment, racemic transtaganolides C (**75a**) and D (**75b**) were prepared in 5 steps from commercial starting materials. Integral to our approach was an Ireland–Claisen rearrangement/intramolecular pyrone Diels–Alder cyclization cascade (ICR/IMPDA) furnishing the stereochemically complex, tricyclic core (**138**) in a single step from a monocyclic achiral precursor (**140**) (Scheme 4.2).[2] Furthermore, a novel Pd-mediated [5+2] annulation reaction of a reactive alkoxyacetylene (**151**) allowed for late-stage formation of the fragile cyclic ketene-acetal (C-ring), the structural trademark of these unique metabolites.

Scheme 4.1. The transtaganolides and basiliolides

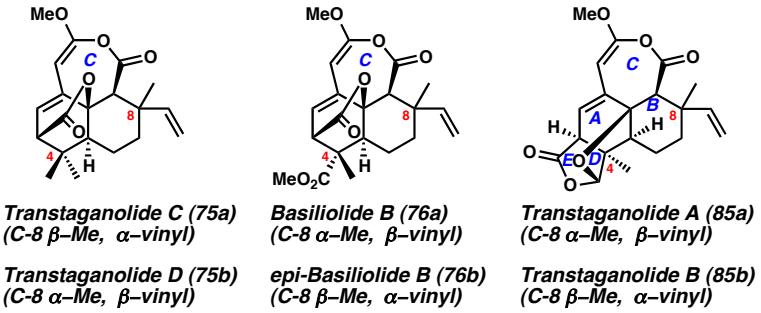

Scheme 4.2. General strategy for total synthesis

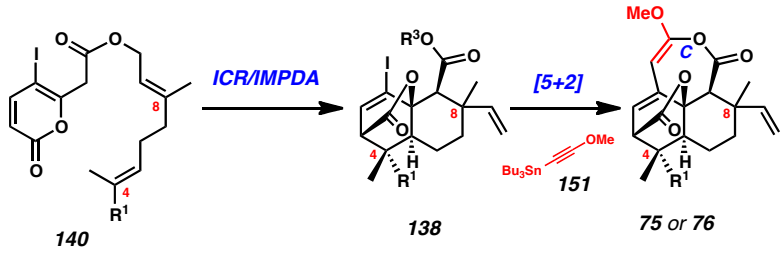

While concise and modular, our approach fell short of achieving two key goals: the preparation of enantioenriched products and the synthesis of transtaganolides A (**85a**) and B (**85b**), the most complex members of the natural product family. Transtaganolides A (**85a**) and B (**85b**) are unique within their class due to their lack of an oxabicyclo[2.2.2]octene structural motif (Scheme 4.1, **85** vs.**75** and **76**). Replacing it is a fused 5-membered lactone (E ring, **85**), which is bridged by an ether linkage (D ring) that contorts the pentacyclic core into a compact, caged structure (Scheme 4.1 and 4.3). Herein, strategies to overcome these synthetic challenges are presented, culminating in the enantioselective total syntheses of (–)-transtaganolide A (**85a**) and (+)-transtaganolide B (**85b**), which to date have eluded total synthesis. Furthermore, (–)-transtaganolide C (**75a**) and (+)-transtaganolide D (**75b**), which were the subject of our previous racemic synthesis, have been prepared enantioslectively. The absolute

configurations of these compounds are also disclosed and discussed within the context of existing biosynthetic hypotheses.[2]

4.2 Strategy for the Enantioselective Syntheses of Transtaganolides A–D

After several unsuccessful attempts to utilize reported methods for asymmetric ester-enolate-Claisen rearrangements on our unique system,[3] we turned to the early work of Ireland and co-workers.[4] They demonstrated the efficient employment of α-acyloxy allylic silanes (e.g., **157** in Scheme 4.3) as chiral, primary alcohol equivalents in Ireland-Claisen rearrangements. We envisioned that the use of such a chiral directing group in our key ICR/IMPDA cyclization cascade could serve as an entry point into the enantioselective synthesis of all members of the natural product family, including transtaganolides A and B.

Scheme 4.3. Retrosynthetic analysis with inclusion of chiral directing group

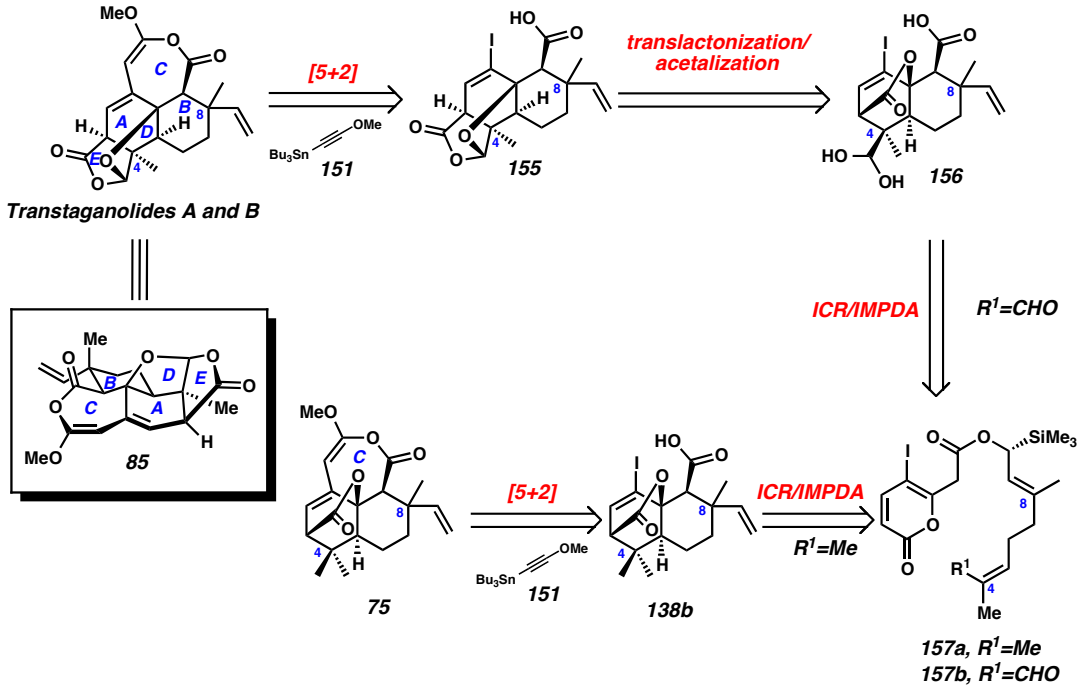

Retrosynthetically, transtaganolides A and B (**85**) could derive from optically active tetracycle **155** by application of our previously disclosed [5+2] annulation technology (Scheme 4.3).[1] We envisioned that the tetracyclic core (**155**) could in turn arise from a translactonization/acetalization reaction of hydrated aldehyde **156**. Similar to our previously disclosed strategy, tricycle **156** could be derived from an ICR/IMPDA cascade of enantioenriched monocyclic precursor **157b** with the requisite aldehyde oxidation state. Notably, enantioenriched transtaganolides C and D (**75**) could be prepared from tricycle **138b**, which could also derive from a chiral pyrone ester such as **157a** by our ICR/IMPDA cascade reaction.

4.3 Enantioselective Total Syntheses of Transtaganolides C and D

Our studies began with the application of this retrosynthetic hypothesis to transtaganolides C (**75a**) and D (**75b**) (Scheme 4.4). Hoppe's enantioenriched geraniol derivative **159** was prepared by treatment of carbamate **158** with *n*-BuLi, freshly distilled (–)-sparteine, and trimethylsilyl chloride.[5] Subsequent reduction of the intermediate carbamate furnished enantioenriched geraniol equivalent **159** in good yield and 89.5% *ee*. Coupling of alcohol **159** to pyrone acid **142b** provided the desired cascade substrate **157a** in good yield. Gratifyingly, exposure of pyrone ester **157a** to our ICR/IMPDA cascade conditions afforded vinyl silanes **160a** and **160b** in 78% yield as a 4:1 mixture of diastereomers with 89.5% *ee* and 80.5% *ee*, respectively. We were pleased to find that subsequent exposure of vinyl silanes **160** to aqueous HBF_4 yielded tricycles **138a** and **138b**. Protection of free acids **138** as silyl esters **161a** and **161b** followed by treatment with stannane **151** and $Pd(PPh_3)_4$ yielded (–)-transtaganolide C (**75a**) and (+)-transtaganolide D (**75b**).

Scheme 4.4. Enantioselective total synthesis of transtaganolides C and D

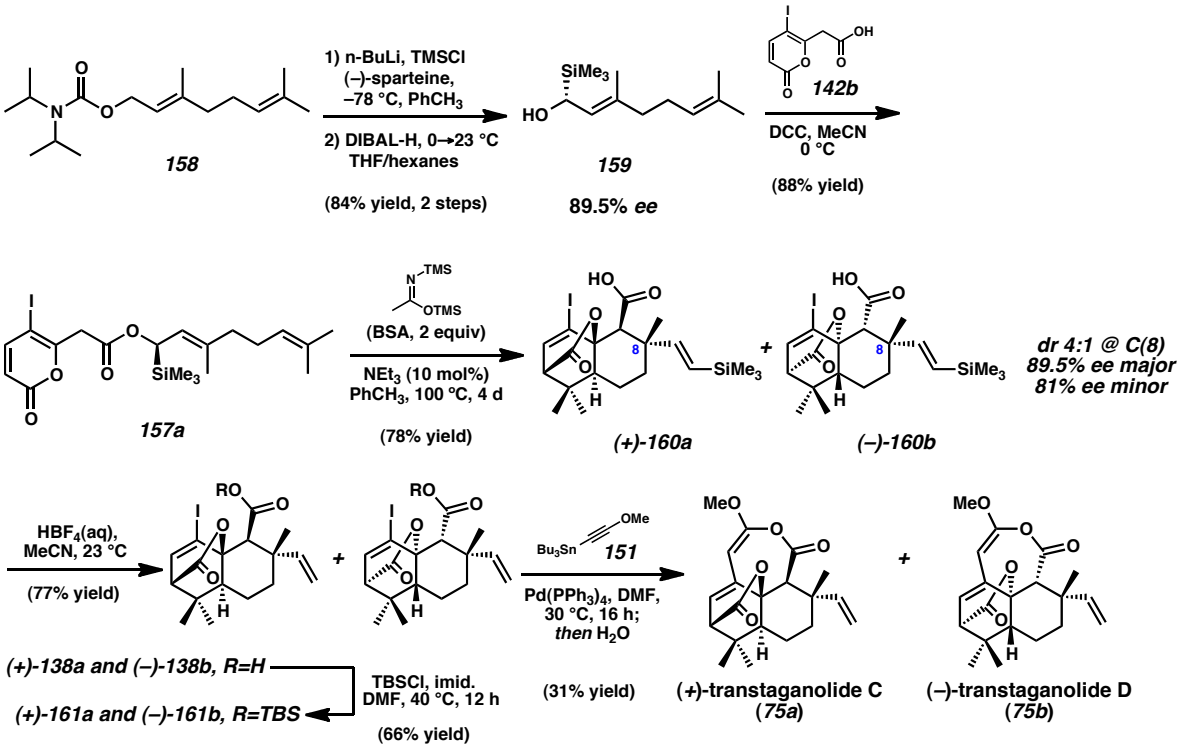

4.4 Enantioselective Total Syntheses of Transtaganolides A and B

Having established the feasibility of the chiral geraniol approach to setting critical stereochemistry, we sought to prepare enantioenriched transtaganolides A (**85a**) and B (**85b**). The most apparent path to this goal relies on the utilization of a chiral *Z*-enal such as **157b** in our ICR/IMPDA cyclization cascade to produce aldehydes **163a** and **163b**, predisposed by proximity to undergo the desired skeletal rearrangement (Scheme 4.5). However, we found that *Z*-enal **157b** was difficult to prepare and configurationally unstable under myriad reaction conditions.[6]

Scheme 4.5. Initial attempts at preparing the tricyclic cores of transtaganolides A and B

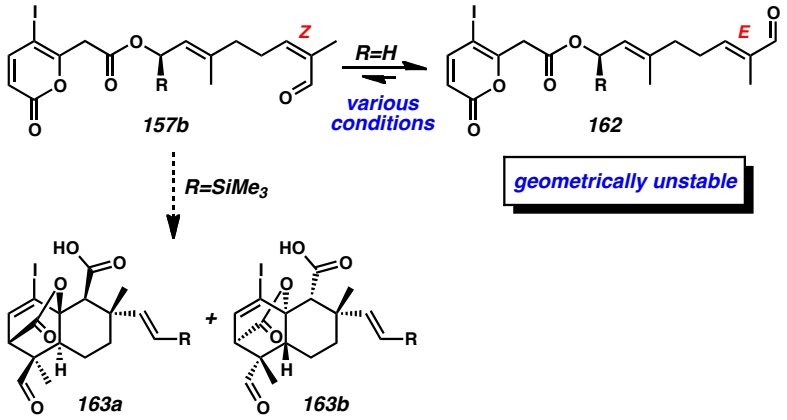

Prompted by these experimental cues, efforts refocused on preparing a protected aldehyde equivalent. Enantioenriched geraniol derivative **159** was protected as the acetate ester under standard conditions (Scheme 4.6).[7] Selective oxidation with *m*-CPBA, followed by oxidation of the intermediate epoxide with periodic acid cleanly provided aldehyde **164**.[8] Utilization of the Still–Gennari modification of the Horner–Wadsworth–Emmons reaction followed by deprotection of the acetate group allowed for formation of *Z*-methylenoate **166** in good yield and excellent diastereoselectivity.[9] Coupling of **166** to iodoacid **142b** yielded ICR/IMPDA cascade substrate, pyrone ester **167**. Prolonged heating of ester **167** with *N,O*-bis(trimethylsilyl)acetamide (BSA) in the presence of a catalytic amount of triethylamine afforded tricycles **168a** and **168b** in synthetically useful yield.

Scheme 4.6. Syntheses of enantioenriched tricyclic cores of transtaganolides A and B

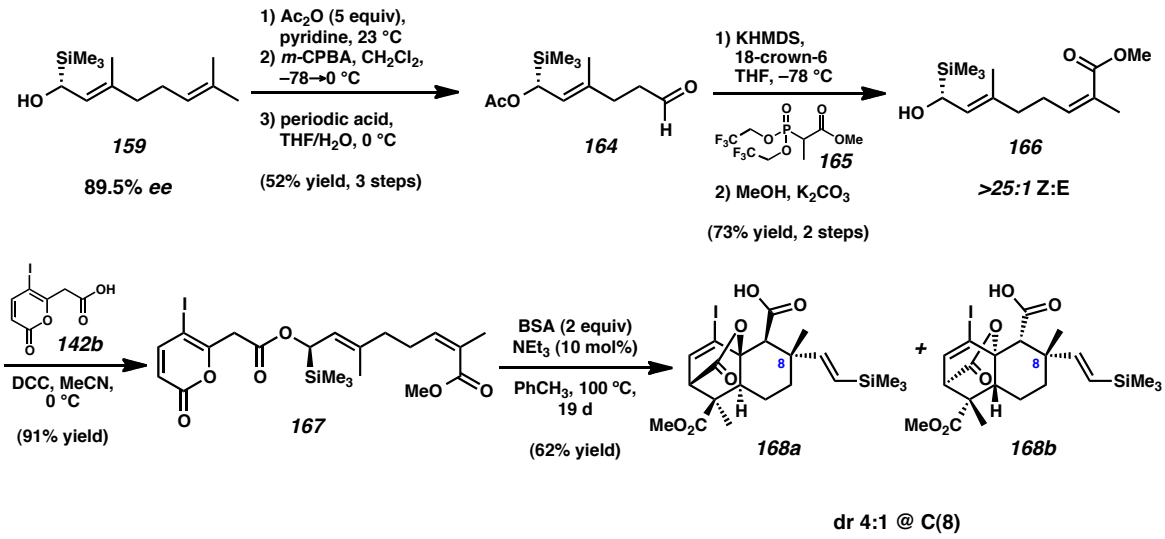

To our delight, brief exposure of acids **168a** and **168b** to an excess of DIBAL-H at low temperature, followed by carefully quenching with acetic acid at low temperatures resulted in clean and chemoselective reduction to the corresponding aldehydes **163a** and **163b** (Scheme 4.7). The crude aldehydes **163**, when exposed to aqueous HBF_4, underwent the desired translactonization/acetalization process and protodesilylation in one pot to yield caged tetracycles **155a** and **155b**. Transient protection of the free acids (**155**) as the TBS-esters (**169**), followed by application of our [5+2] annulation technology allowed for the enantioselective syntheses of (+)-transtaganolide B (**85b**) and (–)-transtaganolide A (**85a**) in good yield and good optical purity.

Scheme 4.7. Enantioselective total syntheses of transtaganolides A and B

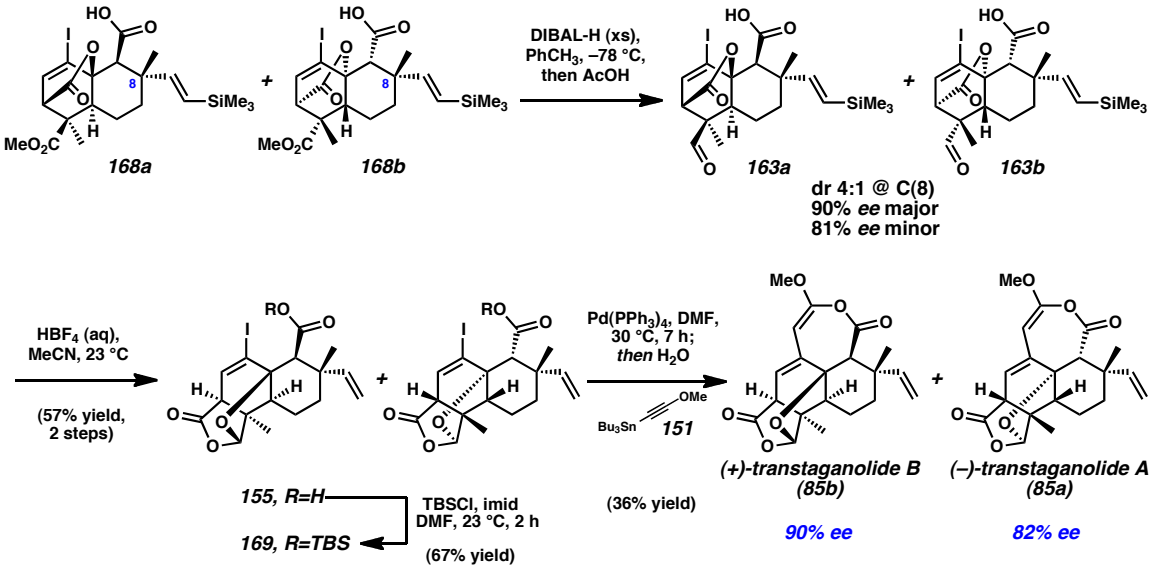

4.5 Biosynthetic Implication of Enantioselective Total Synthesis

Recently, Larsson and co-workers have proposed that the co-isolated prenylated pyrone **89** is the direct biosynthetic precursor of transtaganolides C and D (**75**) (Scheme 4.8).[2b,10] They hypothesized that an unprecedented enzymatic ester-enolate-Claisen rearrangement is responsible for the production of "optically pure" transtaganolides.[2b] Under this scenario, and assuming that the C9 proton is relatively acidic due to the withdrawing nature of the pyrone, we would expect that an enzymatic and presumably enantioselective[11] rearrangement would produce C9 diastereomers **170**, optically pure at C8. The demonstrated propensity of these systems to undergo diastereoselective Diels–Alder rearrangements under allylic strain control,[12] would lead to pseudo-enantiomeric transtaganolides C and D (**75**, Scheme 4.8). Having prepared enantioenriched transtaganolides A–D via an analogous, synthetic enantioselective Ireland–Claisen

rearrangement, we believed that determination of the absolute stereochemistries of the synthetic transtaganolides could provide insight into this biosynthetic hypothesis.

Scheme 4.8. Larsson's biosynthetic proposal

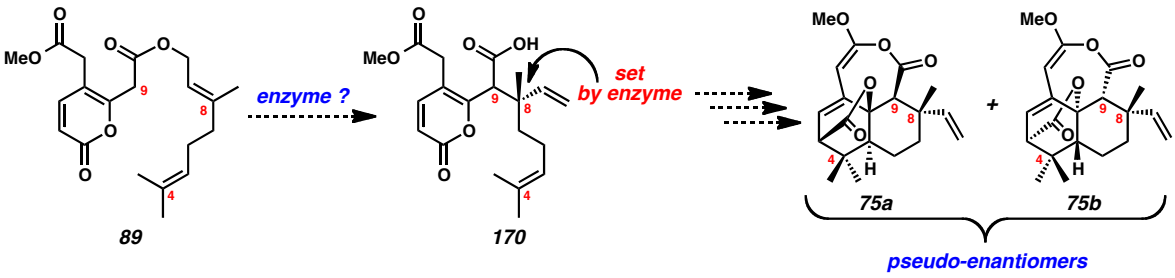

Hoppe has previously established the absolute stereochemistry of geraniol derivatives such as **159** prepared by (–)-sparteine mediated deprotonation as the (*R*)-enantiomer (Scheme 4.6).[5] As acyclic Ireland-Claisen rearrangements prefer chair transition states,[13] we postulated that the Ireland–Claisen rearrangement of esters **157** or **167** could proceed through two ketene-acetal geometry dependent pathways (Scheme 4.9, *Z*-**171** and *E*-**171**). Furthermore, the ensuing Diels–Alder cyclization is known to proceed through allylic ($A_{1,3}$) strain minimized geometries *Z*-**172** and *E*-**172**.[12] These proposed reaction pathways result in the formation of diastereomeric intermediates **160a**/**168a** and **160b**/**168b**. Acid **160a** (R^2=Me) was converted to the corresponding methyl ester (**173**) by treatment with diazomethane, and anomalous dispersion analysis of a single crystal confirmed the hypothesized stereochemistry of **160a** (Scheme 4.10).[14] As **160a** was advanced to (+)-transtaganolide C, we unambiguously assign its absolute structure as **75a** (Scheme 4.4). Furthermore, by analogy we assigned (–) transtaganolide D as **75b** (Scheme 4.4), (–)-transtaganolide A as **85a** and (+)-transtaganolide B as **85b** (Scheme 4.7).

Scheme 4.9. Stereochemical analysis of chiral silane directed ICR/IMPDA

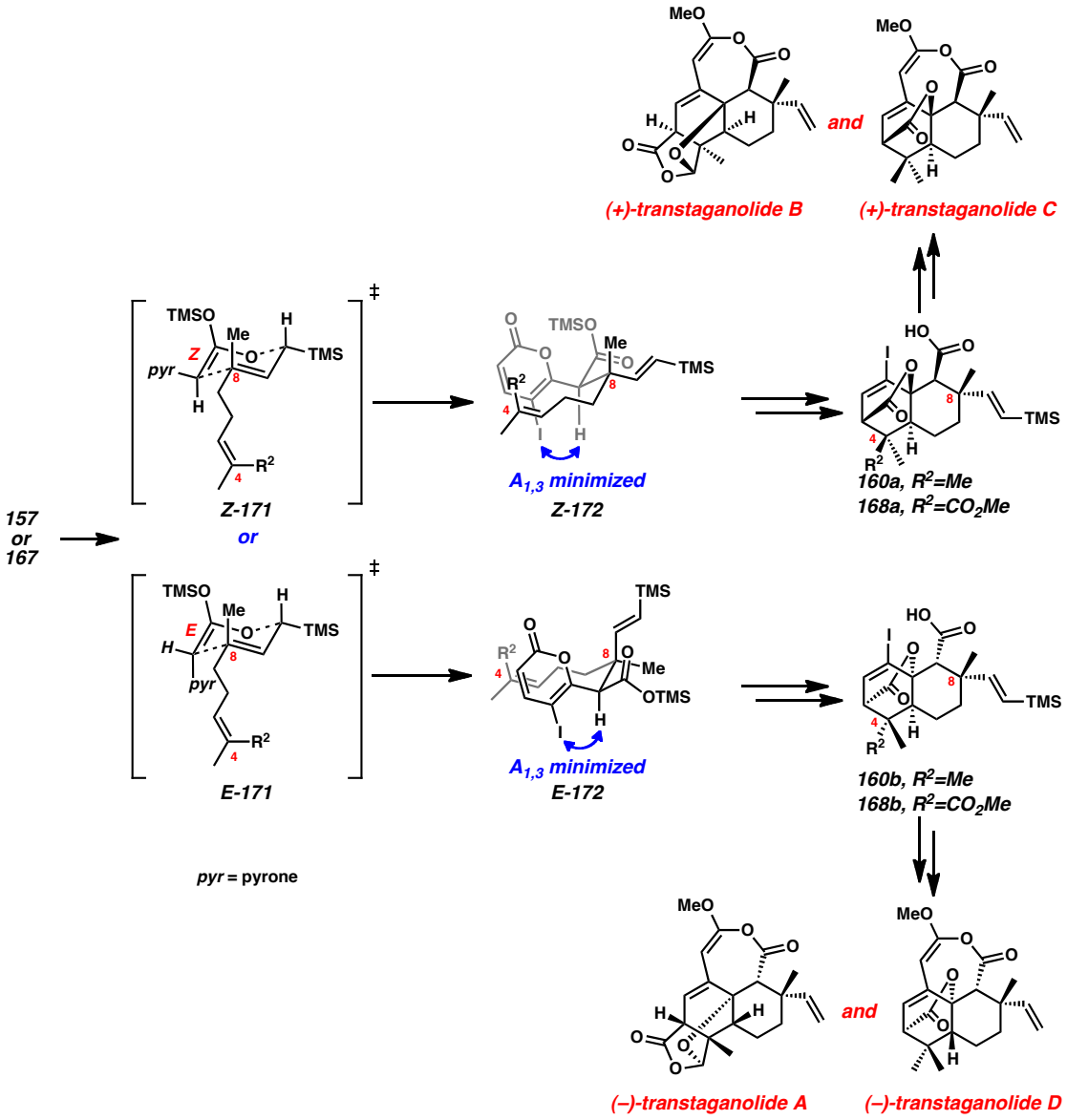

*Scheme 4.10. Determination of the absolute stereochemistry of intermediate **173***

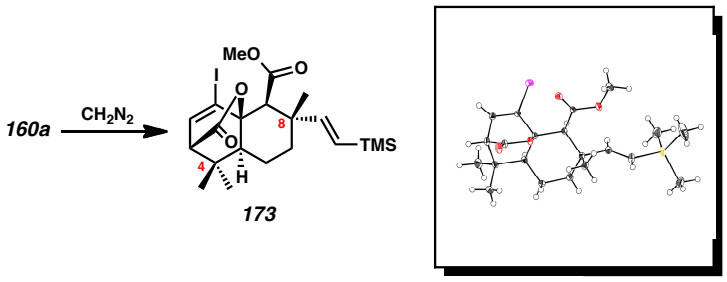

The optical rotations obtained from synthetic and natural transtaganolides A–D

are depicted in Table 4.1.[15] Interestingly, the moderately enantioenriched synthetic transtaganolides uniformly rotate plane polarized light to a greater extent than their naturally occurring counterparts, introducing the possibility that the naturally occurring transtaganolides are scalemates.

Furthermore, while the naturally occurring C8 diastereomeric pairs (e.g., transtaganolides C and D) rotate plane-polarized light in the same direction, the samples derived from a synthetic, enantioselective ICR rotate light oppositely. This data does not support the action of an enzymatic Ireland–Claisen rearrangement, as an enzyme-controlled, and likely asymmetric, Ireland–Claisen rearrangement should have analogous rotations to the synthetic transtaganolides (Scheme 4.8). As demonstrated by our synthetic efforts, the Ireland–Claisen/Diels–Alder cascade of prenylated pyrones similar to **89** is a facile process. As such, the metabolites may therefore be biosynthetically derived from **89**, however without action of an "Ireland–Claisenase" enzyme; any observed optical enrichment may derive from post-biosynthetic resolution or partial resolution (e.g. by the action of esterases and etc.)

Table 4.1. Comparison of the optical rotations of synthetic and natural transtaganolides A–D

	transtaganolide A	transtaganolide B	transtaganolide C	transtaganolide D
synthetic	– 105.4	+ 207.9	+ 49.0	– 41.2
natural	– 44.8	– 25.8	– 10.0	– 14.2

Comparison of the natural compounds to the synthetic counterparts by chiral phase chromatography is needed before a conclusion can be drawn. Unfortunately, efforts to obtain samples of the natural products from the isolation chemists has been

unsuccessful. However at this juncture, the data strongly suggests that prenylated pyrone **89** is not an "Ireland-Claisenase" substrate in the biosynthesis of transtaganolides C and D. As previously proposed, pyrone **89** can still be viewed as a decomposition product of epoxide **107** or oxepine **108**, which can be derived from co-isolated coumarin **103** (Scheme 4.11).[10,15a]

Scheme 4.11. Possible biosynthetic origin of ***89***

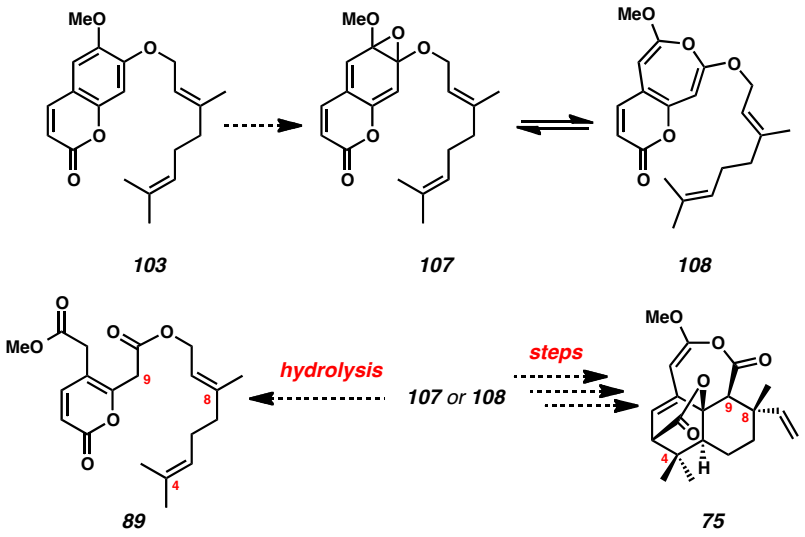

4.5 Conclusion

In conclusion, enantioenriched transtaganolides A–D have been prepared by the use of a chiral geraniol equivalent in an Ireland–Claisen/Diels–Alder cascade that proceeds with excellent stereofidelity. Remarkably, all of the titled natural products were prepared in 10 steps or less from known compounds. Single crystal X-ray diffraction studies of a synthetic intermediate have unambiguously determined the absolute stereochemistry of (+)-transtaganolide C (**75a**). By inference, the absolute stereochemistries of (–)-transtaganolide D (**75b**), (–)-transtaganolide A (**85a**), and (+)-transtaganolide B (**85b**) have been proposed. Finally, analysis of optical rotation data

does not support the role of a putative "Ireland–Claisenase" in the biosynthesis of the transtaganolides.

4.7 Experimental

4.7.1 Materials and Methods

Unless otherwise stated, reactions were performed in flame-dried glassware under an argon or nitrogen atmosphere using dry deoxygenated solvents. Solvents were dried by passage through an activated alumina column under argon. Chemicals were purchased from Sigma-Aldrich Chemical Company and used as received. $Pd(PPh_3)_4$ was prepared using known methods. Thin layer chromatography (TLC), both preparatory and analytical, were performed using E. Merck silica gel 60 F254 pre-coated plates (0.25 mm) and visualized by UV fluorescence quenching, *p*-anisaldehyde, I_2, or $KMnO_4$ staining. ICN Silica gel (particle size 0.032–0.063 mm) was used for flash chromatography. ^1H NMR, and ^{13}C NMR spectra were recorded on a Varian Mercury 300 (at 300 MHz) or on a Varian Unity Inova 500 (at 500 MHz). ^1H NMR spectra are reported relative to $CDCl_3$ (7.26 ppm). Data for ^1H NMR spectra are reported as follows: chemical shift, multiplicity, coupling constant (Hz), integration. Multiplicities are reported as follows: s = singlet, d = doublet, t = triplet, q = quartet, sept. = septet, m = multiplet, bs = broad singlet. ^{13}C NMR spectra are reported relative to $CDCl_3$ (77.0 ppm). FTIR spectra were recorded on a Perkin Elmer SpectrumBX spectrometer and are reported in frequency of absorption (cm^{-1}). HRMS were acquired using an Agilent 6200 Series TOF with an Agilent G1978A Multimode source in electrospray ionization (ESI), atmospheric pressure chemical ionization (APCI) or multimode-ESI/APCI. Crystallographic data were obtained from the Caltech X-ray Diffraction Facility.

4.7.2 Experimental Procedures

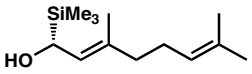

Silane 159. To a 23 °C solution of known diisopropyl geraniol carbamate (**158**) (519 mg, 1.84 mmol) in toluene (9.2 mL, 0.2M) was added freshly distilled (–)-sparteine (635 μL, 1.5 equiv) and TMSCl (352 μL, 1.5 equiv). The solution was then cooled to 78 °C and a solution of 2.5M *n*-BuLi in hexanes (1.11 mL, 1.5 equiv) was added dropwise. The reaction was allowed to stir at –78 °C for 3 hours. The reaction was then quenched at –78 °C by slow addition of MeOH (250 μL) and allowed to warm to 23 °C. The reaction was washed with saturated NH_4Cl (2x 10 mL). Aqueous layers were combined and back extracted with Et_2O (3x 20 mL). The combined organics were than washed with saturated brine (20 mL), dried over $MgSO_4$, and concentrated by rotary evaporation. This crude oil could be taken on without further purification. Purification, if desired, was done via column chromatography (ethyl acetate in hexanes 2⇒10% on SiO_2**)** to yield 602 mg (92% yield) of silylated diisopropyl geraniol carbamate, as a colorless oil.

Silylated diisopropyl geraniol carbamate (2.36 g, 6.68 mmol) was dissolved in THF (67 mL, .1M with respect to substrate) and hexanes (40mL, 1M with respect to DIBAL-H) and cooled to 0 °C. To this 0 °C solution we then slowly added neat DIBAL-H (7.1 mL, 6 equiv) dropwise. After the addition, the reaction was warmed to 23 °C and stirred for 6 hours. The reaction was then cooled to 0 °C and slowly quenched with saturated Rochelle's salt (35 mL) with vigorous stirring to help stop coagulation of the

aluminum salts that precipitate from reaction mixture. After addition of Rochelle's salt, the reaction was allowed to warm to 23 °C and celite (10 g) was added to further prevent coagulation. The suspension was vigorously stirred for another 5 minutes and then filtered through a small pad of celite. The organic layer was then collected, washed with saturated brine (35 mL), dried over $MgSO_4$, and concentrated by rotary evaporation. Once again the crude oil could be taken on without further purification. Purification, if desired, was accomplished by column chromatography (ethyl acetate in hexanes 2⇒20% on SiO_2) to yield 1.38 g (91% yield) of colorless oil **159**. $[\alpha]_D^{20}$ = +69.71 (*c* 1.00 in $CHCl_3$). All spectral data match the literature.[16]

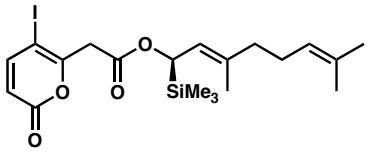

Pyrone ester 157a. To a solution 0 °C of enantioenriched geraniol derivative **159** (202 mg, 0.89 mmol) in MeCN (9 mL, 0.1 M) was added sequentially pyrone acid **142b** (300 mg, 1.2 equiv) and DCC (221 mg, 1.2 equiv). After 20 min at 0 °C, while still cold, the reaction was filtered through a plug of celite using MeCN to remove the excess urea byproduct. The filtrate was collected and concentrated by rotary evaporation. The crude oil was purified by column chromatography (ethyl acetate in hexanes 2⇒10% on SiO_2) to yield 384 mg (88% yield) of ICR/DA precursor **157a** as a colorless oil.

^{1}H NMR (500 MHz, $CDCl_3$) δ 7.46 (d, *J* = 9.7 Hz, 1H), 6.06 (d, *J* = 9.7 Hz, 1H), 5.42 (d, *J* = 10.4 Hz, 1H), 5.14 (dq, *J* = 10.4, 1.2 Hz, 1H), 5.04 (tm, *J* = 6.2, 1H), 3.76 (s, 2H),

2.16 – 2.00 (m, 4H), 1.66 (d, J = 1.4 Hz, 6H), 1.59 (d, J = 1.2 Hz, 3H), 0.01 (s, 9H); ^{13}C NMR (125 MHz, $CDCl_3$) δ 166.6, 160.6, 158.6, 151.4, 138.0, 131.8, 124.1, 120.9, 116.1, 70.5, 69.7, 43.1, 40.0, 26.6, 25.9, 17.9, 17.0, –3.7.

FTIR (Neat Film NaCl) 2959, 2923, 2854, 1741, 1607, 1546, 1445, 1404, 1382, 1336, 1293, 1273, 1249, 1206, 1170, 1134, 1062, 1016, 960, 908, 842, 819, 750 cm^{-1}; HRMS (Multimode-ESI/APCI) m/z calc'd for $C_{20}H_{29}IO_4Si$ $[M–H]^-$: 487.0807, found 487.0821;

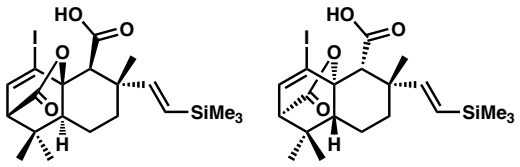

Vinyl silanes 160a and 160b. To a 23 °C solution of pyrone ester **157a** (384 mg, 0.79 mmol) in toluene (4 mL, 0.2M) in a 500 mL sealed tube was added *N,O*-bis(trimetylsilyl)acetamide (BSA) (384 μL, 2 equiv) and NEt_3 (11 μL, 0.1 equiv). This reaction mixture was heated to 110 °C and stirred for 20 minutes. The solution was then cooled to 23 °C and diluted with toluene (450 mL), leaving ample headspace in the sealed tube to allow for solvent expansion which was observed upon heating. The reaction mixture was then re-heated to 100 °C and stirred for 4 days, until completion, which was determined after monitoring by NMR. The reaction mixture was then cooled to 23 °C and 0.02% $HCl_{(aq)}$ (20 mL) was added and the reaction mixture was stirred vigorously for 1 minute. The organic phase was then separated and washed with 0.02% $HCl_{(aq)}$ (3 x 25 mL) making sure aqueous phase is acidic. The aqueous phases were then combined and back extracted with ethyl acetate (3 x 30 mL). All organic phases were

combined, dried with Na_2SO_4, and concentrated by rotary evaporation. The crude oil was purified by column chromatography (ethyl acetate in hexanes with 0.1% AcOH 5⇒30% on SiO_2) to yield 294 mg (77% yield) of a 3:1 diastereomeric mixture of Claisen-Diels-Alder products **160a** and **160b** as white solids.

Major: ^{1}H NMR (300 MHz, $CDCl_3$) δ 6.94 (d, *J* = 6.8 Hz, 1H), 6.12 (d, *J* = 18.9 Hz, 1H), 5.64 (d, *J* = 18.9 Hz, 1H), 3.01 (s, 1H), 2.97 (d, *J* = 6.9 Hz, 1H), 1.72–1.21 (m, 5H), 1.28 (s, 3H), 1.08 (s, 3H), 1.00 (s, 3H), 0.07 (s, 9H); ^{13}C NMR (125 MHz, $CDCl_3$) δ 173.6, 170.8, 155.4, 140.2, 125.3, 98.0, 84.7, 59.3, 56.7, 48.1, 41.3, 38.2, 36.9, 29.9, 24.6, 20.8, 18.5, –1.0.

Minor: ^{1}H NMR (300 MHz, $CDCl_3$) δ 6.94 (d, *J* = 6.8 Hz, 1H), 6.44 (d, *J* = 19.2 Hz, 1H), 5.68 (d, *J* = 19.2 Hz, 1H), 2.95 (d, *J* = 6.8 Hz, 1H), 2.95 (s, 1H) 1.96 (dt, *J* = 13.5, 3.1 Hz, 2H), 1.72–1.21 (m, 3H), 1.31 (s, 3H), 1.04 (s, 3H), 0.99 (s, 3H), 0.06 (s, 9H); ^{13}C NMR (125 MHz, $CDCl_3$) δ 173.4, 169.9, 148.0, 140.5, 127.8, 97.5, 84.8, 61.2, 56.8, 47.9, 40.5, 38.1, 37.0, 29.7, 24.6, 20.7, 18.5, –1.1.

FTIR (Neat Film NaCl) 3075, 3014, 2955, 2671, 2545, 1755, 1713, 1612, 1464, 1455, 1415, 1397, 1386, 1373, 1338, 1286, 1246, 1218, 1174, 1133, 1103, 1048, 1016, 990, 967, 932, 903, 867, 838, 796, 757 cm^{-1}; HRMS (Multimode-ESI/APCI) m/z calc'd for $C_{20}H_{29}IO_4Si$ $[M+H]^+$: 489.0953, found 489.0952; $[\alpha]_D^{20}$ = +13.28 (*c* 2.00 in $CHCl_3$).

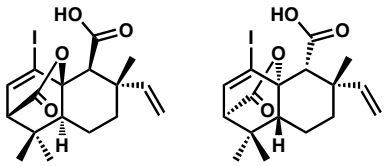

Iodoacids 138a and **138b**. To a 23 °C solution of vinyl silane **160** (36.5 mg, 0.075 mmol) in MeCN (1.5 mL, 0.05M) was added $HBF_{4(aq)}$ (48% w/w, 75 μL, 8 equiv). The reaction was stirred for 4.5 hours and then diluted with ethyl acetate (15 mL). The organic layer was then washed with 0.02% $HCl_{(aq)}$ (3 x 5 mL). The aqueous phases were combined and back extracted with ethyl acetate (3 x 5 mL). The combined organic phases were dried with Na_2SO_4 and concentrated by rotary evaporation. Purification by column chromatography (ethyl acetate in hexanes with 0.1% AcOH 5⇒30% on SiO_2) yielded 27.5 mg (89% yield) of a 3.5:1 diastereomeric mixture of the desilylated tricycles **138a** and **138b** as a white solid. $[\alpha]_D^{20}$ = +42.73 (*c* 1.00 in $CHCl_3$). The spectral data obtained matches that of the reported for the racemic compounds.

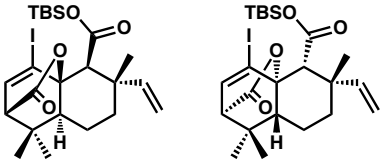

TBS-ester 161. To a 23 °C solution of iodoacid **160** (46 mg, 0.11 mmol,) in DMF (300 μL, 0.35M) were added sequentially imidazole (76 mg, 10 equiv) and TBSCl (84 mg, 5 equiv). The reaction was warmed to 40 °C and then stirred for 12 hours. The solution was then diluted with saturated brine solution (1 mL) and extracted with Et_2O/hexane (1:1) (3 x 2 mL). The combined organic extracts were washed with saturated aqueous $KHSO_4$ (1 mL) and then with saturated brine (3 x 1 mL). The combined organics were dried over Na_2SO_4, and concentrated by rotary evaporation. The crude oil was purified by column chromatography (ethyl acetate in hexane 10⇒50% on SiO_2) to yield 39 mg

(66% yield) of a 4:1 mixture of protected diastereomers **161a** and **161b** as white powders. $[\alpha]_D^{20}$ = +41.42 (*c* 1.00 in $CHCl_3$). The spectral data obtained matches that of the reported for the racemic compounds.

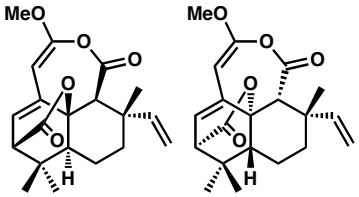

Transtaganolides C and D (75a and 75b). In a nitrogen filled glovebox, to a solution of TBS-esters **161a** and **161b** (13 mg, 0.026 mmol) and $Pd(PPh_3)_4$ (33 mg, 1.1 equiv) in DMF (260 μL, 0.1 M) was added tributyl(2-methoxyethynyl)stananne (**151**) (34 mg, 4 equiv). The reaction was stirred at 31 °C for 14 h. The reaction mixture was then filtered through glass wool and eluted with Et_2O (1.0 mL) (this removes a large excess of the undisolved $Pd(PPh_3)_4$) and is removed from the glovebox. The Et_2O was removed by rotary evaporation, and the reaction was diluted with MeCN (15 mL). To this solution was added pH 7 phosphate buffer (200 μL) and reaction was stirred vigorously at 23 °C for 2 hrs. Upon completion, the reaction was then concentrated by rotary evaporation, as to remove the copious amounts of MeCN, and then diluted with ethyl acetate (4 mL). This was then washed with water (3 x 1 mL) and the combined aqueous washes were back extracted with ethyl acetate (2 x 1 mL). All organics were pooled, dried with Na_2SO_4, and concentrated by rotary evaporation. The crude oil was purified by normal

phase HPLC to yield 1.7 mg (25% yield) of transtaganolide C (**75a**) and 0.9 mg (11% yield) of transtaganolide D (**75b**) as white powders.

Transtaganolides C: $[\alpha]_D^{20} = +49.03$ (*c* 0.09 in $CHCl_3$).

Transtaganolides D: $[\alpha]_D^{20} = -41.14$ (*c* 0.09 in $CHCl_3$).

The spectral data obtained matches that of the reported for the racemic compounds.

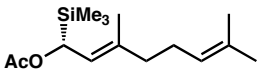

Acetate SI-1. To a 0 °C solution of **159** (256 mg, 1.13 mmol) in pyridine (11 mL, 0.1M) was added acetic anhydride (534 μL, 5 equiv). The reaction was allowed to warm to 23 °C and was stirred for 6 hours until completion as monitored by TLC. Following completion of the reaction, the solution was diluted with ethyl acetate (30 mL) and quenched with saturated $NaHCO_3$ (10 mL). The organic layer was then washed with saturated aqueous $CuSO_4$ (4x 10 mL) until the dark blue color no longer persisted in the aqueous phase. This was followed by another saturated $NaHCO_3$ wash (10 mL), a saturated brine wash (10 mL), and then drying over $MgSO_4$. Concentration by rotary evaporation gave a crude, colorless oil which could be taken on without further purification. Purification, if desired, was done by column chromatography (ethyl acetate in hexanes 2⇒10% on SiO_2) to yield 260 mg (86% yield) of acetate **SI-1**, as a colorless oil.

^{1}H NMR (300 MHz, $CDCl_3$) δ 5.42 (d, *J* = 10.4 Hz, 1H), 5.16 (dm *J* = 10.5 Hz, 1H), 5.10–5.00 (m, 1H), 2.18–1.94 (m, 7H), 1.66 (s, 6H), 1.59 (s, 3H), 0.02 (s, 9H); ^{13}C NMR

(125 MHz, $CDCl_3$) δ 171.1, 137.0, 131.7, 124.2, 121.7, 67.6, 40.0, 26.6, 25.9, 21.4, 17.9, 17.0, -3.7.

FTIR (Neat Film NaCl) 2962, 2927, 2856, 1737, 1443, 1368, 1290, 1248, 1237, 1158, 1109, 1014, 957, 842, 750 cm^{-1}; $[\alpha]_D^{20}$ = +49.50 (*c* 1.00 in $CHCl_3$).

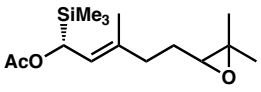

Epoxide SI-2. To a –78 °C solution of acetate **SI-1** (260 mg, 0.97 mmol) in CH_2Cl_2 (10 mL, 0.1M) was added *m*-CPBA (max 77% by weight) (240 mg, 1.1 equiv). The reaction was then removed from the –78 °C bath and placed in a 0 °C. The reaction was then carefully monitored by TLC. After 30 minutes the reaction had reached completion. If the reaction does not reach completion and appears to have stalled, the reaction must first be cooled back to –78 °C prior to the addition of more *m*-CPBA. After addition, the reaction should be once again warmed up to 0 °C and carefully monitored by TLC. If the reaction once again stalls the above protocol is repeated until complete consumption of allyl acetate **SI-1** is observed. The cooling and heating and careful monitoring of the reaction is necessary to prevent over oxidation, an observable byproduct of the reaction. Once the reaction had reached completion, it was quenched with 10% aqueous Na_2SO_3 (5 mL) at 0 °C. The organic layer is then separated from the aqueous and washed again with 10% Na_2SO_3 (5 mL). The combined aqueous layers were then combined and back extracted with CH_2Cl_2 (3x 10 mL). The combined organic layers were washed with saturated $NaHCO_3$ (15 mL), saturated brine (15 mL), and then dried over $MgSO_4$.

Concentration by rotary evaporation gave a crude oil, which was purified by column chromatography (ethyl acetate in hexanes 2⇒10% on SiO_2) to yield 215 mg (78% yield) of **SI-2** as a colorless oil and a 1:1 mixture of diastereomers.

^{1}H NMR (500 MHz, $CDCl_3$) δ 5.40 (d, *J* = 10.3 Hz, 1H), 5.21 (dm, *J* = 10.4, 1H), 2.69 (td, *J* = 6.5, 5.3 Hz, 1H), 2.24 – 2.05 (m, 2H), 2.02 (s, 3H), 1.71 – 2.05 (m, 3H), 1.68 – 1.56 (m, 2H), 1.30 – 1.24 (m, 6H), 0.02 (s, 9H); ^{13}C NMR (125 MHz, $CDCl_3$) δ 171.04, 171.02, 136.32, 136.20, 122.26, 122.09, 67.40, 64.08, 58.49, 58.48, 36.64, 36.56, 27.74, 27.50, 25.03, 25.00, 21.32, 18.86, 18.83, 17.12, 16.94, -3.64.

FTIR (Neat Film NaCl) 2960, 2928, 1736, 1732, 1446, 1377, 1369, 1323, 1291, 1248, 1238, 1123, 1046, 1015, 958, 842, 795, 751, 718 cm^{-1}; HRMS (ESI) m/z calc'd for $C_{15}H_{28}O_3Si$ $[M+Na]^+$: 307.1700, found 307.1706; $[\alpha]_D^{20}$ = +34.03 (*c* 1.00 in $CHCl_3$).

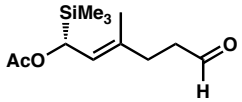

Aldehyde 164. To a solution of epoxide **SI-2** (244 mg, 0.86 mmol) in THF (8.6 mL, 0.1M) and water (4.8 mL, 0.18M) at 0 °C was added periodic acid (391 mg, 2 equiv). The reaction stirred for 7 hours then diluted with Et_2O (25 mL) and quenched with saturated $NaHCO_3$ (10 mL). The aqueous layer was separated from the organic layer and back extracted with Et_2O (2 x 10 mL). The combined organics were washed with saturated brine (3x 15 mL), dried over $MgSO_4$, and concentrated by rotary evaporation.

Purification by column chromatography (ethyl acetate in hexanes 5⇒25% on SiO_2) yielded 161 mg (77% yield) of aldehyde **164** as a colorless oil.

^{1}H NMR (300 MHz, $CDCl_3$) δ 9.74 (t, *J* = 1.7 Hz, 1H), 5.37 (d, *J* = 10.3 Hz, 1H), 5.18 (dm, *J* = 10.3, 1H), 2.58 – 2.47 (m, 2H), 2.41 – 2.28 (m, 2H), 2.01 (s, 3H), 0.00 (s, 9H); ^{13}C NMR (75 MHz, $CDCl_3$) δ 202.1, 171.0, 134.9, 122.7, 67.3, 42.2, 32.0, 21.3, 17.1, -3.7.

FTIR (Neat Film NaCl) 3432, 2958, 2902, 2823, 2720, 2479, 2113, 1732, 1415, 1368, 1291, 1248, 1142, 1115, 1046, 1016, 958, 842, 769, 752, 718 cm^{-1}; HRMS (ESI) m/z calc'd for $C_{12}H_{22}O_3Si$ $[M+Na]^+$: 265.1230, found 265.1232; $[\alpha]_D^{20}$ = +41.93 (*c* 1.00 in $CHCl_3$).

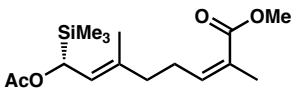

(*Z*)-Enone SI-3. To a –78 °C solution of KHMDS (35 mg, 1.2 equiv) in THF (2 mL) was added a solution of Stille-Genari reagent **165** (53.5 mg, 0.16 mmol, 1.1 equiv) and 18-crown-6 (193.5 mg, 5 equiv) in THF (600 μL). After stirring the reaction mixture for 10 minutes at –78 °C, a solution of aldehyde **164** (35.5 mg, 0.146 mmol, 1 equiv) in THF (600 μL) was added. The total volume of THF is set to 3.2 mL, which is a 0.05M solution with respect to Stille-Genari reagent **165**. The reaction was stirred at –78 °C for 20 minutes and then quenched with a saturated NH_4Cl solution (1 mL) at –78 °C. After allowing the reaction mixture to warm to 23 °C the reaction mixture was diluted with Et_2O (10 mL) and washed with saturated NH_4Cl (1 x 3 mL). Aqueous layers were

combined and back extracted with Et_2O (2 x 3 mL). The combined organic layers were washed with saturated brine (10 mL), dried over MgSO4, and concentrated by rotary evaporation. Purification was accomplished by column chromatography (ethyl acetate in hexanes 2⇒10% on SiO_2) to yield 42.5 mg (93% yield) of exclusively the *Z*-isomer of enone **SI-3** as a colorless oil.

^{1}H NMR (300 MHz, $CDCl_3$) δ 5.88 (tm, *J* = 7.2 Hz, 1H), 5.39 (d, *J* = 10.3 Hz, 1H), 5.17 (dm, *J* = 10.5 Hz, 1H), 3.72 (s, 3H), 2.58 (q, *J* = 7.5 Hz, 2H), 2.11 (t, *J* = 7.3 Hz, 2H), 2.02 (s, 3H), 1.88 – 1.85 (m, 3H), 1.67 – 1.66 (m, 3H), 0.01 (s, 9H); ^{13}C NMR (75 MHz, $CDCl_3$) δ 168.4, 143.0, 136.3, 127.2, 122.3, 67.4, 51.3, 39.4, 27.9, 21.3, 20.8, 16.9, -3.7. FTIR (Neat Film NaCl) 2954, 2928, 2855, 1722, 1649, 1453, 1434, 1368, 1289, 1248, 1238, 1199, 1131, 1104, 1085, 1015, 958, 842, 769, 751 cm^{-1}; HRMS (ESI) m/z calc'd for $C_{16}H_{28}O_4Si$ $[M+Na]^+$: 335.1649, found 335.1648; $[\alpha]_D^{20}$ = +49.43 (*c* 1.00 in $CHCl_3$).

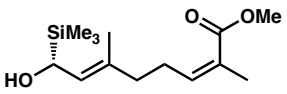

Alcohol 166. To a 23 °C solution of (*Z*)-enone **SI-3** (143 mg, 0.458 mmol) in MeOH (10 mL, 0.05M) was added K_2CO_3 (32 mg, 0.5 equiv). The resulting suspension was then stirred for 2.5 days until complete deprotection was observed. Following completion, the reaction was diluted with Et_2O (100 mL) and washed with water (2 x 75 mL). The combined aqueous washes with then back extracted with Et_2O (3 x 75 mL). All organic phases were combined, washed with saturated brine (100 mL), dried over $MgSO_4$, and concentrated by rotary evaporation. Purification was accomplished by column

chromatography (ethyl acetate in hexanes 5⇒10% on SiO_2) to yield 96 mg (78%) of the *Z*-isomer of alcohol **166** as a colorless oil.

^{1}H NMR (300 MHz, $CDCl_3$) δ 5.89 (tm, *J* = 7.3 Hz, 1H), 5.27 (dm, *J* = 10.1 Hz, 1H), 4.16 (d, *J* = 10.1 Hz, 1H), 3.71 (s, 3H), 2.63 – 2.52 (m, 2H), 2.11 (t, *J* = 7.3 Hz, 2H), 1.88 – 1.84 (m, 3H), 1.58 (d, *J* = 1.2 Hz, 3H), 0.01 (s, 9H); ^{13}C NMR (75 MHz, $CDCl_3$) δ 168.5, 142.9, 134.3, 127.2, 126.9, 64.5, 51.4, 39.5, 28.0, 20.8, 16.7, -4.0.

FTIR (Neat Film NaCl) 3424, 2953, 2928, 2854, 1719, 1648, 1454, 1437, 1382, 1366, 1331, 1246, 1198, 1129, 1083, 1032, 978, 856, 841, 791, 749 cm^{-1}; HRMS (ESI) m/z calc'd for $C_{14}H_{26}O_3Si$ $[M+Na]^+$: 293.1543, found 293.1538; $[\alpha]_D^{20}$ = +56.83 (*c* 1.00 in $CHCl_3$).

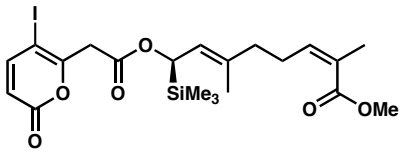

Pyrone ester 167. To a 0 °C solution of alcohol **166** (297 mg, 1.10 mmol) in MeCN (11mL, 0.1M) was added sequentially pyrone acid **142b** (339 mg, 1.1 equiv) and DCC (250 mg, 1.1 equiv). After 20 min at 0 °C, while still cold, the reaction was filtered through a plug of celite using MeCN to remove the excess urea byproduct. The filtrate was collected and concentrated by rotary evaporation. The crude oil was purified by column chromatography (ethyl acetate in hexanes 2⇒10% on SiO_2) to yield 534 mg (91% yield) of pyrone ester **167** as a yellow oil.

^{1}H NMR (300 MHz, $CDCl_3$) δ 7.46 (d, *J* = 9.7 Hz, 1H), 6.06 (d, *J* = 9.8 Hz, 1H), 5.88 (tm, *J* = 7.2 Hz, 1H), 5.41 (d, *J* = 10.4 Hz, 1H), 5.16 (dm, *J* = 10.4 Hz, 1H), 3.76 (s, 2H), 3.73 (s, 3H), 2.59 (tdm, *J* = 7.3, 7.2 Hz, 2H), 2.13 (t, *J* = 7.3 Hz, 2H), 1.87 (d, *J* = 1.4 Hz, 3H), 1.67 (d, *J* = 1.3 Hz, 3H), 0.01 (s, 9H); ^{13}C NMR (75 MHz, $CDCl_3$) δ 166.6, 160.5, 158.5, 151.4, 142.9, 137.3, 127.2, 121.5, 116.1, 70.5, 69.6, 51.4, 43.1, 39.4, 27.9, 20.9, 16.9, -3.7.

FTIR (Neat Film NaCl) 2953, 2923, 2854, 1742, 1648, 1607, 1546, 1451, 1434, 1405, 1382, 1365, 1336, 1249, 1202, 1172, 1131, 1085, 1062, 1016, 960, 842, 764, 751, 729 cm^{-1}; HRMS (Multimode-ESI/APCI) m/z calc'd for $C_{21}H_{29}IO_6Si$ $[M–H]^–$: 531.0705, found 531.0712; $[\alpha]_D^{20}$ = +17.79 (*c* 1.00 in $CHCl_3$).

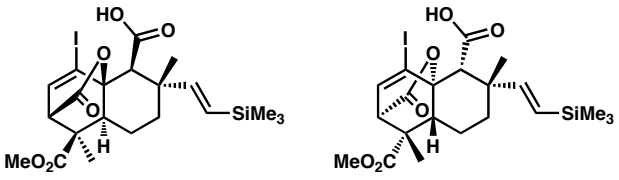

Vinyl silanes 168. To a 23 °C solution of pyrone ester **167** (298 mg, 0.560 mmol) in toluene (2.8 mL, 0.2M) in a 500 mL sealed tube was added BSA (274 μL, 2 equiv) and NEt_3 (8 μL, 0.1 equiv). The reaction mixture was heated to 110 °C and stirred for 20 minutes. The mixture was then cooled to 23 °C and diluted with toluene (450 mL), leaving ample headspace in the sealed tube to allow for solvent expansion which was observed upon heating. The reaction mixture was then re-heated to 100 °C and stirred for 19 days, until completion, which was determined after monitoring by NMR. The reaction

mixture was then cooled back to 23 °C and 0.02% $HCl_{(aq)}$ (20 mL) was added and the reaction mixture was stirred vigorously for 1 minute. The organic phase was then separated and washed with 0.02% $HCl_{(aq)}$ (3 x 25 mL). The aqueous phases were then combined and back extracted with ethyl acetate (3 x 30 mL). All organic phases were combined, dried with Na_2SO_4, and concentrated by rotary evaporation. The crude oil was purified by column chromatography (ethyl acetate in hexanes with 0.1% acetic acid 5⇒30% on SiO_2) to yield 186 mg (62% yield) of a 3:1 mixture of ICR/DA diastereomers **168a** and **168b** as a yellow solid. It is important to note that compound **168**, and all subsequent compounds in the total synthesis have very poor solubility in most common organic solvents excluding ethyl acetate. Therefore all transfers of products should be accomplished using ethyl acetate and vessels should be repeatedly washed.

Major: ^{1}H NMR (500 MHz, $CDCl_3$) δ 6.96 (d, *J* = 7.0 Hz, 1H), 6.09 (d, *J* = 18.8 Hz, 1H), 5.64 (d, *J* = 18.8 Hz, 1H), 3.74 (s, 3H), 3.36 (d, *J* = 7.0 Hz, 1H), 2.96 (s, 1H), 1.98 – 1.36 (m, 5H), 1.27 (s, 6H), 0.06 (s, 9H); ^{13}C NMR (125 MHz, $CDCl_3$) δ 173.5, 172.1, 168.9, 154.9, 139.8, 125.8, 99.8, 83.8, 59.2, 52.7, 51.5, 49.5, 49.2, 41.4, 37.9, 24.6, 20.8, 18.7, -1.0.

Minor: ^{1}H NMR (500 MHz, $CDCl_3$) δ 6.95 (d, *J* = 6.9 Hz, 1H), 6.41 (d, *J* = 19.1 Hz, 1H), 5.64 (d, *J* = 19.1 Hz, 1H), 3.70 (s, 3H), 3.34 (d, *J* = 7.1 Hz, 1H), 2.91 (s, 1H), 1.98 – 1.36 (m, 5H), 1.30 (s, 3H), 1.25 (s, 3H), 0.06 (s, 9H); ^{13}C NMR (125 MHz, $CDCl_3$) δ 173.3, 171.9, 168.0, 147.5, 140.1, 128.1, 99.2, 83.9, 61.2, 52.5, 51.5, 49.6, 49.0, 40.6, 37.6, 29.6, 24.6, 20.7, -1.1.

FTIR (Neat Film NaCl) 3077, 2952, 1773, 1736, 1611, 1492, 1459, 1453, 1382, 1309, 1276, 1247, 1184, 1161, 1122, 1047, 1019, 989, 970, 935, 870, 838, 783, 754 cm^{-1};

HRMS (Multimode-ESI/APCI) m/z calc'd for $C_{21}H_{29}IO_6Si$ $[M+H]^+$: 533.0851, found 533.0847; $[\alpha]_D^{20}$ = +10.47 (*c* 1.00 in $CHCl_3$).

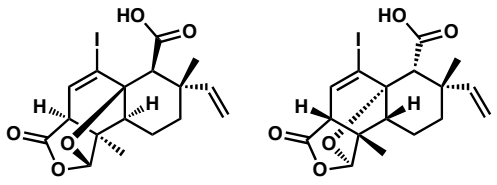

Tetracycle 155. It is important to note that the selective single hydride reduction of methyl ester **168** was only made possible using a glass cannula as it allows for the precise temperature control necessary to exact the transformation on such a complex substrate bearing many electrophilic carbonyl functionalities (Figure SI-1). A solution of vinyl silane **168** (31 mg, 0.06 mmol) in toluene (600 μL, 0.1M) was stirred in the receiving chamber of the glass cannula at –78 °C (the entire glass cannula is placed in a –78 °C bath submerging both chambers and the cannula itself). A freshly made 1M solution of DIBAL-H (300 μL, 5 equiv) in toluene was added to the addition chamber of the glass cannula, further diluted with toluene (500 μL), and stirred at –78 °C. Once both solutions and the entire glass cannula were sufficiently cooled, the –78 °C solution of DIBAL-H was slowly added to vinyl silane **168** dropwise. The reaction was stirred for another 10 minutes and then slowly quenched by a –78 °C solution of AcOH (200 μL) in toluene (1.5 mL) via the addition chamber of the glass cannula. Once complete, the reaction vessel was removed from the –78 °C bath, allowed to warm to 23 °C, and then diluted with ethyl acetate (10 mL). The reaction was washed with a 1% solution of AcOH in

water (3 x 2 mL) and the aqueous phases were combined and back extracted with ethyl acetate (2 x 2 mL). All organic phases were pooled, dried over Na_2SO_4, and concentrated by rotary evaporation to give the desired aldehyde **163** as an orange-brown solid. Aldehyde **163** was used immediately in the following tandem cyclization, TMS cleavage protocol without further purification.

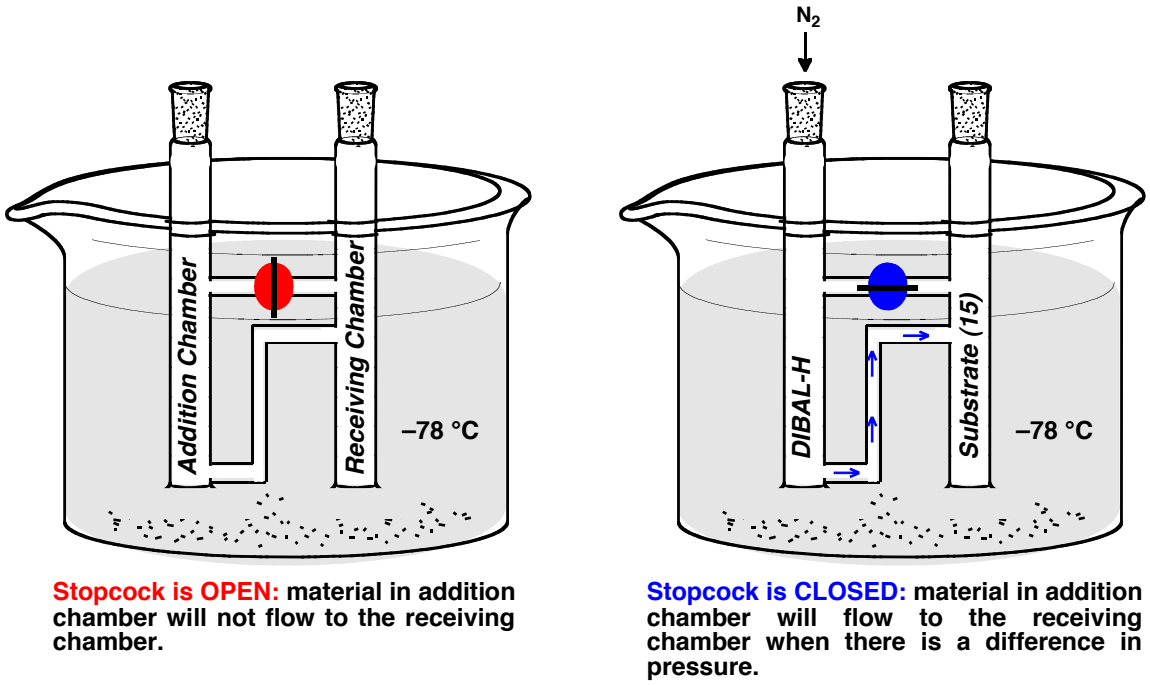

Figure 4.1. Reaction schematic for the single hydride reduction of vinyl silanes **168** using a glass cannula

To a 23 °C solution of the crude aldehyde products **163** in MeCN (150 μL, 0.4M assuming quantitative yield from the reduction) was added aqueous HBF_4 (48% w/w, 100 μL, 13 equiv). The reaction was stirred at 23 °C for 8 hours and then diluted with ethyl acetate (5 mL). This was washed with pH 2–3 water (0.02% HCl solution) (3 x 1 mL), and the aqueous phases were back extracted with ethyl acetate (2 x 1 mL). All organics

were pooled, dried over Na_2SO_4, and concentrated by rotary evaporation. Purification was accomplished by column chromatography (ethyl acetate in hexanes with 0.1% acetic acid 5⇒30% on SiO_2) to yield 15 mg (57% yield over 2 steps) of a 2.5:1 mixture of the reduced, cyclized, and desilylated diastereomers **155** as a yellow solid.

Major: ^{1}H NMR (500 MHz, $CDCl_3$) δ 6.69 (d, *J* = 5.8 Hz, 1H), 6.03 (dd, *J* = 17.3, 10.8 Hz, 1H), 5.75 (s, 1H), 5.10 (d, *J* = 10.9 Hz, 1H), 5.04 (d, *J* = 17.4 Hz, 1H), 3.08 (d, *J* = 5.9 Hz, 1H), 2.92 (s, 1H), 2.21 – 2.14 (m, 1H), 1.97 – 1.38 (m, 4H), 1.36 (s, 3H), 1.19 (s, 3H); ^{13}C NMR (125 MHz, $CDCl_3$) δ 173.1, 169.5, 147.1, 136.1, 112.3, 108.9, 107.3, 87.1, 61.5, 54.7, 49.1, 48.8, 39.7, 36.2, 20.1, 18.8, 15.9.

Minor: ^{1}H NMR (500 MHz, $CDCl_3$) δ 6.69 (d, *J* = 5.8 Hz, 1H), 6.07 (dd, *J* = 17.5, 11.0 Hz, 1H), 5.67 (s, 1H), 5.12 (d, *J* = 11.1 Hz, 1H), 5.08 (d, *J* = 17.5 Hz, 1H), 3.07 (d, *J* = 5.9 Hz, 1H), 2.88 (s, 1H), 2.21 – 2.14 (m, 1H), 1.97 – 1.38 (m, 4H), 1.36 (s, 3H), 1.33 (s, 3H); ^{13}C NMR (125 MHz, $CDCl_3$) δ 173.2, 169.7, 139.5, 136.3, 114.6, 108.8, 107.0, 87.1, 63.1, 54.7, 49.3, 48.8, 39.4, 36.3, 29.6, 20.0, 15.8.

FTIR (Neat Film NaCl) 3300, 3077, 3007, 2958, 2933, 2873, 1785, 1748, 1708, 1456, 1375, 1286, 1239, 1217, 1199, 1182, 1157, 1115, 1083, 1046, 1034, 992, 964, 957, 910, 895, 873, 829, 814, 796, 752 cm^{-1}; HRMS (Multimode-ESI/APCI) m/z calc'd for $C_{17}H_{19}IO_5$ $[M+H]^+$: 431.0350 found 431.0359; $[\alpha]_D^{20}$ = +18.71 (*c* 0.94 in $CHCl_3$).

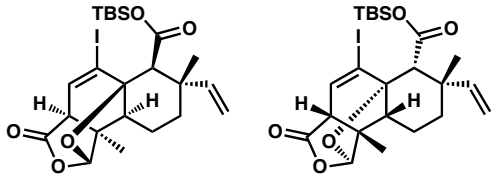

TBS-esters 169. To a 23 °C solution of acetal **163** (15 mg, 0.034 mmol) in DMF (600 μL, 0.055M) were added sequentially imidazole (14 mg, 6 equiv) and TBSCl (21 mg, 4 equiv). The reaction was stirred at 23 °C for 2 hours. The reaction mixture was then diluted with saturated brine (2 mL) and extracted with ethyl acetate/hexane (1:1) (4 x 3 mL). The combined organic extracts were washed with saturated aqueous $NaHCO_3$ (3 mL) and then with saturated brine (2 x 3 mL). The combined organics were dried over Na_2SO_4, and concentrated by rotary evaporation. The crude oil was purified by column chromatography (ethyl acetate in hexane 10⟹50% on SiO_2) to yield 12.5 mg (67% yield) of a 4:1 mixture of diastereomers **169a** and **169b** as a white solid.

Major: ^{1}H NMR (500 MHz, $CDCl_3$) δ 6.61 (d, *J* = 6.0 Hz, 1H), 6.00 (dd, *J* = 17.5, 10.6 Hz, 1H), 5.68 (s, 1H), 4.99 (d, *J* = 10.8 Hz, 1H), 4.98 (d, *J* = 17.3 Hz, 1H), 2.98 (dd, *J* = 6.0, 0.8 Hz, 1H), 2.80 (s, 1H), 2.08 – 2.00 (m, 1H), 1.90 – 1.35 (m, 4H), 1.29 (s, 3H), 1.18 (s, 3H), 0.92 (s, 9H), 0.31 (s, 3H), 0.25 (s, 3H); ^{13}C NMR (125 MHz, $CDCl_3$) δ 174.4, 169.7, 149.2, 135.4, 110.9, 110.0, 109.8, 87.0, 61.1, 55.1, 49.5, 48.7, 40.0, 37.4, 25.7, 20.6, 18.2, 17.7, 16.0, -4.7.

Minor: ^{1}H NMR (500 MHz, $CDCl_3$) δ 6.61 (d, *J* = 6.1 Hz, 1H), 6.26 (dd, *J* = 17.6, 11.0 Hz, 1H), 5.58 (s, 1H), 5.03 (dd, *J* = 11.1, 1.1 Hz, 1H), 4.97 (dd, *J* = 17.7, 1.2 Hz, 1H), 2.96 (dd, *J* = 6.1, 0.9 Hz, 1H), 2.72 (s, 1H), 2.08 – 2.00 (m, 1H), 1.90 – 1.35 (m, 4H), 1.32 (s, 3H), 1.26 (s, 3H), 0.93 (s, 9H), 0.31 (s, 3H), 0.25 (s, 3H); ^{13}C NMR (125 MHz, $CDCl_3$) δ 174.5, 169.9, 141.4, 135.6, 112.8, 109.9, 109.4, 87.0, 62.6, 55.1, 49.6, 48.9, 39.6, 37.7, 30.4, 25.6, 20.6, 17.6, 15.9, -4.8.

FTIR (Neat Film NaCl) 3083, 2930, 2857, 1784, 1716, 1638, 1601, 1471, 1463, 1413, 1390, 1362, 1338, 1317, 1282, 1250, 1235, 1222, 1196, 1183, 1160, 1144, 1115, 1084, 1049, 1036, 1000, 960, 942, 908, 895, 895, 884, 868, 843, 828, 816, 787, 752 cm^{-1}; HRMS (Multimode-ESI/APCI) m/z calc'd for $C_{23}H_{33}IO_5Si$ $[M+H]^+$: 545.1215, found 545.1218; $[\alpha]_D^{20}$ = +49.09 (*c* 1.00 in $CHCl_3$).

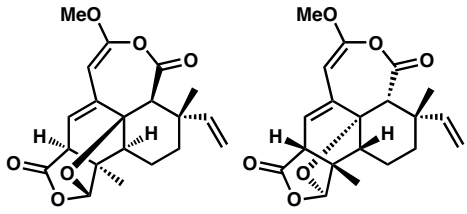

Transtaganolides B and A (85b and 85a). In a nitrogen filled glovebox, to a solution of TBS-ester **169** (9 mg, 0.0165 mmol) and $Pd(PPh_3)_4$ (21 mg, 1.1 equiv) in DMF (165 μL, 0.1M) was added tributyl(2-methoxyethynyl)stananne (**151**) (22 mg, 4 equiv). The heterogeneous reaction mixture was vigorously stirred at 31 °C for 7.5 h. The reaction mixture was then filtered through a glass wool with MeCN (1.5 mL) (this removes a large excess of the undisolved $Pd(PPh_3)_4$ and is removed from the glovebox. Outside of the glovebox, pH 7 phosphate buffer (75 μL) was added to the MeCN solution, which was then vigorously stirred for 36 hr. The reaction was then concentrated by rotary evaporation, as to remove some of the copious amounts of MeCN, and then diluted with ethyl acetate (2 mL). This was washed with water (3 x 750 μL) and the combined aqueous washes were back extracted with ethyl acetate (2 x 750 μL). All organics were pooled, dried with Na_2SO_4, and concentrated by rotary evaporation. The crude oil was

purified by normal phase HPLC to yield 0.6 mg (12% yield) of transtaganolide A (**85a**) and 1.5 mg (24% yield) of transtaganolide B (**85b**) as white powders.

Transtaganolide B: ^{1}H NMR (500 MHz, $CDCl_3$) δ 5.80 (dd, *J* = 17.4, 10.8 Hz, 1H), 5.65 (s, 1H), 5.58 (dd, *J* = 6.0, 0.9 Hz, 1H), 5.05 (d, *J* = 17.5 Hz, 1H), 5.02 (d, *J* = 10.8 Hz, 1H), 4.96 (s, 1H), 3.68 (s, 3H), 3.12 (d, *J* = 6.0 Hz, 1H), 3.08 (s, 1H), 1.94 (dd, *J* = 12.3, 6.3 Hz, 1H), 1.72 (ddt, *J* = 13.1, 6.3, 3.3 Hz, 1H), 1.63 (dt, *J* = 13.3, 3.3 Hz, 1H), 1.55 (s, 3H), 1.55–1.35 (m, 2H), 1.33 (s, 3H); ^{13}C NMR (125 MHz, $CDCl_3$) δ 175.6, 163.8, 154.5, 146.7, 144.2, 119.4, 112.7, 109.8, 87.7, 84.4, 56.5, 51.6, 49.8, 49.5, 48.8, 38.1, 37.0, 20.1, 19.4, 15.9.

HRMS (Multimode-ESI/APCI) m/z calc'd for $C_{20}H_{22}O_6$ $[M–H]^-$: 357.1344, found 357.1356; $[\alpha]_D^{20}$ = +207.93 (*c* 0.15 in $CHCl_3$).

Transtaganolide A: ^{1}H NMR (500 MHz, $CDCl_3$) δ 6.90 (dd, *J* = 17.9, 11.1 Hz, 1H), 5.62 (s, 1H), 5.60 (dd, *J* = 5.9, 1.0 Hz, 1H), 5.12 (ddd, *J* = 11.1, 1.1, 0.6 Hz, 1H), 5.03 (dd, *J* = 17.9, 1.1 Hz, 1H), 4.98 (s, 1H), 3.70 (s, 3H), 3.11 (dt, *J* = 5.9, 0.8 Hz, 1H), 2.98 (s, 1H), 1.95 (dd, *J* = 12.3, 6.3 Hz, 1H), 1.83 (ddd, *J* = 12.9, 3.7, 2.6 Hz, 1H), 1.60–1.30 (m, 3H), 1.30 (s, 3H), 1.22 (s, 3H);; HRMS (Multimode-ESI/APCI) m/z calc'd for $C_{20}H_{22}O_6$ $[M–H]^-$: 357.1344, found 357.1356; $[\alpha]_D^{20}$ = –98.76 (*c* 0.06 in $CHCl_3$).

4.8 References and Notes

1) Nelson, H. M.; Murakami, K.; Virgil, S. C.; Stoltz, B. M. *Angew. Chem., Int. Ed.* **2011**, *50*, 3688–3691.

2) a) Nelson, H. M.; Stoltz, B. M. *Tetrahedron Lett.* **2009**, *50*, 1699–1701. b) Larsson, R.; Sterner, O.; Johansson, M. *Org. Lett.* **2009**, *11*, 657–660.

3) a) Corey, E. J.; Lee, D. H. *J. Am. Chem. Soc.* **1991**, *113*, 4026–4028. b) Kazmaier, U.; Krebs, A. *Angew. Chem., Int. Ed.* **1995**, *34*, 2012–2014.

4) Ireland, R. E.; Varney, M. D. *J. Am. Chem. Soc.* **1984**, *106*, 3668–3670.

5) Zeng, W.; Fröhlich, R.; Hoppe, D. *Tetrahedron* **2005**, *61*, 3281–3287.

6) Even under mild esterification conditions, i.e. low-temperature DCC coupling, isomerization would occur. Compounding the issue was a very difficult separation of the E and Z isomers via chomatography. The isomers were able to be separated by HPLC, however, any attempts to induce the Ireland–Claisen rearrangement resulted in isomerization as well.

7) Snyder, S. A.; Treitler, D. S. *Angew. Chem., Int. Ed.* **2009**, *48*, 7899–7903.

8) Fillion, E.; Beingessner, R. L. *J. Org. Chem.* **2003**, *68*, 9485–9488.

9) Still, W. C.; Gennari, C. *Tetrahedron Lett.* **1983**, *24*, 4405–4408.

10) Rubal, J. J.; Moreno-Dorado, F. J.; Guerra, F. M.; Zacarias, D. J.; Abderrahmane, S.; Mohamed, A.; Fouad, M.; Raul, R. G.; Massanet, G. M. *Phytochemistry* **2007**, *68*, 2480–2486.

11) Batista, J. M.; López, S. N.; Da Silva Mota, J.; Vanzolini, K. L.; Cass, Q. B.; Rinaldo, D.; Vilegas, W.; Da Silva Bolzani, V.; Kato, M. J.; Furlan, M. *Chirality* **2009**, *21*, 799–801.

12) Kozytska, M. V.; Dudley, G. B. *Tetrahedron Lett.* **2008**, *49*, 2899–2901.

13) a) Ireland, R. E.; Wipf, P.; Xiang, J. N. *J. Org. Chem.* **1991**, *56*, 3572–3582. b) Gu, S. E.; Schoenebeck, F.; Aviyente, V.; Houk, K. N. *J. Org. Chem.* **2010**, *75*, 2115–2118.

14) Comparison of CD spectra to the bulk material confirmed that the mounted crystal represented the major enantiomer in the 89.5% ee bulk.

15) a) Appendino, G.; Prosperini, S.; Valdivia, C.; Ballero, M.; Colombano, G.; Billington, R. A.; Genazzani, A. A.; Sterner, O. *J. Nat. Prod.* **2005**, *68*, 1213–1217. b) Saouf, A.; Guerra, F. M.; Rubal, J. J.; Moreno-Dorado, F. J.; Akssira, M.; Mellouki, F.; Lopez, M.; Pujadas, A. J.; Jorge, Z. D.; Massanet, G. M. *Org. Lett.* **2005**, *7*, 881–884.

APPENDIX 7

Synthetic Summary: Enantioselective Total Syntheses of Transtaganolides A–D

Scheme A7.1. Enantioselective total synthesis of transtaganolides C and D

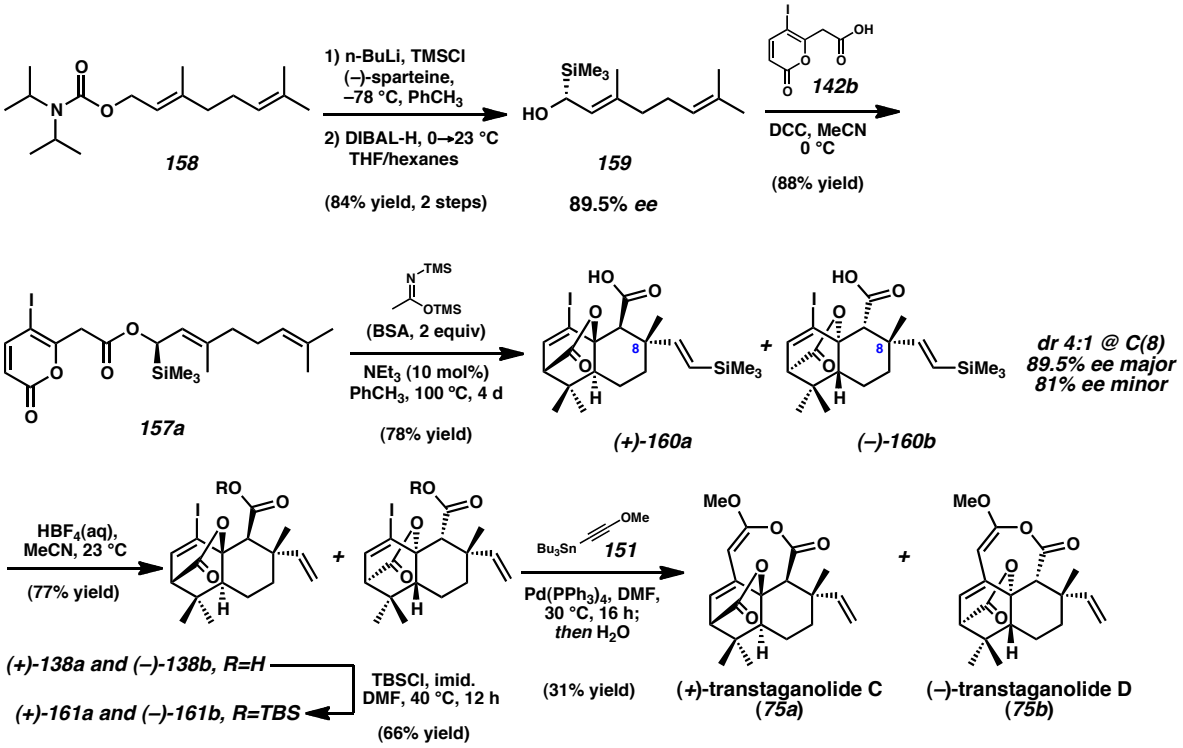

Scheme A7.2. Syntheses of enantioenriched tricyclic cores of transtaganolides A and B

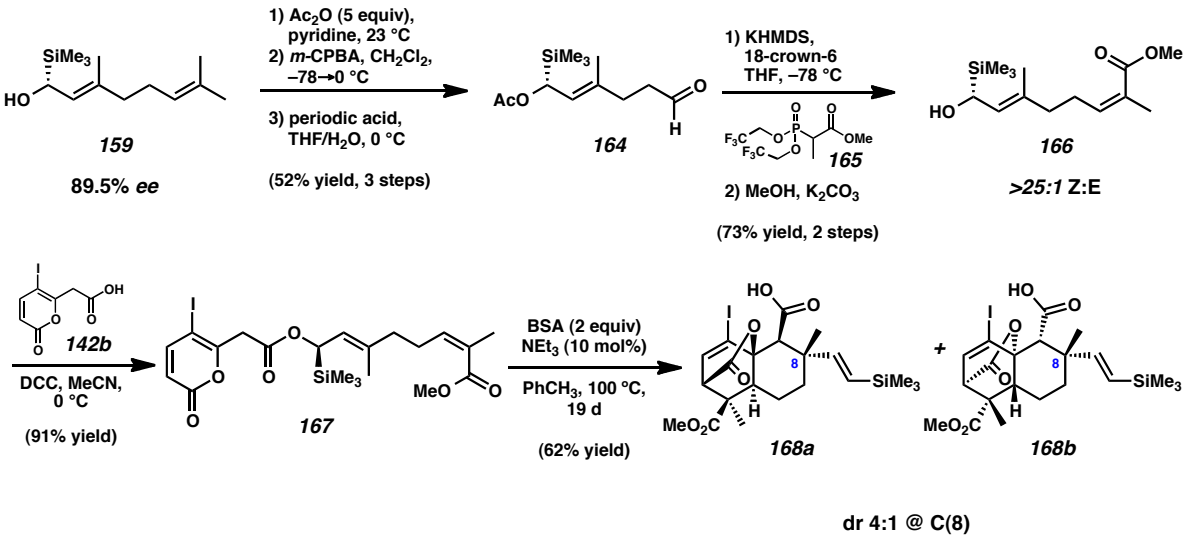

Scheme A7.3. Enantioselective total syntheses of transtaganolides A and B

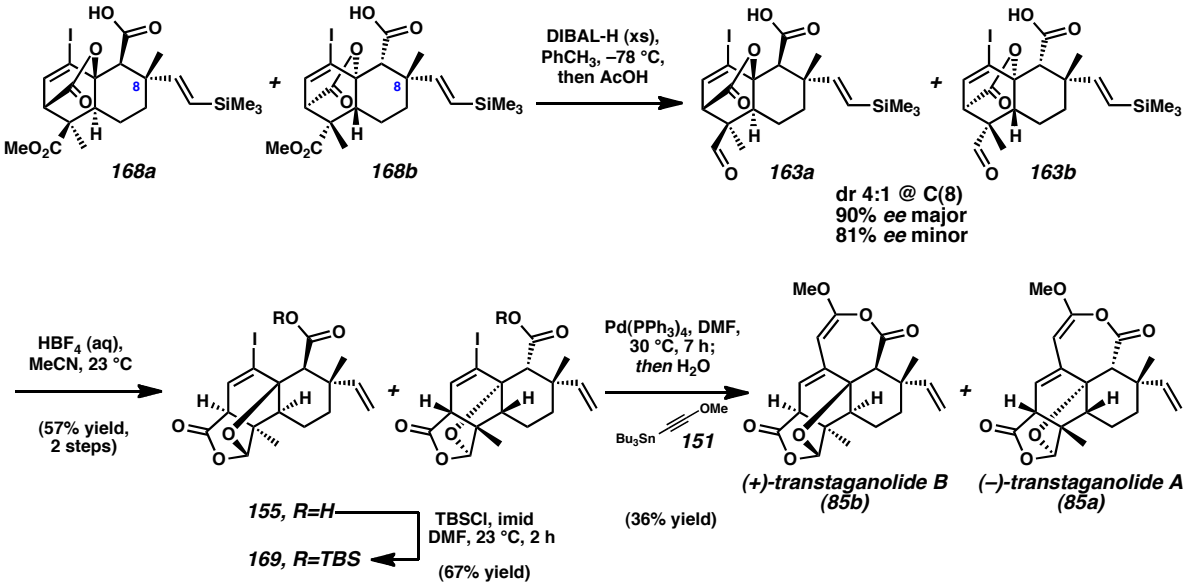

APPENDIX 8

Spectra Relevant to: The Enantioselective Total Syntheses of Transtaganolides A–D and the Biosynthetic Implications

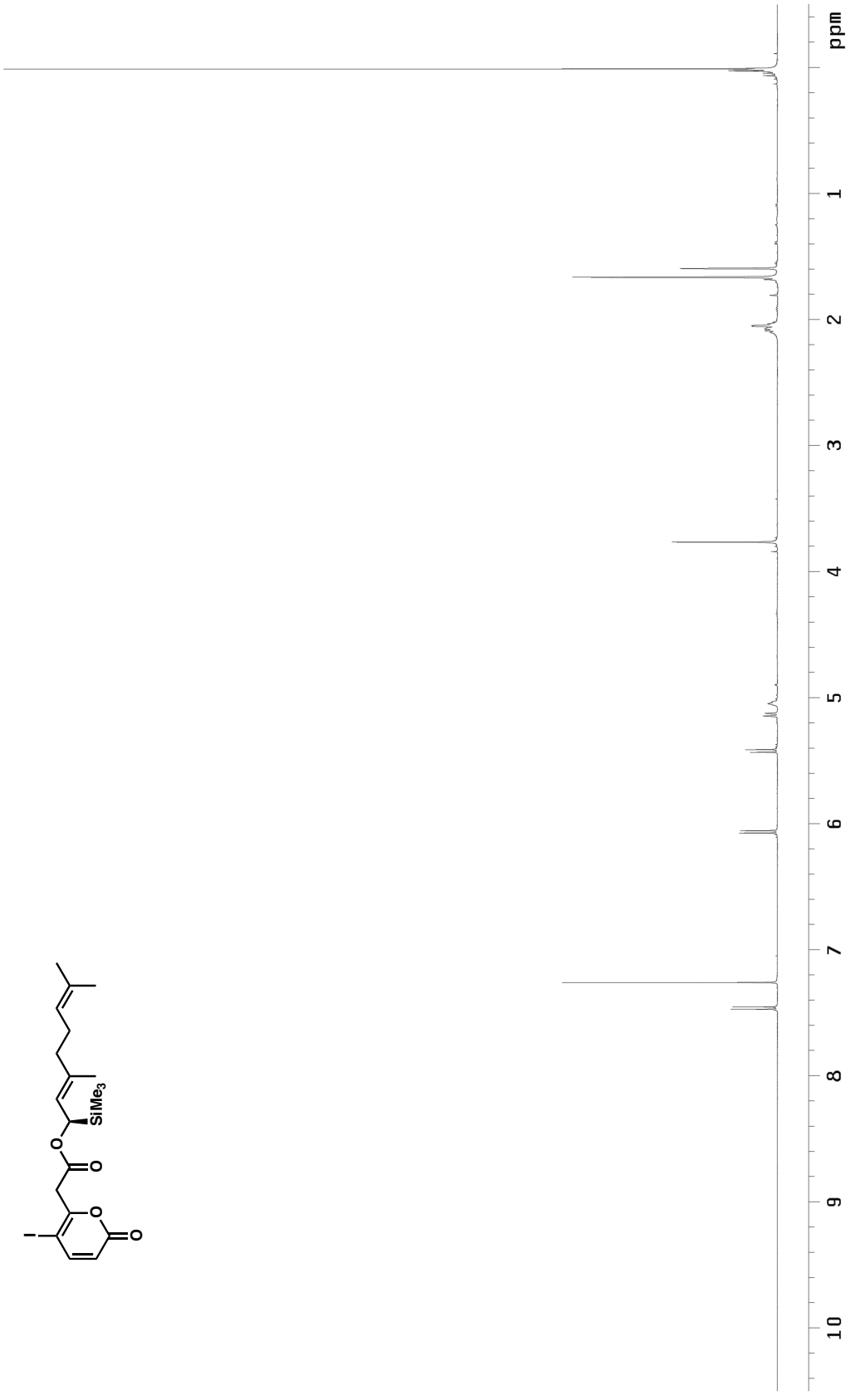

Figure A8.1.1 ^{1}H NMR (500 MHz, $CDCl_3$) of compound **157**

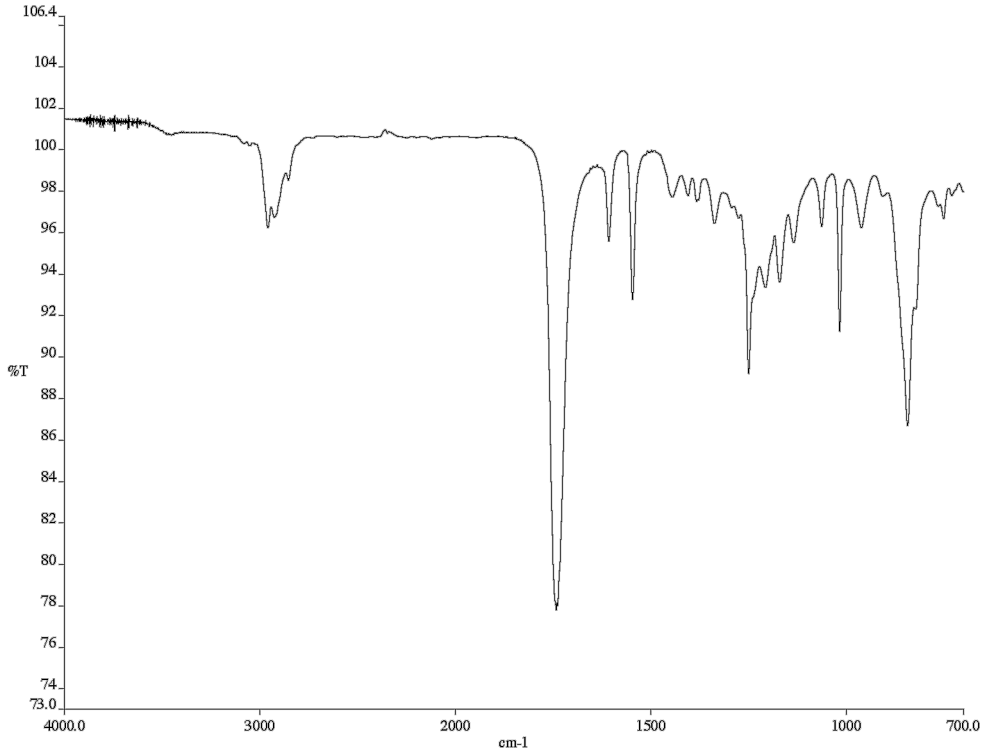

Figure A8.1.2 Infrared spectrum (thin film/NaCl) of compound **157**

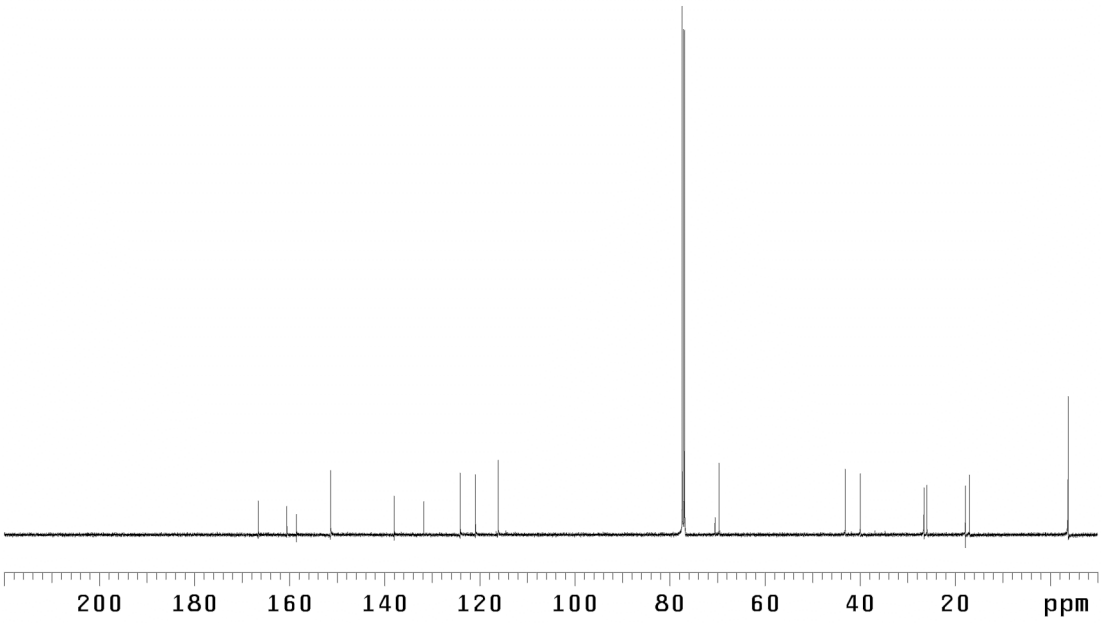

Figure A8.1.3 ^{13}C NMR (125 MHz, $CDCl_3$) of compound **157**

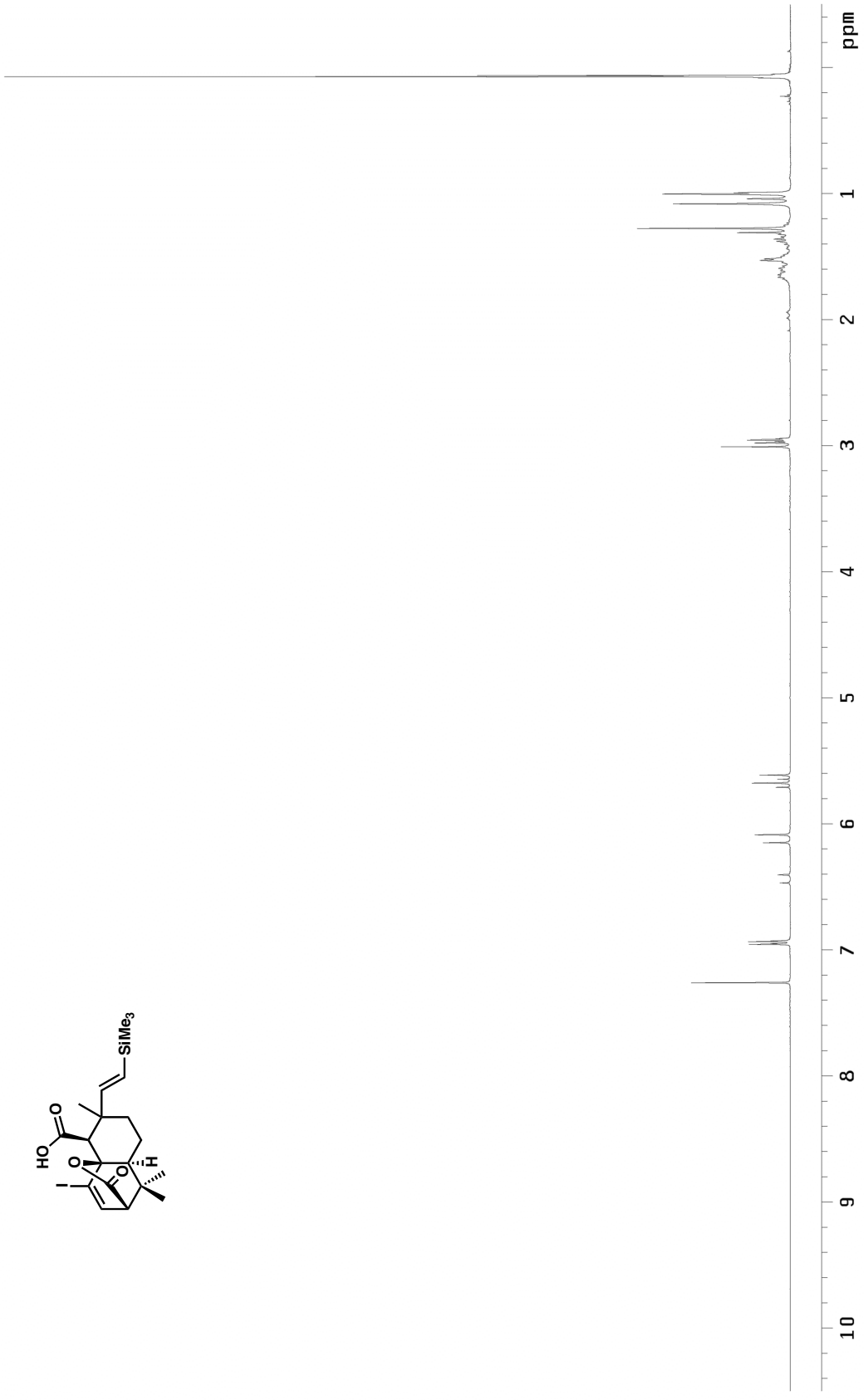

Figure A8.2.1 ^{1}H NMR (500 MHz, $CDCl_3$) of compound **160**

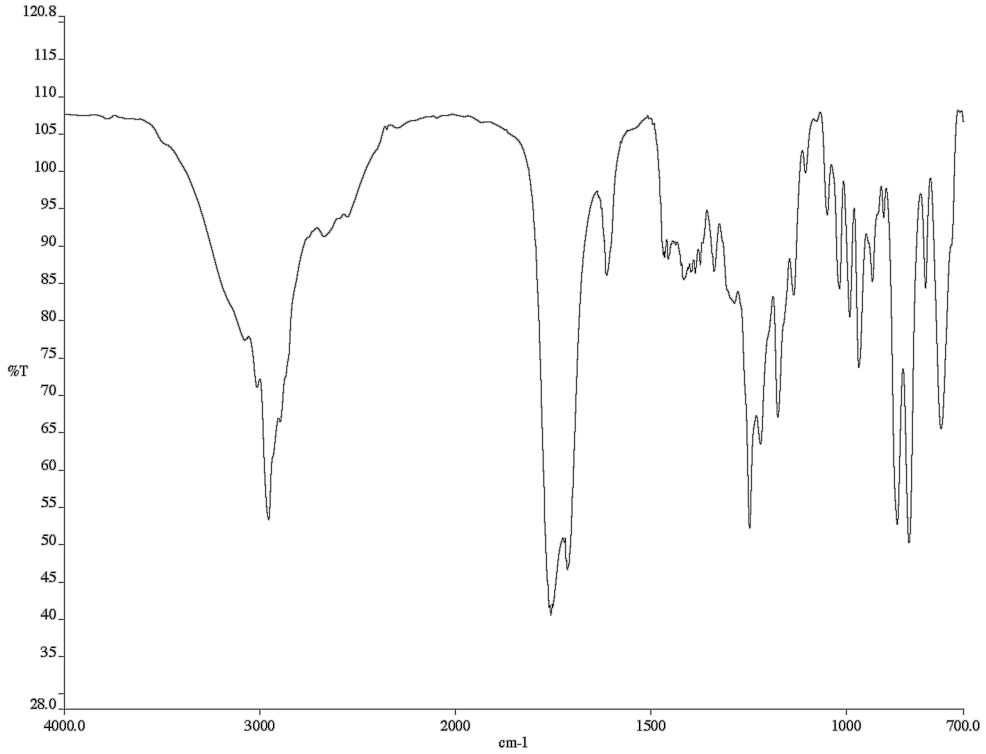

Figure A8.2.2 Infrared spectrum (thin film/NaCl) of compound **160**

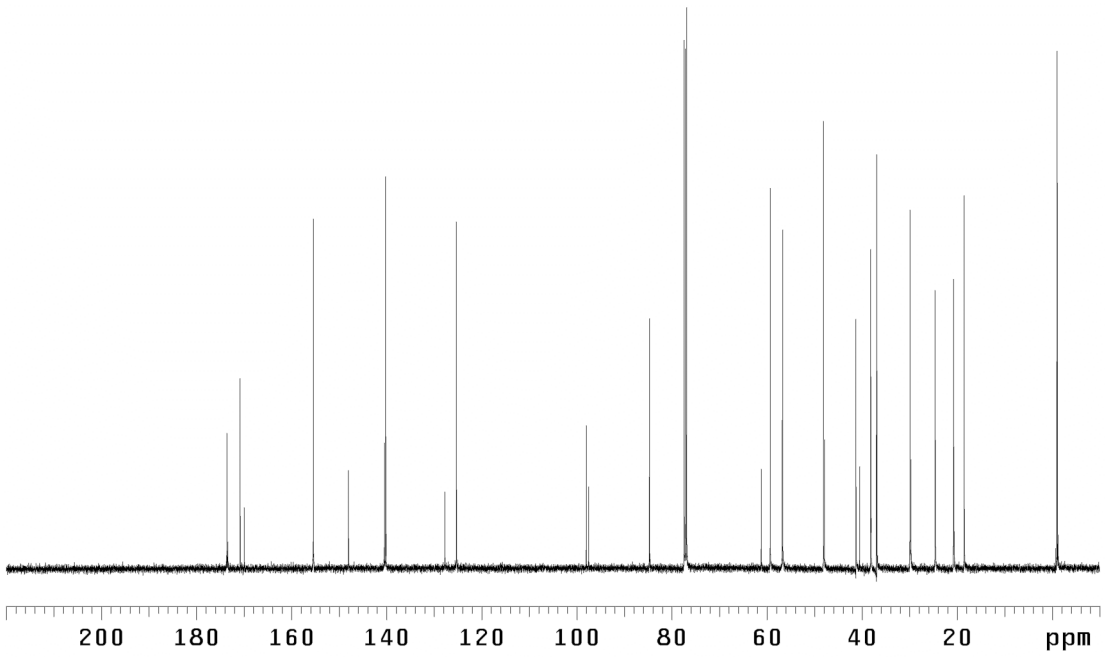

Figure A8.2.3 ^{13}C NMR (125 MHz, $CDCl_3$) of compound **160**

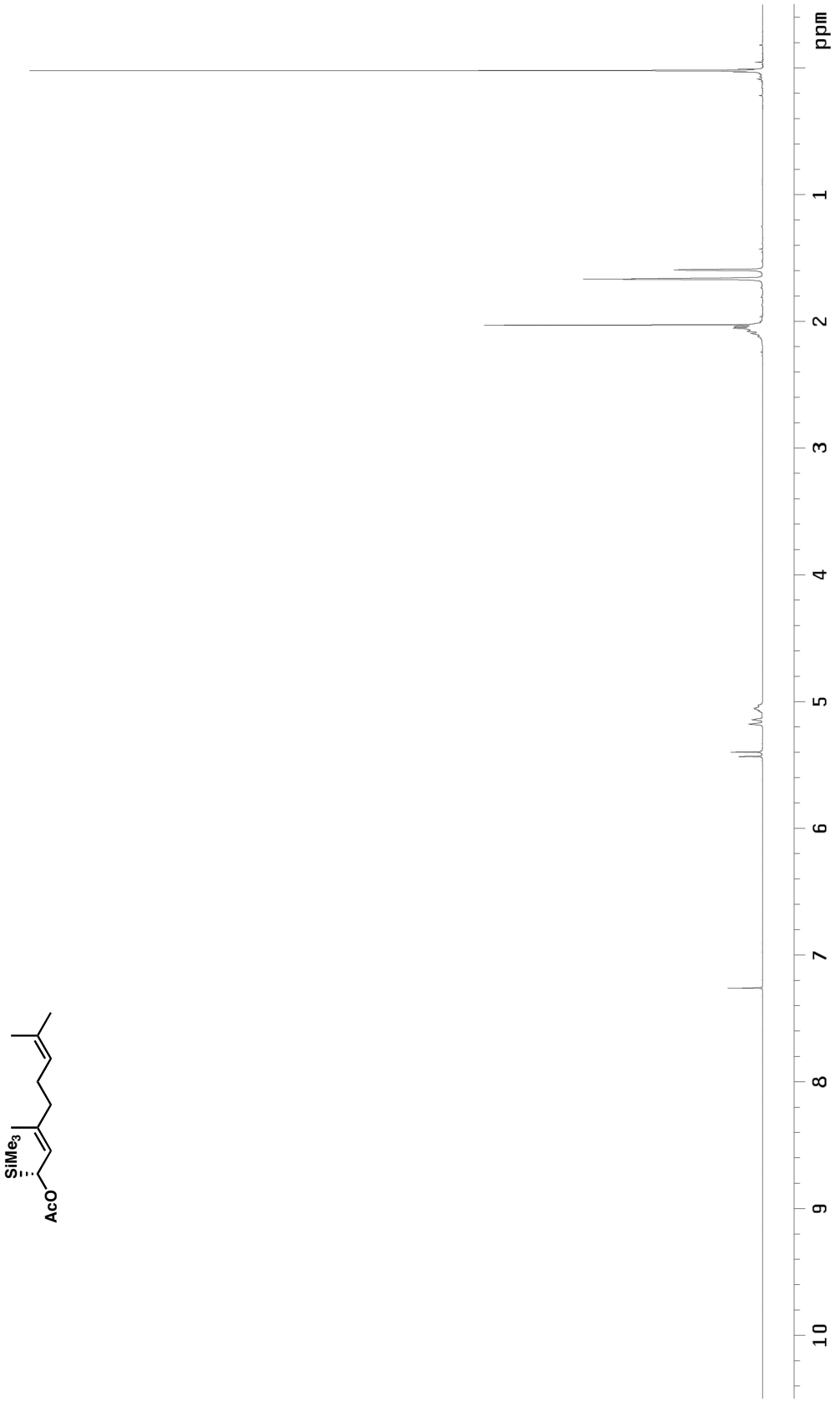

Figure A8.3.1 ^{1}H NMR (500 MHz, $CDCl_3$) of compound **SI-1**

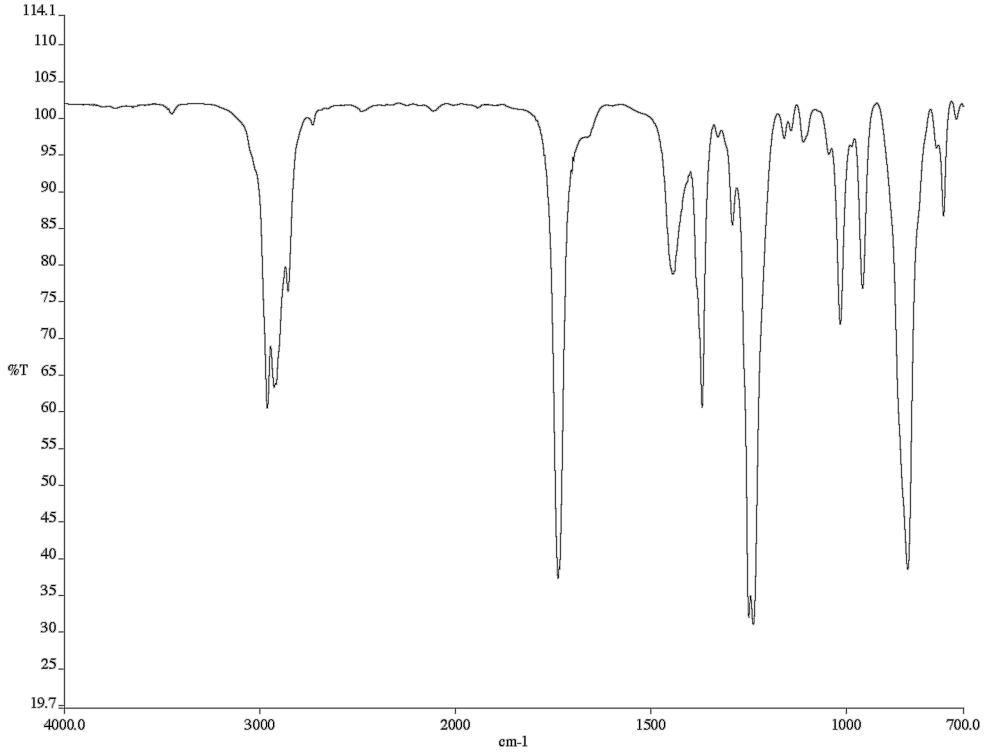

Figure A8.3.2 Infrared spectrum (thin film/NaCl) of compound **SI-1**

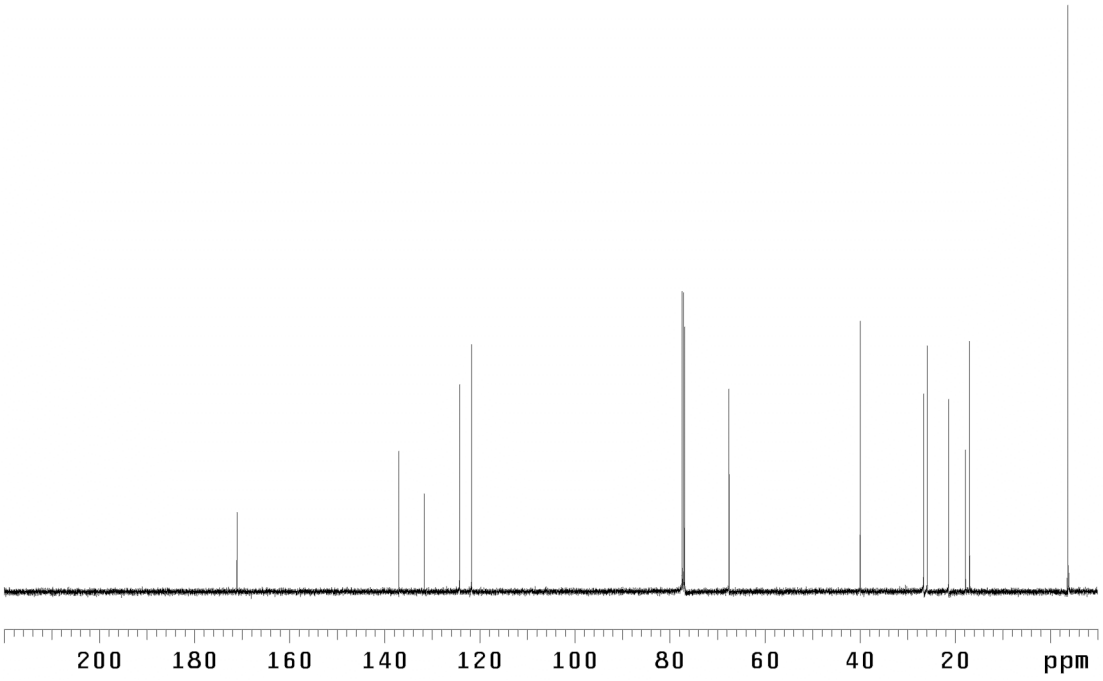

Figure A8.3.3 ^{13}C NMR (125 MHz, $CDCl_3$) of compound **SI-1**

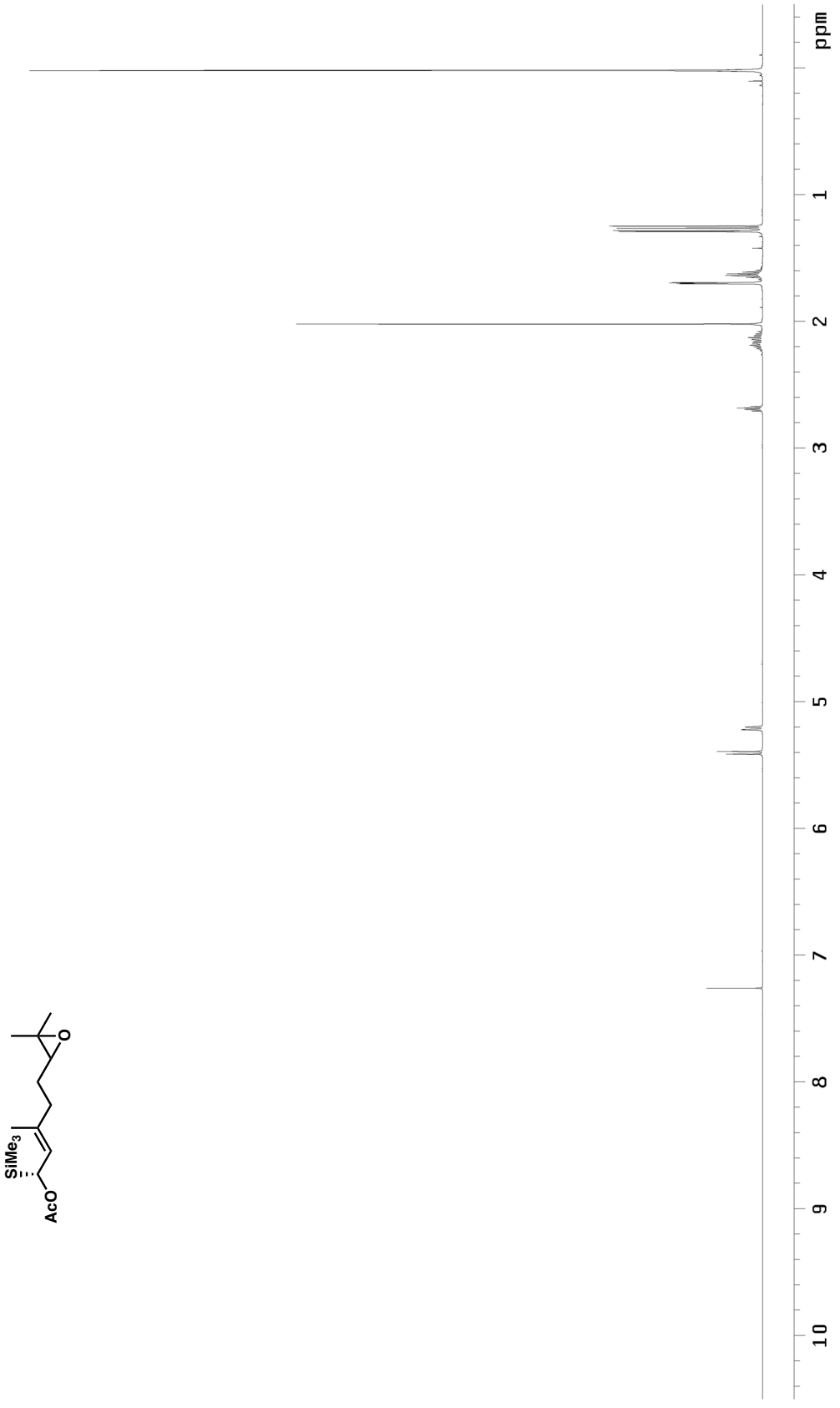

Figure A8.4.1 ^{1}H NMR (500 MHz, $CDCl_3$) of compound **SI-2**

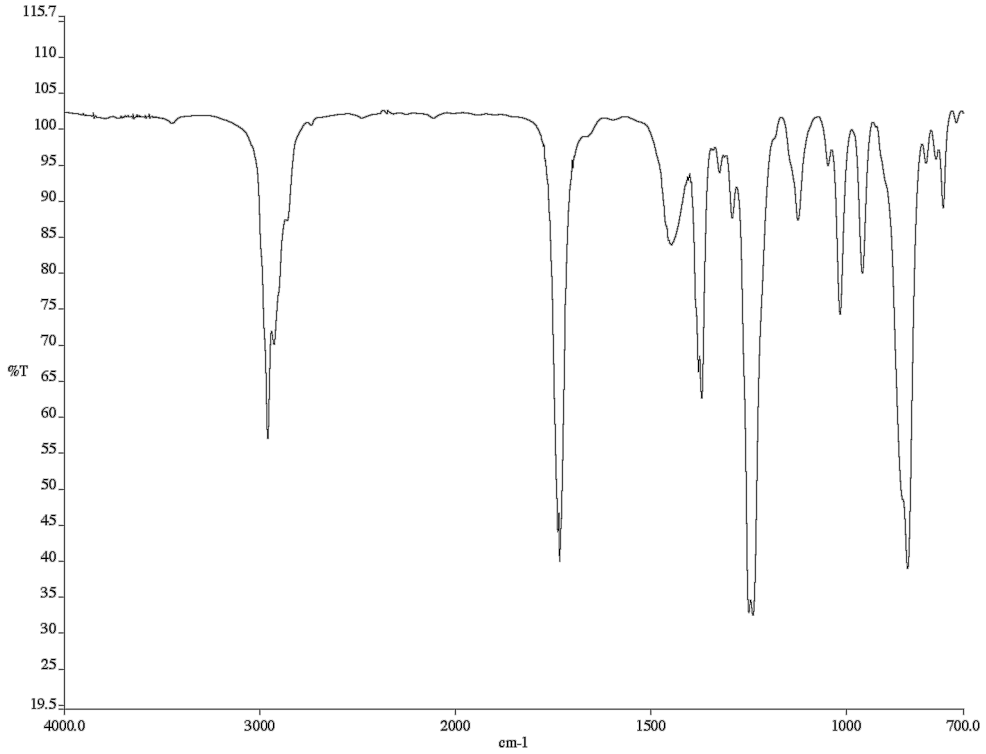

Figure A8.4.2 Infrared spectrum (thin film/NaCl) of compound **SI-2**

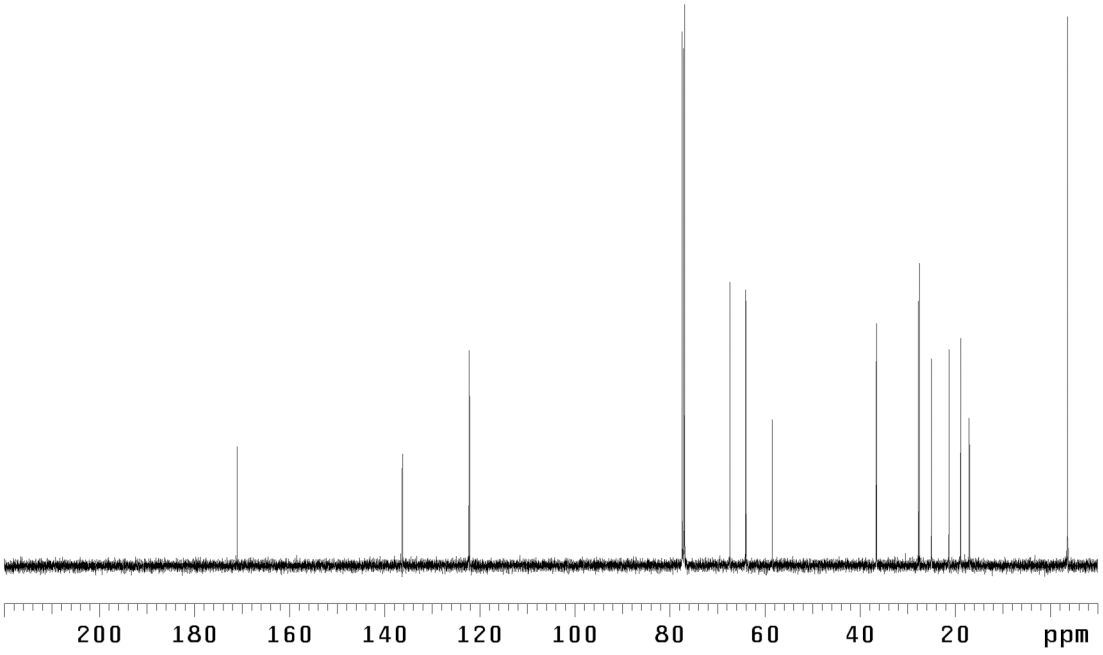

Figure A8.4.3 ^{13}C NMR (125 MHz, $CDCl_3$) of compound **SI-2**

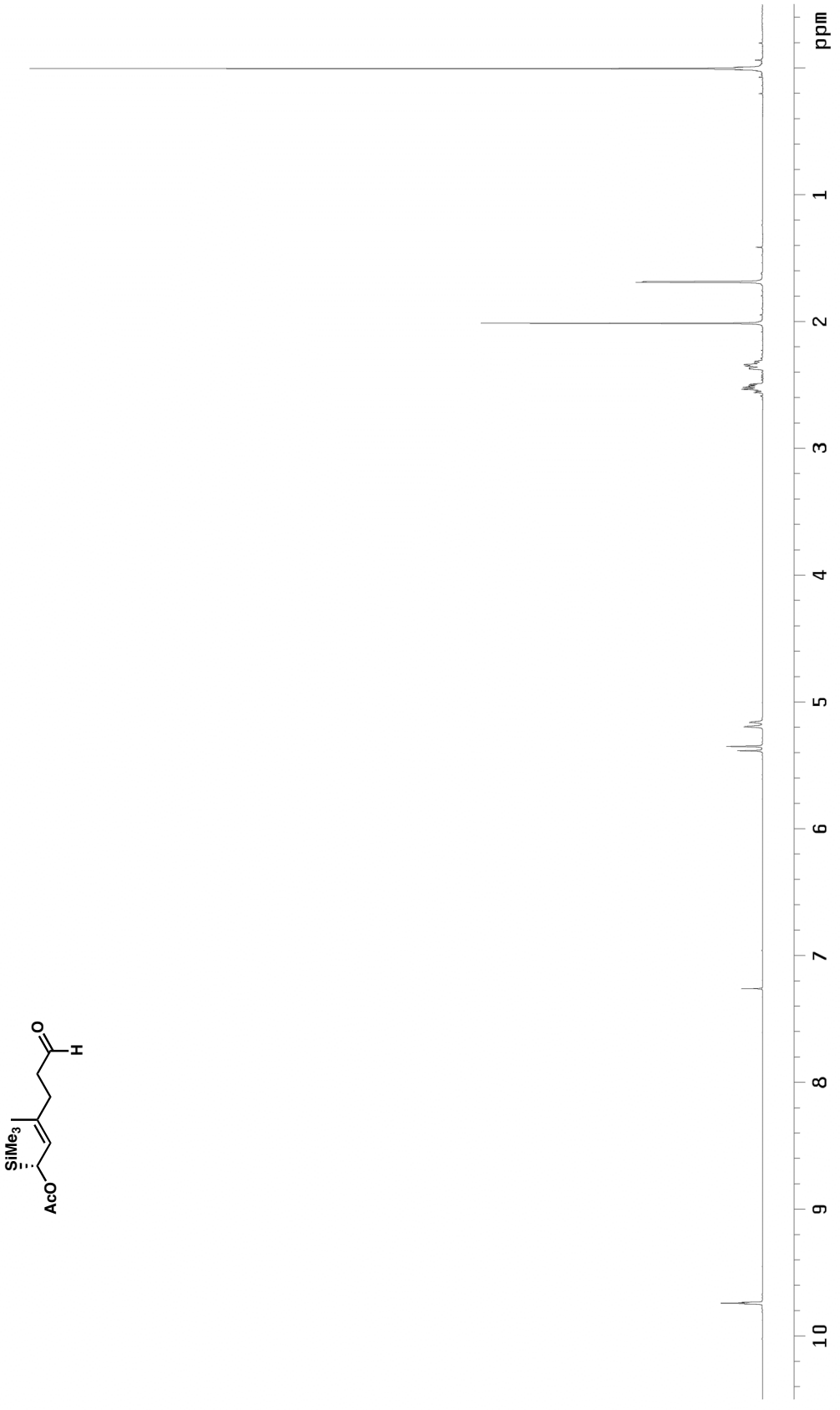

Figure A8.5.1 ^{1}H NMR (500 MHz, $CDCl_3$) of compound **164**

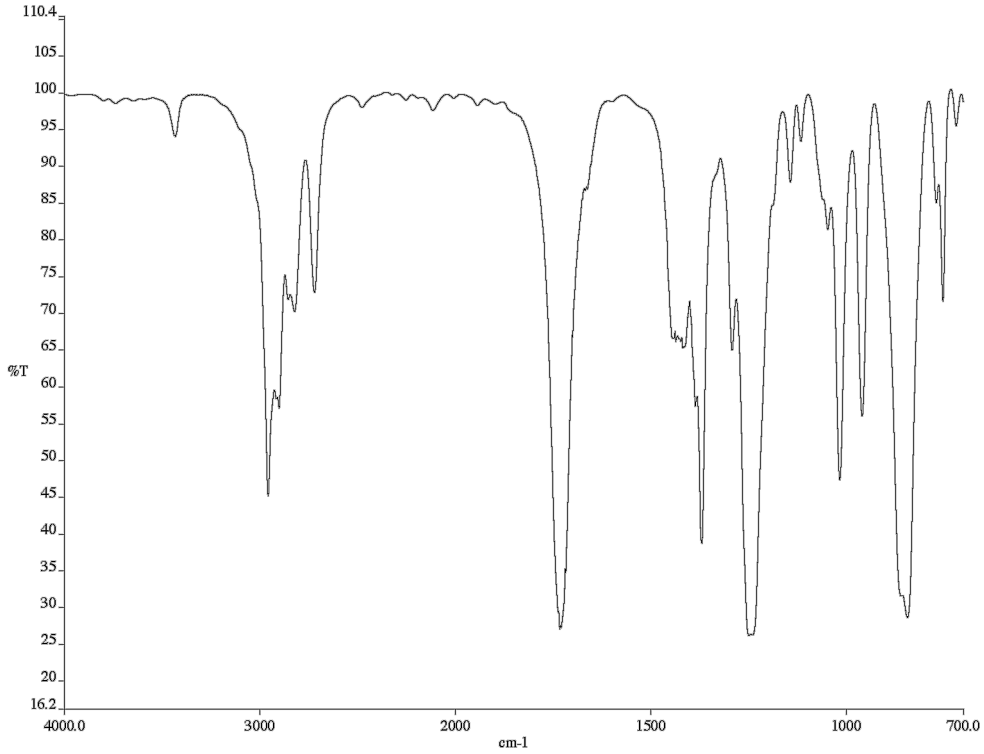

Figure A8.5.2 Infrared spectrum (thin film/NaCl) of compound **164**

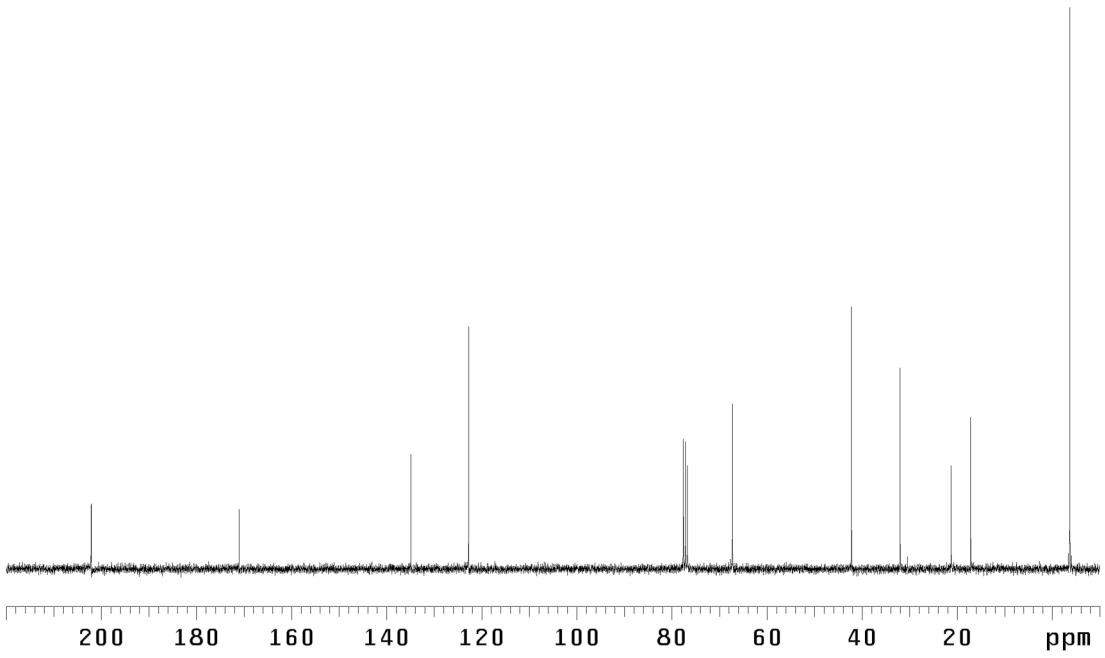

Figure A8.5.3 ^{13}C NMR (125 MHz, $CDCl_3$) of compound **164**

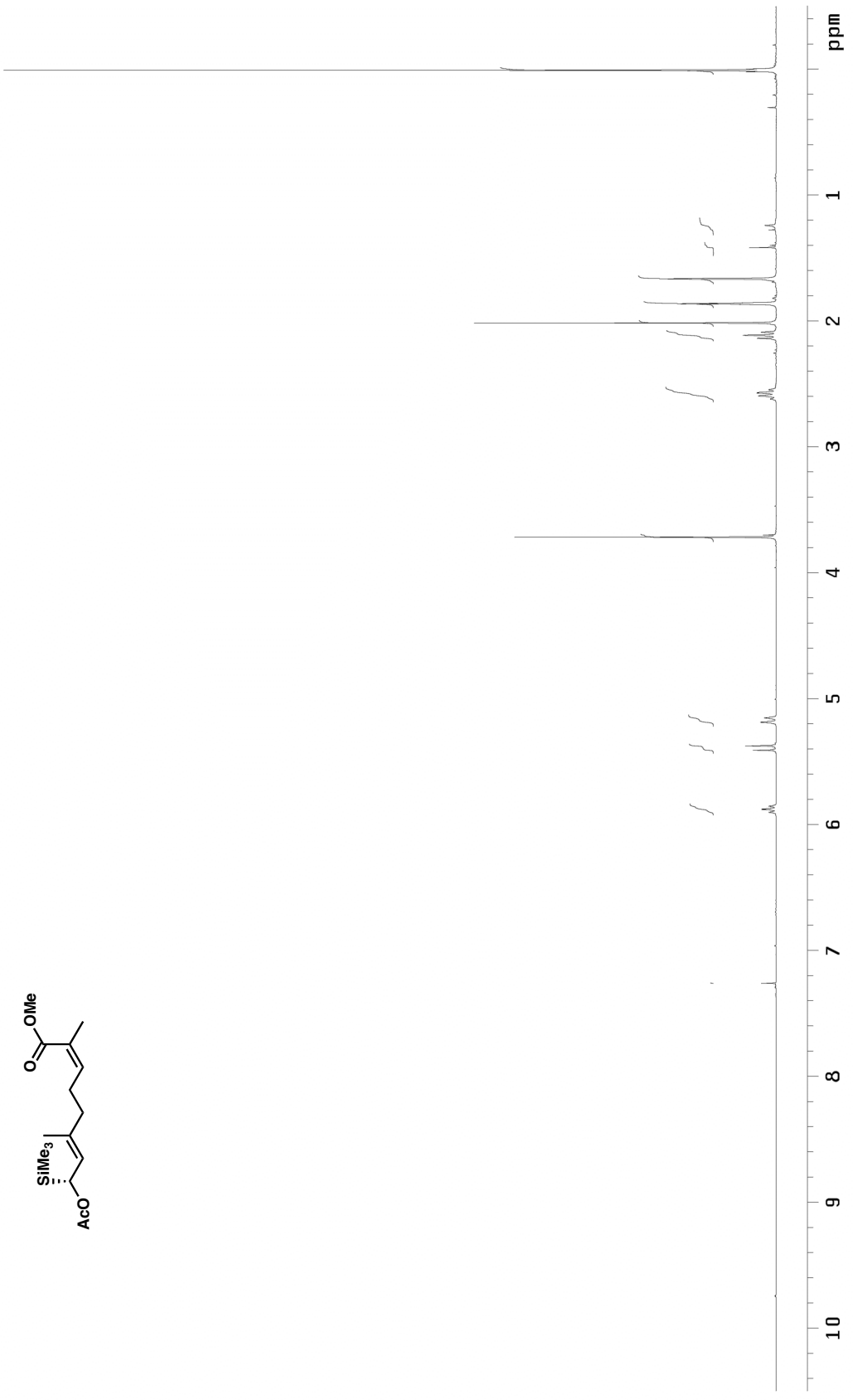

Figure A8.6.1 ^{1}H NMR (500 MHz, $CDCl_3$) of compound **SI-3**

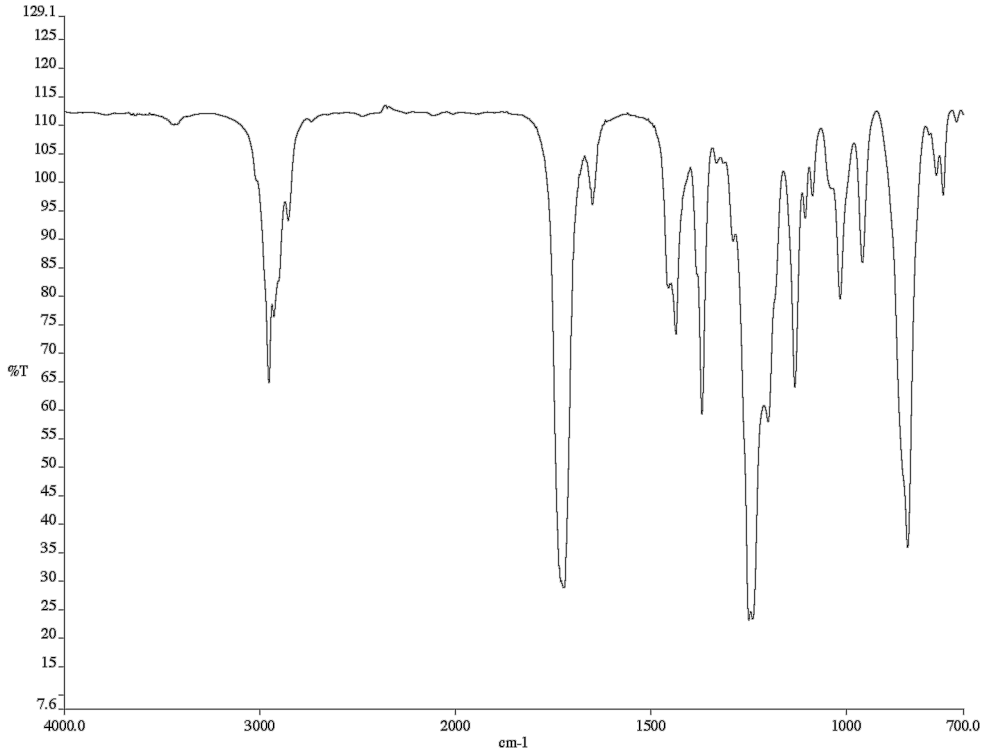

Figure A8.6.2 Infrared spectrum (thin film/NaCl) of compound **SI-3**

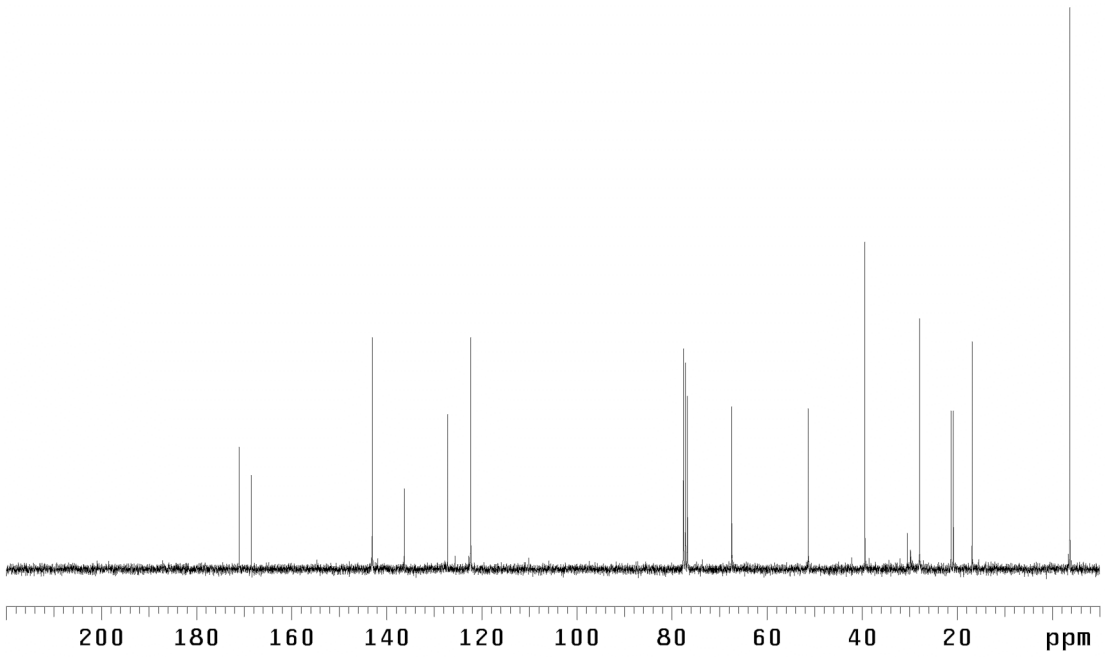

Figure A8.6.3 ^{13}C NMR (125 MHz, $CDCl_3$) of compound **SI-3**

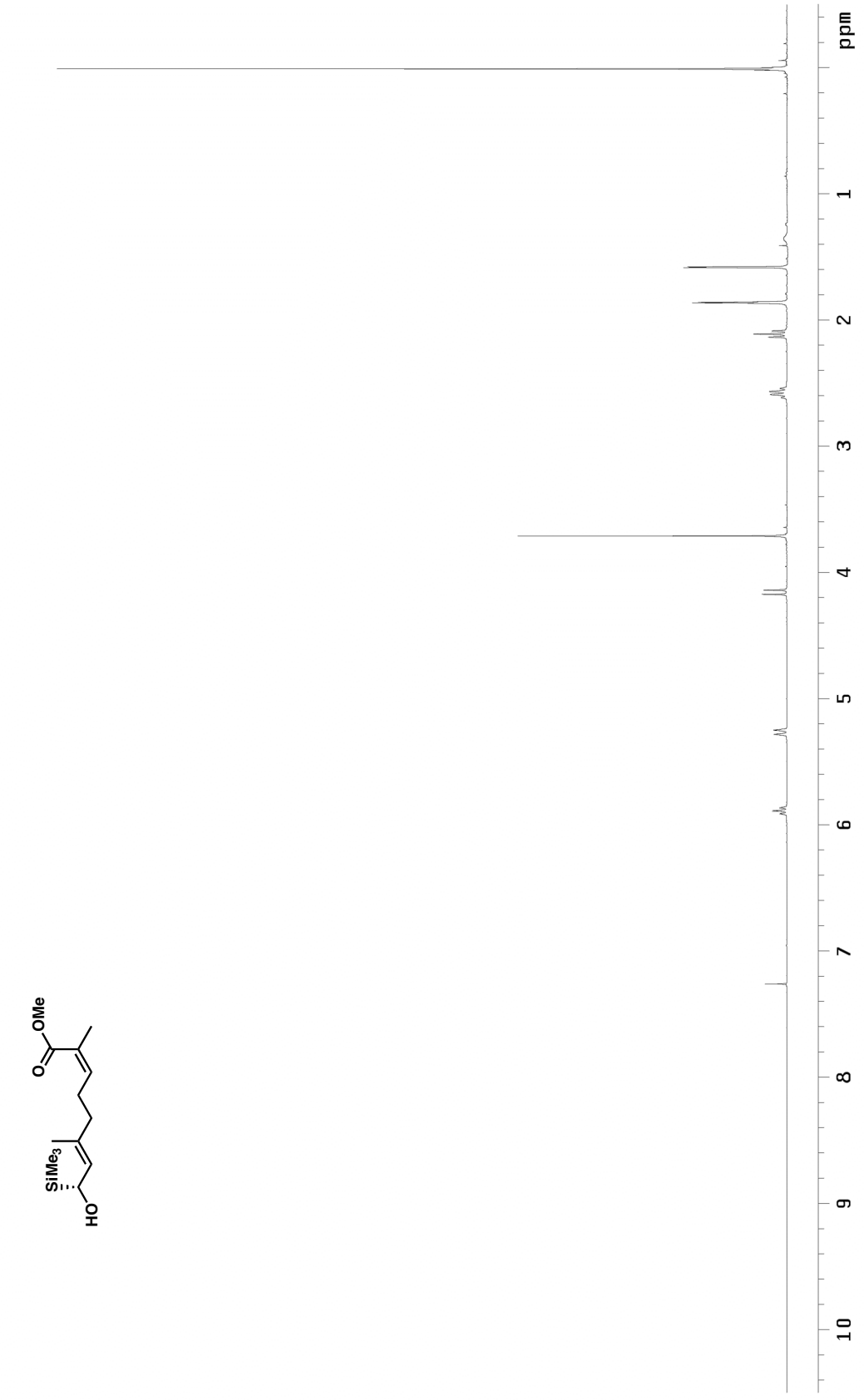

Figure A8.7.1 ^{1}H NMR (500 MHz, $CDCl_3$) of compound **166**

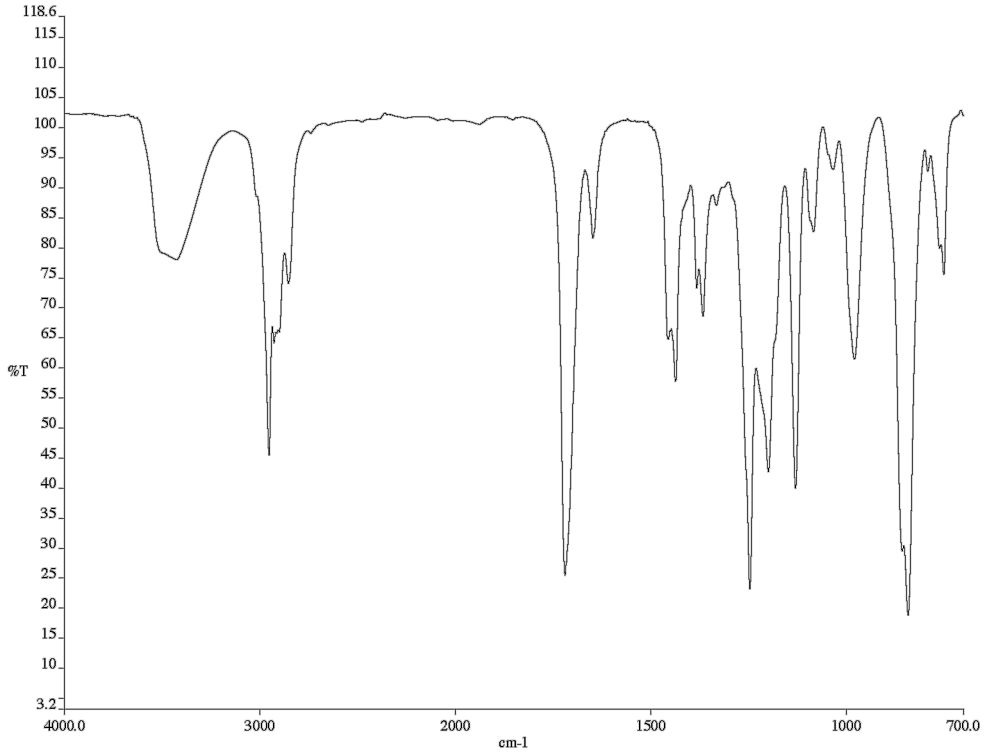

Figure A8.7.2 Infrared spectrum (thin film/NaCl) of compound **166**

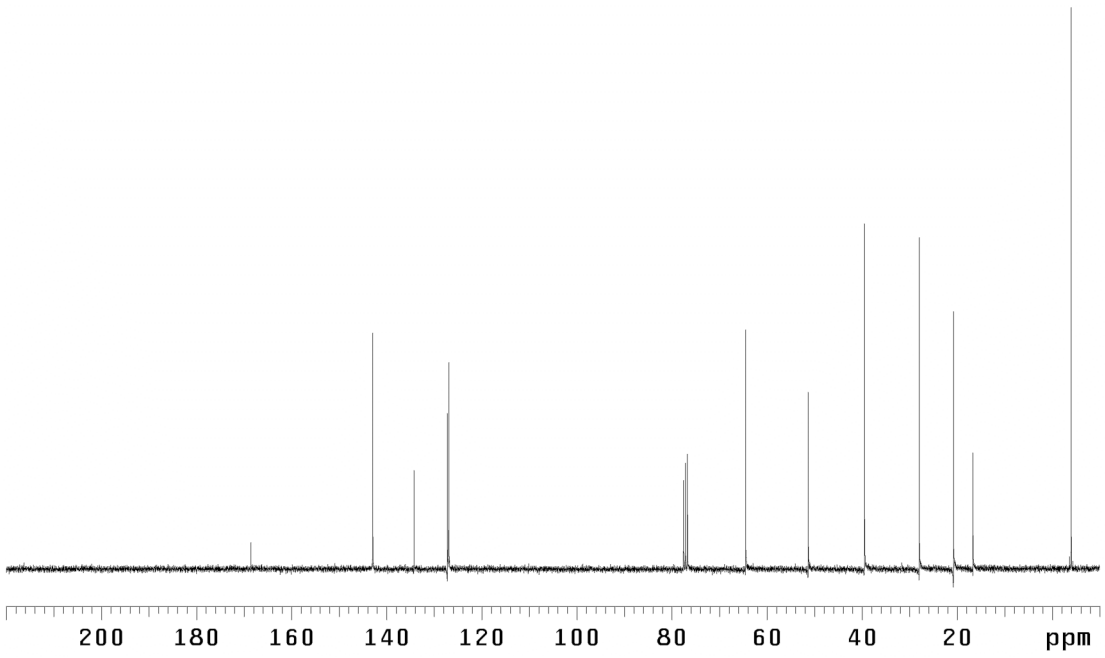

Figure A8.7.3 ^{13}C NMR (125 MHz, $CDCl_3$) of compound **166**

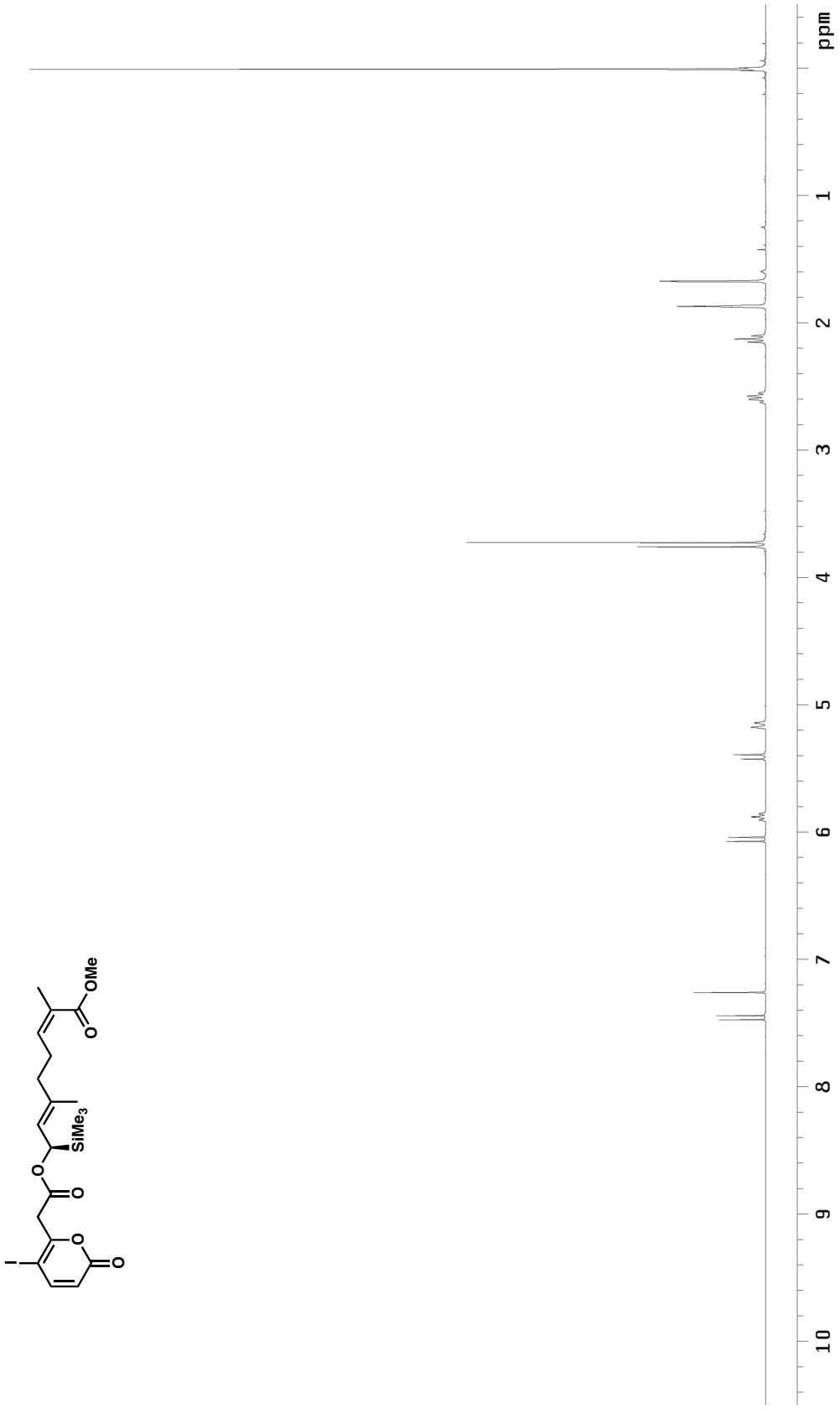

Figure A8.8.1 ^{1}H NMR (500 MHz, $CDCl_3$) of compound **167**

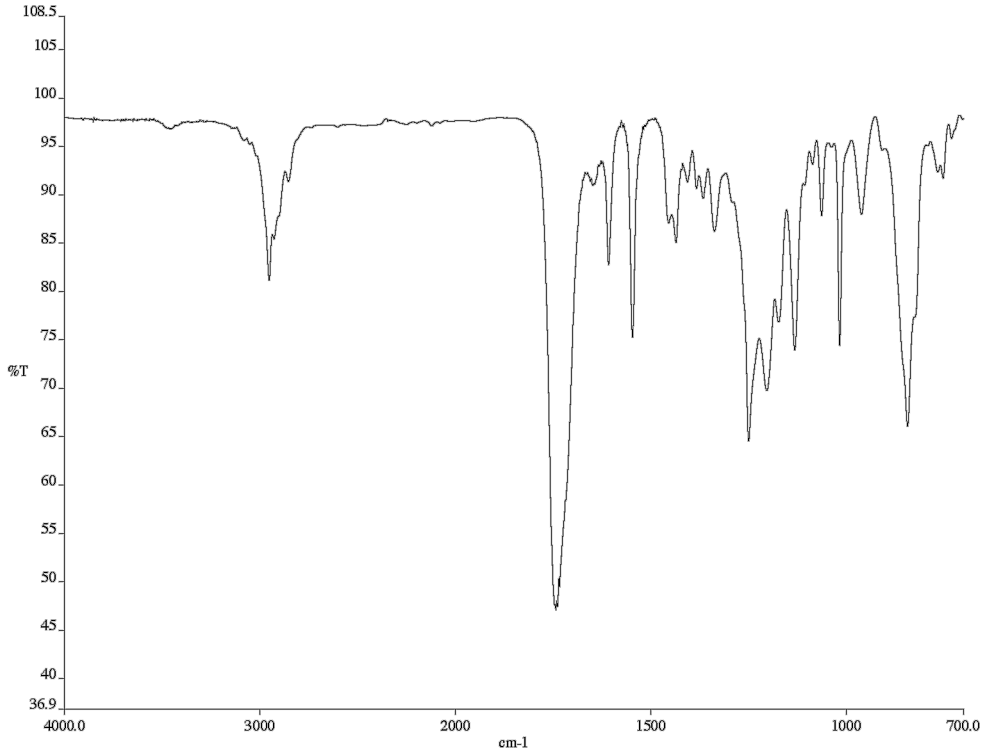

Figure A8.8.2 Infrared spectrum (thin film/NaCl) of compound **167**

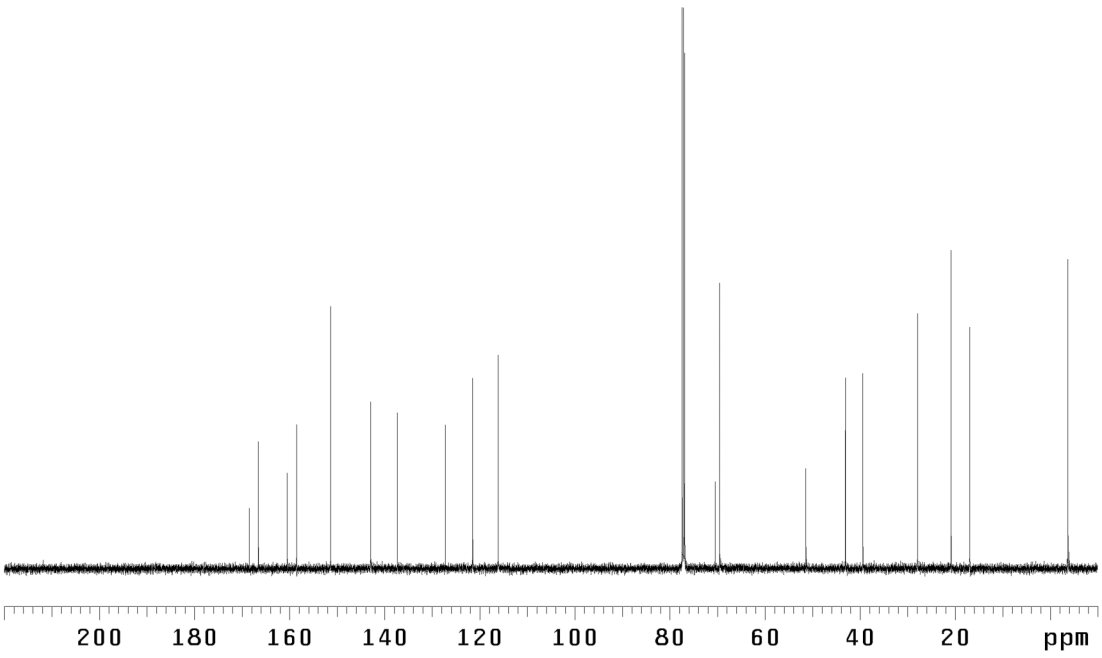

Figure A8.8.3 ^{13}C NMR (125 MHz, $CDCl_3$) of compound **167**

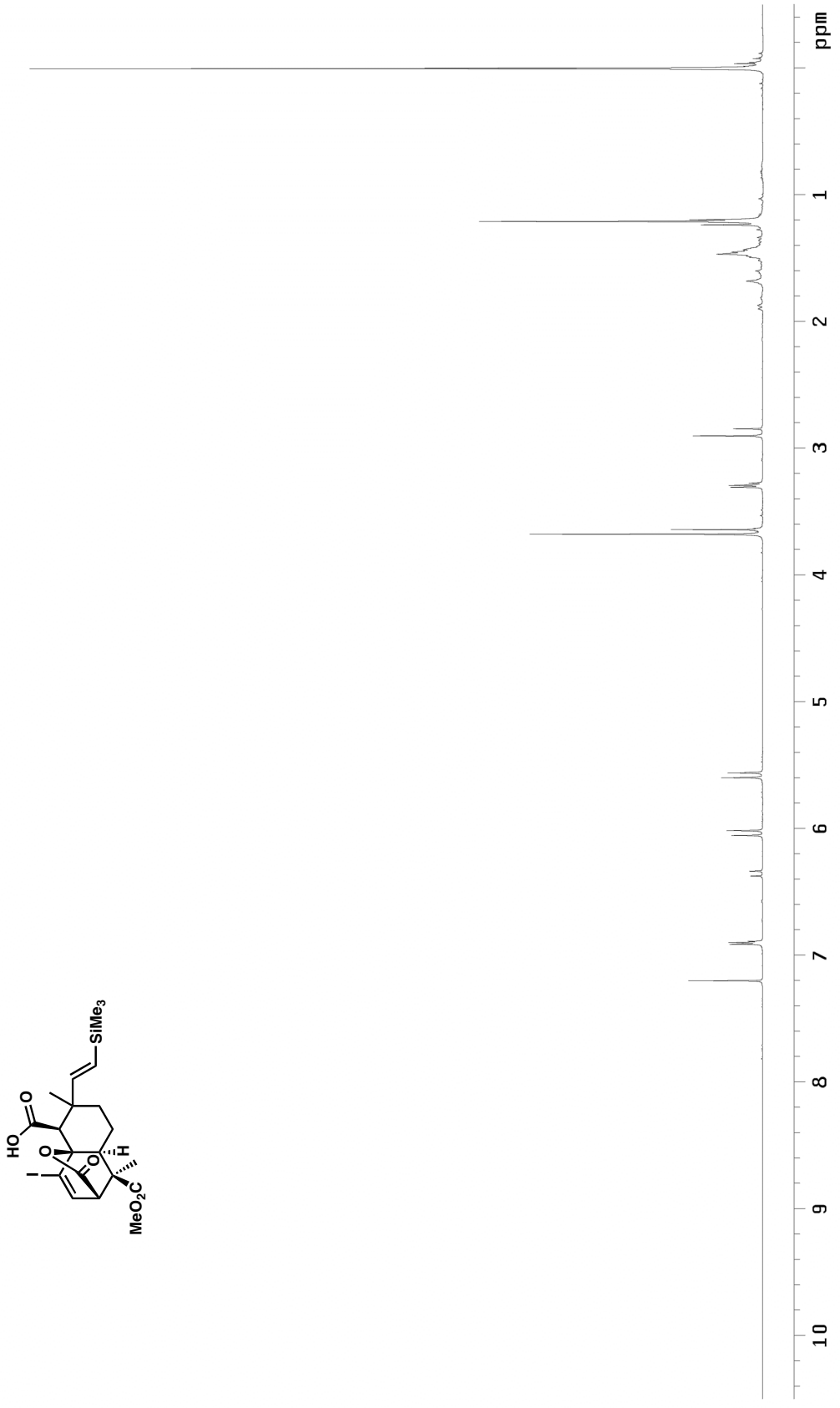

Figure A8.9.1 ^{1}H NMR (500 MHz, $CDCl_3$) of compound **168**

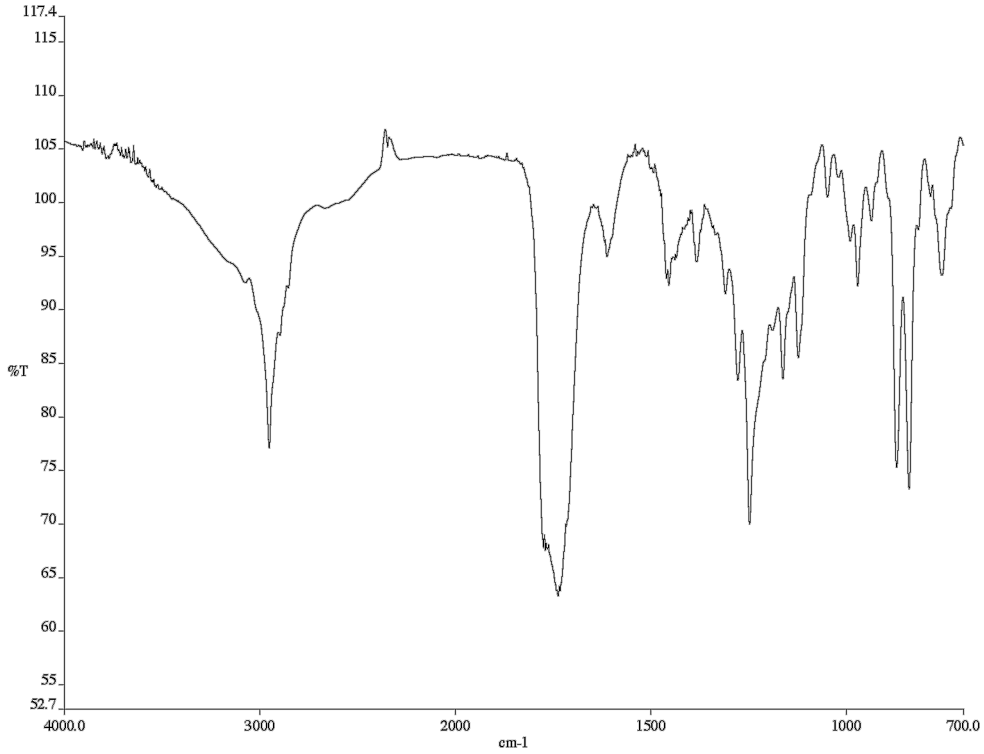

Figure A8.9.2 Infrared spectrum (thin film/NaCl) of compound **168**

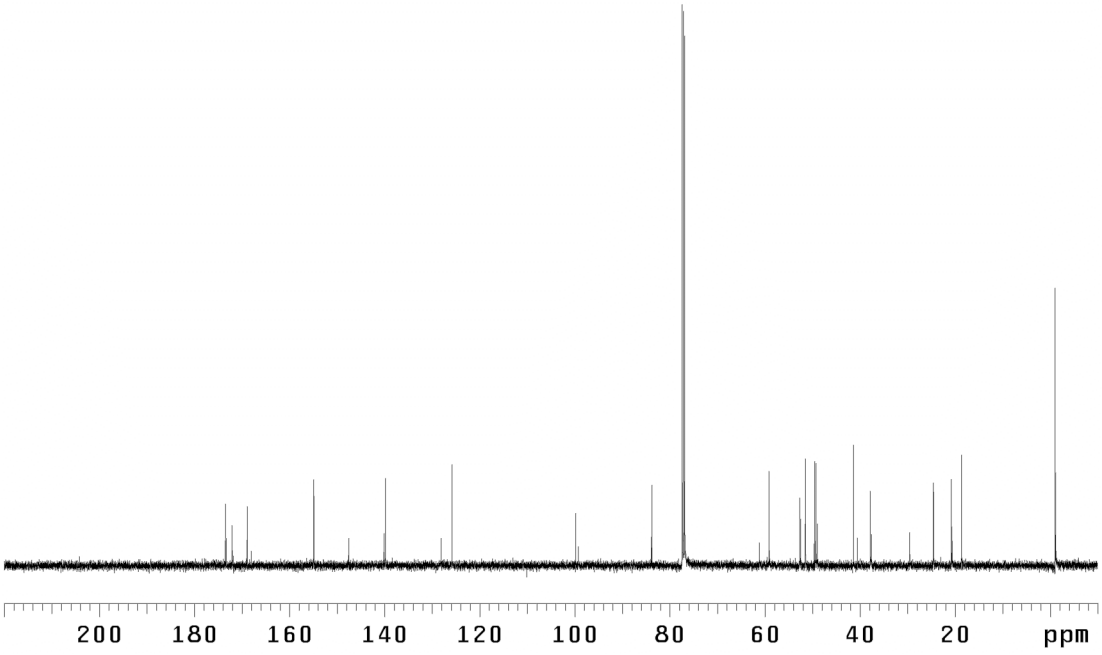

Figure A8.9.3 ^{13}C NMR (125 MHz, $CDCl_3$) of compound **168**

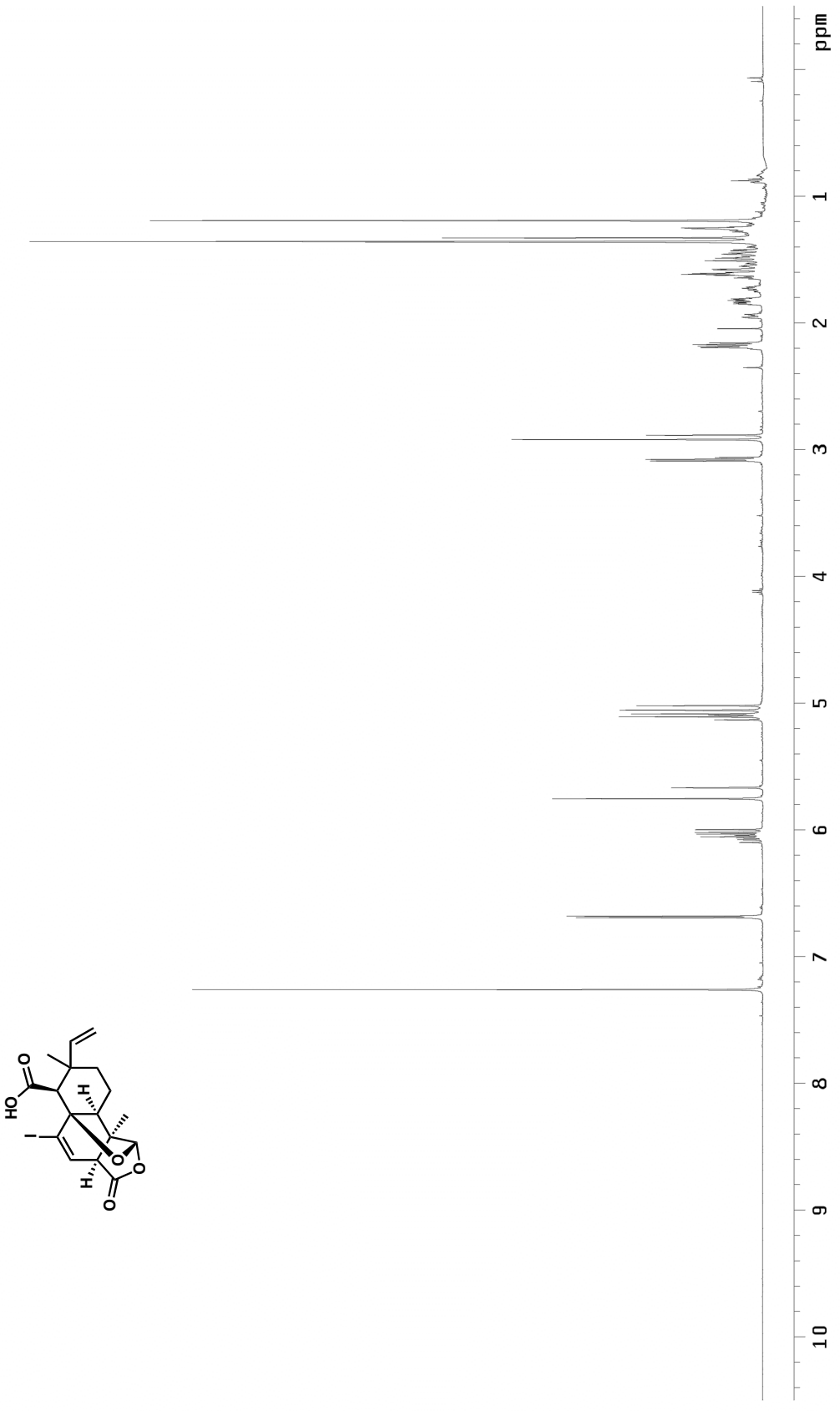

Figure A8.10.1 ^{1}H NMR (500 MHz, $CDCl_3$) of compound **155**

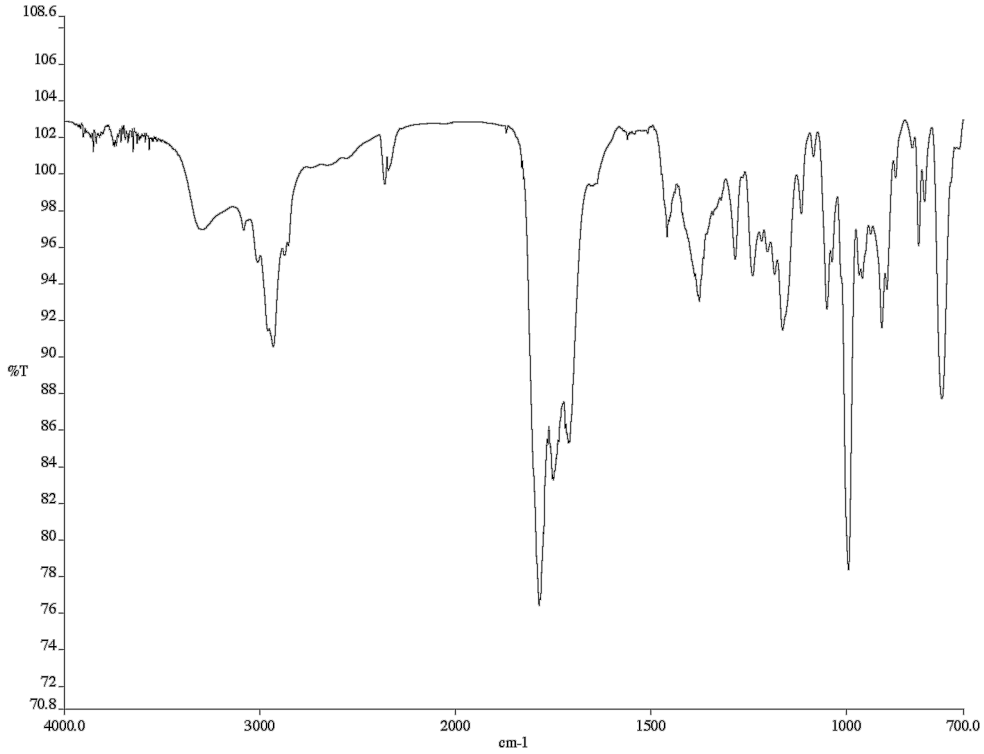

Figure A8.10.2 Infrared spectrum (thin film/NaCl) of compound **155**

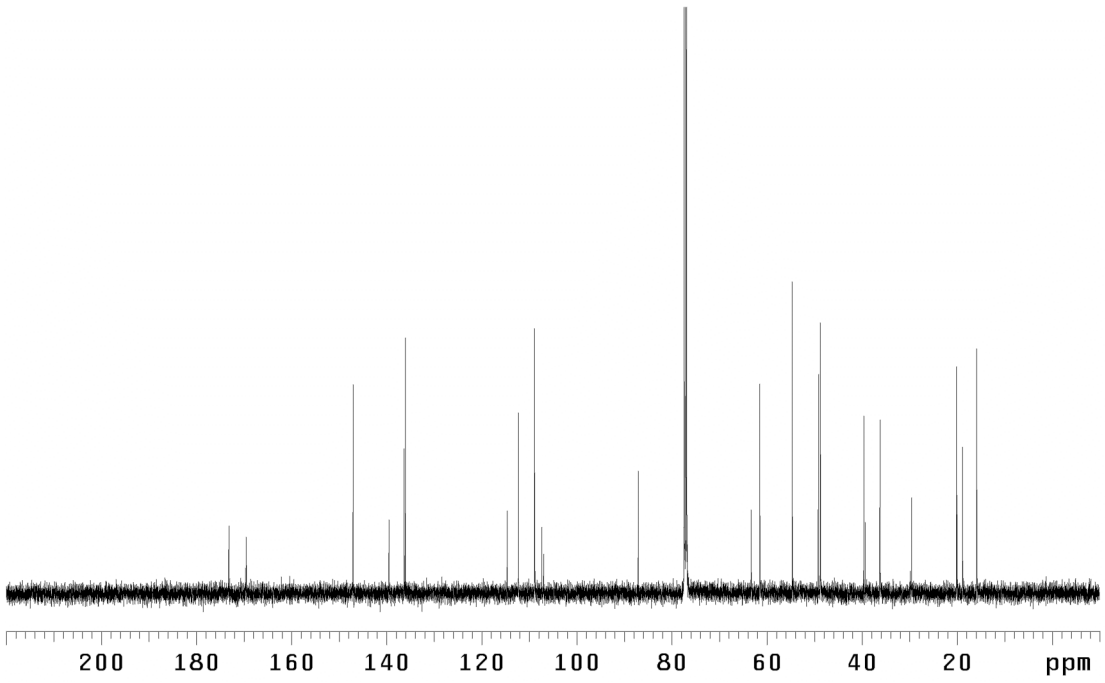

Figure A8.10.3 ^{13}C NMR (125 MHz, $CDCl_3$) of compound **155**

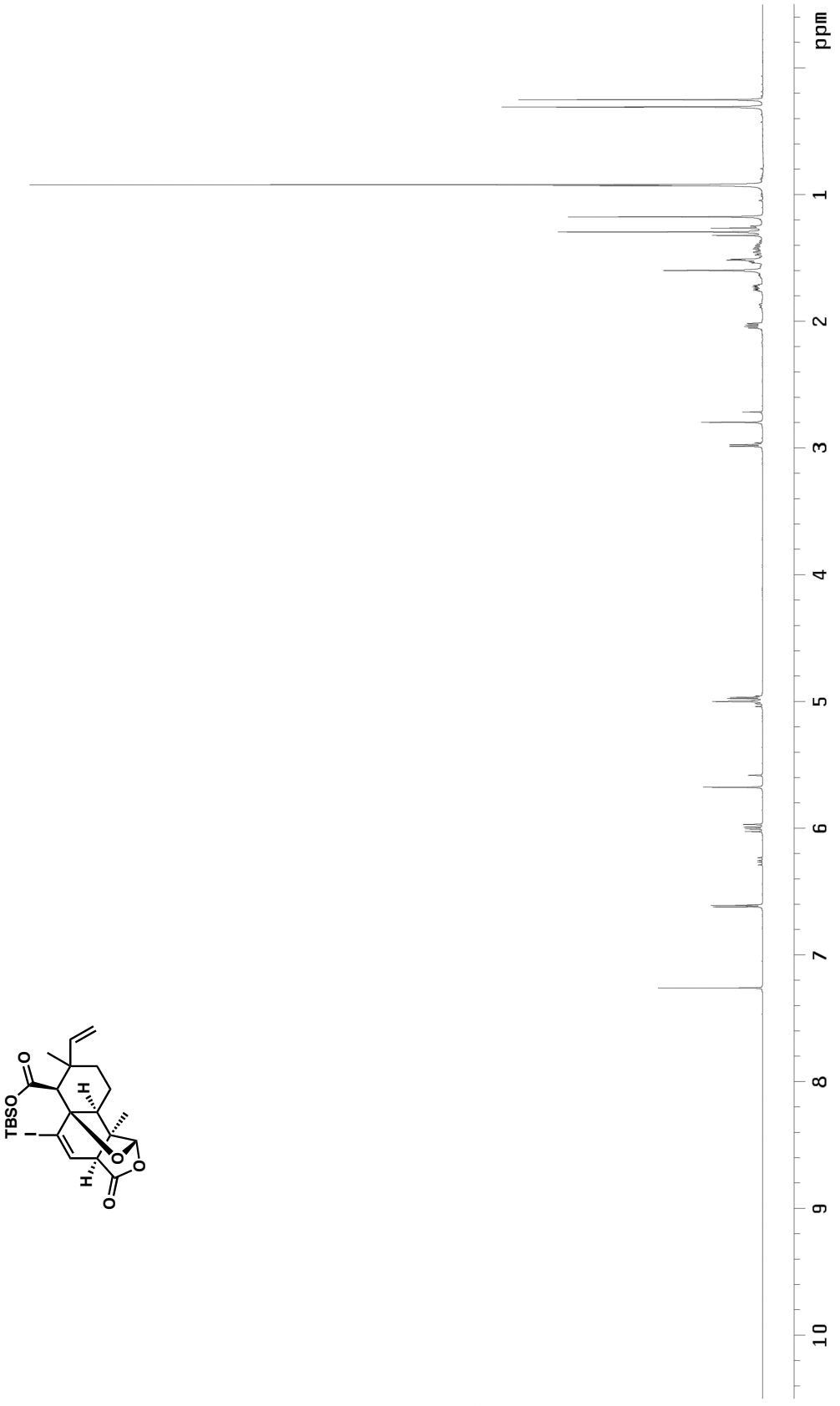

Figure A8.11.1 ^{1}H NMR (500 MHz, $CDCl_3$) of compound **169**

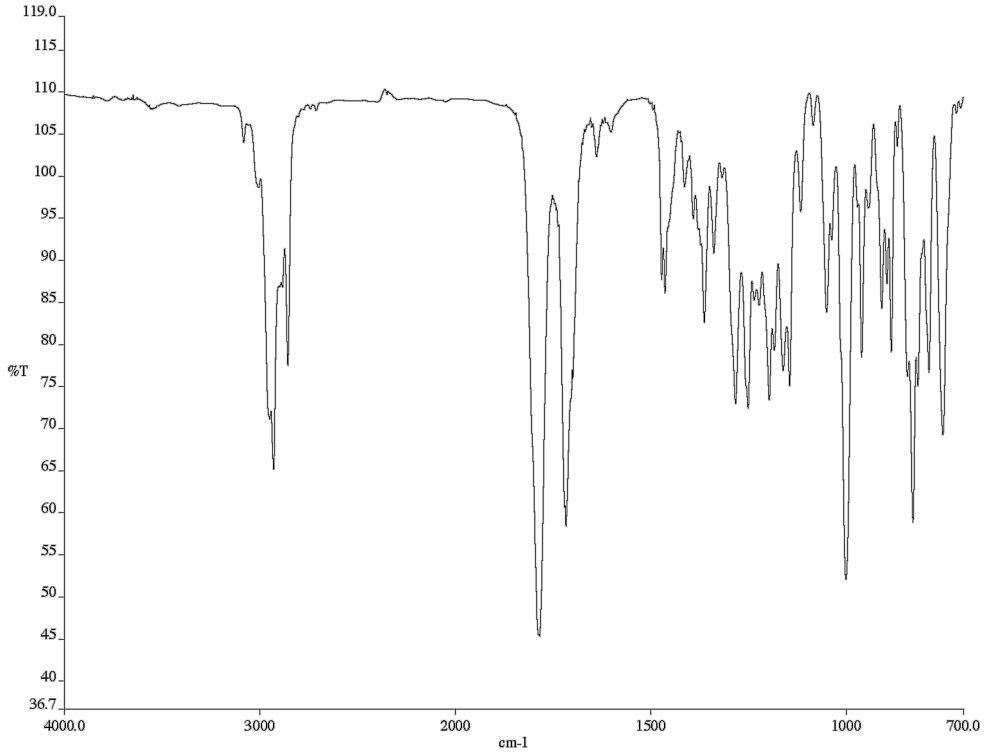

Figure A8.11.2 Infrared spectrum (thin film/NaCl) of compound **169**

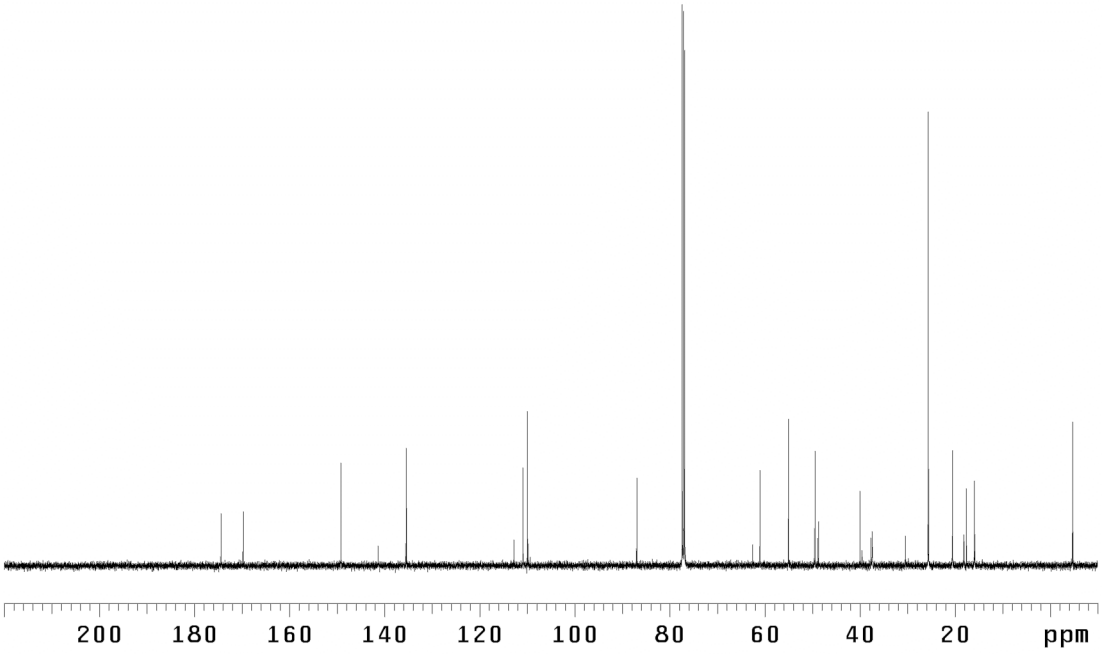

Figure A8.11.3 ^{13}C NMR (125 MHz, $CDCl_3$) of compound **169**

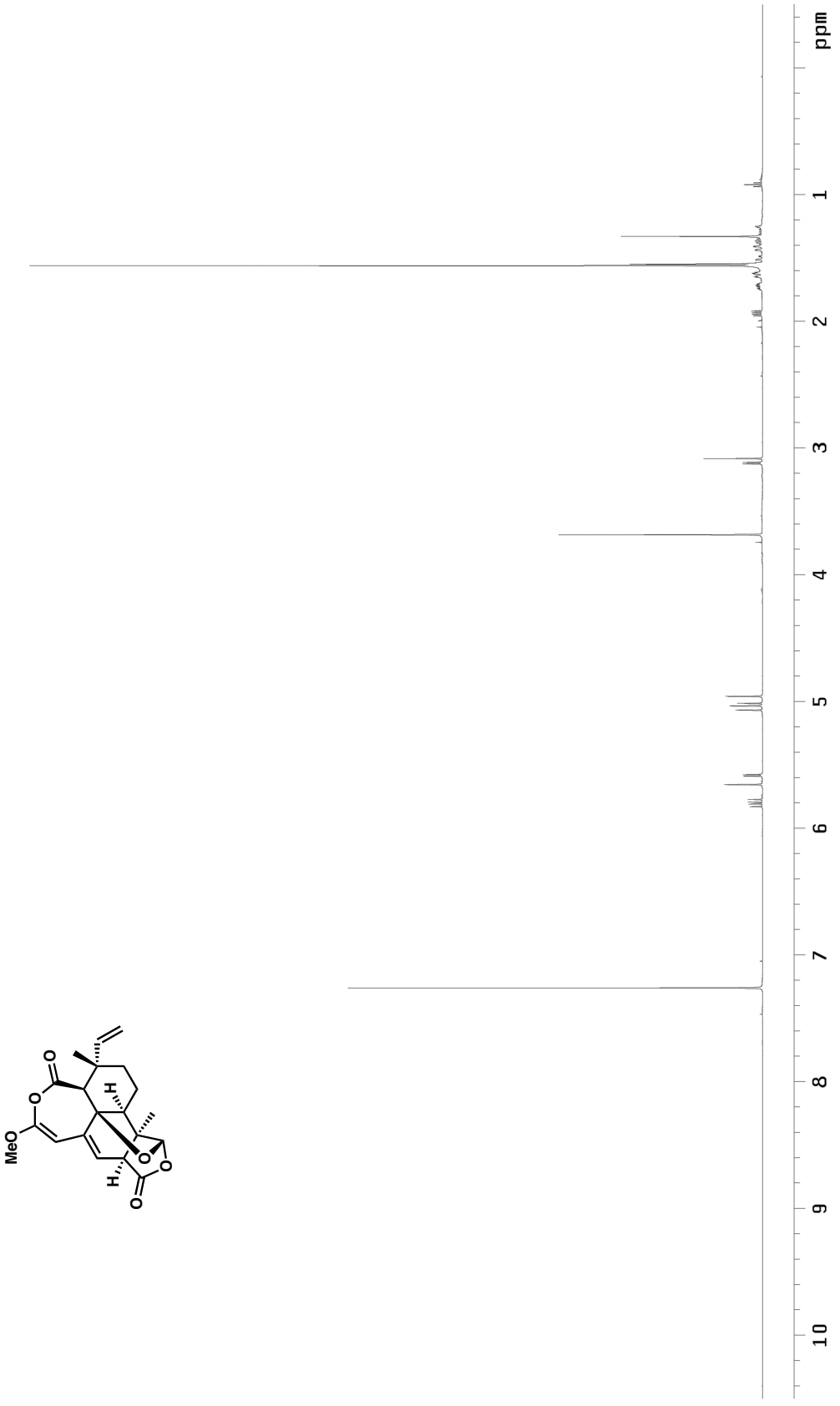

Figure A8.12.1 ^{1}H NMR (500 MHz, $CDCl_3$) of compound **85b**

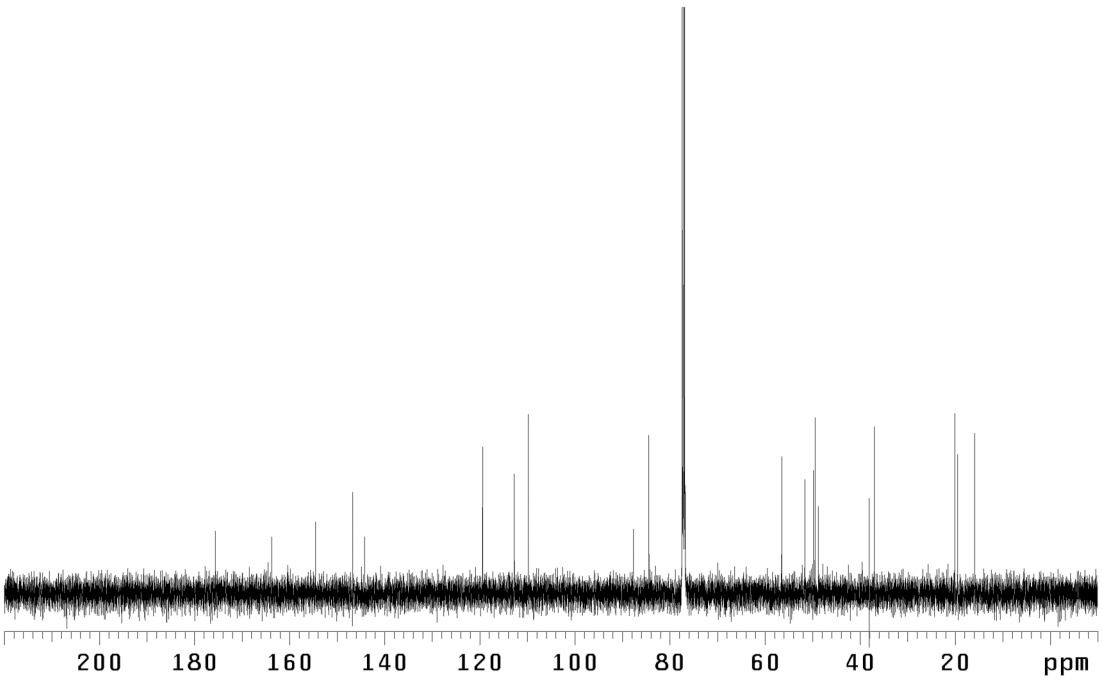

Figure A8.12.3 ^{13}C NMR (125 MHz, $CDCl_3$) of compound **85b**

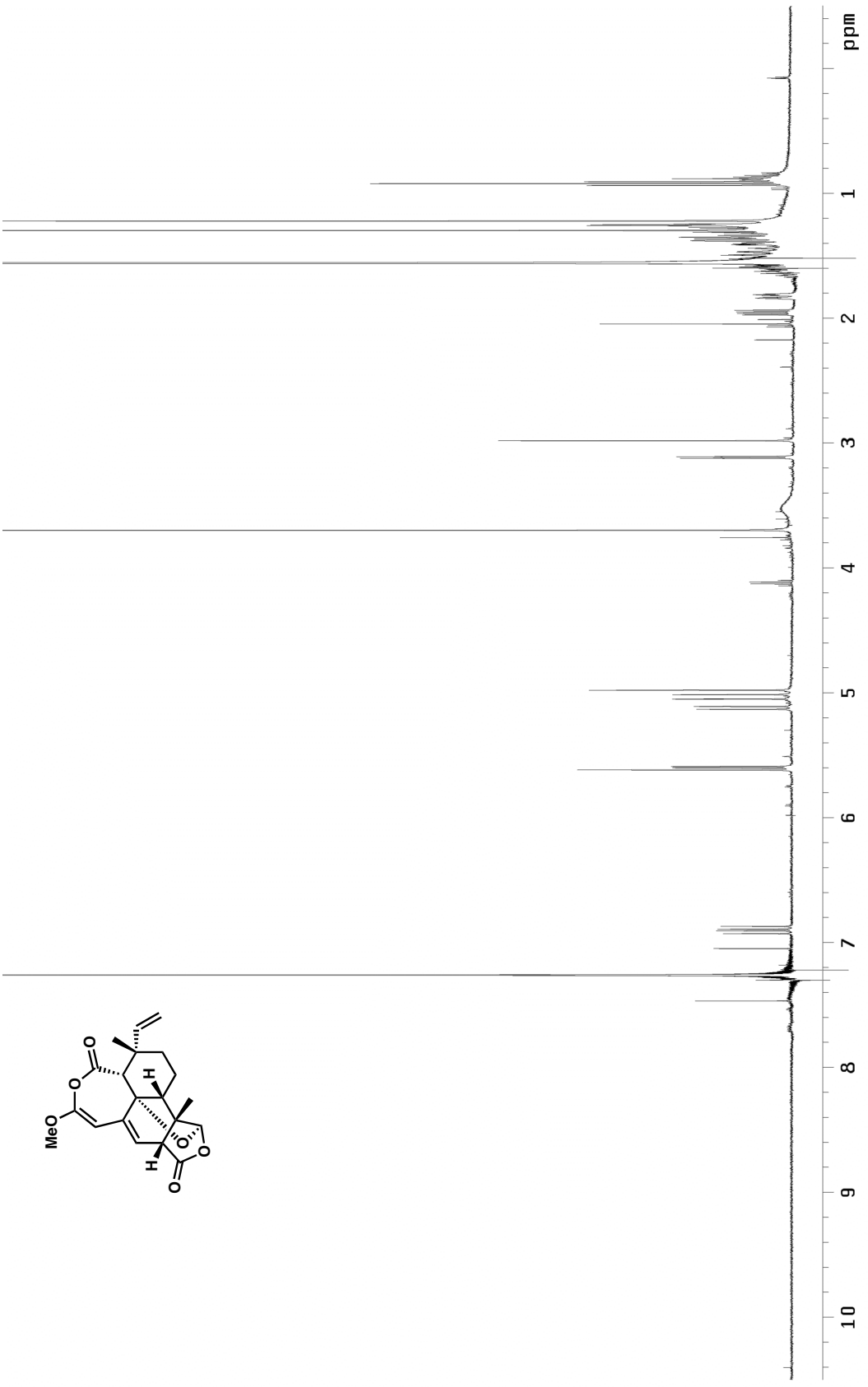

Figure A8.13.1 ^{1}H NMR (500 MHz, $CDCl_3$) of compound **85a**

APPENDIX 9

X-Ray Data Relevant to Chapter 4

*Figure A9.1. Ortep diagram of **173**. The crystallographic data have been deposited in the Cambridge Database (CCDC) and has been placed on hold pending further instructions.*

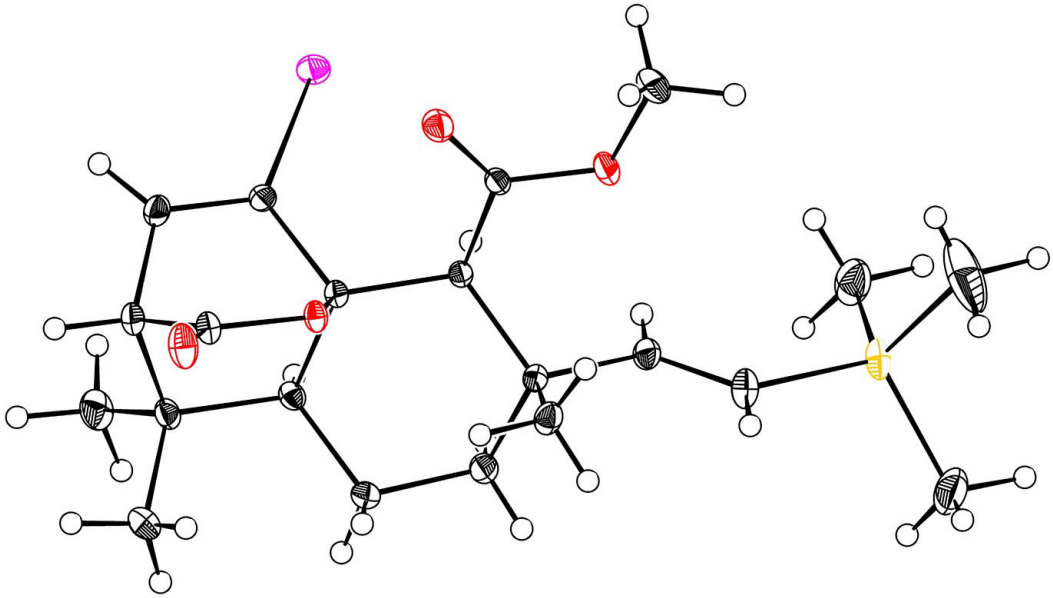

*Table A9.1 Crystal data and structure analysis details for **173**.*

Empirical formula	C21 H31 I O4 Si
Formula weight	502.45
Crystallization solvent	Hexanes/Pentane
Crystal shape	block
Crystal color	colourless
Crystal size	0.28 x 0.3 x 0.38 mm

Data Collection

Preliminary photograph(s)	rotation
Type of diffractometer	Bruker APEX-II CCD

Wavelength	0.71073 ≈ MoK	
Data collection temperature	100 K	
Theta range for 9418 reflections used		
in lattice determination	2.69 to 49.27∞	
Unit cell dimensions	a = 7.8106(6) ≈	α= 90∞
	b = 9.9557(9) ≈	β= 90∞
	c = 29.925(3) ≈	γ = 90∞
Volume	2326.9(3) $\approx^3$	
Z	4	
Crystal system	orthorhombic	
Space group	P 21 21 21 (# 19)	
Density (calculated)	1.434 g/cm^3	
F(000)	1024	
Theta range for data collection	2.2 to 51.0∞	
Completeness to theta = 25.00∞	99.9%	
Index ranges	-16 ≤ h ≤ 8, -21 ≤ k ≤ 21, -61 ≤ l ≤ 65	
Data collection scan type	and scans	
Reflections collected	91039	
Independent reflections	24693 [R_{int}= 0.0329]	
Reflections > 2σ(I)	22910	
Average σ(I)/(net I)	0.0301	
Absorption coefficient	1.45 mm^{-1}	
Absorption correction	Semi-empirical from equivalents	
Max. and min. transmission	0.8799 and 0.8128	

Structure Solution and Refinement

Primary solution method	dual
Secondary solution method	difmap
Hydrogen placement	geom

Refinement method	Full-matrix least-squares on F^2
Data / restraints / parameters	24693 / 0 / 368
Treatment of hydrogen atoms	refall
Goodness-of-fit on F^2	1.71
Final R indices [I>2σ(I), 22910 reflections]	R1 = 0.0322, wR2 = 0.0520
R indices (all data)	R1 = 0.0364, wR2 = 0.0525
Type of weighting scheme used	calc
Weighting scheme used	calc w=1/[^2^(Fo^2^)]
Max shift/error	0.002
Average shift/error	0.000
Absolute structure parameter	-0.001(5)
Largest diff. peak and hole	2.58 and -2.43 e∑≈$^{-3}$

Programs Used

Cell refinement	SAINT V8.18C (Bruker-AXS, 2007)
Data collection	APEX2 2012.2-0 (Bruker-AXS, 2007)
Data reduction	SAINT V8.18C (Bruker-AXS, 2007)
Structure solution	SHELXS-97 (Sheldrick, 1990)
Structure refinement	SHELXL-97 (Sheldrick, 1997)
Graphics	DIAMOND 3 (Crystal Impact, 1999)

Table A9.2. Atomic coordinates (x 10^4) and equivalent isotropic displacement parameters (≈^{2}x 10^3) for 173. U(eq) is defined as one third of the trace of the orthogonalized U^{ij} tensor.

	x	y	z	U_{eq}

I(1)	3229(1)	3273(1)	1007(1)	15(1)
Si(1)	8286(1)	9598(1)	296(1)	18(1)
O(1)	5867(1)	5072(1)	2118(1)	11(1)
O(2)	5592(1)	4487(1)	2829(1)	19(1)
O(3)	3205(1)	6242(1)	1658(1)	17(1)
O(4)	4368(1)	7639(1)	1154(1)	18(1)
C(1)	6046(1)	4527(1)	1664(1)	10(1)
C(2)	6004(1)	5727(1)	1341(1)	10(1)
C(3)	7647(1)	6616(1)	1326(1)	12(1)
C(4)	9209(1)	5673(1)	1298(1)	17(1)
C(5)	9286(1)	4665(1)	1680(1)	15(1)
C(6)	7759(1)	3724(1)	1662(1)	12(1)
C(7)	7701(1)	2636(1)	2044(1)	13(1)
C(8)	5895(1)	2726(1)	2272(1)	13(1)
C(9)	4551(1)	2554(1)	1916(1)	14(1)
C(10)	4638(1)	3483(1)	1598(1)	12(1)
C(11)	5751(1)	4138(1)	2445(1)	12(1)
C(12)	4363(1)	6542(1)	1412(1)	11(1)
C(13)	2917(1)	8524(1)	1196(1)	21(1)
C(14)	7682(1)	7423(1)	893(1)	14(1)
C(15)	8219(1)	8682(1)	840(1)	17(1)
C(16)	7633(2)	8455(1)	-168(1)	29(1)
C(17)	6799(3)	11047(2)	328(1)	51(1)
C(18)	10497(2)	10244(2)	195(1)	31(1)
C(19)	7776(1)	7534(1)	1736(1)	15(1)
C(20)	9053(1)	2839(1)	2411(1)	20(1)
C(21)	7953(1)	1234(1)	1846(1)	20(1)

Table A9.3. Bond lengths [≈] and angles [∞] for 173.

I(1)-C(10)	2.0931(7)
Si(1)-C(15)	1.8650(8)
Si(1)-C(16)	1.8677(12)
Si(1)-C(17)	1.8543(14)
Si(1)-C(18)	1.8672(13)
O(1)-C(1)	1.4684(9)
O(1)-C(11)	1.3539(10)
O(2)-C(11)	1.2063(11)
O(3)-C(12)	1.2049(10)
O(4)-C(12)	1.3363(10)
O(4)-C(13)	1.4404(11)
C(1)-C(2)	1.5377(11)
C(1)-C(6)	1.5580(11)
C(1)-C(10)	1.5261(11)
C(2)-H(2)	1.015(14)
C(2)-C(3)	1.5596(10)
C(2)-C(12)	1.5307(10)
C(3)-C(4)	1.5419(12)
C(3)-C(14)	1.5258(11)
C(3)-C(19)	1.5320(12)
C(4)-H(4A)	1.008(15)
C(4)-H(4B)	0.875(17)
C(4)-C(5)	1.5223(12)
C(5)-H(5A)	1.052(15)
C(5)-H(5B)	0.959(14)
C(5)-C(6)	1.5178(12)
C(6)-H(6)	1.030(13)

C(6)-C(7)	1.5739(12)
C(7)-C(8)	1.5698(11)
C(7)-C(20)	1.5367(12)
C(7)-C(21)	1.5297(13)
C(8)-H(8)	1.004(16)
C(8)-C(9)	1.5052(12)
C(8)-C(11)	1.5022(12)
C(9)-H(9)	0.930(16)
C(9)-C(10)	1.3303(11)
C(13)-H(13A)	0.951(16)
C(13)-H(13B)	0.993(14)
C(13)-H(13C)	0.904(18)
C(14)-H(14)	0.928(14)
C(14)-C(15)	1.3312(13)
C(15)-H(15)	0.997(18)
C(16)-H(16A)	0.915(17)
C(16)-H(16B)	1.04(2)
C(16)-H(16C)	1.020(18)
C(17)-H(17A)	0.80(3)
C(17)-H(17B)	1.01(2)
C(17)-H(17C)	0.99(2)
C(18)-H(18A)	1.020(18)
C(18)-H(18B)	0.93(2)
C(18)-H(18C)	0.88(2)
C(19)-H(19A)	0.904(15)
C(19)-H(19B)	0.952(15)
C(19)-H(19C)	0.886(16)
C(20)-H(20A)	0.920(16)
C(20)-H(20B)	0.950(17)

C(20)-H(20C)	0.924(16)
C(21)-H(21A)	1.003(14)
C(21)-H(21B)	0.889(18)
C(21)-H(21C)	0.987(16)

C(15)-Si(1)-C(16)	110.06(5)
C(15)-Si(1)-C(18)	109.60(5)
C(17)-Si(1)-C(15)	108.59(6)
C(17)-Si(1)-C(16)	109.91(9)
C(17)-Si(1)-C(18)	108.64(10)
C(18)-Si(1)-C(16)	110.01(6)
C(11)-O(1)-C(1)	114.95(6)
C(12)-O(4)-C(13)	116.59(7)
O(1)-C(1)-C(2)	106.94(6)
O(1)-C(1)-C(6)	105.89(6)
O(1)-C(1)-C(10)	107.66(6)
C(2)-C(1)-C(6)	114.54(6)
C(10)-C(1)-C(2)	115.60(6)
C(10)-C(1)-C(6)	105.64(6)
C(1)-C(2)-H(2)	105.4(8)
C(1)-C(2)-C(3)	116.17(6)
C(3)-C(2)-H(2)	107.3(8)
C(12)-C(2)-C(1)	110.08(6)
C(12)-C(2)-H(2)	103.7(8)
C(12)-C(2)-C(3)	113.09(6)
C(4)-C(3)-C(2)	107.88(7)
C(14)-C(3)-C(2)	109.73(6)
C(14)-C(3)-C(4)	105.03(6)
C(14)-C(3)-C(19)	111.41(7)

C(19)-C(3)-C(2)	111.72(6)
C(19)-C(3)-C(4)	110.80(7)
C(3)-C(4)-H(4A)	109.0(8)
C(3)-C(4)-H(4B)	108.2(11)
H(4A)-C(4)-H(4B)	110.6(13)
C(5)-C(4)-C(3)	113.04(7)
C(5)-C(4)-H(4A)	109.2(8)
C(5)-C(4)-H(4B)	106.8(10)
C(4)-C(5)-H(5A)	110.4(8)
C(4)-C(5)-H(5B)	106.8(8)
H(5A)-C(5)-H(5B)	109.1(12)
C(6)-C(5)-C(4)	110.45(7)
C(6)-C(5)-H(5A)	111.9(8)
C(6)-C(5)-H(5B)	108.1(8)
C(1)-C(6)-H(6)	106.3(7)
C(1)-C(6)-C(7)	109.03(6)
C(5)-C(6)-C(1)	111.02(7)
C(5)-C(6)-H(6)	108.4(7)
C(5)-C(6)-C(7)	114.99(7)
C(7)-C(6)-H(6)	106.6(7)
C(8)-C(7)-C(6)	107.59(6)
C(20)-C(7)-C(6)	114.06(7)
C(20)-C(7)-C(8)	107.40(7)
C(21)-C(7)-C(6)	110.09(7)
C(21)-C(7)-C(8)	109.68(7)
C(21)-C(7)-C(20)	107.94(7)
C(7)-C(8)-H(8)	110.6(9)
C(9)-C(8)-C(7)	108.20(6)
C(9)-C(8)-H(8)	114.9(9)

C(11)-C(8)-C(7)	105.71(7)
C(11)-C(8)-H(8)	109.7(9)
C(11)-C(8)-C(9)	107.34(7)
C(8)-C(9)-H(9)	119.6(9)
C(10)-C(9)-C(8)	113.10(7)
C(10)-C(9)-H(9)	127.0(9)
C(1)-C(10)-I(1)	123.83(5)
C(9)-C(10)-I(1)	120.64(6)
C(9)-C(10)-C(1)	114.63(7)
O(1)-C(11)-C(8)	112.82(6)
O(2)-C(11)-O(1)	119.90(8)
O(2)-C(11)-C(8)	127.25(8)
O(3)-C(12)-O(4)	123.87(7)
O(3)-C(12)-C(2)	125.54(7)
O(4)-C(12)-C(2)	110.58(6)
O(4)-C(13)-H(13A)	107.9(10)
O(4)-C(13)-H(13B)	110.3(8)
O(4)-C(13)-H(13C)	110.2(12)
H(13A)-C(13)-H(13B)	109.1(12)
H(13A)-C(13)-H(13C)	114.6(15)
H(13B)-C(13)-H(13C)	104.8(14)
C(3)-C(14)-H(14)	113.4(9)
C(15)-C(14)-C(3)	127.14(8)
C(15)-C(14)-H(14)	119.3(9)
Si(1)-C(15)-H(15)	116.0(10)
C(14)-C(15)-Si(1)	125.05(7)
C(14)-C(15)-H(15)	118.5(10)
Si(1)-C(16)-H(16A)	108.5(10)
Si(1)-C(16)-H(16B)	110.7(10)

Si(1)-C(16)-H(16C)	113.9(11)
H(16A)-C(16)-H(16B)	106.6(15)
H(16A)-C(16)-H(16C)	112.0(15)
H(16B)-C(16)-H(16C)	104.8(15)
Si(1)-C(17)-H(17A)	105(2)
Si(1)-C(17)-H(17B)	110.7(13)
Si(1)-C(17)-H(17C)	103.4(14)
H(17A)-C(17)-H(17B)	103(2)
H(17A)-C(17)-H(17C)	126(2)
H(17B)-C(17)-H(17C)	108.5(18)
Si(1)-C(18)-H(18A)	111.1(11)
Si(1)-C(18)-H(18B)	109.9(13)
Si(1)-C(18)-H(18C)	104.1(16)
H(18A)-C(18)-H(18B)	109.8(16)
H(18A)-C(18)-H(18C)	108.5(18)
H(18B)-C(18)-H(18C)	113(2)
C(3)-C(19)-H(19A)	112.9(10)
C(3)-C(19)-H(19B)	112.8(9)
C(3)-C(19)-H(19C)	110.1(9)
H(19A)-C(19)-H(19B)	104.8(13)
H(19A)-C(19)-H(19C)	105.1(13)
H(19B)-C(19)-H(19C)	110.7(13)
C(7)-C(20)-H(20A)	107.2(10)
C(7)-C(20)-H(20B)	110.3(10)
C(7)-C(20)-H(20C)	110.6(9)
H(20A)-C(20)-H(20B)	107.5(13)
H(20A)-C(20)-H(20C)	111.0(14)
H(20B)-C(20)-H(20C)	110.3(14)
C(7)-C(21)-H(21A)	107.9(8)

C(7)-C(21)-H(21B)	114.7(12)
C(7)-C(21)-H(21C)	113.7(9)
H(21A)-C(21)-H(21B)	110.7(12)
H(21A)-C(21)-H(21C)	109.6(12)
H(21B)-C(21)-H(21C)	100.0(14)

Symmetry transformations used to generate equivalent atoms:

Table A9.4. Anisotropic displacement parameters ($\approx^2$x 10^4) for hmn03. The anisotropic displacement factor exponent takes the form: $-2\pi^2$ [$h^2 a^{*2} U^{11}$ + ... + 2 h k a* b* U^{12}]

	U^{11}	U^{22}	U^{33}	U^{23}	U^{13}	U^{12}
I(1)	153(1)	162(1)	141(1)	-20(1)	-36(1)	-19(1)
Si(1)	248(1)	130(1)	151(1)	45(1)	40(1)	16(1)
O(1)	155(2)	82(2)	85(2)	0(2)	5(2)	6(2)
O(2)	318(4)	150(3)	106(2)	8(2)	23(2)	13(2)
O(3)	139(2)	179(3)	181(2)	39(2)	29(2)	33(2)
O(4)	154(2)	162(3)	233(3)	93(2)	1(2)	34(2)
C(1)	116(2)	85(3)	86(2)	1(2)	-1(2)	3(2)
C(2)	110(2)	91(3)	94(2)	6(2)	-6(2)	-1(2)
C(3)	120(2)	109(3)	117(3)	16(2)	-6(2)	-15(2)
C(4)	117(3)	181(4)	200(4)	68(3)	24(2)	9(2)
C(5)	106(3)	166(4)	192(3)	48(3)	-7(2)	8(2)
C(6)	119(2)	112(3)	115(3)	6(2)	5(2)	24(2)
C(7)	148(3)	98(3)	148(3)	17(2)	-11(2)	20(2)
C(8)	167(3)	90(3)	131(3)	22(2)	-1(2)	2(2)

C(9)	149(3)	98(3)	160(3)	5(2)	2(2)	-15(2)
C(10)	115(2)	103(3)	128(3)	-4(2)	-16(2)	-9(2)
C(11)	161(3)	103(3)	108(3)	14(2)	5(2)	7(2)
C(12)	118(2)	99(3)	118(3)	7(2)	-19(2)	9(2)
C(13)	192(4)	165(4)	271(4)	34(3)	-35(3)	58(3)
C(14)	151(3)	149(3)	115(3)	23(2)	9(2)	-11(2)
C(15)	237(3)	132(3)	147(3)	26(2)	28(3)	-6(3)
C(16)	380(6)	294(6)	191(4)	60(4)	-41(3)	-109(4)
C(17)	732(12)	401(8)	403(8)	181(7)	221(8)	366(9)
C(18)	363(6)	296(6)	274(5)	104(5)	-16(4)	-138(5)
C(19)	190(3)	143(3)	124(3)	8(3)	-24(2)	-49(3)
C(20)	189(3)	211(4)	188(4)	57(3)	-58(3)	5(3)
C(21)	238(4)	119(3)	256(4)	-9(3)	21(3)	51(3)

Table A9.5. Hydrogen coordinates (x 10^3) and isotropic displacement parameters (≈^{2}x 10^3) for hmn03.

	x	y	z	U_{iso}
H(2)	585(2)	532(1)	103(1)	16(3)
H(4A)	917(2)	517(1)	100(1)	18(3)
H(4B)	1014(2)	616(2)	132(1)	23(4)
H(5A)	937(2)	517(2)	199(1)	20(3)
H(5B)	1030(2)	414(1)	164(1)	11(3)
H(6)	779(2)	321(1)	136(1)	10(3)
H(8)	581(2)	208(2)	253(1)	24(4)
H(9)	384(2)	181(2)	192(1)	22(3)
H(13A)	197(2)	811(2)	105(1)	28(4)
H(13B)	316(2)	940(1)	105(1)	16(3)
H(13C)	273(2)	872(2)	149(1)	38(5)
H(14)	735(2)	693(2)	64(1)	17(3)
H(15)	848(2)	923(2)	111(1)	37(5)
H(16A)	657(2)	812(2)	-11(1)	30(4)
H(16B)	845(2)	763(2)	-19(1)	40(5)
H(16C)	768(2)	889(2)	-48(1)	42(5)
H(17A)	587(4)	1072(3)	33(1)	80(10)
H(17B)	680(3)	1156(2)	4(1)	65(6)
H(17C)	731(3)	1162(2)	56(1)	59(6)
H(18A)	1056(2)	1077(2)	-10(1)	37(5)
H(18B)	1127(3)	953(2)	19(1)	48(6)
H(18C)	1068(3)	1080(2)	42(1)	58(6)

H(19A)	875(2)	802(2)	174(1)	22(4)
H(19B)	777(2)	705(2)	201(1)	23(4)
H(19C)	694(2)	814(2)	173(1)	21(3)
H(20A)	885(2)	220(2)	263(1)	23(4)
H(20B)	892(2)	370(2)	255(1)	25(4)
H(20C)	1014(2)	275(2)	229(1)	24(4)
H(21A)	910(2)	121(2)	170(1)	14(3)
H(21B)	714(2)	98(2)	166(1)	31(4)
H(21C)	788(2)	50(2)	207(1)	25(4)

Comprehensive Bibliography

Abderrahmane, A.; Guerra, F. M.; Rubal J. J.; Moreno-Durado, F. J.; Akssira, M.; Mellouki, F.; Lopez, M.; Pujadas, A. J.; Jorge, Z. D.; Massanet, G. M. *Org. Lett.* **2005**, *5,* 881–884.

Afarinkia, K.; Posner, G. H. *Tetrahedron Lett.* **1992**, *33*, 7839–7842.

Afarinkia, K.; Vinader, V.; Nelson, T. D.; Posner, G. H. *Tetrahedron* **1992**, *48*, 9111–9171.

Afarinkia, K; Bearpark, M. J.; Ndibwami, A. *J. Org. Chem.* **2005**, *70,* 1122–1133.

Appendino, G.; Prosperini, S.; Valdivia, C.; Ballero, M.; Colombano, G.; Billington, R. A.; Genazzani, A. A.; Sterner, O. *J. Nat. Prod.* **2005**, *68*, 1213–1217.

Baran, P. S.; Burns, N. Z. *J. Am. Chem. Soc.* **2006**, *128*, 3908–3909.

Batista, J. M.; López, S. N.; Da Silva Mota, J.; Vanzolini, K. L.; Cass, Q. B.; Rinaldo, D.; Vilegas, W.; Da Silva Bolzani, V.; Kato, M. J.; Furlan, M. *Chirality* **2009**, *21*, 799–801.

Batsanov, A. S.; Knowles, J. P.; Whiting, A. *J. Org. Chem.* **2007**, *72*, 2525–2532.

Boger, D. L.; Brotherton, C. E. *J. Org. Chem.* **1984**, *49*, 4050–4055.

Breitmaier, E.; *Terpenes: Flavors, Fragrances, Pharmaca, Phermones*; WILEY-VCH: New York, 2006

Carmona, D.; Lamata, M. P.; Oro, L. A. *Coord. Chem. Rev.* **2000**, *200*, 717–772.

Carroll, M. F., *J. Chem. Soc. (Resumed)* **1940**, 704–706.

Christensen, S. B.; Larsen, I. K.; Rasmussen, U.; Christophersen, C. *J. Org. Chem.* **1982**, *47,* 649-652.

Christensen, S.B.; Andersen, A.; Smitt, U.W. *Prog. Chem. Org. Nat. Prod* **1997**, *71*, 130–167.

Corey, E. J. *Angew. Chem. Int. Ed.* **2002**, *41*, 1650–1667.

Corey, E. J.; Lee, D. H. *J. Am. Chem. Soc.* **1991**, *113*, 4026–4028.

Corey, E. J.; Venkateswarlu, A. *J. Am. Chem. Soc.* **1972**, *94*, 6190–6191.

Corey, E. J.; Watt, D. S., *J. Am. Chem. Soc.* **1973,** *95*, 2303–2311.

Dai, C.; Fu, G. C. *J. Am. Chem. Soc.* **2001**, *122*, 2719–2724.

Diels, O.; Alder, K. *Liebigs Ann. Chem.* **1931**, *490*, 257–266.

Diels, O.; Alder, K. *Liebigs Ann. Chem.* **1928**, *460*, 98–122.

Dombroski, J. R.; Schuerch, C. *Macromolecules (Washington, DC, U. S.)* **1970**, *3*, 257–260.

Dyke, S. F.; Sainsbury, M.; Brown, D. W.; Clipperton, R. D. J. *Tetrahedron* **1970**, *26*, 5969–5980.

Eicher, T.; Hauptmann, S.; 6.3 *2H*-Pyran-*2*-one. The Chemistry of Heterocycles, 2nd edition. Wiley-VCH: New York, 2003; pp. 233–256.

Fillion, E.; Beingessner, R. L. *J. Org. Chem.* **2003**, *68*, 9485–9488.

Futami, T.; Miyagishi, M.; Taira, K. *J. Biol. Chem.* **2005**, *280*, 826–831.

Goldstein, E. *J. Mol. Struct. THEOCHEM* **1987**, *151,* 297–305.

Grewe, R.; Kersten, S. *Ber.* **1967**, *100*, 2546.

Gu, S. E.; Schoenebeck, F.; Aviyente, V.; Houk, K. N. *J. Org. Chem.* **2010**, *75*, 2115–2118.

Guimaraes, C. R. W.; Udier-Blagovic, M.; Jorgensen, W. L. *J. Am. Chem. Soc.* **2005**, *127*, 3577–3588.

Hall, D. J.; Van den Berghe, H. M.; Dove, A. P. *Polym Int* **2011**, *60*, 1149–1157.

Ireland, R. E.; Wipf, P.; Xiang, J. N. *J. Org. Chem.* **1991**, *56*, 3572–3582.

Ireland, R. E.; Varney, M. D. *J. Am. Chem. Soc.* **1984**, *106*, 3668–3670.

Jones, E. R. H.; Eglington, G.; Whiting, M. C.; Shaw, B. L. *Org. Synth.* **1954**, *34*, 46–49.

Jorgensen, K. A. *Angew. Chem. Int. Ed.* **2000**, *39*, 3558–3588.

Juhl, M.; Tanner, D. *Chem. Soc. Rev.* **2009**, *38*, 2983–2992.

Kametani, T.; Hibino, S. *Advances in Heterocyclic Chemistry* **1987**, *42*, 245–333.

Kazmaier, U.; Krebs, A. *Angew. Chem. Int. Ed.* **1995**, *34*, 2012–2014.

Kelly, W. L. *Org. Biomol. Chem.* **2008**, *6*, 4483–4493.

Kelly, W. L., *Nature* **2011,** *473*, 35–36.

Kim, H. J.; Ruszczycky, M. W.; Liu, H. W. *Curr. Opin. Chem. Biol.* **2012**, *16*, 124–131.

Kim, H. J.; Ruszczycky, M. W.; Choi, S. H.; Liu, Y. N.; Liu, H. W., *Nature* **2011,** *473*, 109–112.

Kobuke, Y. *J. Syn. Org. Chem. Jpn.* **1972**, *30*, 992–1005.

Kozytska, M. V.; Dudley, G. B. *Tetrahedron Lett.* **2008**, *49*, 2899–2901.

Larsson, R.; Sterner, O.; Johansson, M. *Org. Lett.* **2009**, *11*, 657–660.

Löffler, A.; Himbert, G. *Synthesis* **1992**, *5*, 495–498.

Lytton, J.; Westlin, M.; Hanley, M. R. *J. Biol. Chem.* **1991**, *26*, 17067–17071.

Marshall, J. A. in *Organometallics in Synthesis: A Manual,* Ed.: M. Schlosser, John Wiley & Sons Ltd., West Sussex, **2002**, pp. 457.

Mawhinney, T. P.; Madson, M. A. *J. Org. Chem.* **1982**, *47*, 3336–3339.

Mizoguchi, H.; Oguri, H.; Tsuge, K.; Oikawa, H., *Org. Lett.* **2009,** *11*, 3016–3019.

Narasaka, K.; Shimada, S.; Osoka, K.; Iwasawa, N. *Synthesis* **1991**, 1171–1172.

Navarette, C.; Sancho, R.; Caballero, F. J.; Pollastro, F.; Fiebich, B. L.; Sterner, O.; Appendino, G.; Muñoz, E. *J. Pharmacol. Exp. Ther.* **2006**, *319*, 422-430

Nelson, H. M.; Murakami, K.; Virgil, S. C.; Stoltz, B. M. *Angew. Chem. Int. Ed.* **2011**, *50*, 3688–3691.

Nelson, H. M.; Stoltz, B. M. *Tetrahedron Lett.* **2009**, *50*, 1699–1701.

Nelson, H. M.; Stoltz, B. M. *Org. Lett.* **2007**, *10*, 25–28.

Nicolaou, K. C.; Snyder, S. A.; Montagnon, T.; Vassilikogiannakis, G. *Angew. Chem. Int. Ed.* **2002**, *41*, 1668–1698.

Nicolaou, K. C.; Yang, Z.; Liu, J. J.; Ueno, H.; Nantermet, P. G.; Guy, R. K.; Claiborne, C. F.; Renaud, J.; Couladouros, E. A.; Paulvannan, K.; Sorensen, E. J. *Nature* **1994**, *367*, 630–634.

Nicolaou, K. C.; Liu, J. J.; Yang, Z.; Ueno, H.; Sorensen, E. J.; Claiborne, C. F.; Guy, R. K.; Hwang, C. K.; Nakada, M.; Nantermet, P. G. *J. Am. Chem. Soc.* **1995**, *117*, 634–644.

Nicolaou, K. C.; Nantermet, P. G.; Ueno, H.; Guy, R. K.; Couladouros, E. A.; Sorensen, E. J. *J. Am. Chem. Soc.* **1995**, *117*, 624–633.

Nicolaou, K. C.; Ueno, H.; Liu, J. J.; Nantermet, P. G.; Yang, Z.; Renaud, J.; Paulvannan, K.; Chadha, R. *J. Am. Chem. Soc.* **1995**, *117*, 653–659.

Nicolaou, K. C.; Yang, Z.; Liu, J. J.; Nantermet, P. G.; Claiborne, C. F.; Renaud, J.; Guy, R. K.; Shibayama, K. *J. Am. Chem. Soc.* **1995**, *117*, 645–652.

Nmomiya, I.; Naito, T.; Iehii, H.; Ishida, T.; Ueda, M.; Harada, K. *J. Chem. Soc., Perkin Trans. 1* **1975**, 762.

Oguri, H.; Yamagishi, Y.; Hiruma, T.; Oikawa, H., *Org. Lett.* **2008,** *11*, 601-604.

Oguri, H.; Hiruma, T.; Yamagishi, Y.; Oikawa, H.; Ishiyama, A.; Otoguro, K.; Yamada, H.; Omura, S., *J. Am. Chem. Soc.* **2011,** *133*, 7096–7105.

Okamura, H.; Urabe, F.; Hamada, T.; Iwagawa, T. *B. Chem. Soc. Jpn.* **2012**, *85*, 631–633.

Ose, T.; Watanabe, K.; Mie, T.; Honma, M.; Watanabe, H.; Yao, M.; Oikawa, H.; Tanaka, I. *Nature* **2003,** *422*, 185–189.

Pagani, A.; Pollastro, F.; Spera, S.; Ballero, M.; Sterner, O.; Appendino, G. *Nat. Prod. Commun.* **2007**, *2*, 637–642.

Perchellet, E. M.; Gali, H. U.; Gao, X. M.; Perchellet, J. *Int. J. Cancer* **2006**, *55,* 1036–1043.

Pérez, D.; Guitián, E.; Castedo, L. *J. Org. Chem.* **1992**, *57*, 5911–5917.

Posner, G. H.; Dai, H.; Afarinkia, K.; Murthy, N. N.; Guyton, K. Z.; Kensler, T. W. *J. Org. Chem.* **1993**, *58*, 7209–7215.

Posner, G. H.; Nelson, T. D.; Kinter, C. M.; Afarankia, K. *Tetrahedron Lett.* **1991**, *32*, 5295–5298.

Posner, G. H.; Harrison, W. *J. Chem. Soc., Chem. Commun.* **1985,** *285*, 1786–1787.

Posner, G. H.; Wettlaufer, D. G. *Tetrahedron Lett.* **1986**, *27*, 667–670.

Posner, G. H.; Switzer, C. *J. Org. Chem.* **1987**, *52*, 1642–1644.

Posner, G. H.; Wettlaufer, D. G. *J. Am. Chem. Soc.* **1986**, *108*, 7373–7377.

Posner, G. H.; Carry, J. C.; Lee, J. K.; Bull, D. S.; Dai, H. Y. *Tetrahedron Lett.* **1994**, *35*, 1321–1324.

Raucher, S.; Bray, B. L. *J. Org. Chem.* **1987**, *52*, 2332–2333.

Rubal, J. J.; Moreno-Dorado, F. J.; Guerra, F. M.; Zacarias, D. J.; Abderrahmane, S.; Mohamed, A.; Fouad, M.; Raul, R. G.; Massanet, G. M. *Phytochemistry* **2007**, *68*, 2480–2486.

Sakamoto, T.; Yasuhara, A.; Kondo, Y.; Yamanaka, H.; *Synlett* **1992**, *6*, 502.

Sakamoto, T.; Yasuhara, A.; Kondo, Y.; Yamagishi, Y. *Chem. Pharm. Bull.* **1994**, *42*, 2032–2035

Saouf, A.; Guerra, F. M.; Rubal, J. J.; Moreno-Dorado, F. J.; Akssira, M.; Mellouki, F.; Lopez, M.; Pujadas, A. J.; Jorge, Z. D.; Massanet, G. M. *Org. Lett.* **2005**, *7*, 881–884.

Schmidt, R. R. *Acc. Chem. Res.* **1986**, *19*, 250–259.

Serafimov, J. M.; Westfeld, T.; Meier, B. H.; Hilvert, D., *J. Am. Chem. Soc.* **2007,** *129*, 9580.

Shibuya, H.; Ohashi, K.; Narita, N.; Ishida, T.; Kitigawa, I. *Chem*. *Pharm*. *Bull*. **1994**, *42*, 293–299.

Shusheri, N. P. *Usp. Khim.* **1974**, *43*, 1771–1793.

Snyder, C. D.; Rapoport, H. *J. Am. Chem. Soc.* **1973**, *95*, 7821–7828.

Snyder, S. A.; Treitler, D. S. *Angew. Chem., Int. Ed.* **2009**, *48*, 7899–7903.

Still, W. C.; Gennari, C. *Tetrahedron Lett.* **1983**, *24*, 4405–4408.

Tadano, K.-i. *Eur. J. Org. Chem.* **2009**, 4381–4394.

Takao, K.; Munakata, R.; Tadano, K. *Chem. Rev.* **2005**, *105*, 4779–4807.

Tasdelen, M. A. *Polym Chem-Uk* **2011**, *2*, 2133–2145.

Tietze, L. F.; Kettschau, G. *Stereoselective Heterocyclic Synthesis I* **1997**, *189*, 1–120.

Treiman, T.; Caspersen, C.; Christensen, S. B.; *Trends Pharma. Sciences,* **1998**, *19*, 131–135.

Waldmann, H. *Synthesis-Stuttgart* **1994**, 535–551.

Wang, Y.; Li, H.; Wang, Y.-Q.; Liu, Y.; Foxman, B. M.; Deng, L. *J. Am. Chem. Soc.* **2007**, *129*, 6364.

Wasserman, H. H.; Wharton, H. H. *J. Am. Chem. Soc.* **1960**, *82*, 661–665.

Watanabe, K.; Oikawa, H.; Yagi, K.; Ohashi, S.; Mie, T.; Ichihara, A.; Hornma, M. *J. Biochem.* **2000**, *127*, 467–473.

Werkhoven, T. M.; van Nipsen, R.; Lugtenburg J. *Eur. J. Org. Chem*. **1999**, *11*, 2909–2914.

Wu, W.; Min, L.; Zhu, L.; Lee, C.-S. *Adv. Synth. Catal.* **2011**, *353*, 1135–1145.

Yamaguchi, H.; Bhalla, K.; Wang, H.-G., *Cancer Res*. **2003**, *63*, 1483–1489.

Zeng, W.; Fröhlich, R.; Hoppe, D. *Tetrahedron* **2005**, *61*, 3281–3287.

Zhou, X. ; Wu, W.; Liu, X.; Lee, C.-S. *Org. Lett.* **2008**, *10*, 5525–5528.

INDEX

B

C

D

E

F

G

H

I

K

L

M

N

O

P

R

S

T

X

Y

ABOUT THE AUTHOR

Hosea Martin Nelson was born in San Francisco September 15, 1977, to Jimmy L. Nelson and Patricia E. Snider. Hosea spent much of his childhood fishing, playing sports, and trying to avoid doing homework. In high school, he spent most of his time working out and throwing shot put, eventually competing in several nationally renowned track meets and the CIF state championships. Hosea earned his GED in 1999.

Shortly after earning his high school equivalency, Hosea went on to attend community college at the City College of San Francisco. During this time he fell in love with science and began working in the labs of Leticia Marquez-Magana at San Francisco State University. Hosea transferred to UC Berkeley in the Fall of 2002, where he earned a Bachelor's degree in Chemistry in 2004.

He then moved to Pasadena in 2006 to begin his Ph.D. studies under the guidance of Prof. Brian Stoltz. Hosea received his degree for his work on the total synthesis of the transtaganolide natural products. Hosea will be returning to the Bay Area as a postdoctoral scholar in the labs of Prof. F. Dean Toste at UC Berkeley.